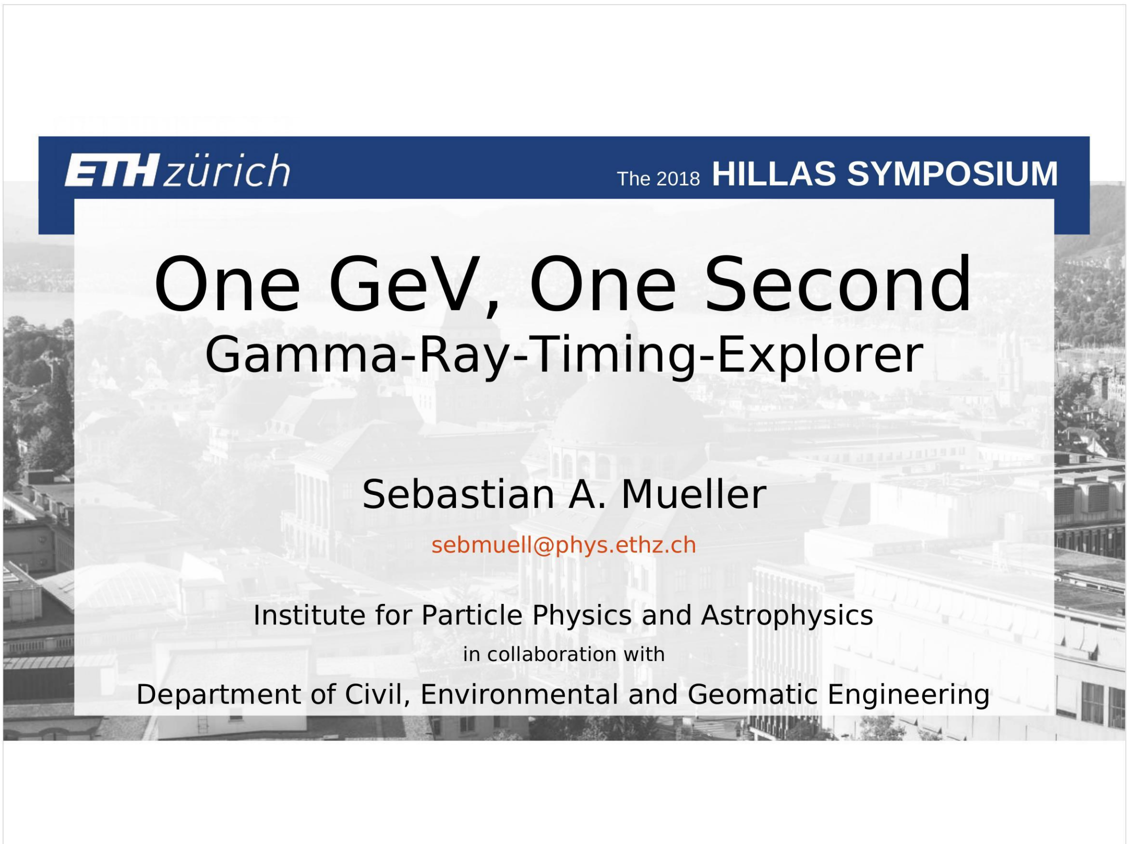

I want to thank the colleagues and friends of Micheal Hillas for introducing me to this beautiful mind, charming colleague, and persistent architect behind the legacy of ground based gamma-ray-astronomy. Presenting my findings on a symposium in memory of Micheal Hillas, makes me the proudest phd-student under the gamma-ray-sky.

--- Begin of talk ---

One Giga Electron Volt, One second gamma-ray-timing-explorer.

Hallo everybody, my name is Sebastian Achim Mueller.

I am a phd-student at ETH Zurich in the group of Adrian Biland, and this is my doctoral-thesis.

Contents lists available at ScienceDirect

Astroparticle Physics

journal homepage: www.elsevier.com/locate/astropartphys

Bokeh mirror alignment for Cherenkov telescopes

M.L. Ahnen[a], D. Baack[d], M. Balbo[b], M. Bergmann[c], A. Biland[a], M. Blank[c], T. Bretz[a], K.A. Bruegge[d], J. Buss[d], M. Domke[d], D. Dorner[c], S. Einecke[d], C. Hempfling[c], D. Hildebrand[a], G. Hughes[a], W. Lustermann[a], K. Mannheim[c], S.A. Mueller[a,*], D. Neise[a], A. Neronov[b], M. Noethe[d], A.-K. Overkemping[d], A. Paravac[c], F. Pauss[a], W. Rhode[d], A. Shukla[a], F. Temme[d], J. Thaele[d], S. Toscano[b], P. Vogler[a], R. Walter[b], A. Wilbert[c]

* Corresponding author
S. A. Mueller

doi.org/10.1016/j.astropartphys.2016.05.003

My findings originate in mirror-alignment which I started in Dortmund and then published during my phd in Zurich.

A look into the Bokeh,

Contents lists available at ScienceDirect

Astroparticle Physics

journal homepage: www.elsevier.com/locate/astropartphys

Normalized and asynchronous mirror alignment for Cherenkov telescopes

M.L. Ahnen[a], D. Baack[d], M. Balbo[b], M. Bergmann[c], A. Biland[a], M. Blank[c], T. Bretz[a], K.A. Bruegge[d], J. Buss[d], M. Domke[d], D. Dorner[c], S. Einecke[d], C. Hempfling[c], D. Hildebrand[a], G. Hughes[a], W. Lustermann[a], K. Mannheim[c], S.A. Mueller[a,*], D. Neise[a], A. Neronov[b], M. Noethe[d], A.-K. Overkemping[d], A. Paravac[c], F. Pauss[a], W. Rhode[d], A. Shukla[a], F. Temme[d], J. Thaele[d], S. Toscano[b], P. Vogler[a], R. Walter[b], A. Wilbert[c]

* Corresponding author
S. A. Mueller

doi.org/10.1016/j.astropartphys.2016.05.005

And the normalized and asynchronous mirror alignment will motivate my findings presented here.

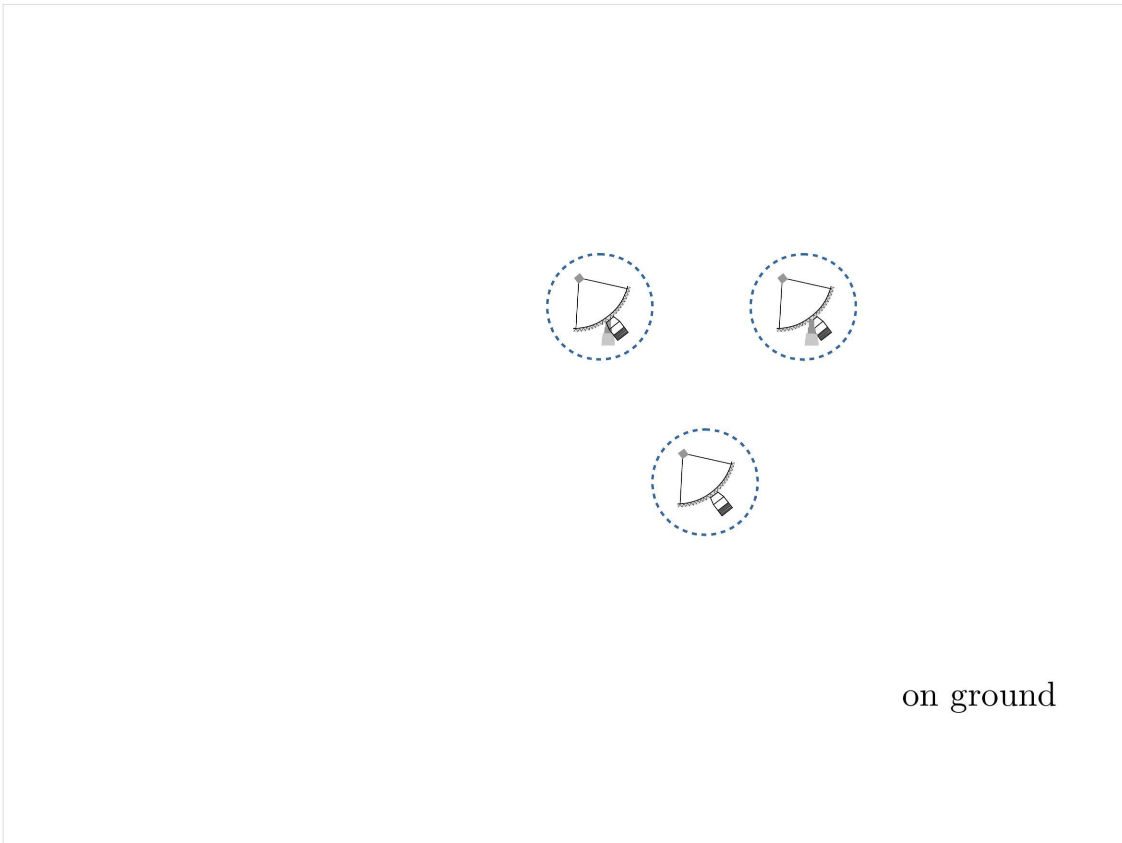

With multiple telescopes

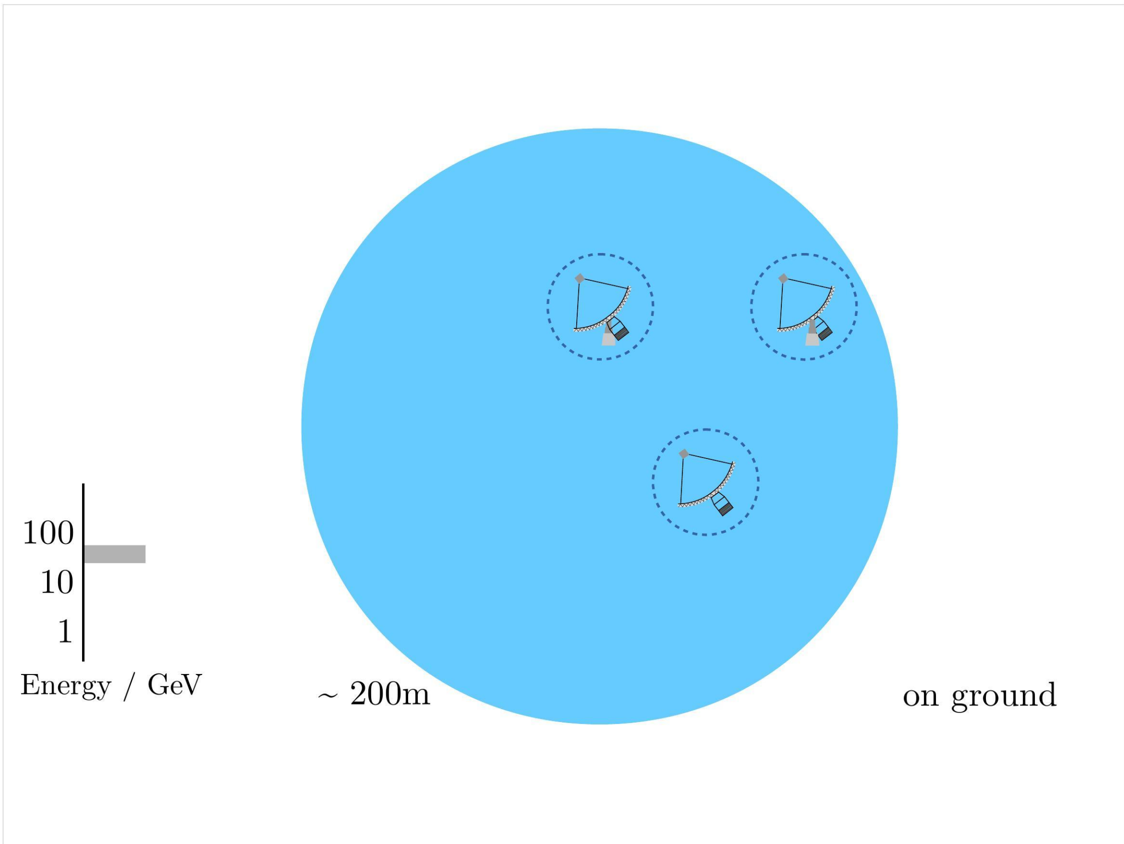

within a pool of Cherenkov-photons emitted by an air-shower

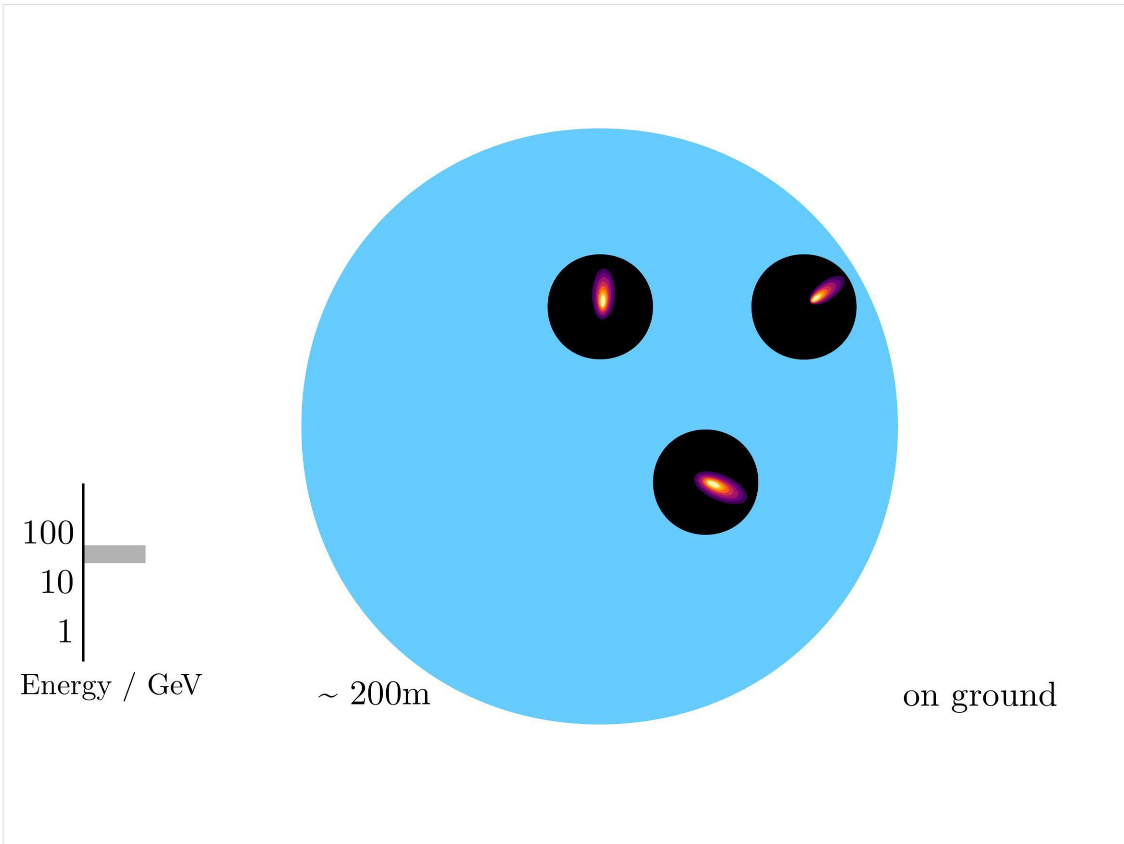

We can have stereo images.

We can reconstruct Hillas-ellipses

And we can reconstruct the cosmic particle’s trajectory.

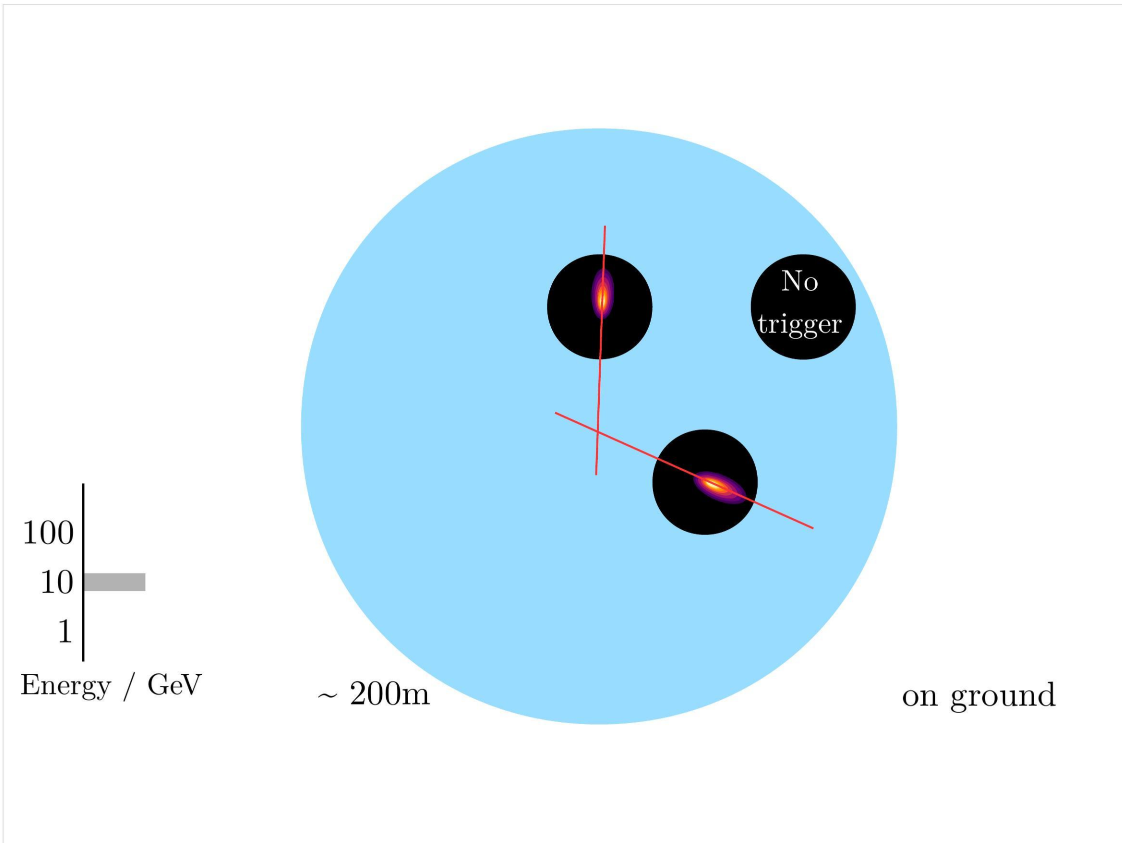

When the cosmic particle’s energy is lower, not all telescopes will trigger.

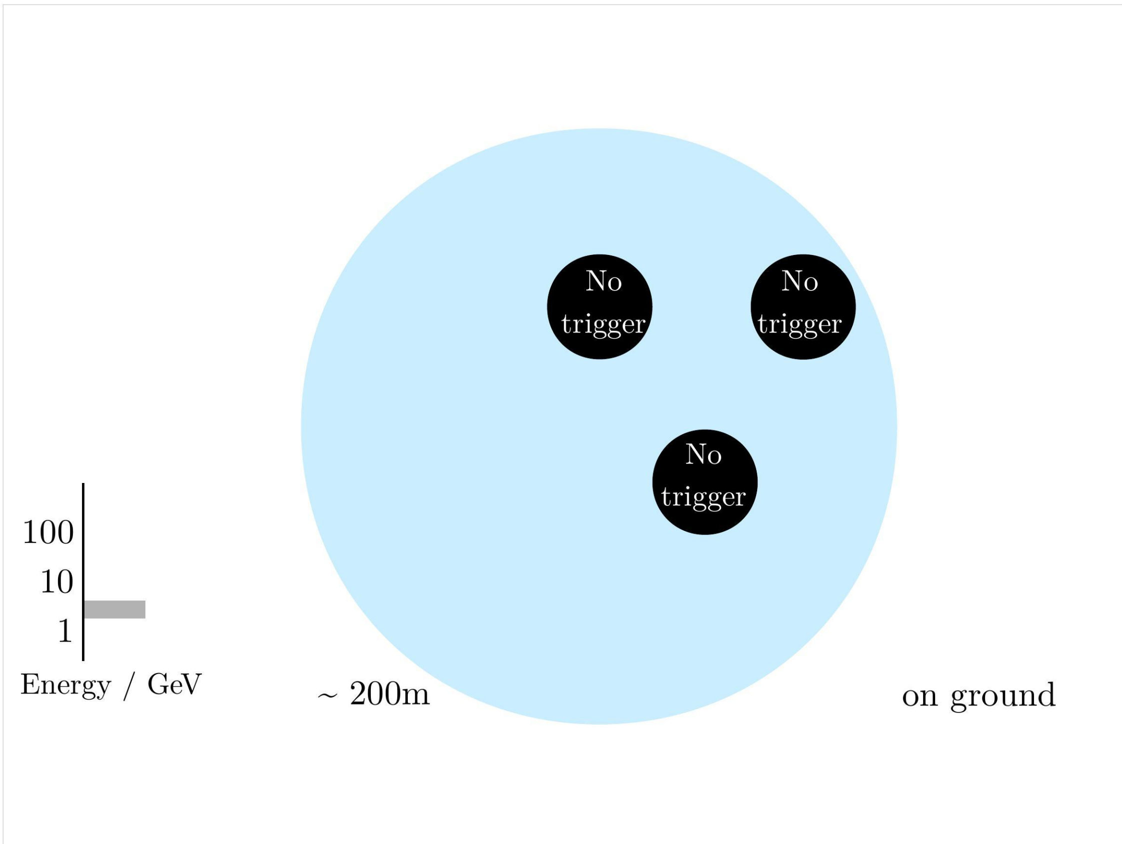

When the cosmic particle’s energy is too low, none of the telescopes will trigger.

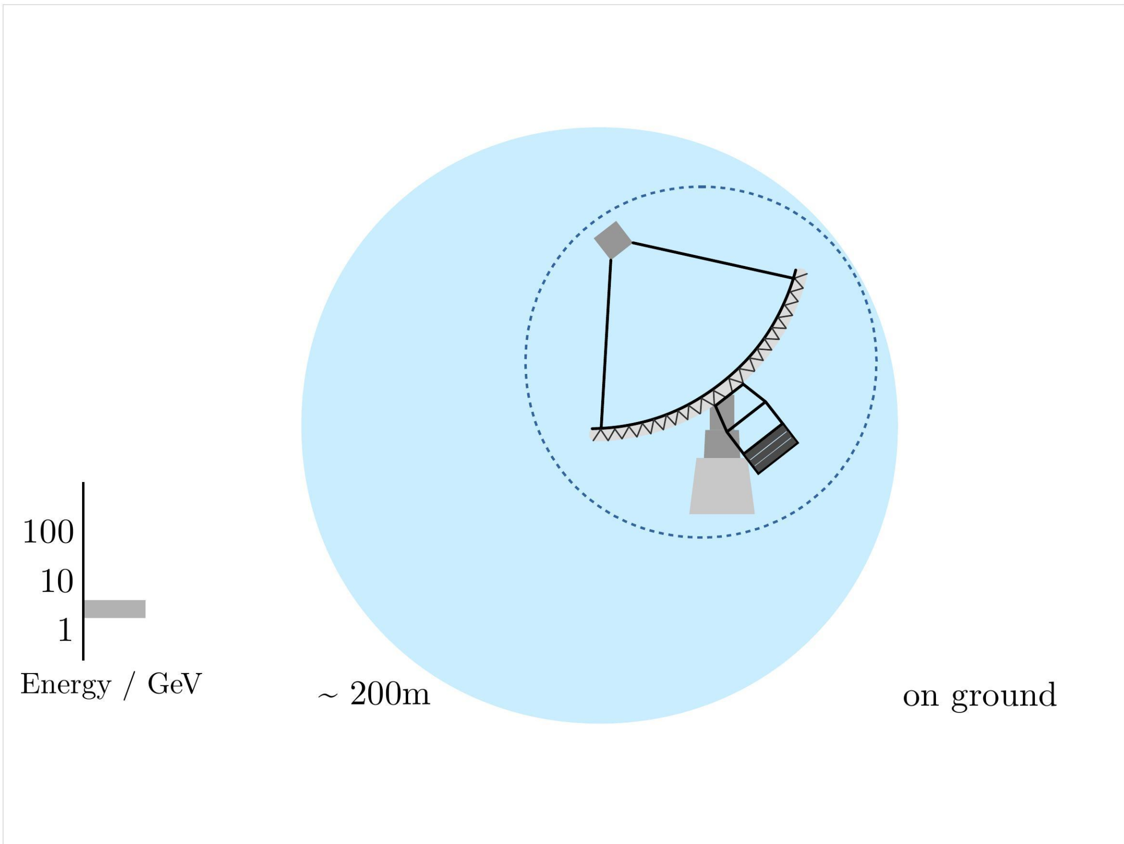

We need to collect more Cherenkov-photons in a single and large telescope.

But when we look at its images

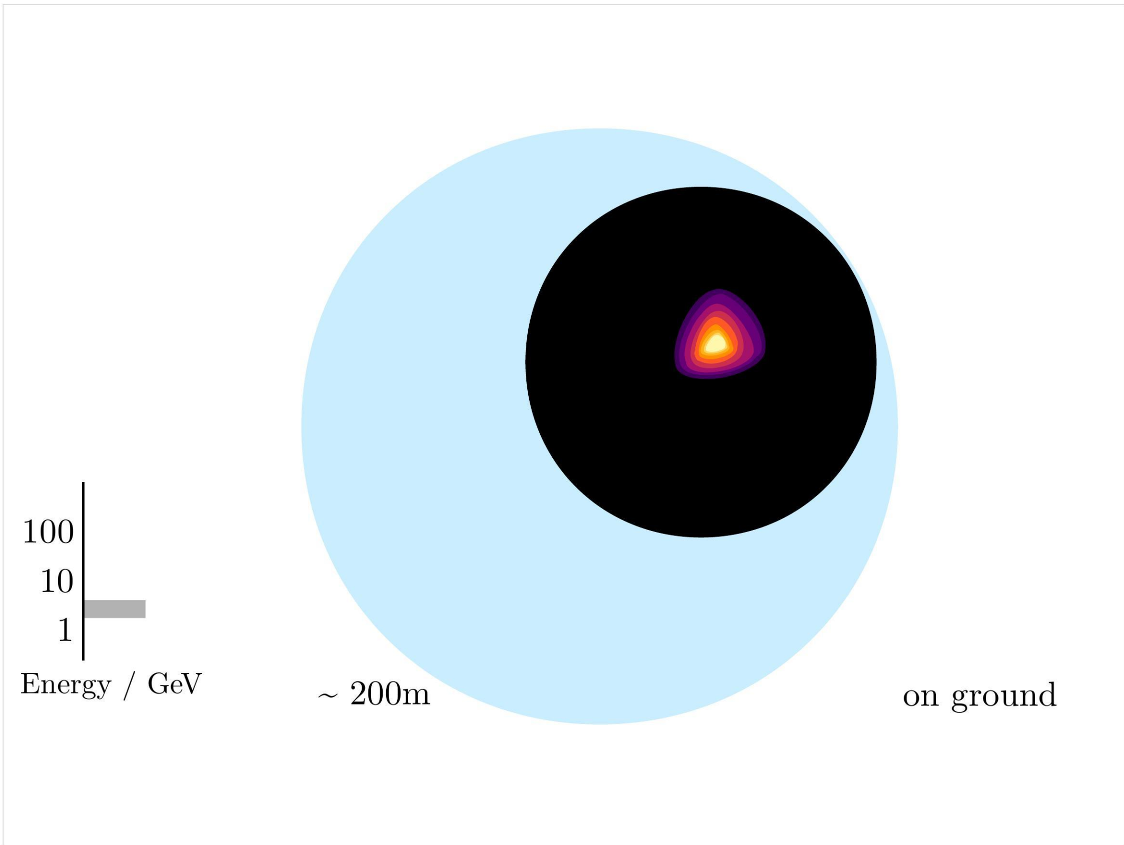

We find that they are blurred.

Here we do not find ellipses.

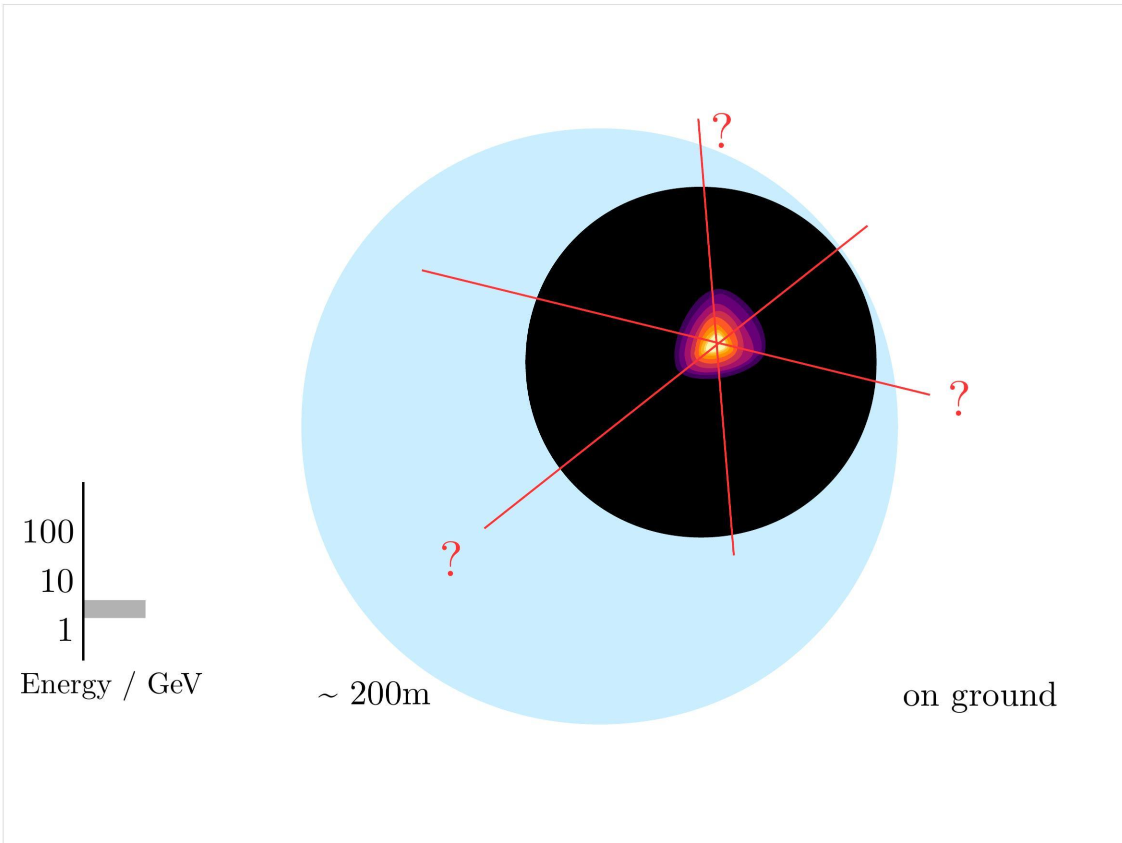

We can not easily reconstruct the trajectory of the cosmic-particle.

We are approaching the limit of a narrow depth-of-field.

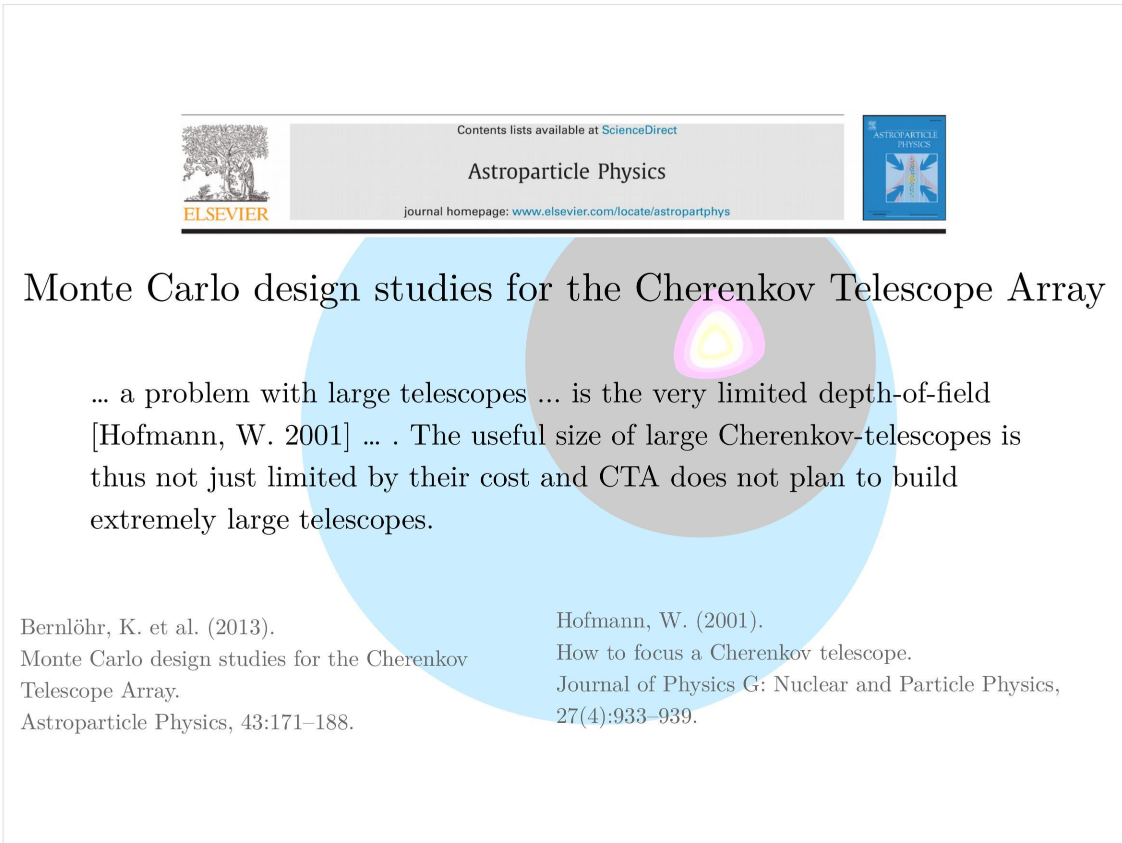

In the Monte Carlo design study for the Cherenkov Telescope array it says:

A problem with large telescopes is the very limited depth-of-field.

The useful size of large Cherenkov-telescopes is thus not just limited by their corst and CTA does not plan to build extremely large telescopes.

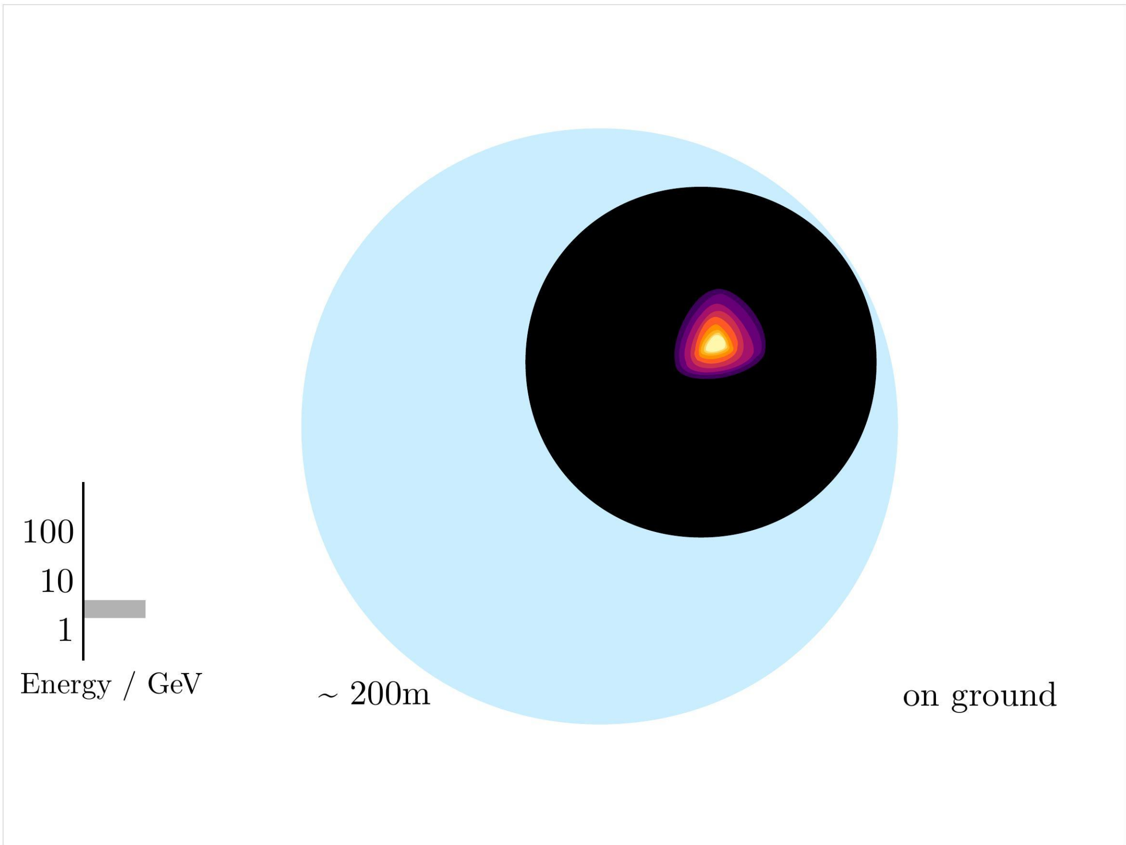

The image of a large telescope is

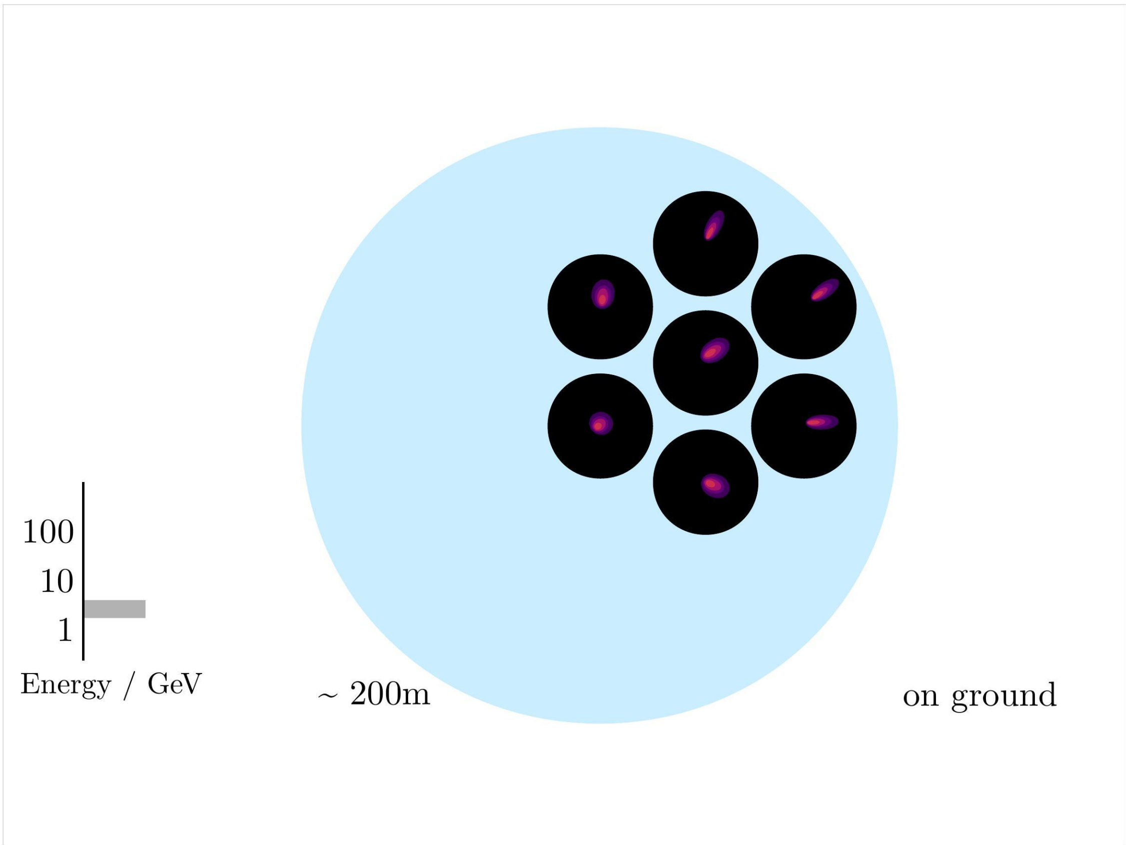

the sum of the images recorded by

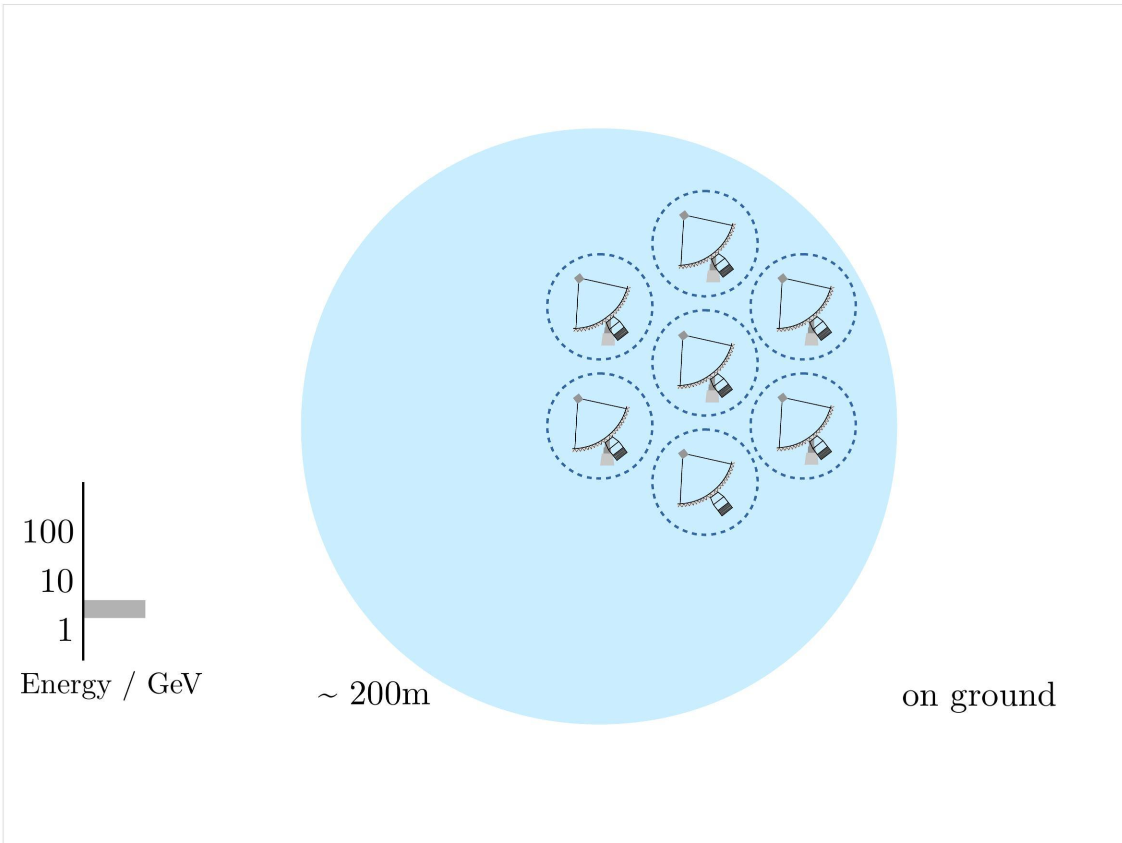

Multiple small telescopes within the large telescope's aperture.

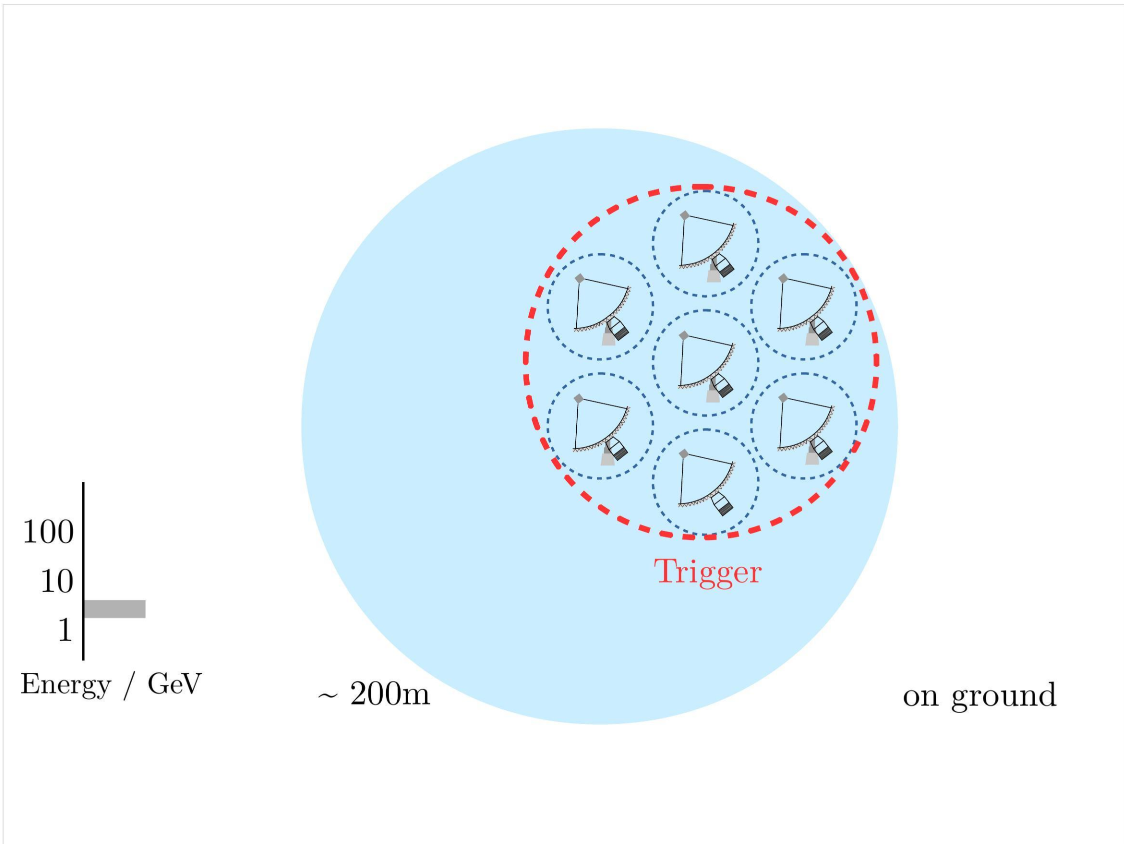

If we had a trigger that had instantaneous access to all these individual telescopes

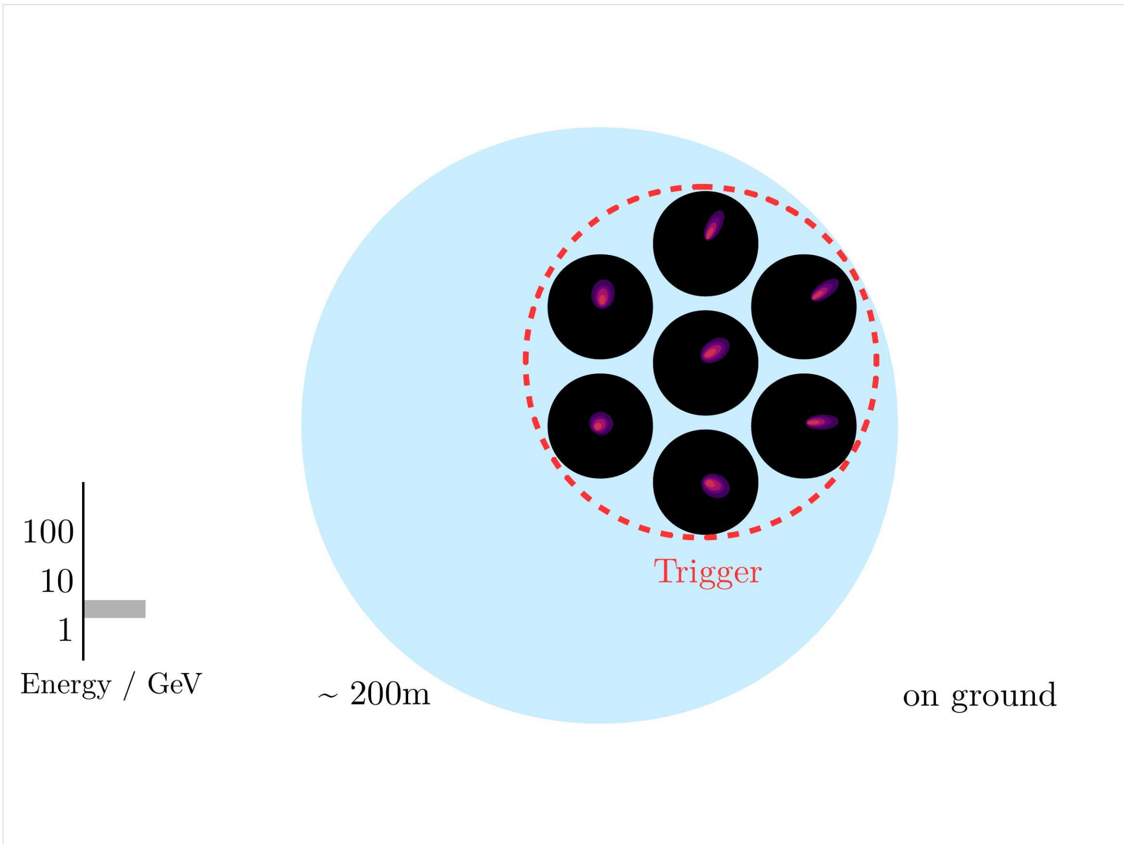

We could record these individual images.

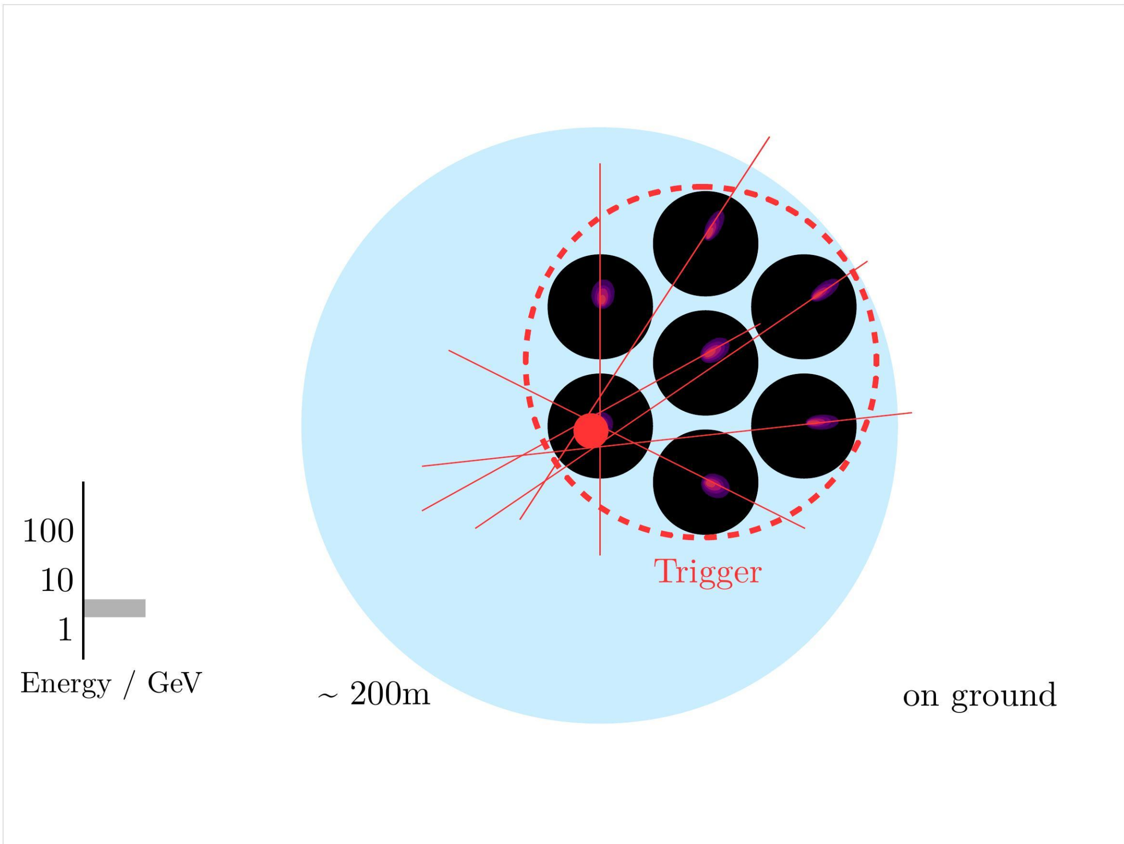

And then reconstruct the cosmic particle's trajectory.

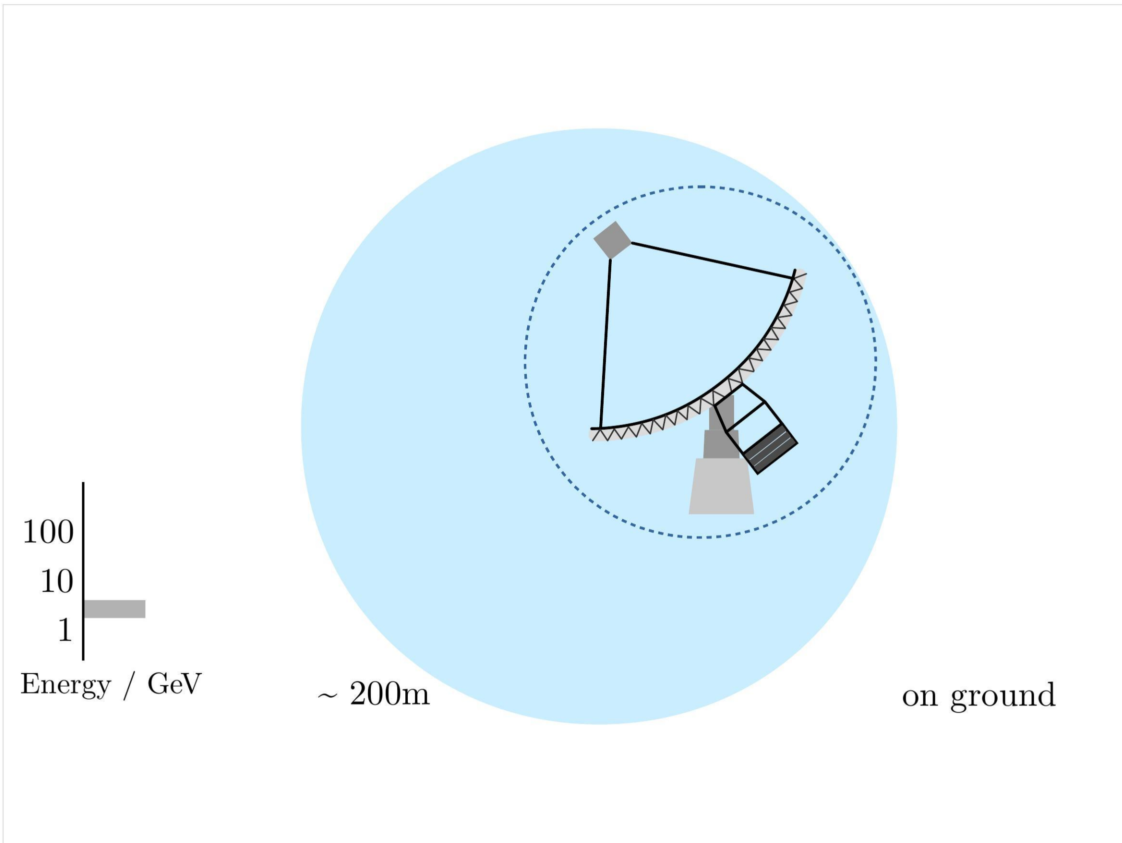

Although a large telescope collects more light, we lose information.

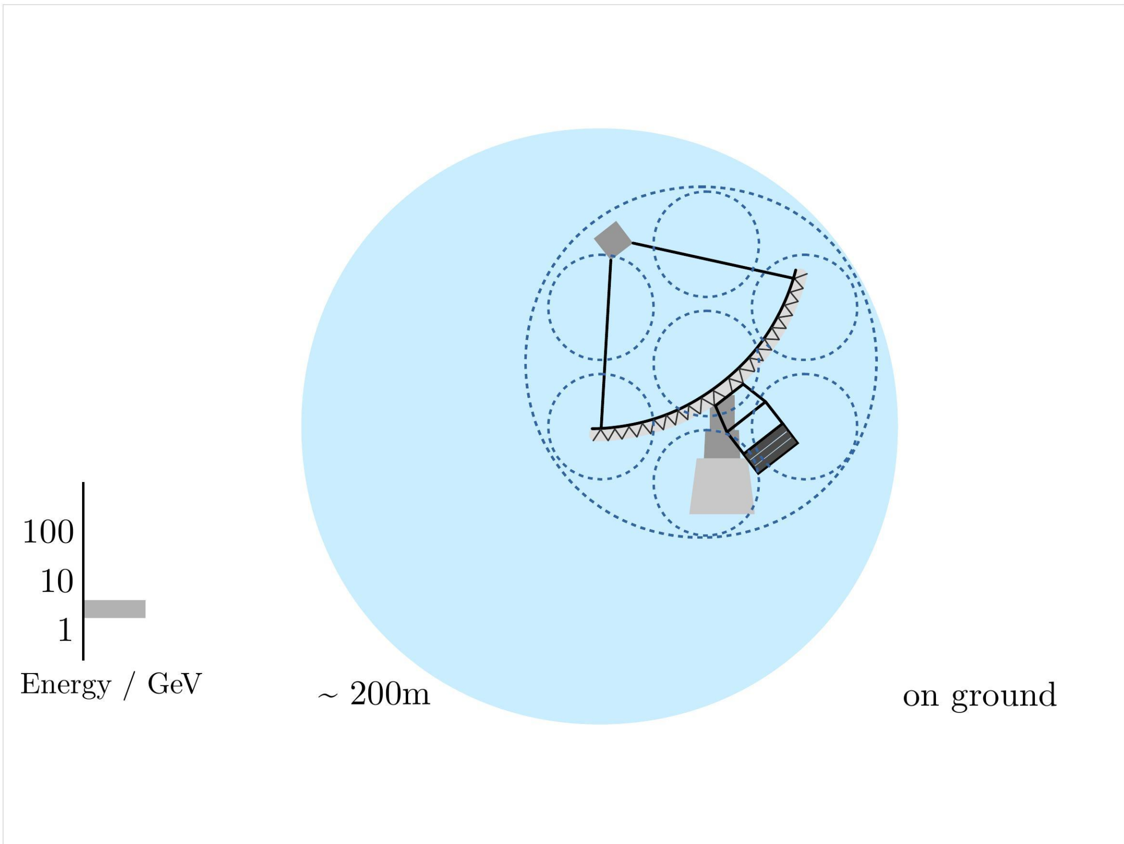

Unfortunately we can not segment the large telescope's aperture

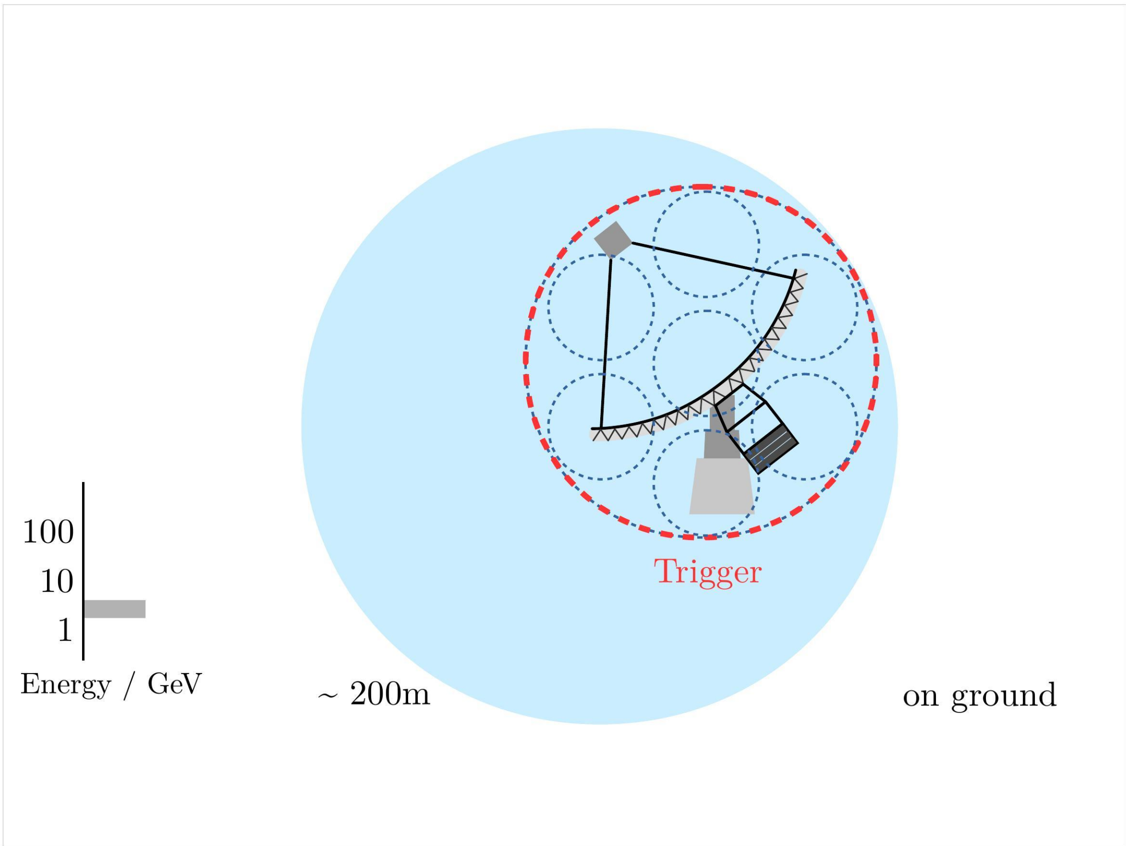

And have both:

A low energy-threshold,

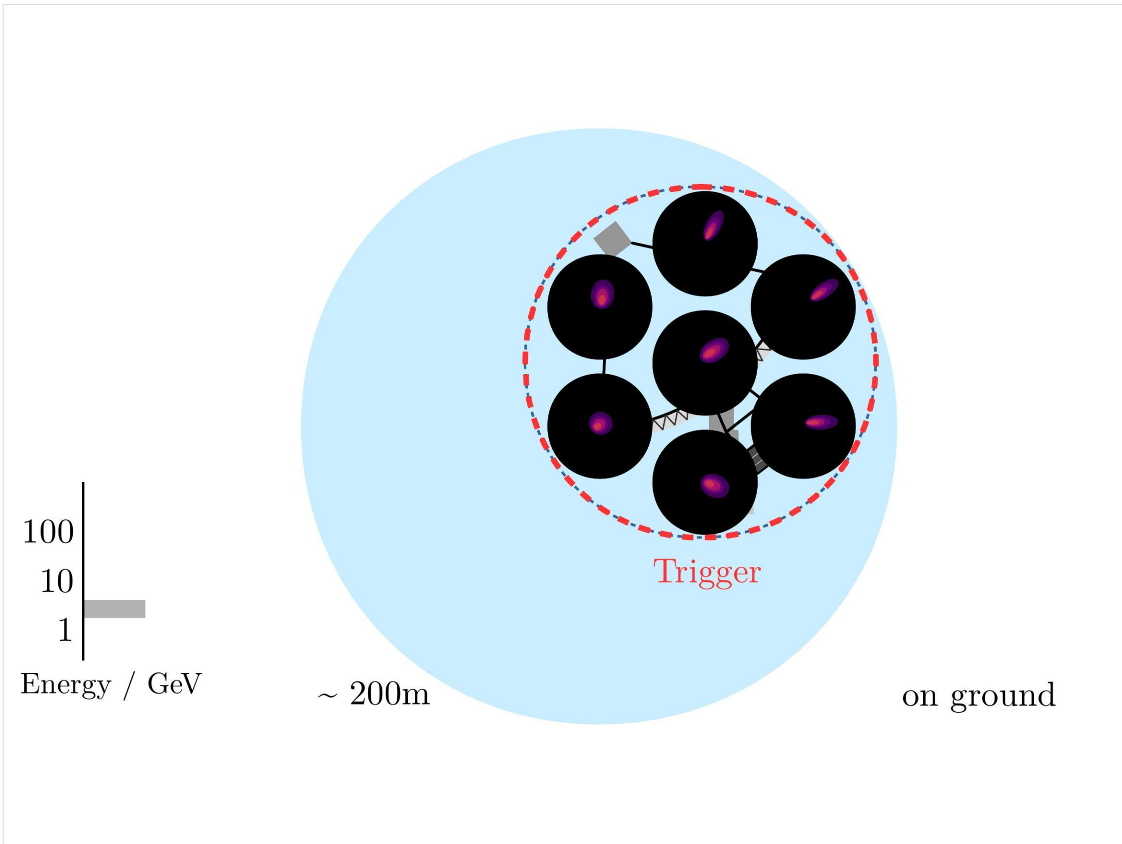

and a high stereo-reconstruction-power.

… Well at least until now…

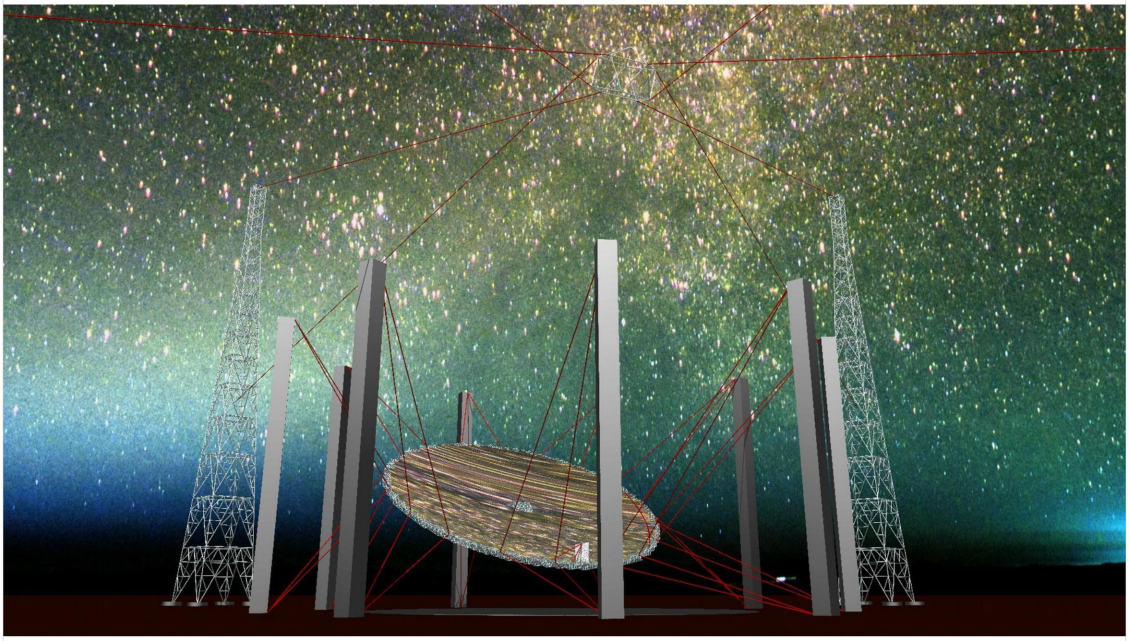

In the race for the lowest possible energy-threshold, Cherenkov-telescopes have become bigger, and now reached their physical limits.

I propose to break with the Cherenkov-telescope, with the far-seeing-instrument, to overcome these physical limits by building an all-seeing-instrument.

My proposed Cherenkov-plenoscope requires much less structural rigidity and turns a narrow depth-of-field into three-dimensional reconstruction-power.

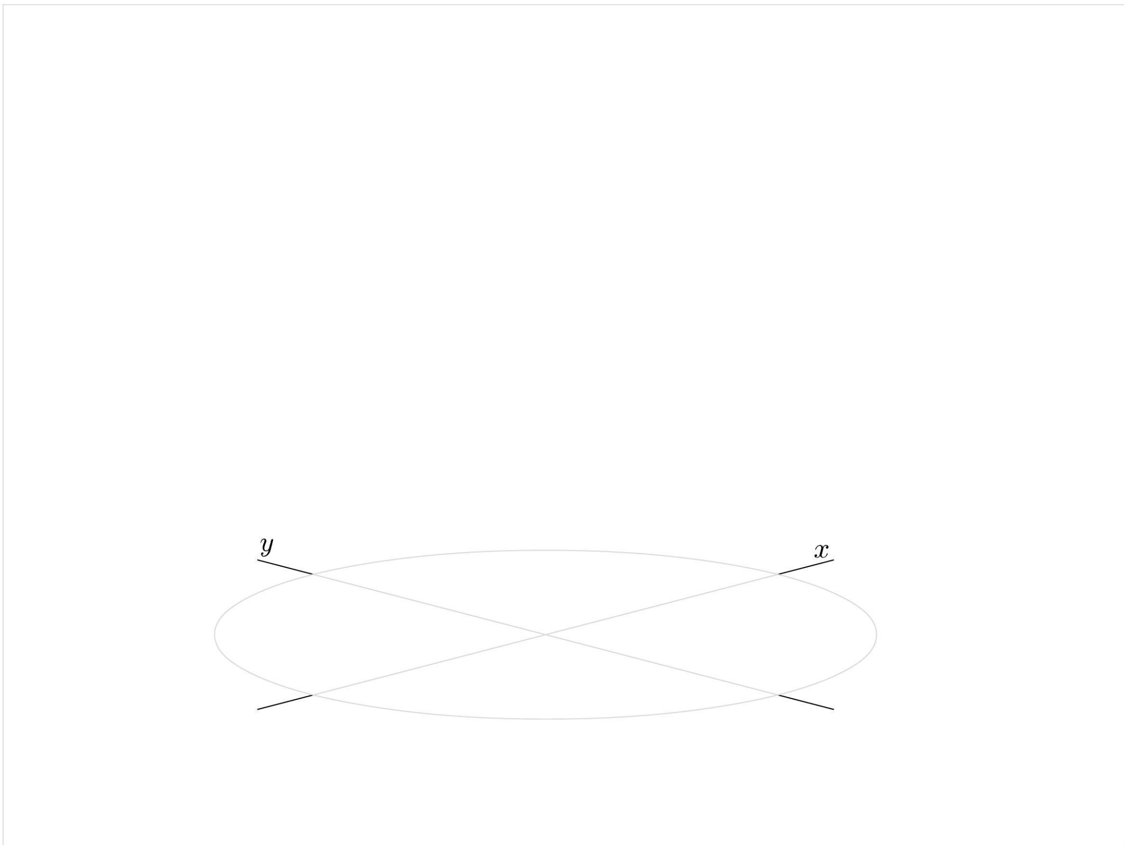

On the aperture-plane

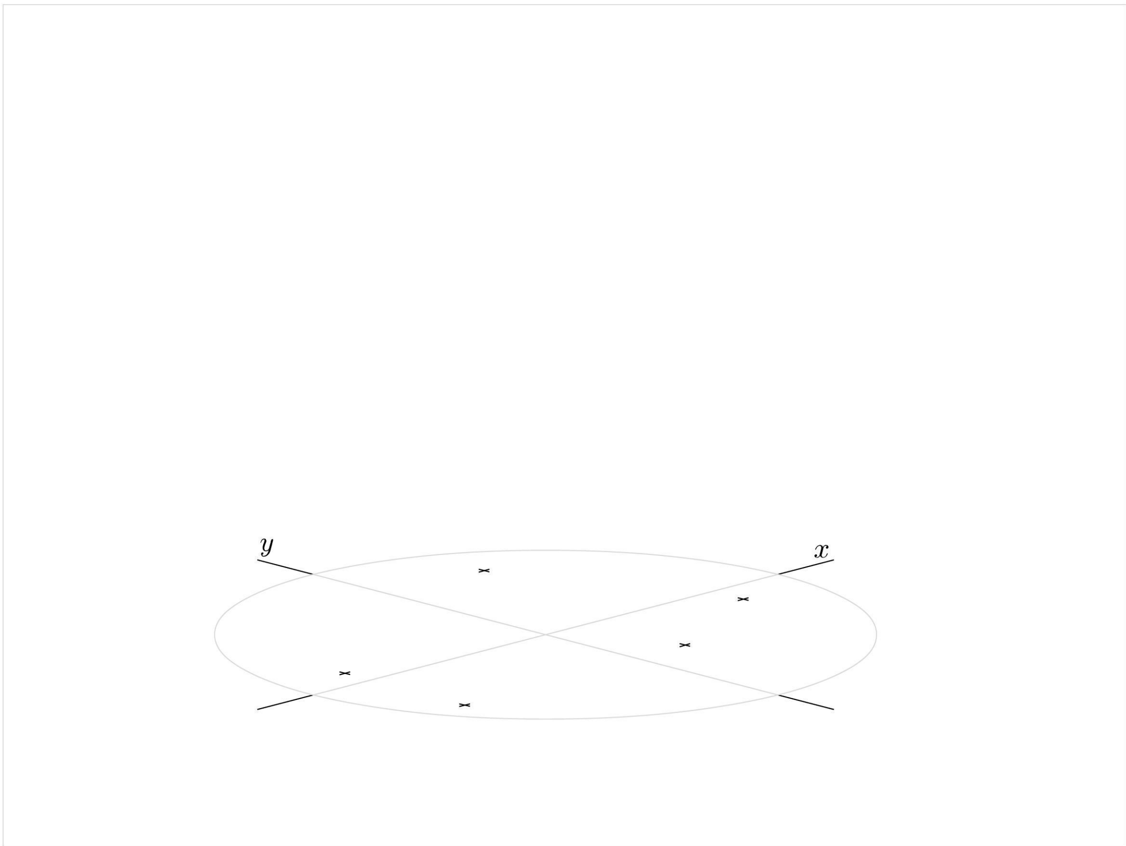

The photons support-positions,

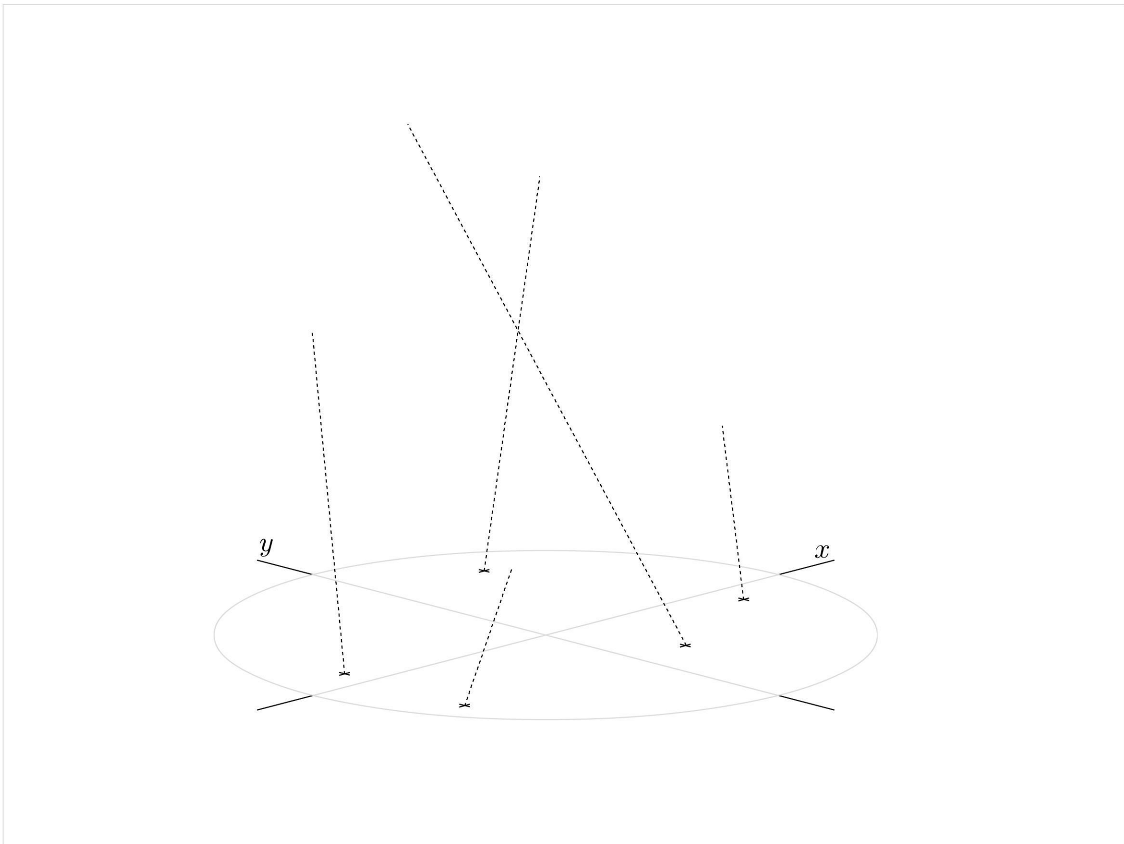

Incident-directions,

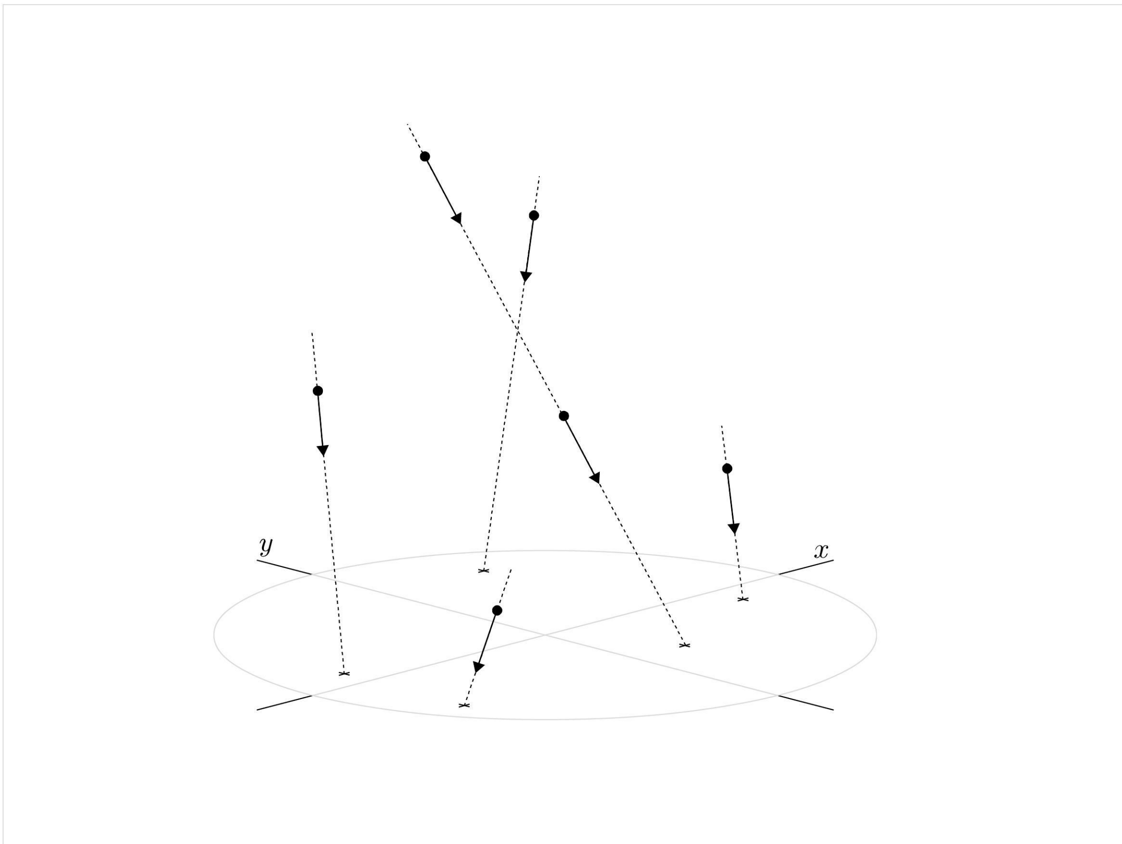

And arrival times, are the five observables accessible to Cherenkov-astronomy.

This is the plenum.

$$[c_x, c_y, \qquad t]$$

The Cherenkov-telescope bins the photons based on their incident-directions in (c_x), and (c_y), and their arrival times (t) into a three dimensional intensity-histogram.

$$[c_x, c_y, \qquad t]$$

Image-sequence

We call this intensity-histogram the image-sequence.

$$[c_x, c_y, x, y, t]$$

Now the Cherenkov-PLENOSCOPE bins the photons based on their incident-directions in (c_x), and (c_y), their support-positions in (x) and (y), and their arrival times (t) into a five dimensional intensity-histogram.

$$[c_x, c_y, x, y, t]$$

Light-field-sequence

We call this intensity-histogram a light-field-sequence.

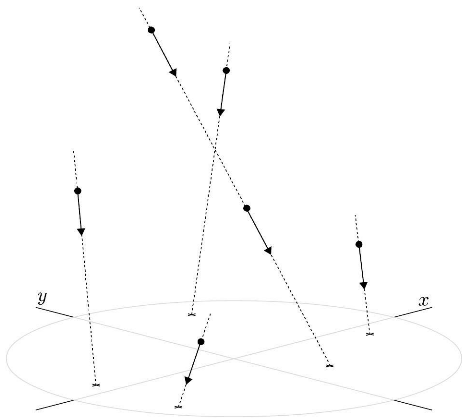

$$[c_x, c_y, x, y, t]$$

Light-field-sequence

Each bin corresponds to a three-dimensional ray supported on the aperture-plane, and pointing up into the night-sky.

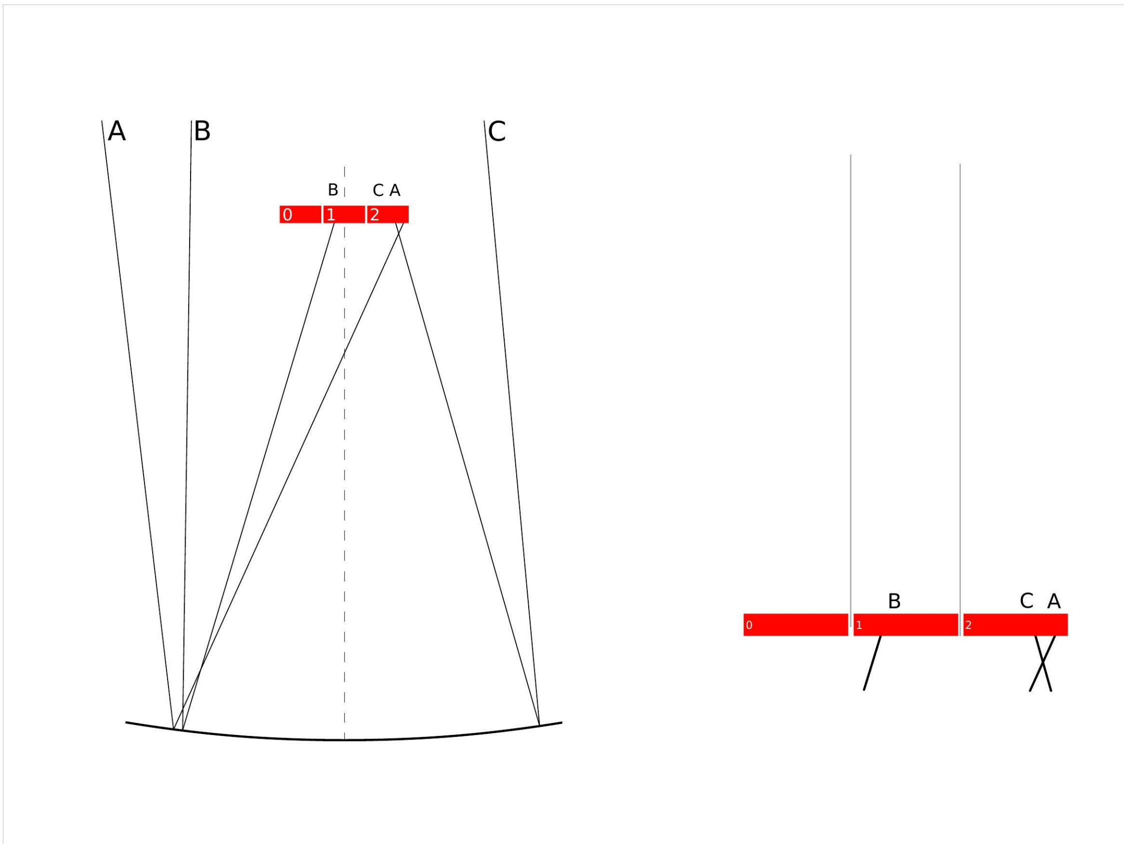

The Cherenkov-telescope and its image-sensor

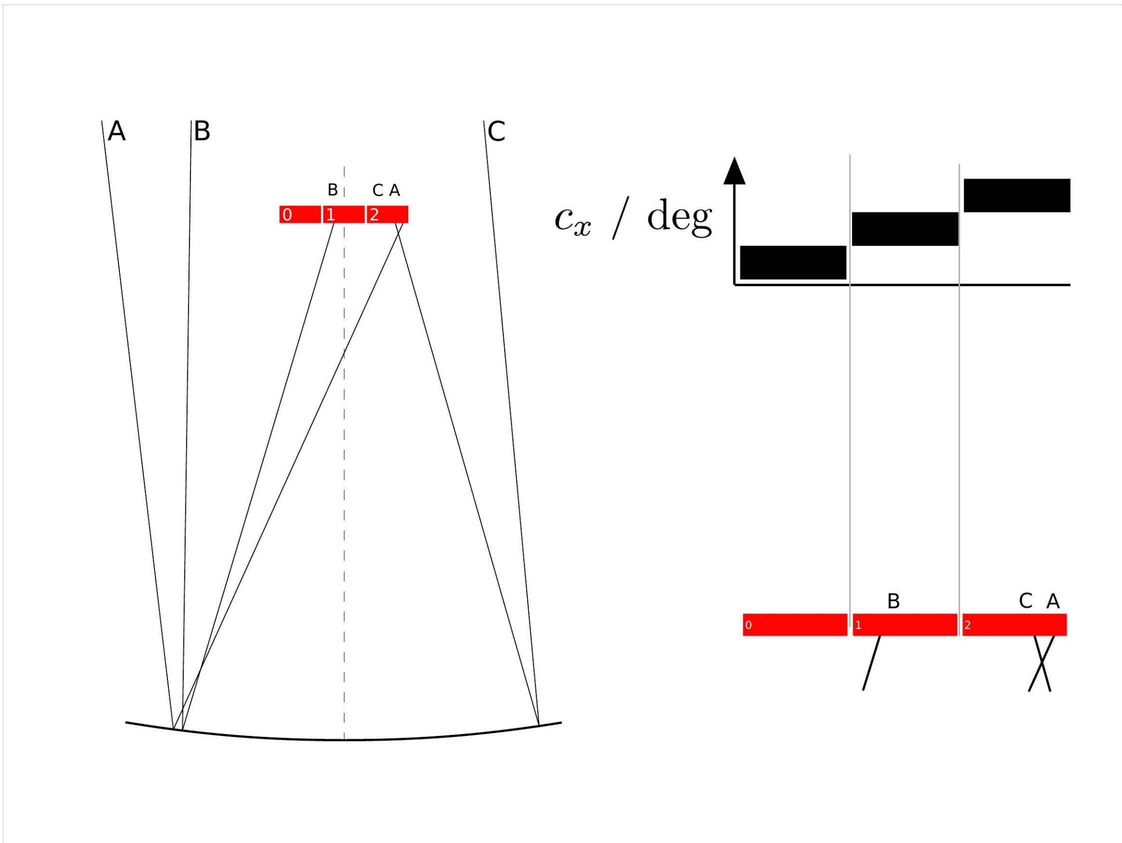

Can distinguish different incident-directions in c_x.

Each photo-sensor samples a different incident-direction.

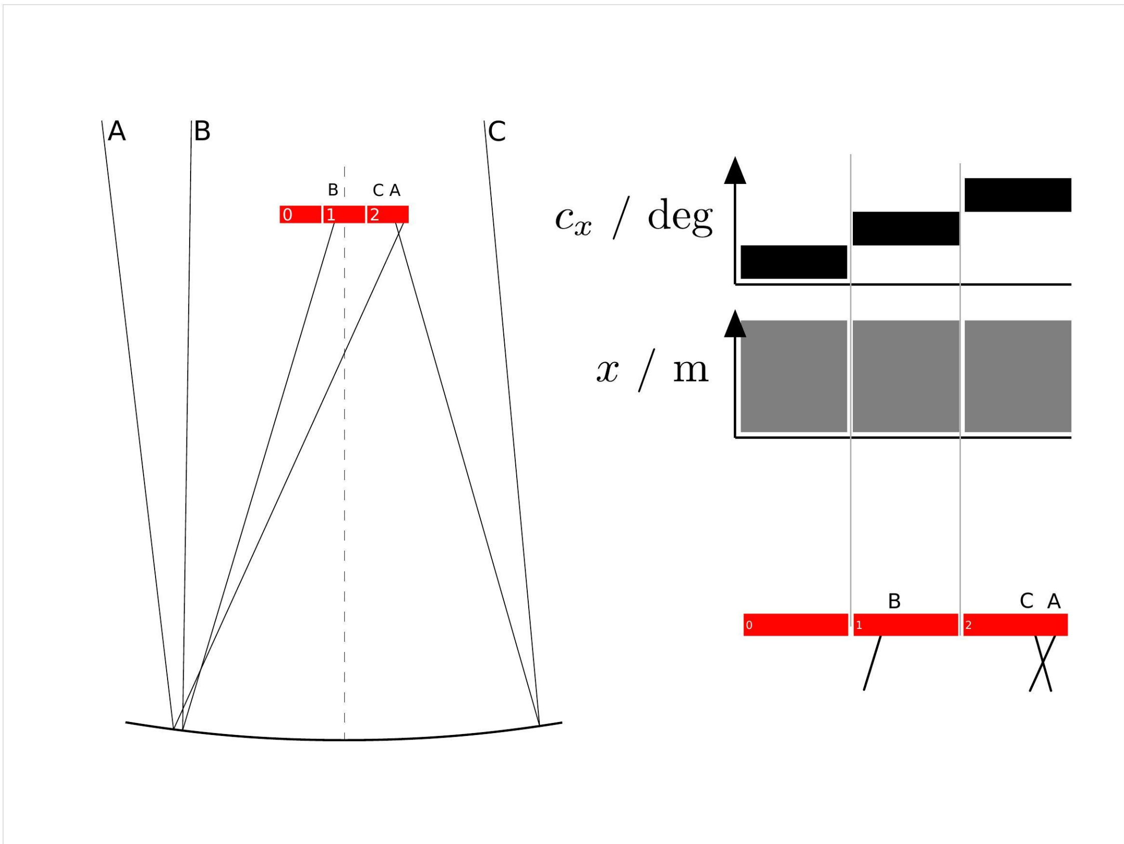

But the image-sensor can not distinguish the different support-position along the telescope’s aperture in (x).

The Cherenkov-telescope can perceive that the photons A, and C have the same incident-directions, but it can not perceive that A and C have different support-positions.

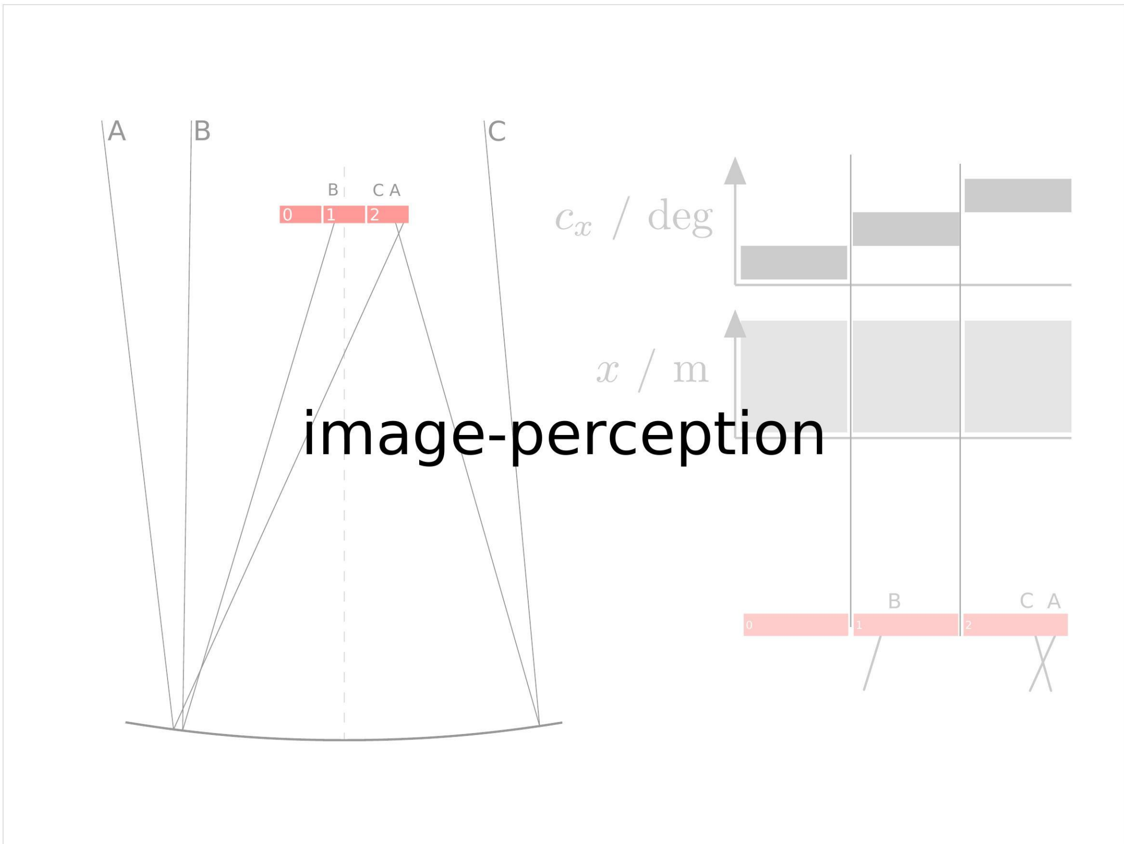

This is image-perception.

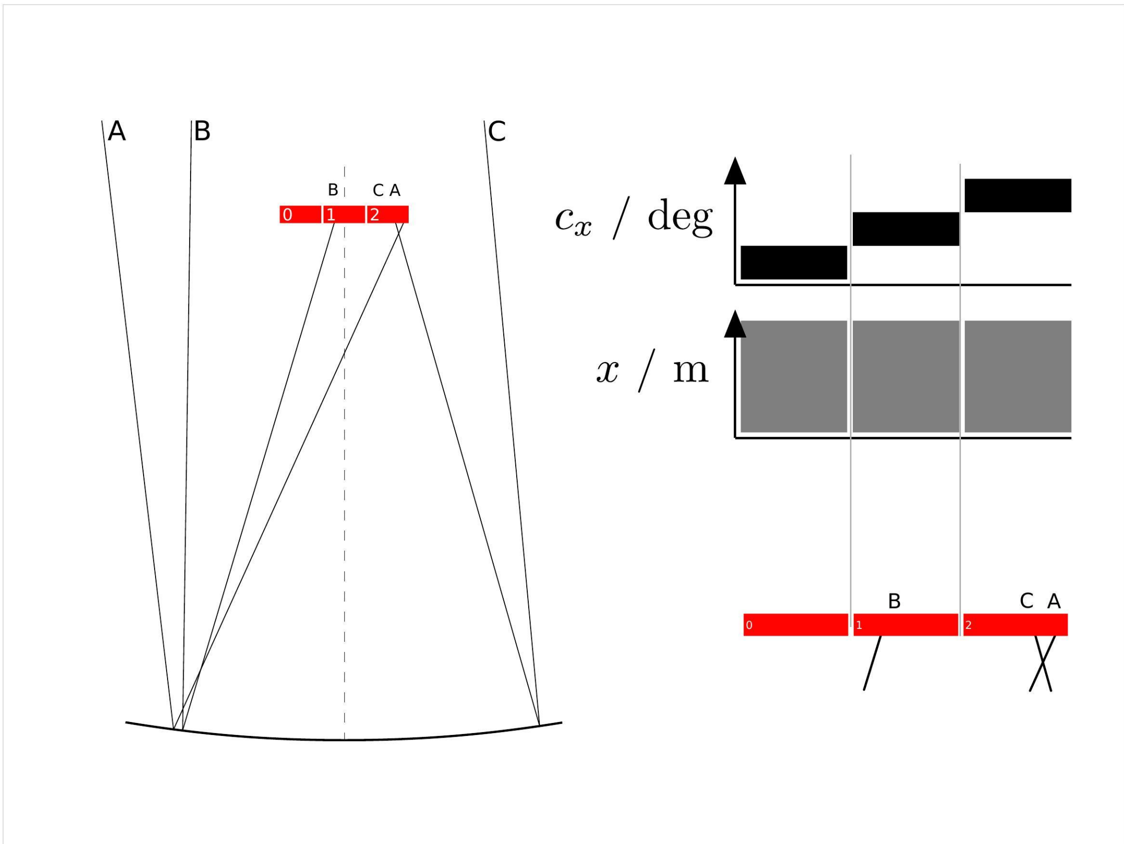

Now, instead of an image-sensor, my Cherenkov-plenoscope has a light-field-sensor, and a light-field-sensor is an array of small cameras.

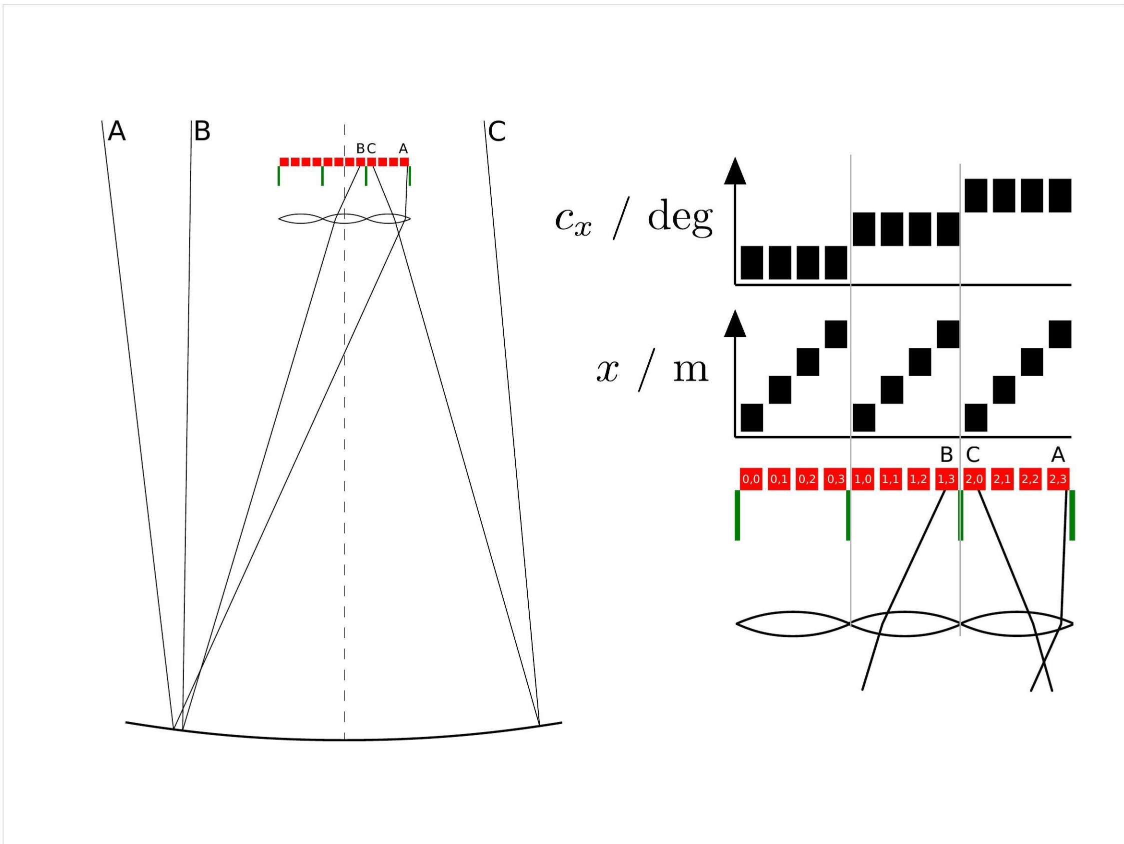

Each small camera is composed from a lens and an array of photo-sensors.

Note the hierarchy among the photo-sensors.

All photo-sensors within a small camera correspond to the same incident-direction.

But each individual photo-sensor within a small camera corresponds to a distinct support-position.

The Cherenkov-plenoscope can perceive all the different incident-directions and support-positions of the photons (A), (B), and (c), using its individual photo-sensors.

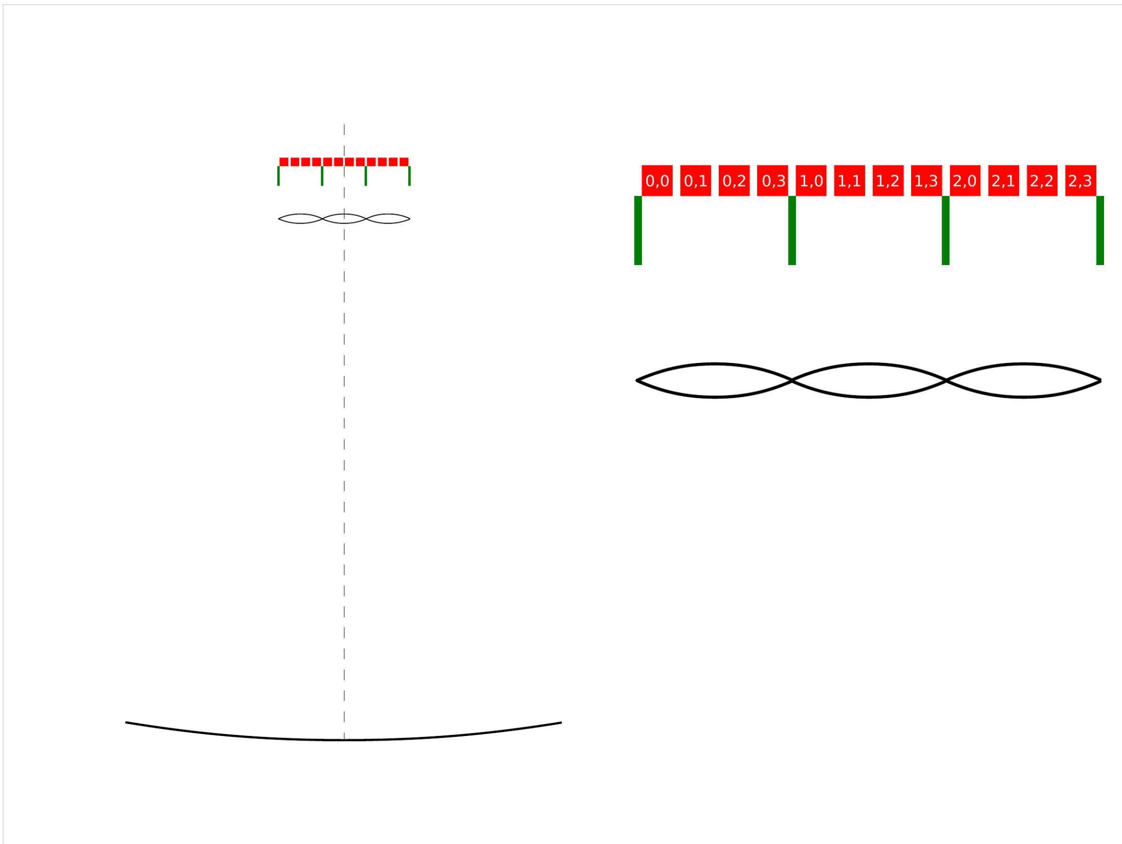
0,0
0,1
0,2
0,3
1,0
1,1
1,2
1,3
2,0
2,1
2,2
2,3

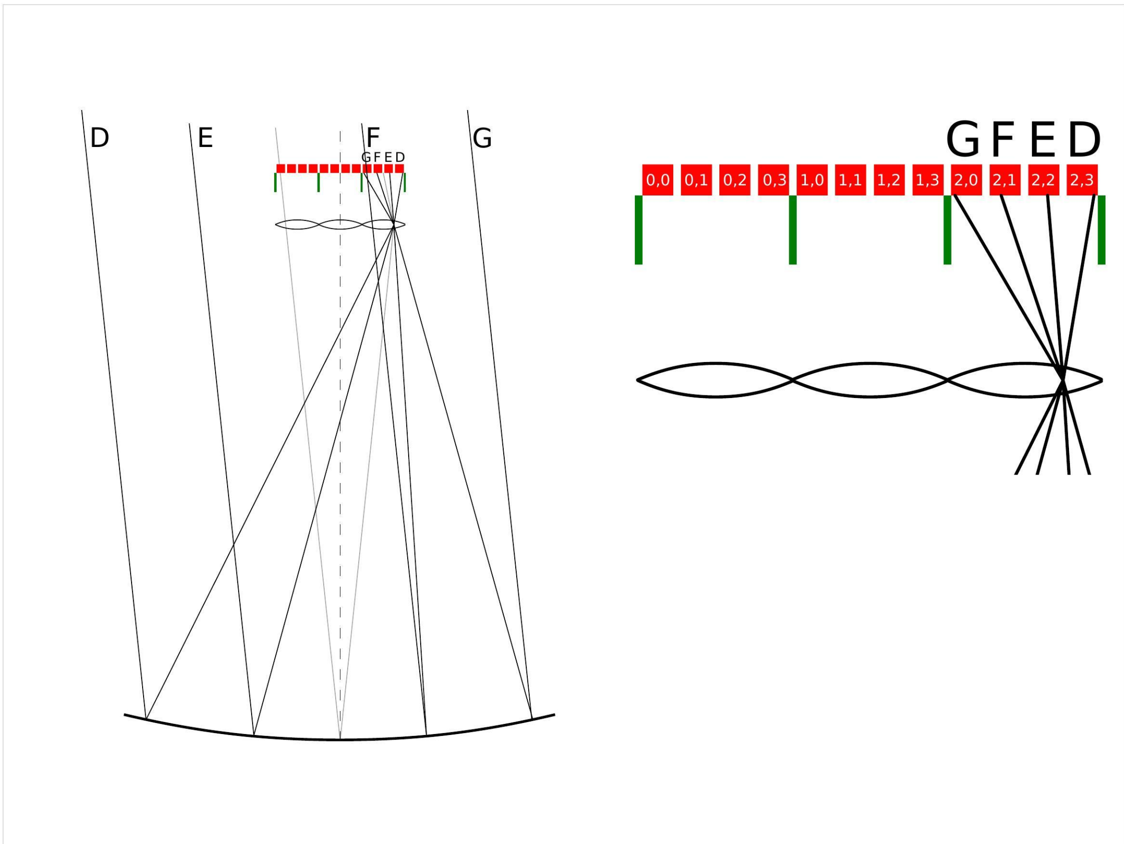

When a photon enters a lens, the Cherenkov-plenoscope perceives the incident-direction of this photon.

And when a photon is absorbed in a photo-sensor, the Cherenkov-plenoscope perceives the support-position of this photon.

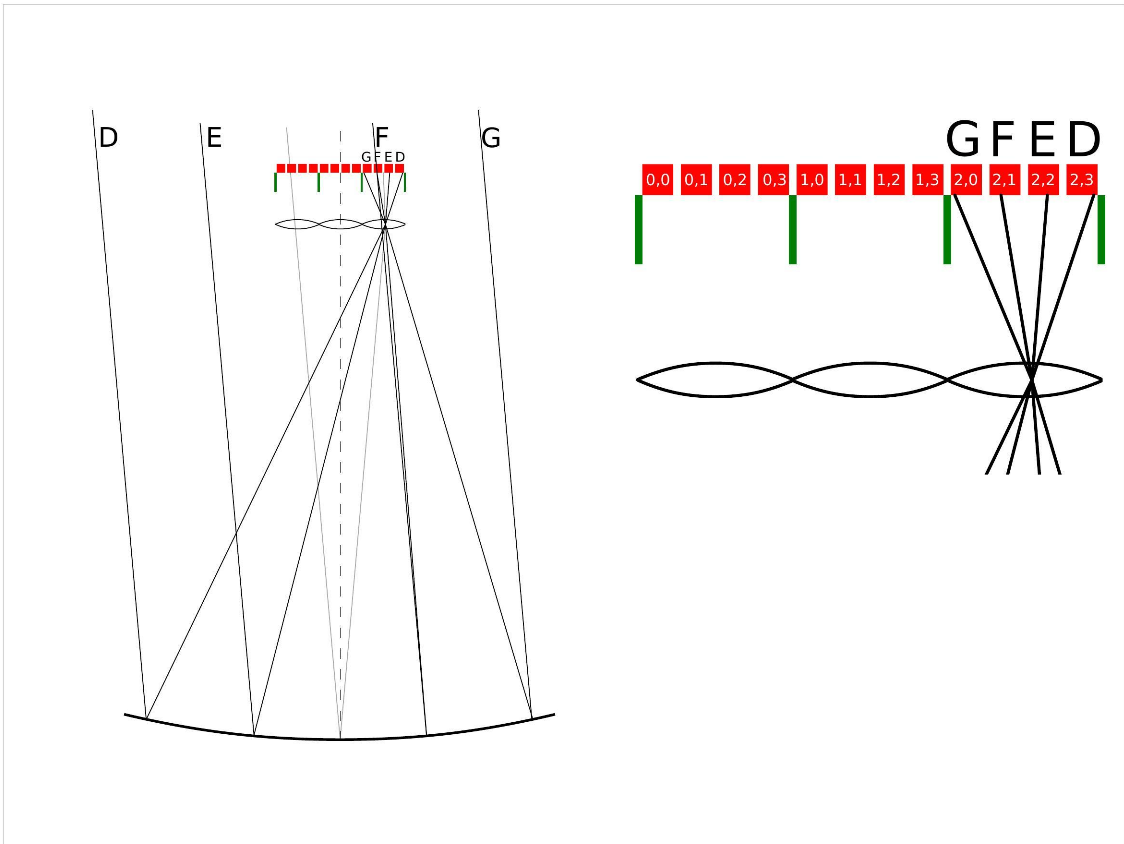

D
E
F
G
G F E D
G F E D
0,0
0,1
0,2
0,3
1,0
1,1
1,2
1,3
2,0
2,1
2,2
2,3

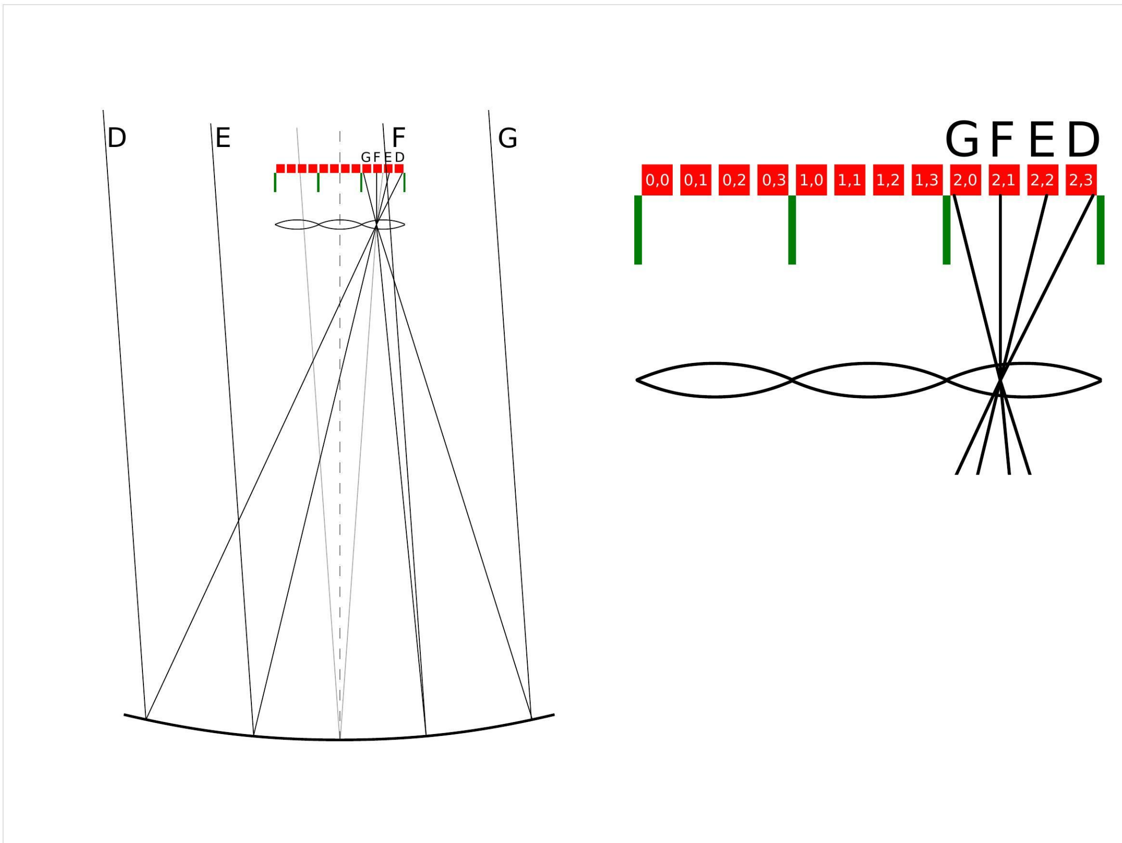
D
E
F
G
G F E D
0,0
0,1
0,2
0,3
1,0
1,1
1,2
1,3
2,0
2,1
2,2
2,3

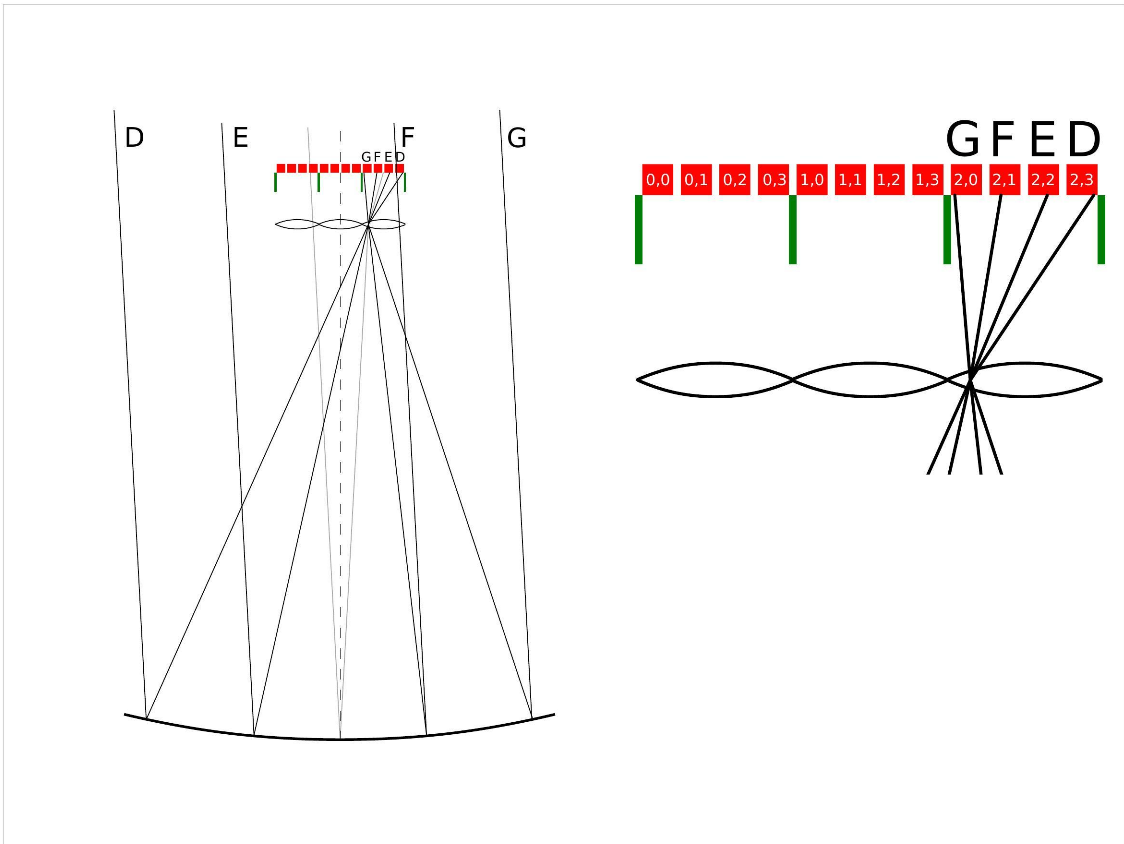
D
E
F
G
G F E D
0,0
0,1
0,2
0,3
1,0
1,1
1,2
1,3
2,0
2,1
2,2
2,3

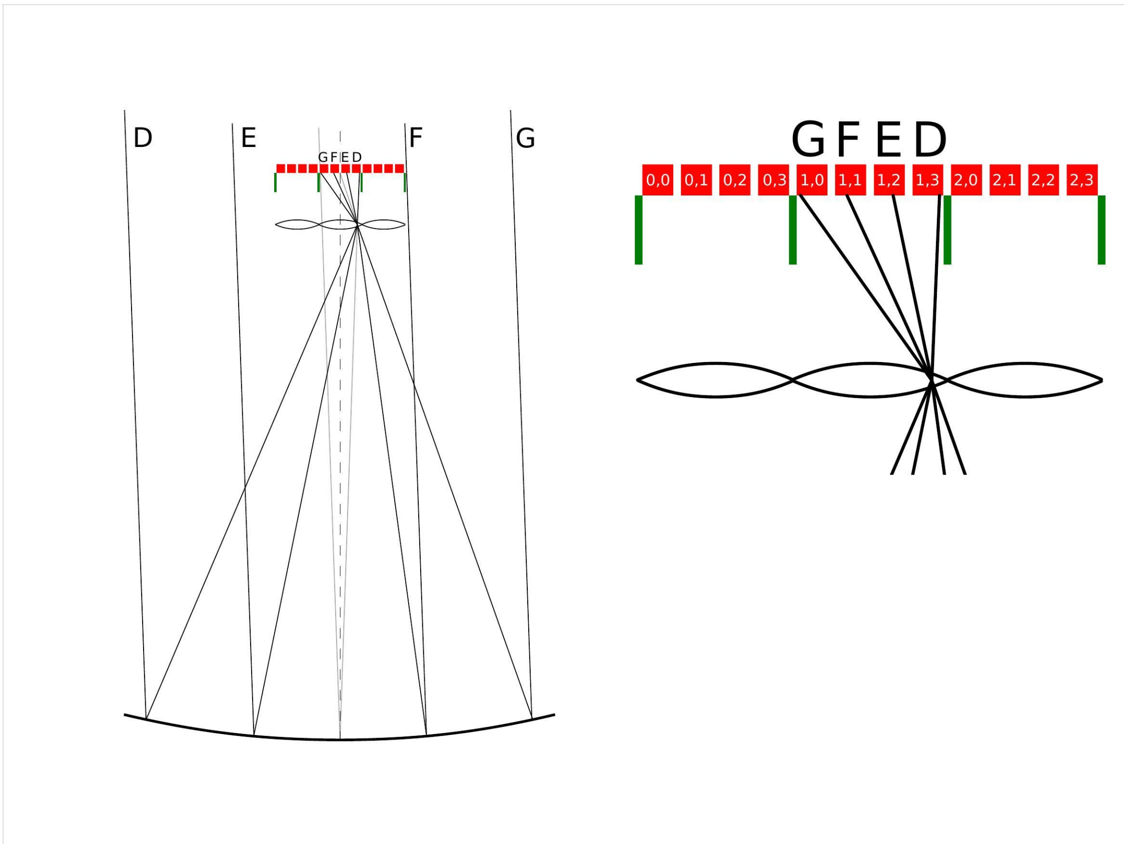

D
E
F
G
G F E D
G F E D
0,0
0,1
0,2
0,3
1,0
1,1
1,2
1,3
2,0
2,1
2,2
2,3

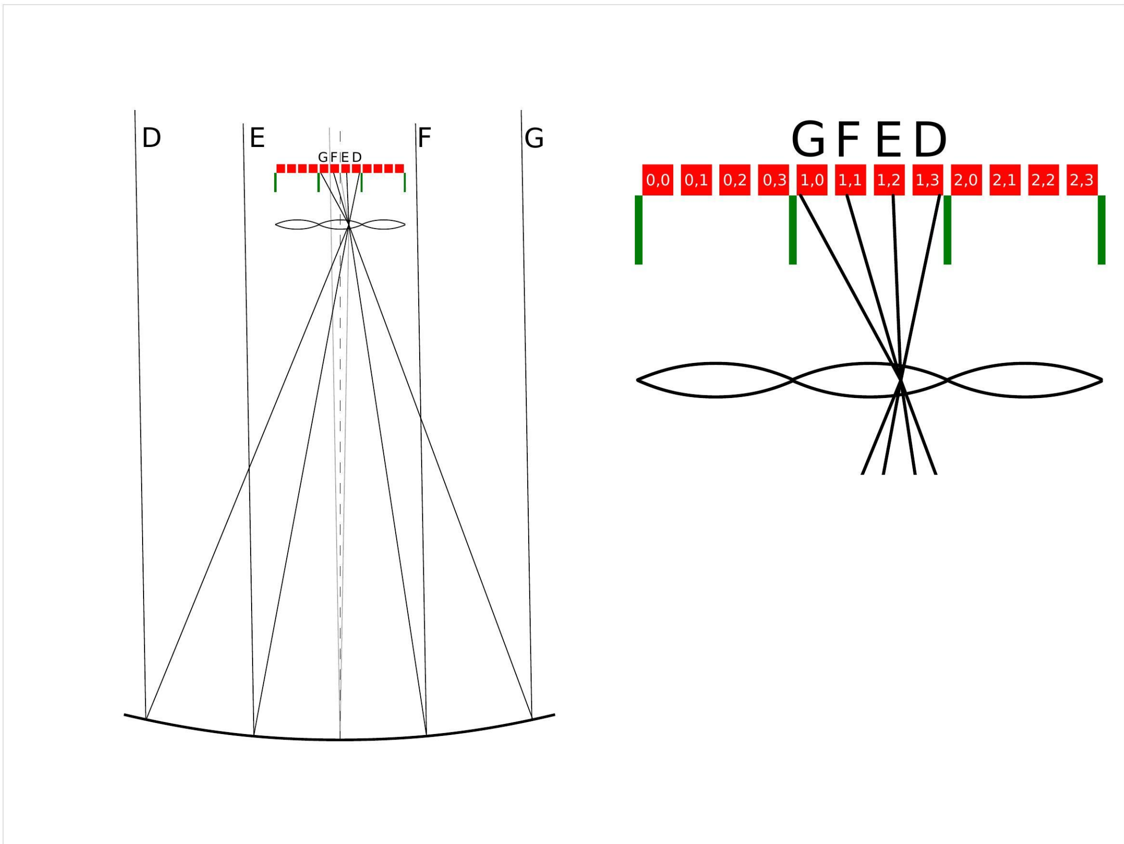

D
E
F
G
G F E D
0,0 0,1 0,2 0,3 1,0 1,1 1,2 1,3 2,0 2,1 2,2 2,3

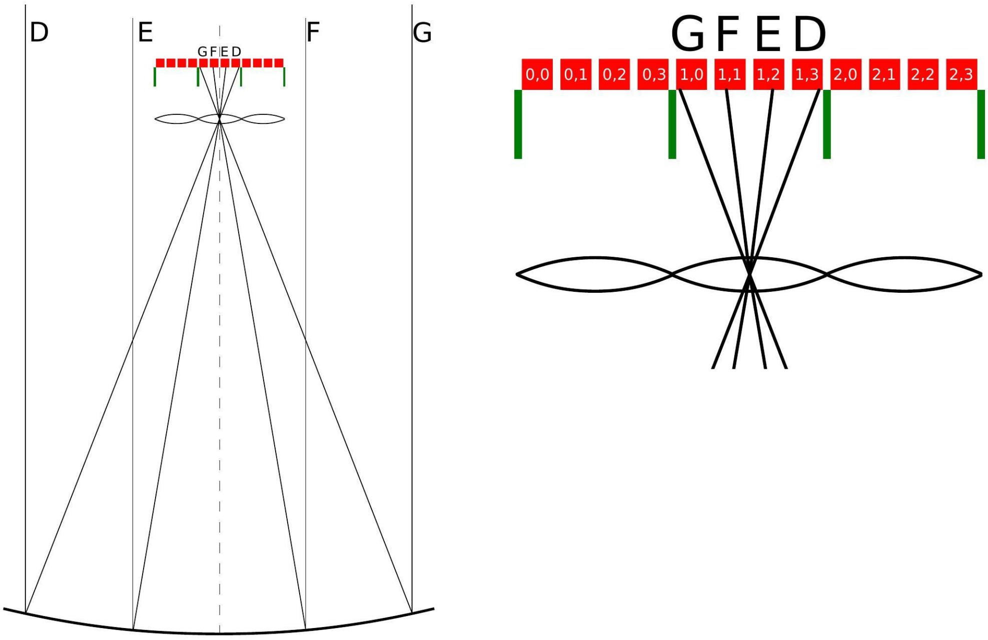

D
E
F
G
G F E D
0,0
0,1
0,2
0,3
1,0
1,1
1,2
1,3
2,0
2,1
2,2
2,3

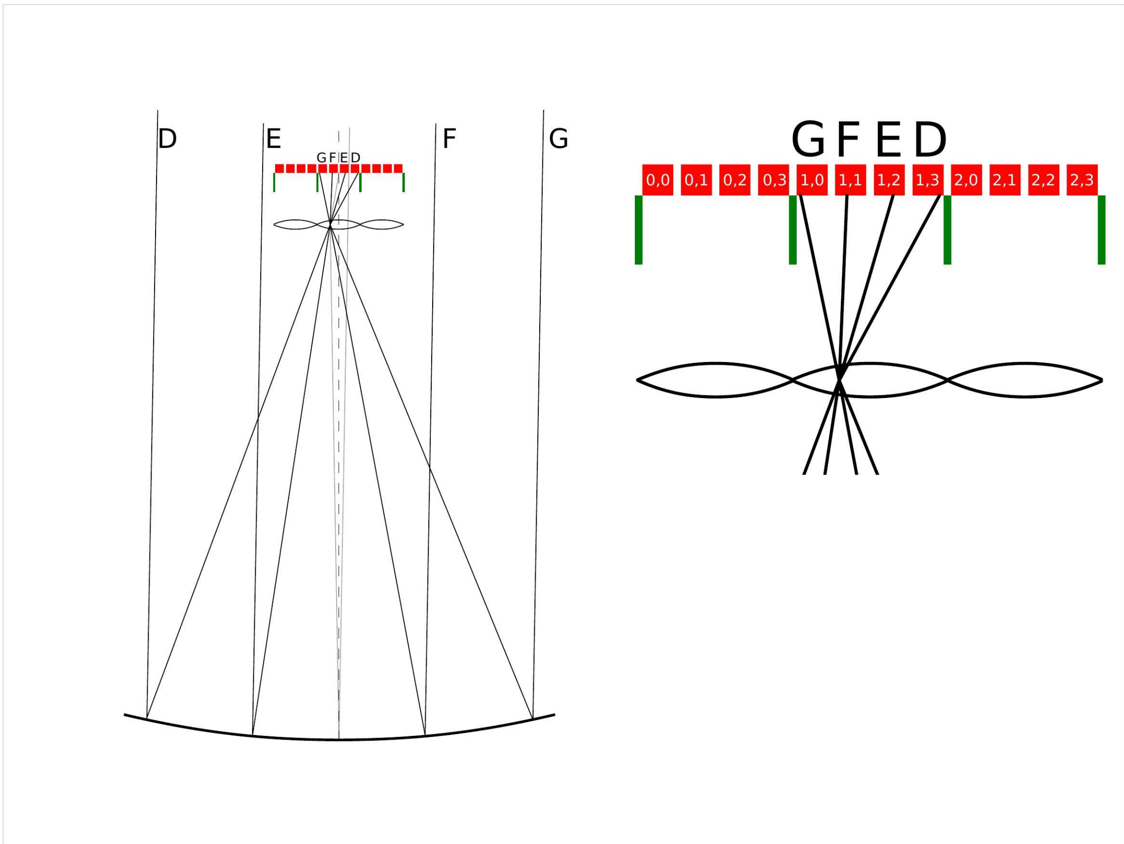
D
E
F
G
GFED
GFED
0,0
0,1
0,2
0,3
1,0
1,1
1,2
1,3
2,0
2,1
2,2
2,3

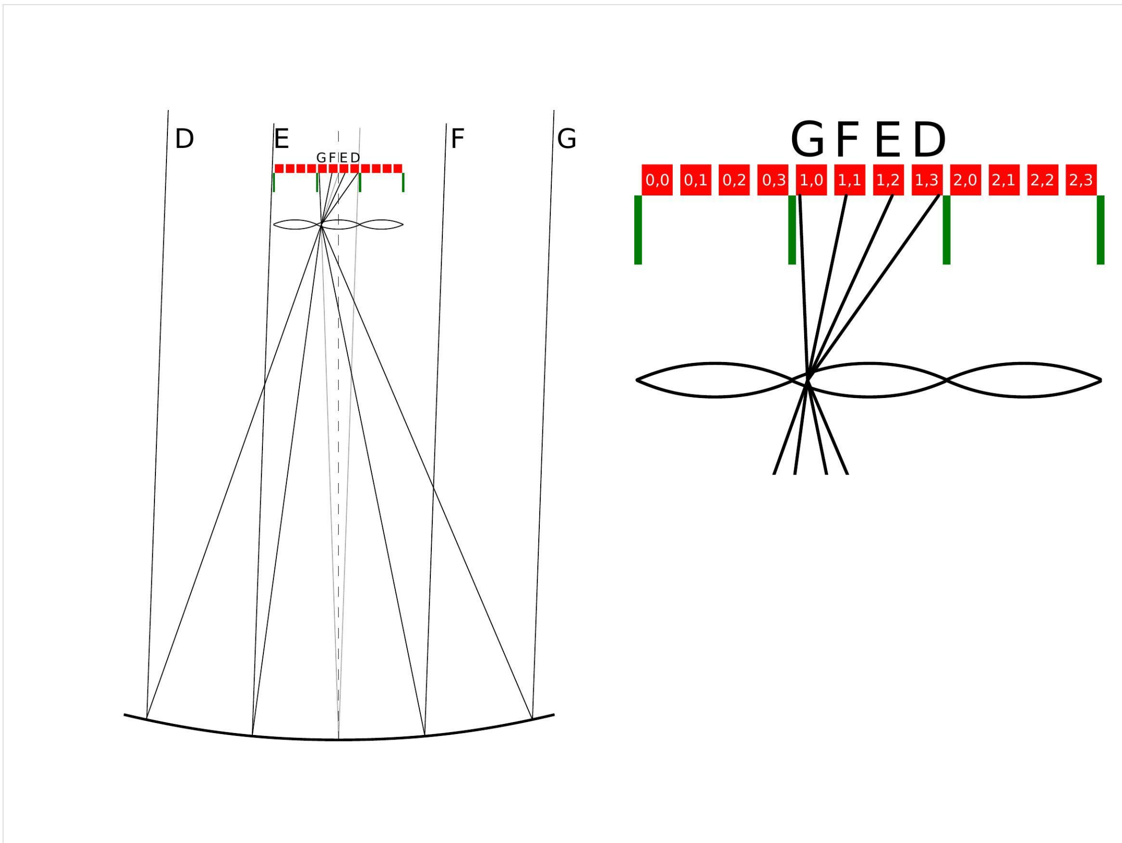

D
E
GFED
F
G
GFED
0,0
0,1
0,2
0,3
1,0
1,1
1,2
1,3
2,0
2,1
2,2
2,3

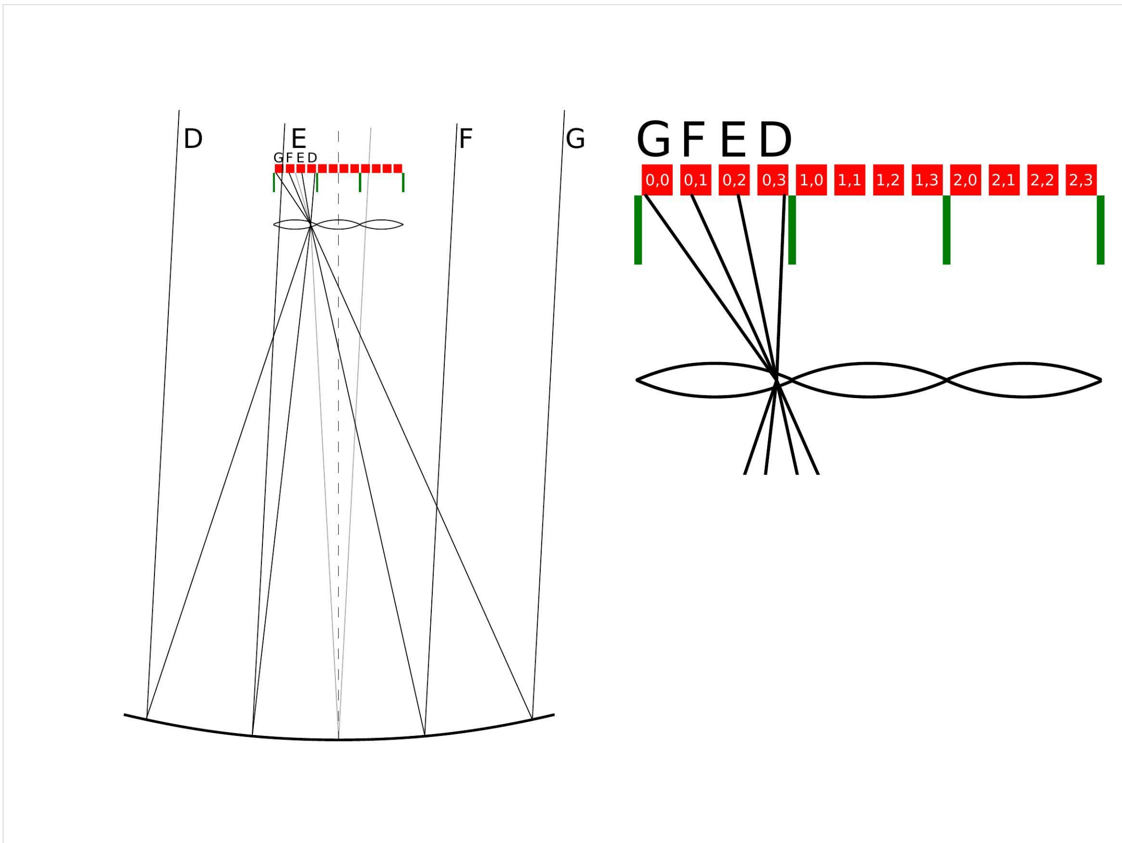
D
E
F
G
G F E D
G F E D
0,0
0,1
0,2
0,3
1,0
1,1
1,2
1,3
2,0
2,1
2,2
2,3

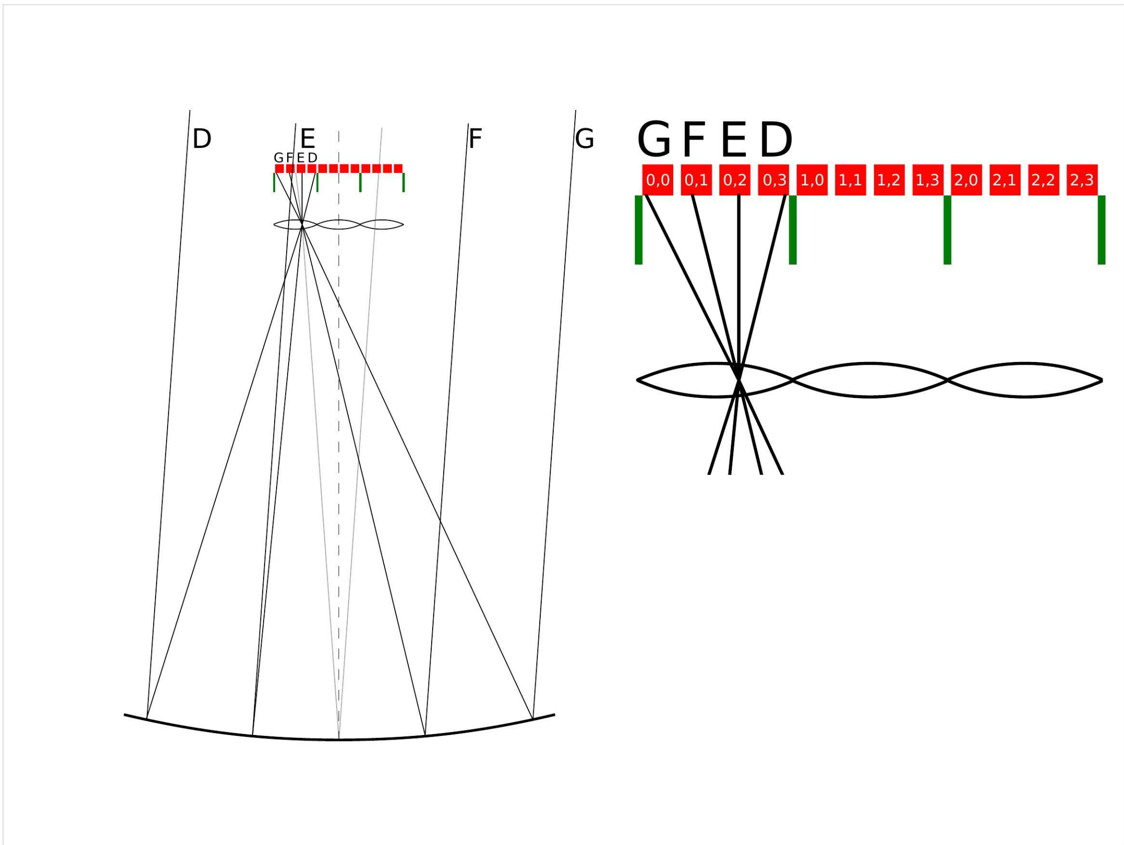

D
E
F
G
GFED
G F E D
0,0
0,1
0,2
0,3
1,0
1,1
1,2
1,3
2,0
2,1
2,2
2,3

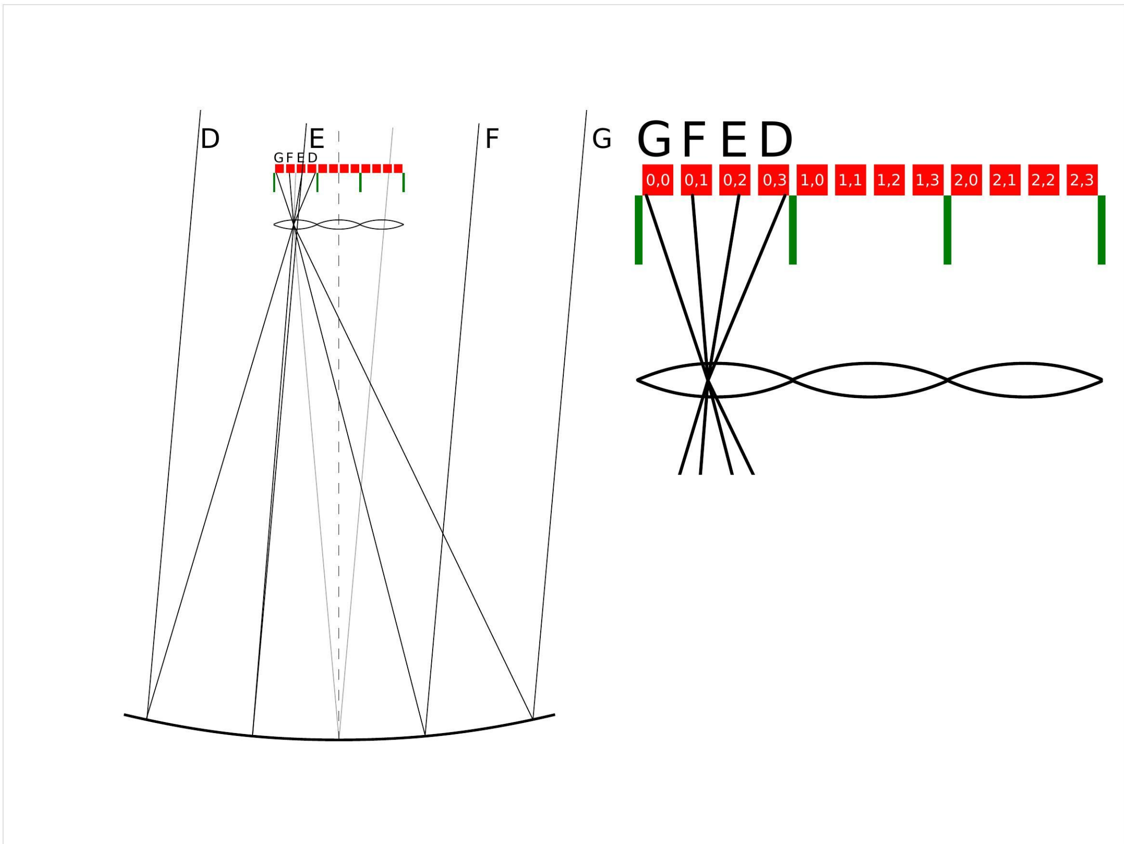

D
E
F
G
GFED
0,0
0,1
0,2
0,3
1,0
1,1
1,2
1,3
2,0
2,1
2,2
2,3

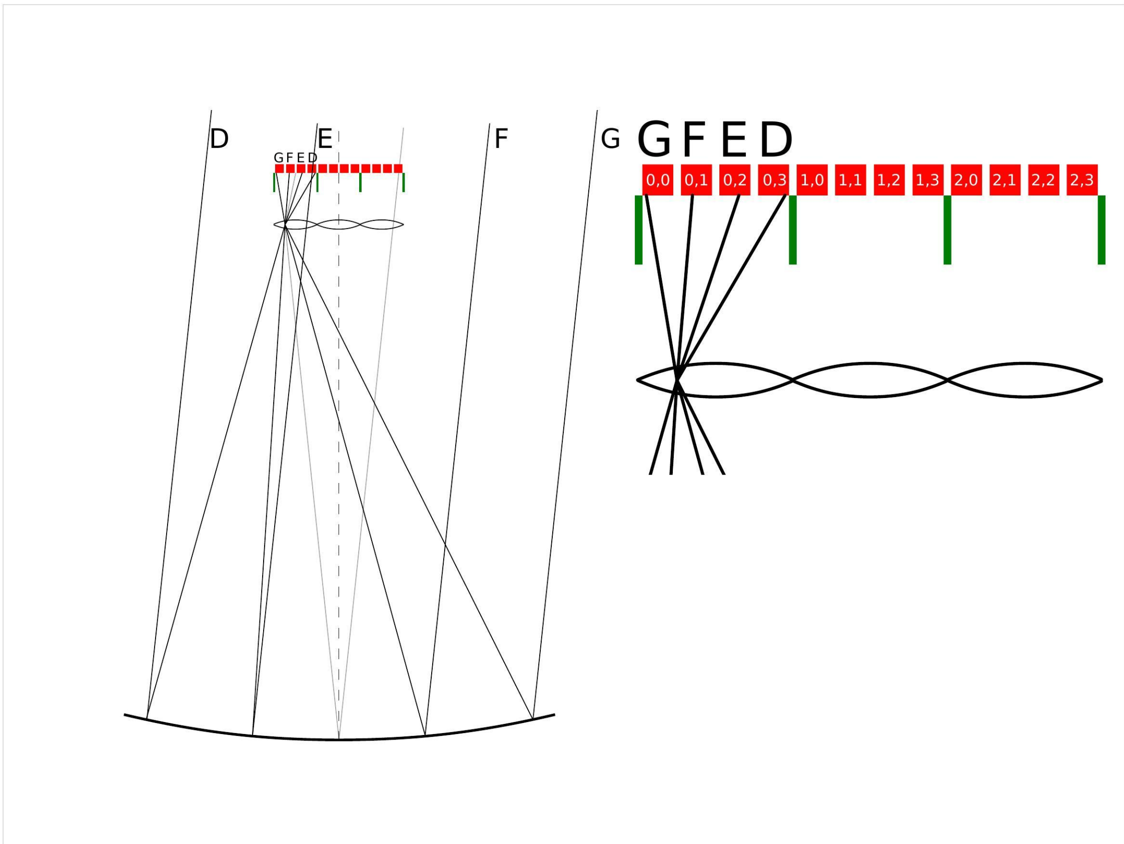

D
E
F
G
G F E D
G F E D
0,0
0,1
0,2
0,3
1,0
1,1
1,2
1,3
2,0
2,1
2,2
2,3

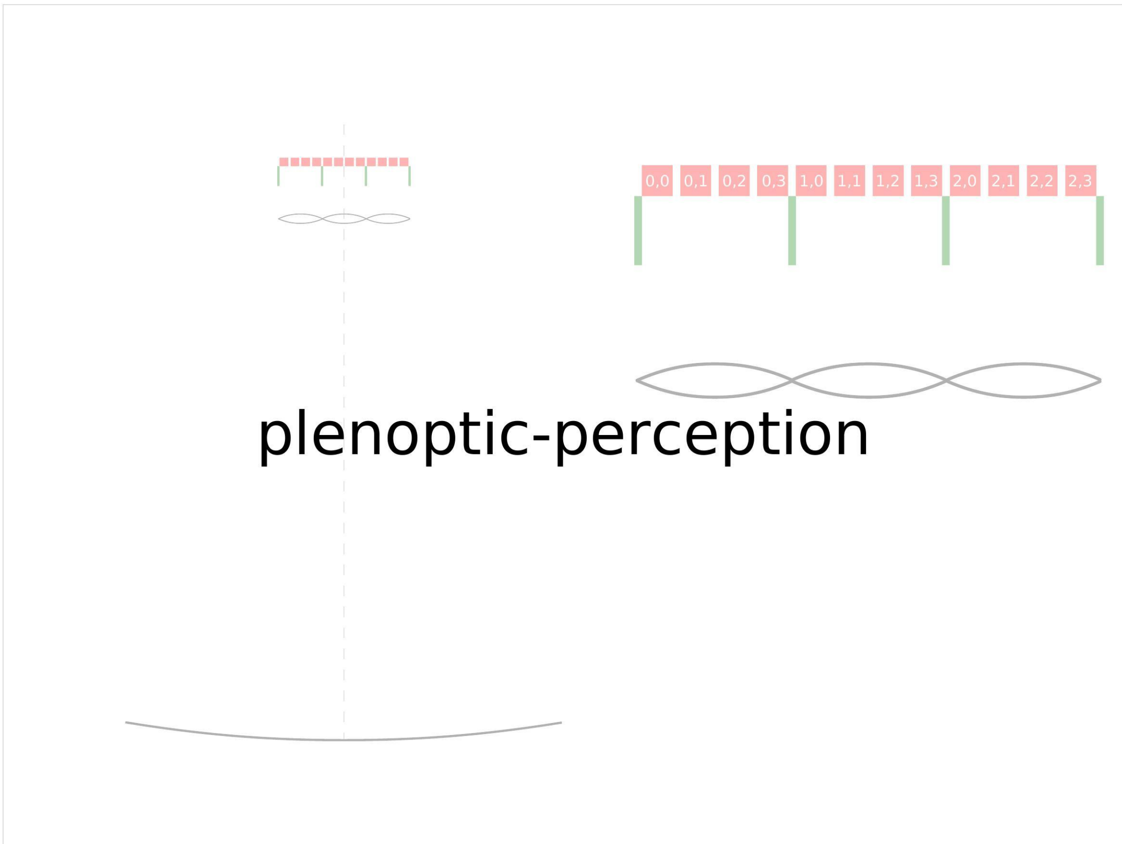

This is plenoptic-perception.

ÉPREUVES RÉVERSIBLES DONNANT LA SENSATION DU RELIEF;

Par M. G. LIPPMANN (1).

1. La plus parfaite des épreuves photographiques actuelles ne montre que l'un des aspects de la réalité ; elle se réduit à une image unique fixée dans un plan, comme le serait un dessin ou une peinture tracée à la main. La vue directe de la réalité offre, on le sait, infiniment plus de variété. On voit les objets dans l'espace, en vraie grandeur et en relief, et non dans un plan. De plus leur aspect change avec les positions de l'observateur ; les différents plans de la vue se déplacent alors les uns par rapport aux autres ; la perspective

G. LIPPMANN, J. PHYS. THEOR. APPL. 7 821-825, 1908

In nineteen o eight, the French physicist G. Lippmann was bored by paintings and images.

He wanted to have a window to look through.

donc un large faisceau qui converge vers A (voir *fig.* 1) : c'est un faisceau large, puisqu'il a pour base toute la plaque sensible, ou du moins toute la partie de cette plaque d'où le point A était visible (1).

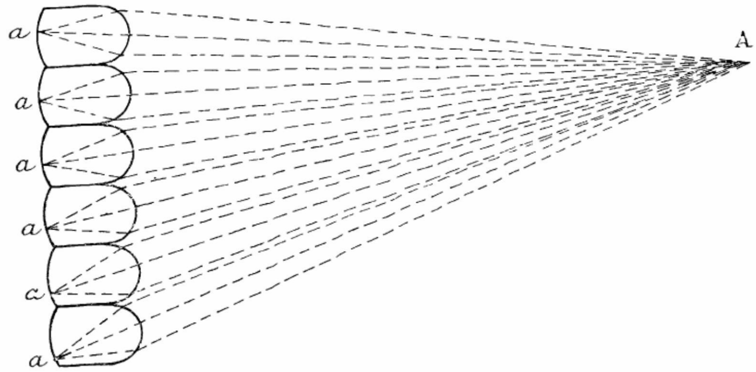

G. LIPPMANN, J. PHYS. THEOR. APPL. 7 821-825, 1908

FIG. 1.

In his publication he illustrated how this might be implemented with an array of lenses.

Light Field Photography with a Hand-held Plenoptic Camera

Ren Ng* Marc Levoy* Mathieu Brédif* Gene Duval† Mark Horowitz* Pat Hanrahan*
*Stanford University †Duval Design

(2005). Stanford Computer Science Technical Report CSTR, 2(11).

And then it took almost one hundred years until clever students in Stanford build the first hand-held plenoptic camera.

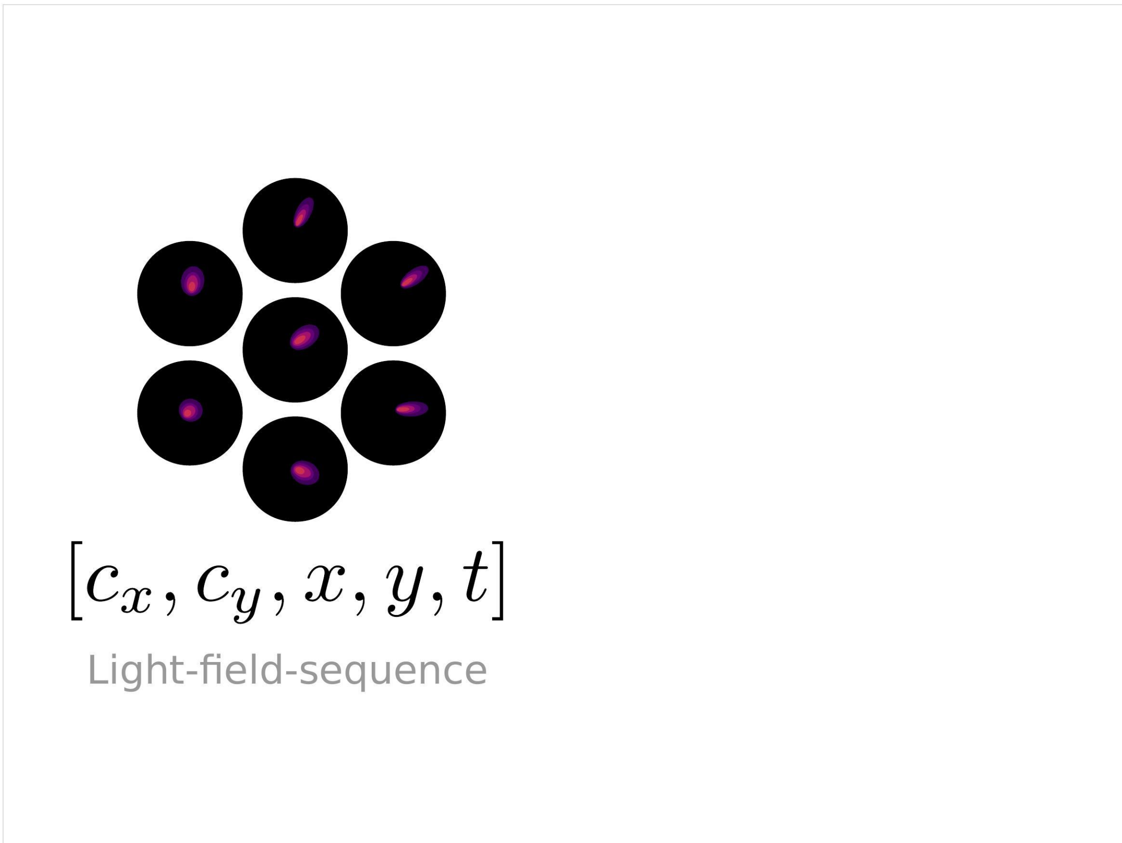

In general, the light-field-sequence recorded by a plenoscope is equivalent to

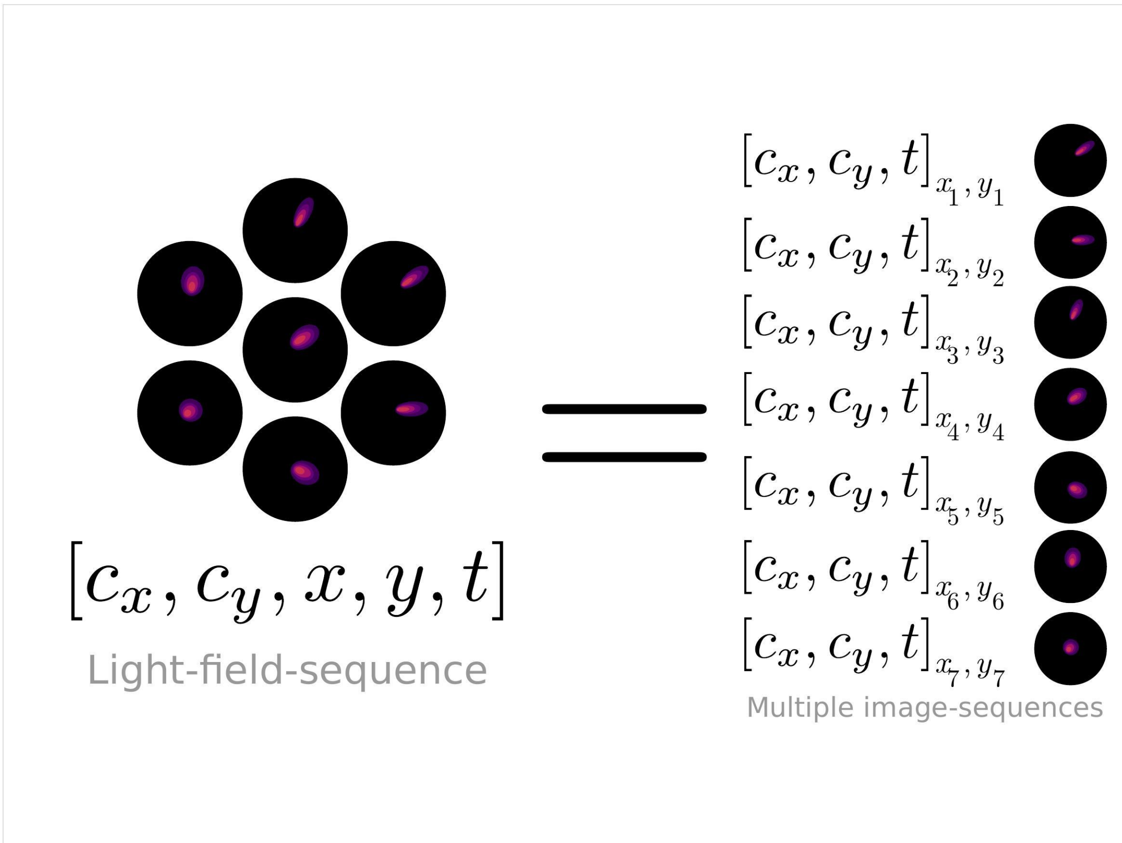

the image-sequences recorded by an array of telescopes located at the different support-positions (x) and (y).

However, in the particular case of Cherenkov-astronomy, the Cherenkov-plenoscope has one crucial advantage over the array of Cherenkov-telescopes:

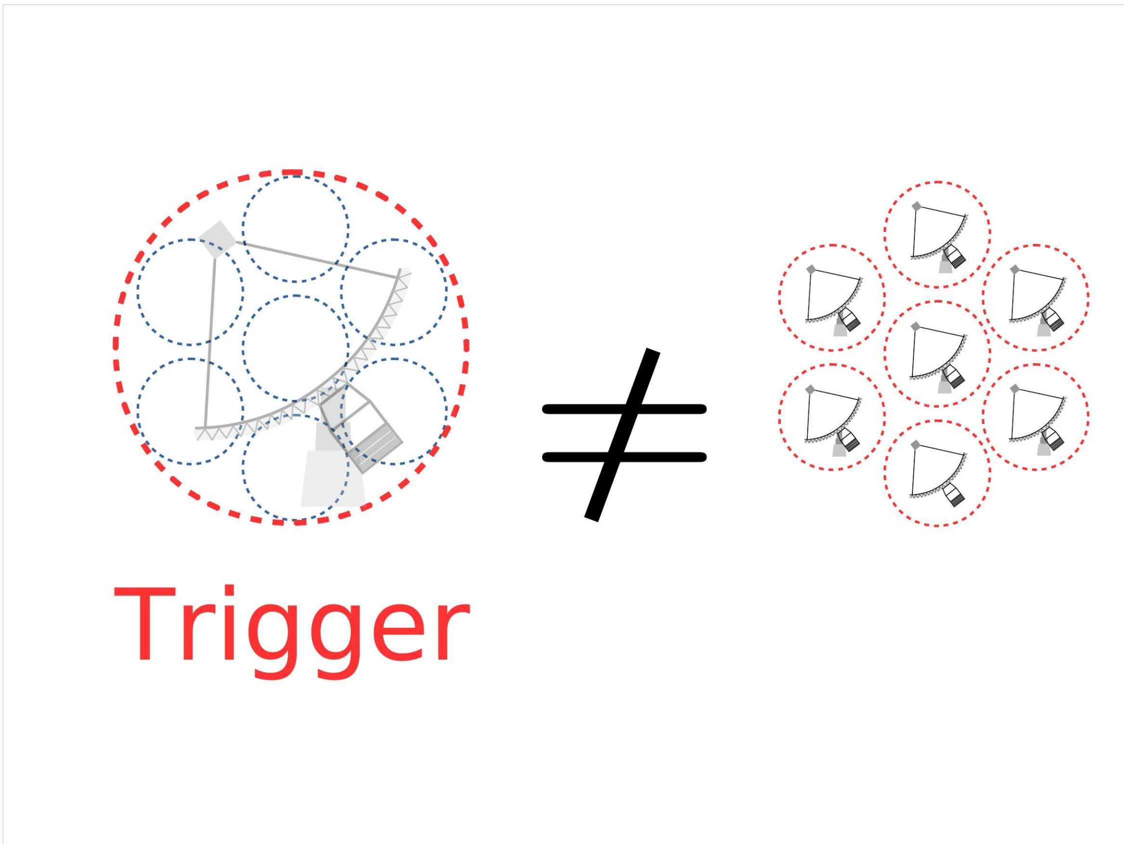

Its trigger.

In the array of Cherenkov-telescopes, it is a huge technological challenge to reorganize signals from being grouped by telescopes on the aperture-plane into signals being grouped by incident-directions on the sky-dome, as it is needed for the trigger-decision.

Here I propose one specific Cherenkov-plenoscope which is designed to take full advantage of plenoptic-perception in order to drive the energy-threshold down to one Giga-electron-volt.

With an energy-threshold of one Giga electron Volt, the Cherenkov-plenoscope could become the Portal to enter the sub-second highly variable gamma-ray-sky.

Optics

of

PORTAL
CHERENKOV-PLENOSCOPE

The optics of Portal

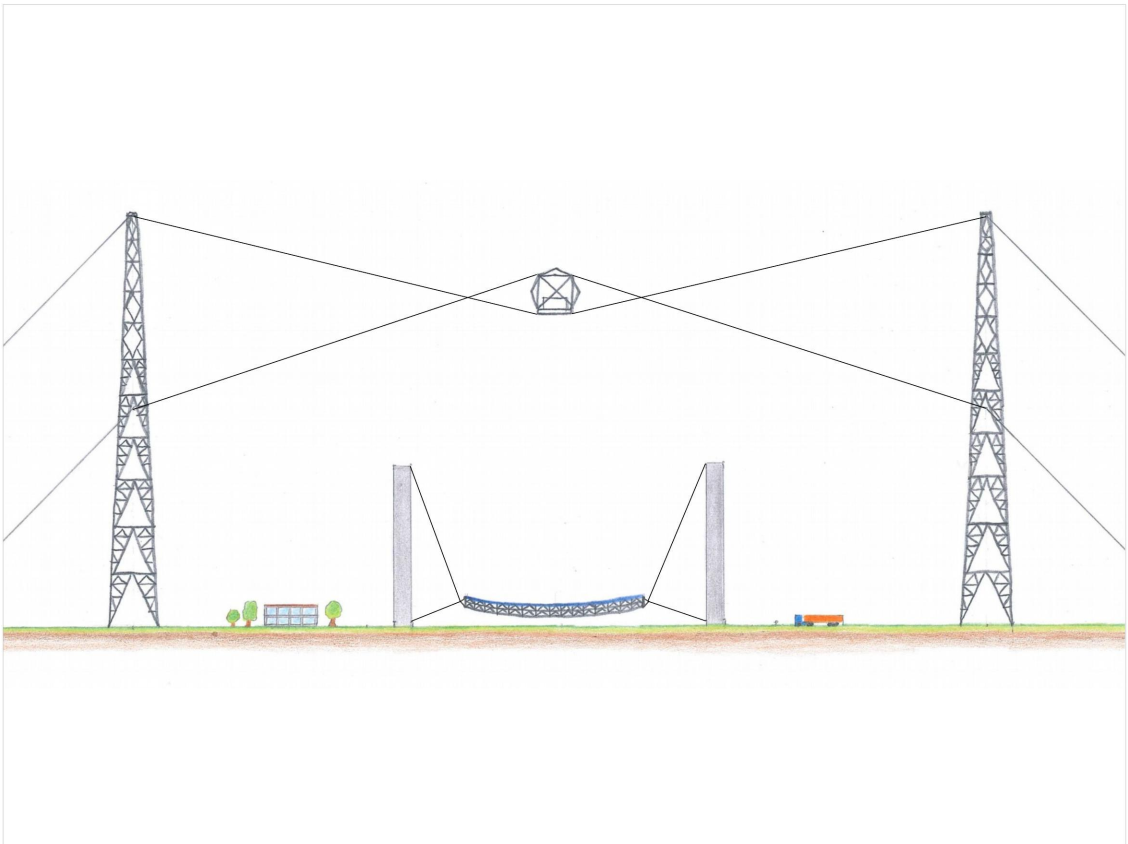

Portal has a large imaging-reflector.

And a light-field-sensor.

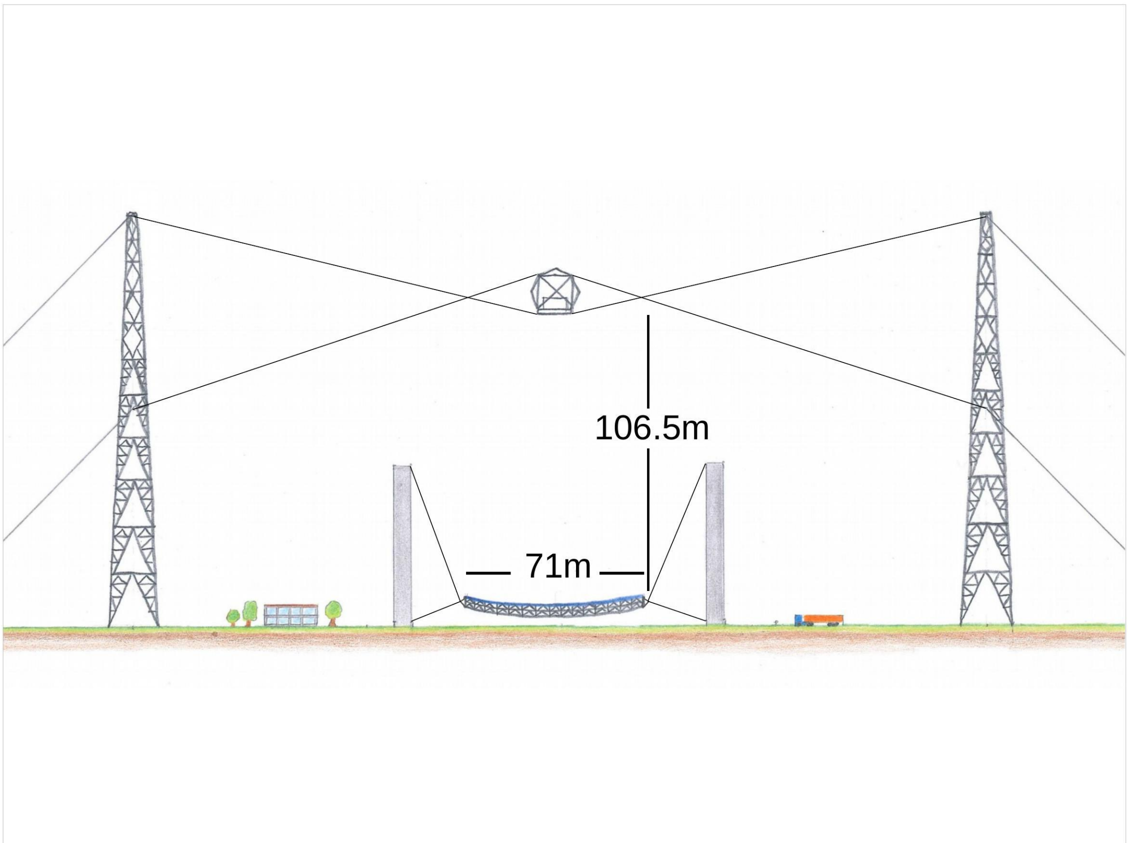

The imaging-reflector has seventy one meter diameter and a one hundred and six point five meter focal-length.

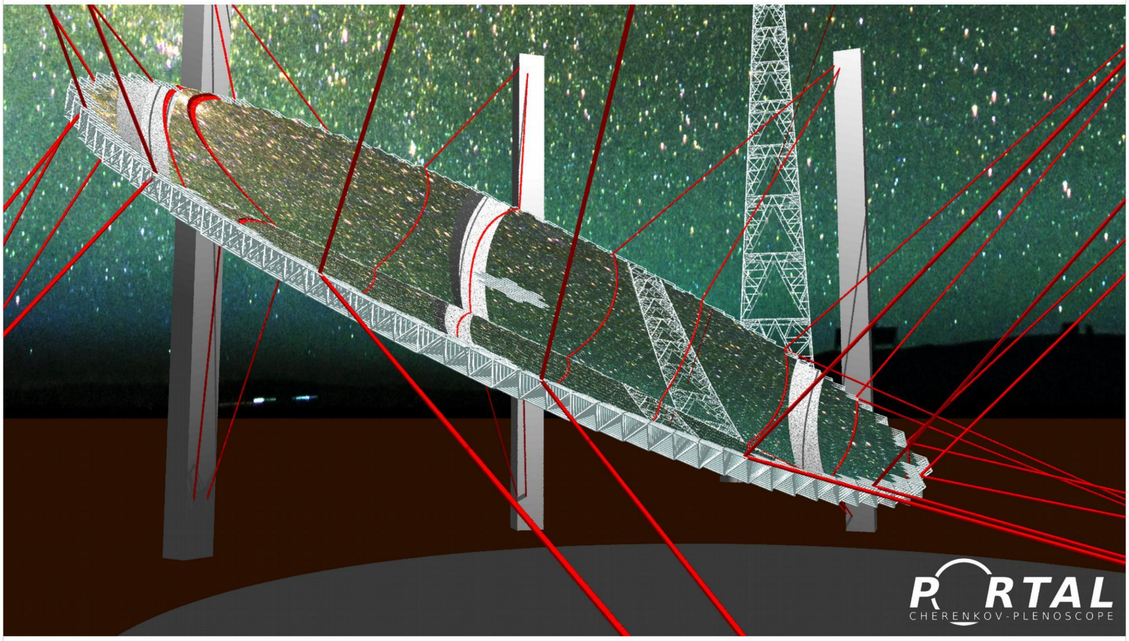

Portal's imaging-reflector is composed from small mirror-facets which are mounted on a space-truss.

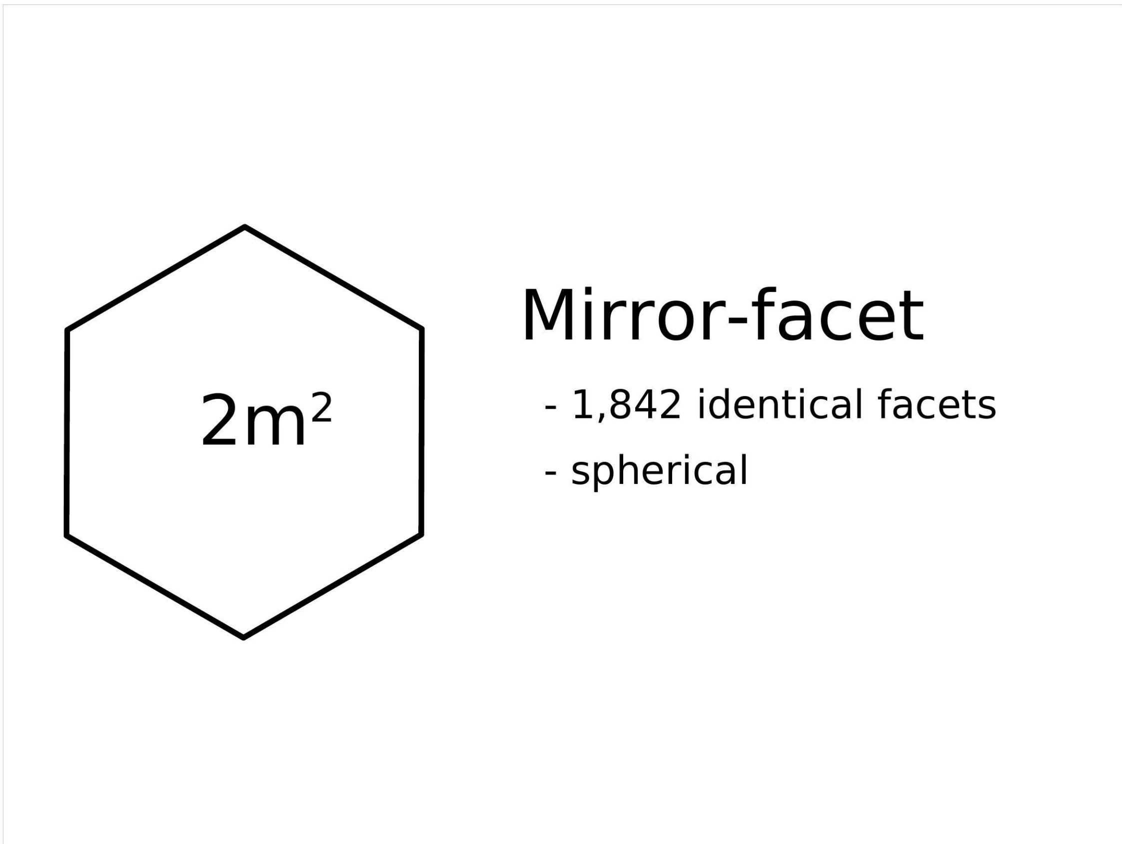

The one thousand eight hundred forty two identical, and spherical mirror-facets have two meter-square reflective area each.

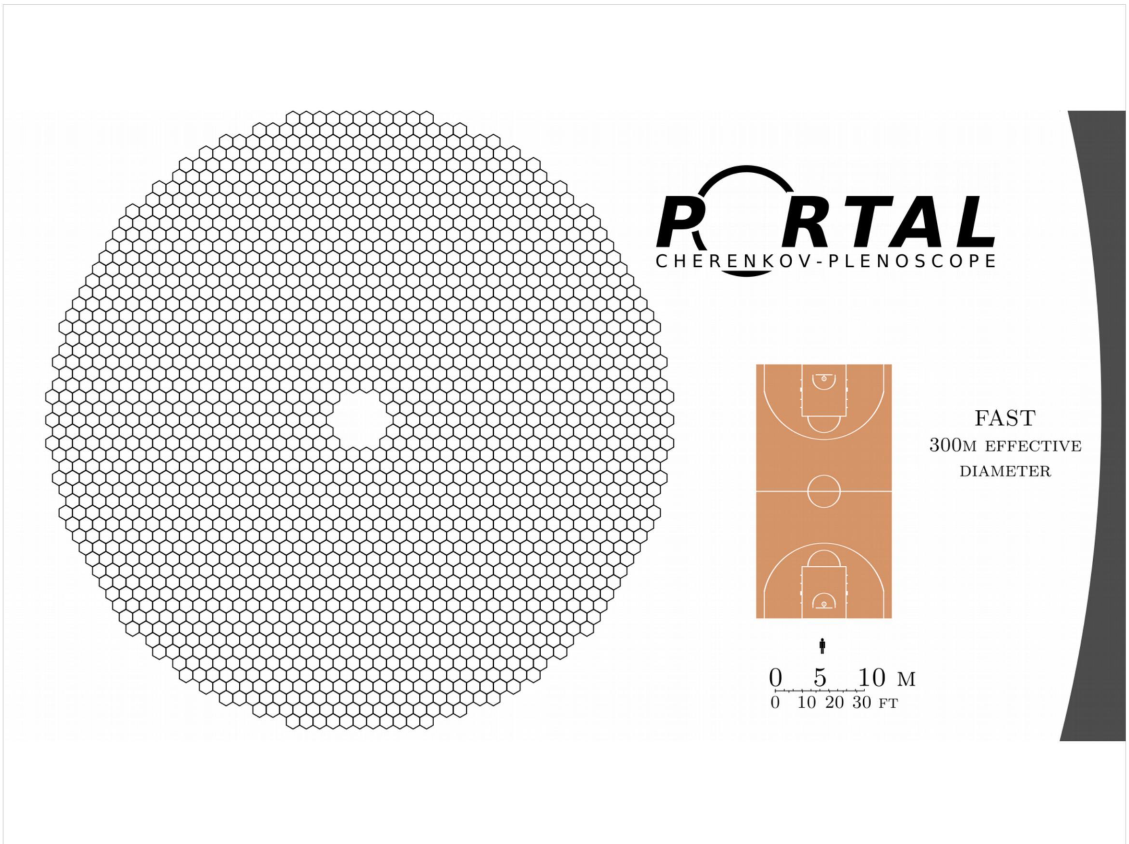
PORTAL
CHERENKOV-PLENOSCOPE
FAST
300M EFFECTIVE DIAMETER
0 5 10 M
0 10 20 30 FT

Portals is

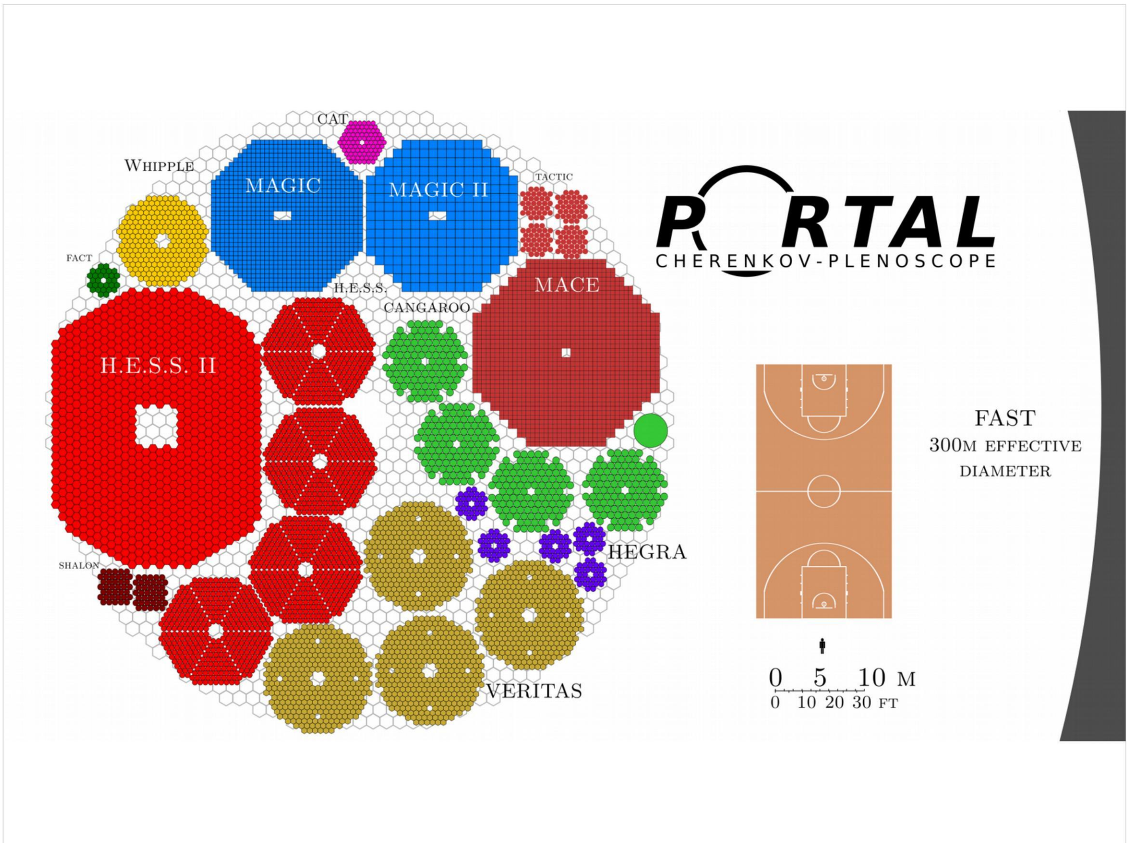

Truly large. (pause and wait for 10s)

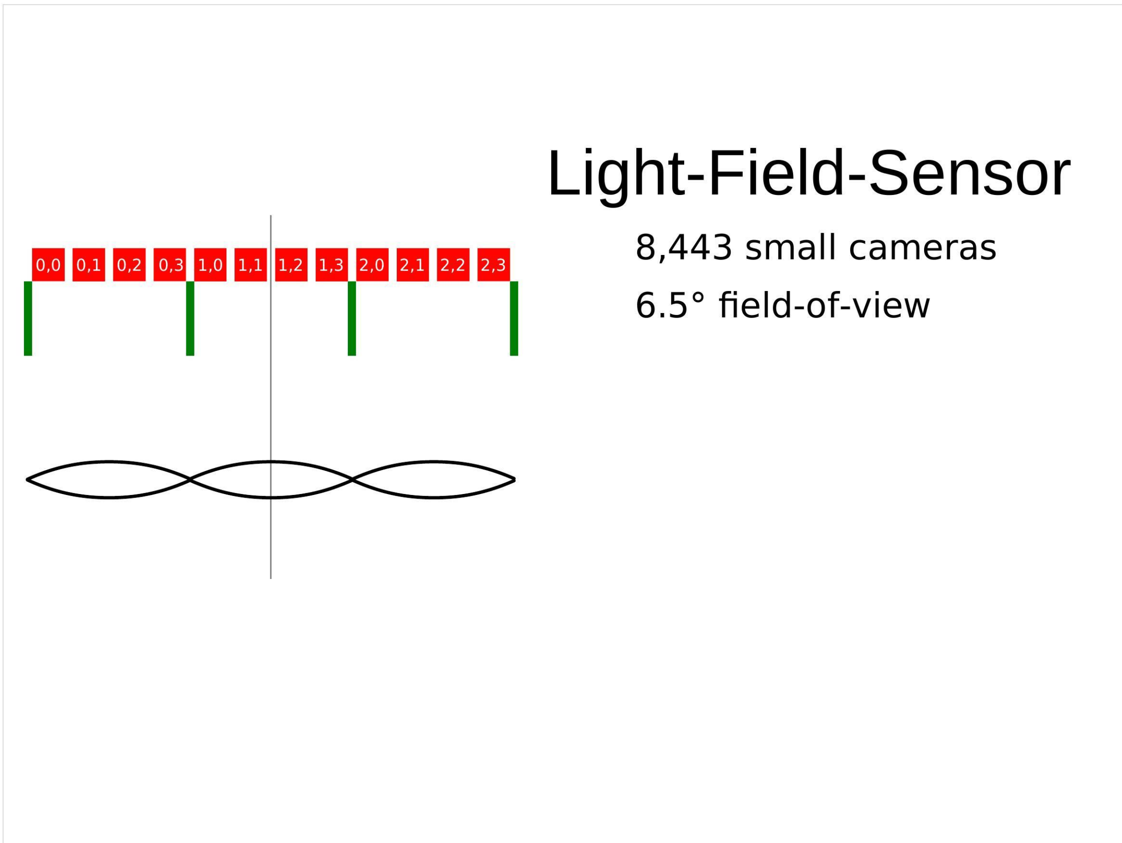

Portal’s light-field-sensor is composed from eight thousand four hundred forty three small cameras, and covers six point five degrees field-of-view.

Plenoptic-perception has severe consequences.

Measuring the full trajectory of photons, in contrast to only measuring the photons incident-directions allows Portal to synthesize images from the light-field which are:

Light-Field-Sensor

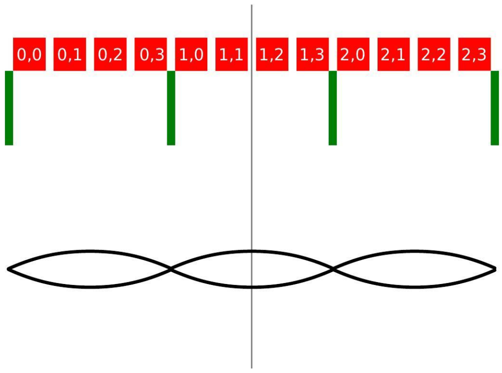

8,443 small cameras

6.5° field-of-view

- Free of distortions

Free of distortions.

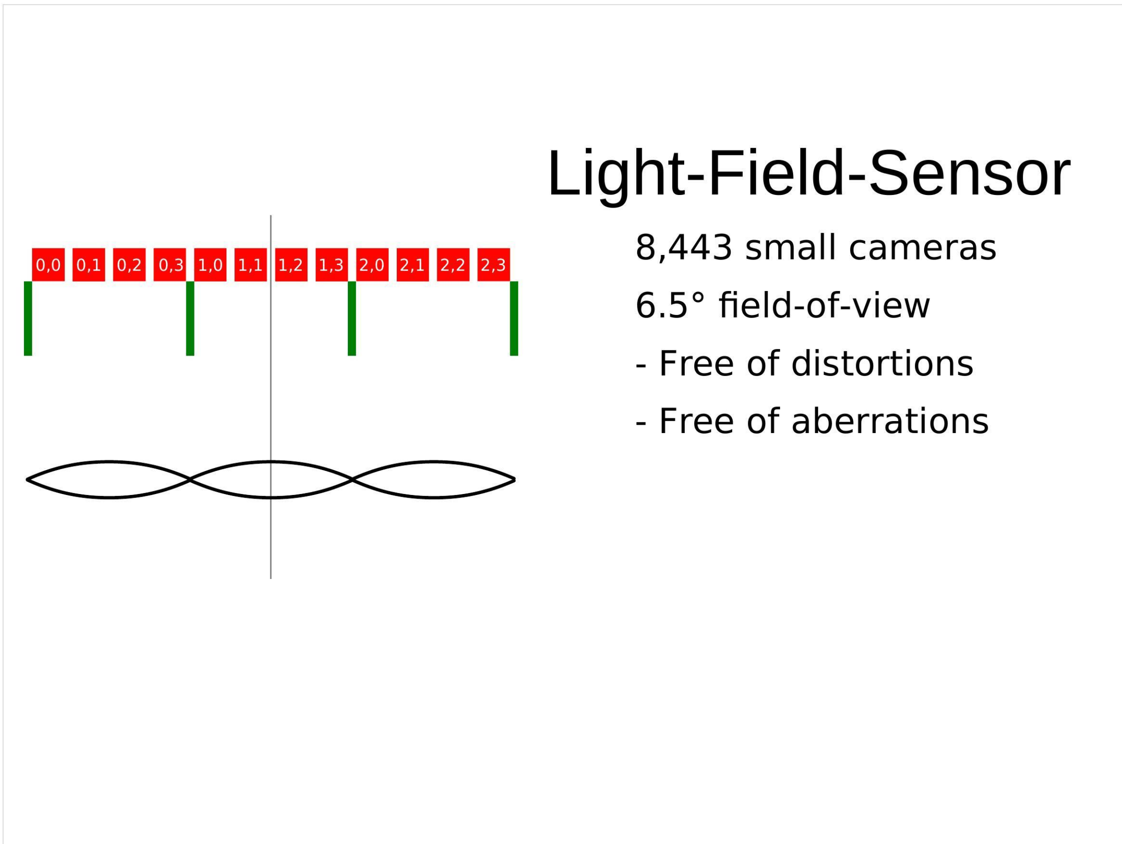

free of aberrations.

Light-Field-Sensor

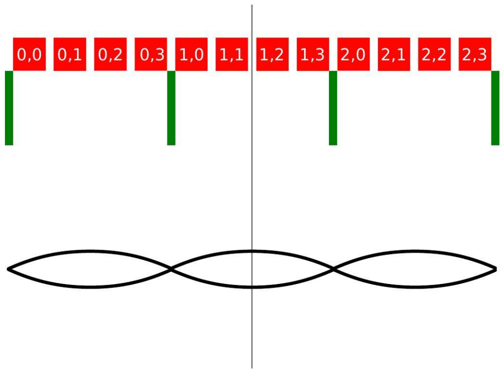

8,443 small cameras

6.5° field-of-view

- Free of distortions
- Free of aberrations
- Isochronous images

Perfectly isochronous across the whole field-of-view

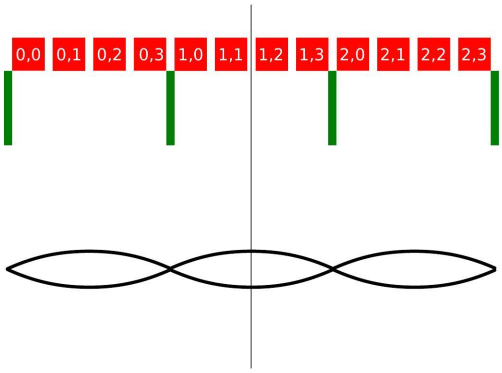

Light-Field-Sensor

8,443 small cameras

6.5° field-of-view

- Free of distortions
- Free of aberrations
- Isochronous images
- Refocus in post

And re focusable in post after the air-shower has been recorded.

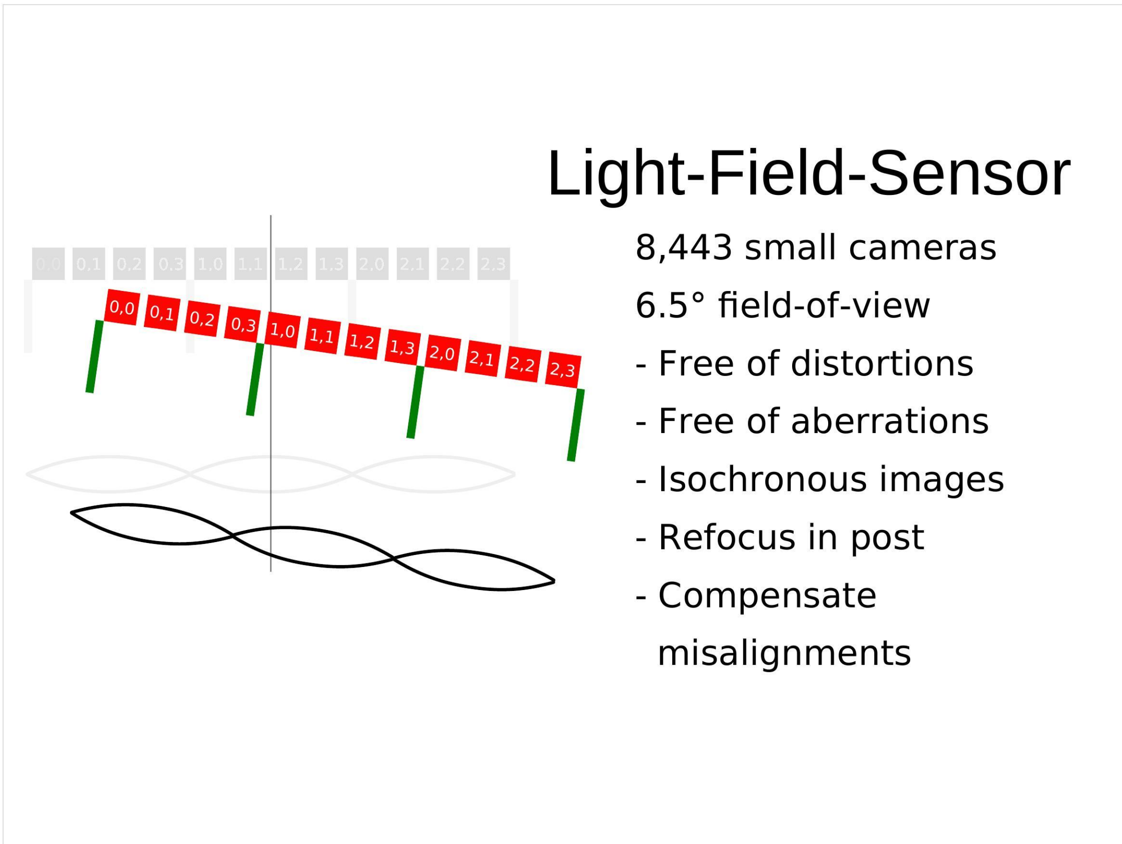

And all of this is even possible when the light-field-sensor is misaligned with respect to the imaging-reflector, as long this misalignment is known.

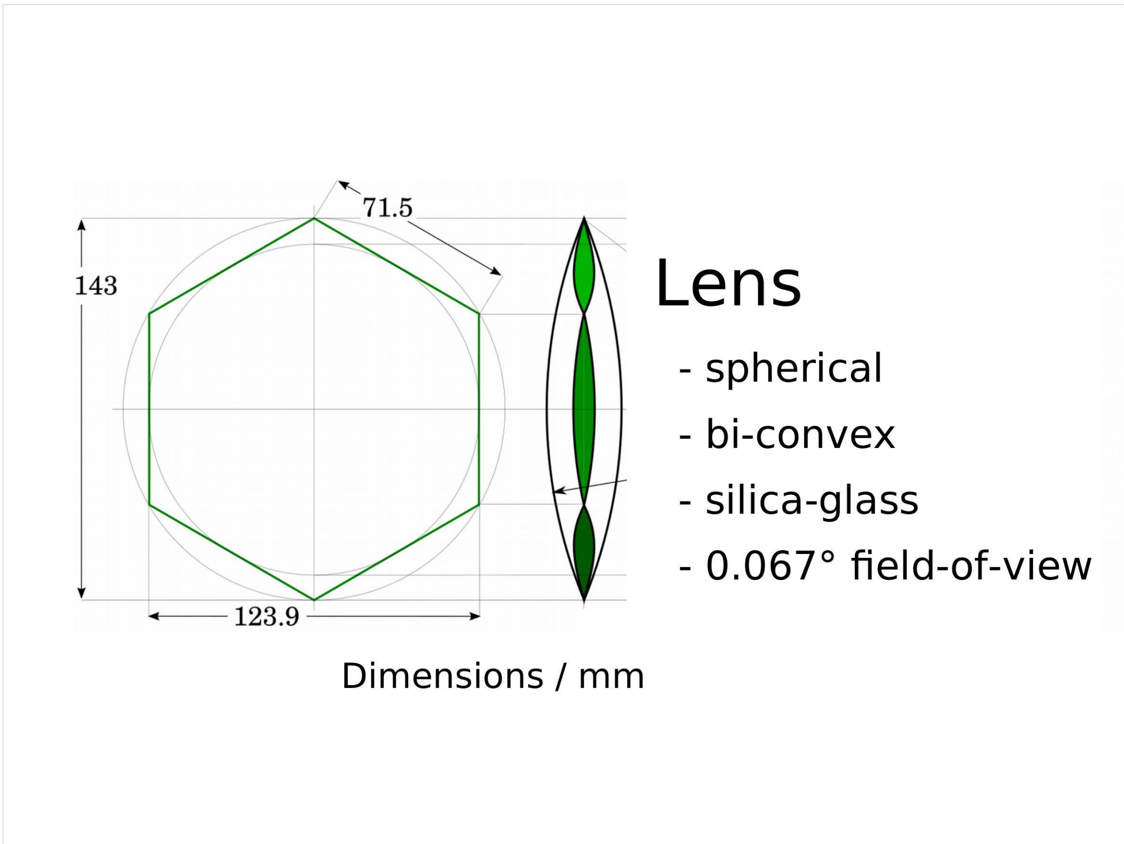

The spherical and bi-convex lenses in Portal's small cameras are made from UV transparent silica-glass.

Each small camera has point oh six seven degrees field-of-view.

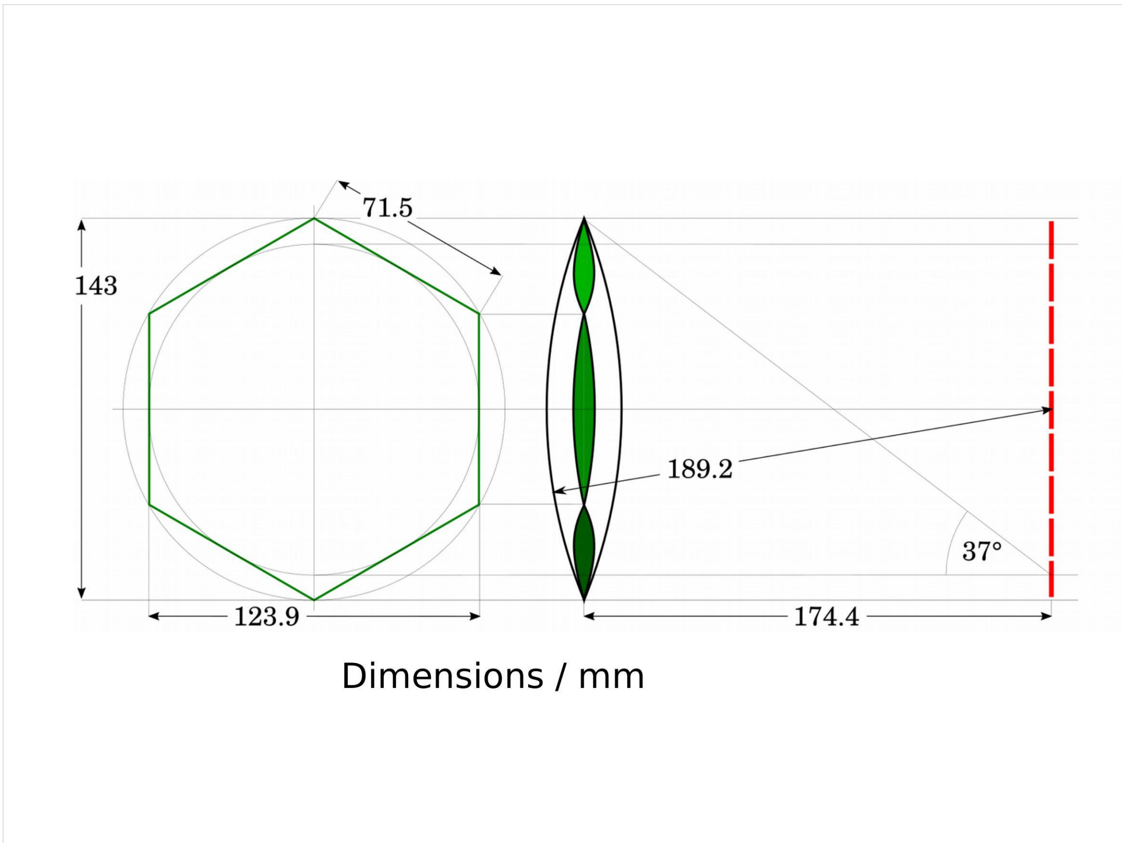

In the back of the small camera is an array of sixty one photo-sensors.

Each photo-sensor has about two centimeter-square each.

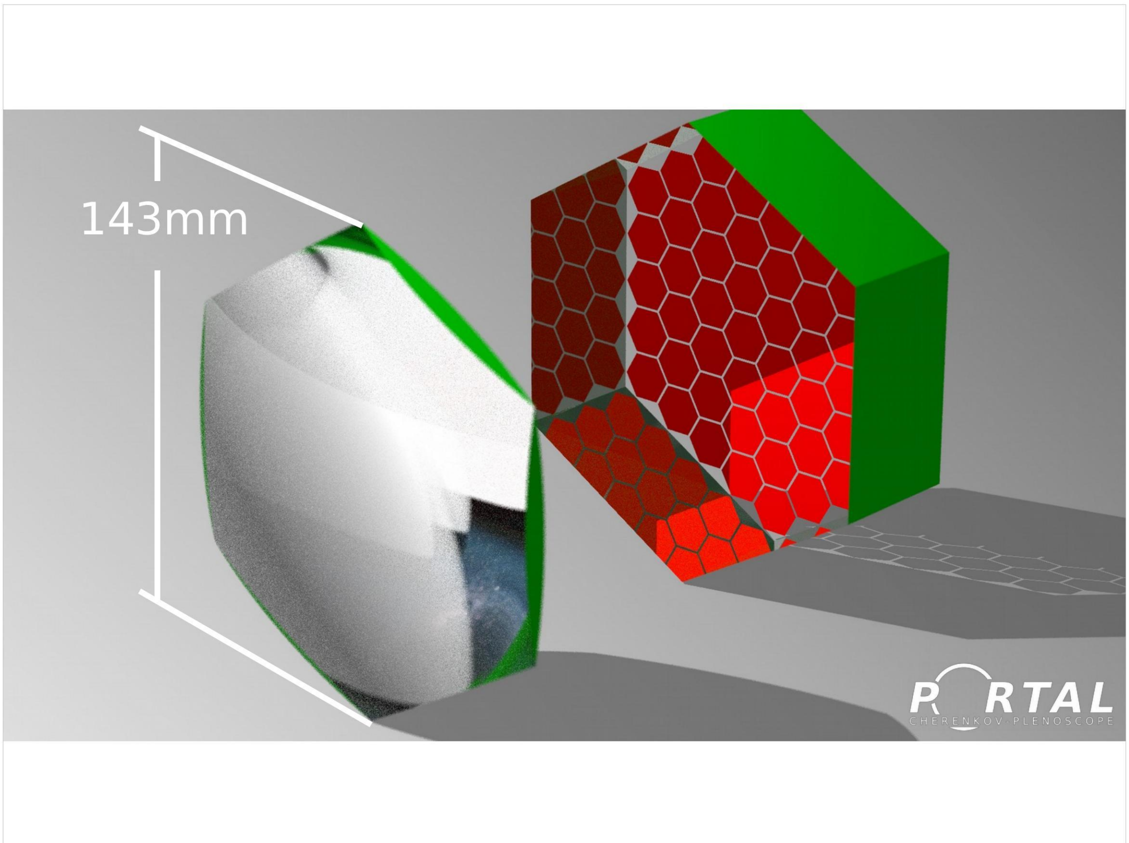

This is a single small camera in Portal’s light-field-sensor.

For us to have a look, I shortened the green walls which would otherwise reach down to the lens for mechanical support.

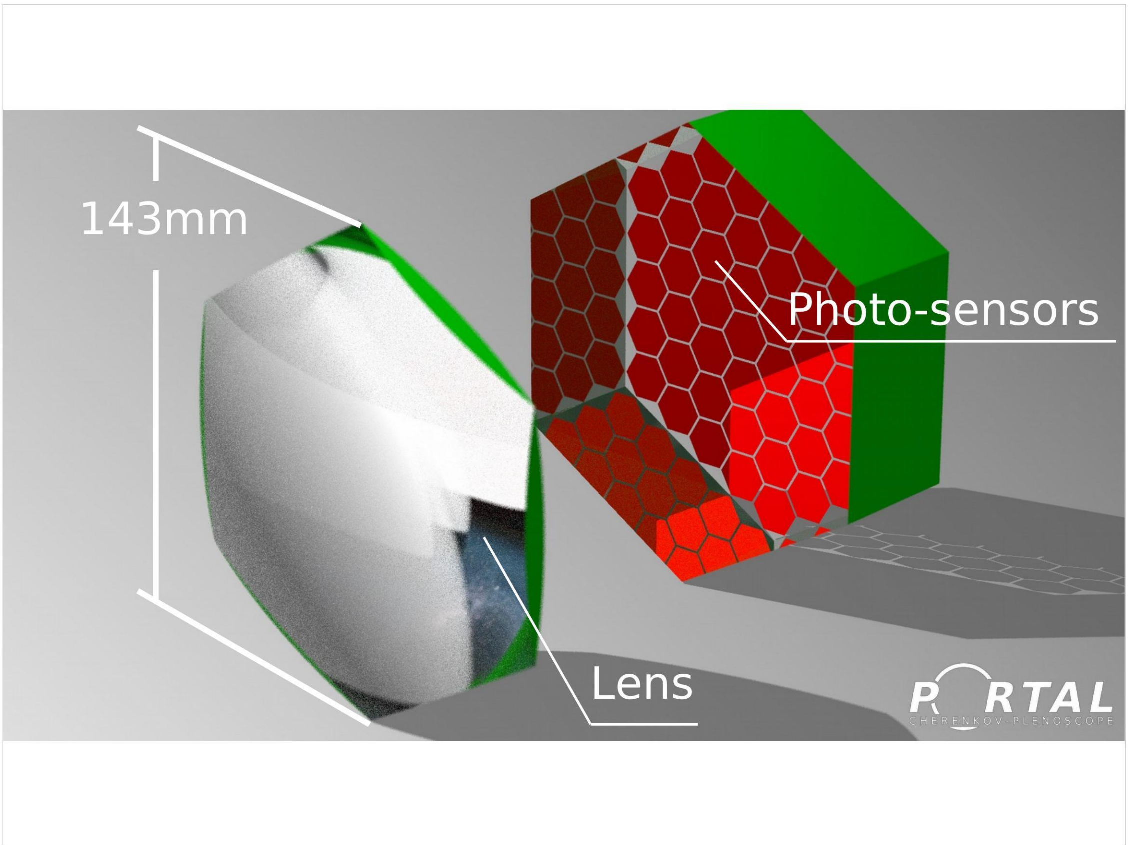

In the front is the lens, and in the back is the array of photo-sensors.

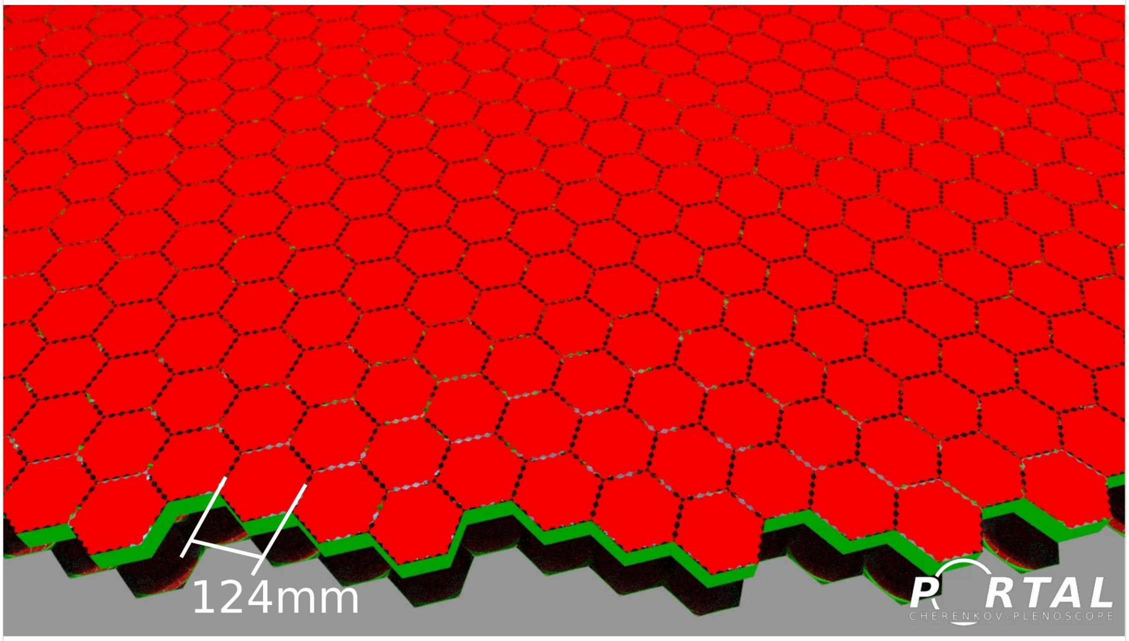

In Portal’s light-field-sensor

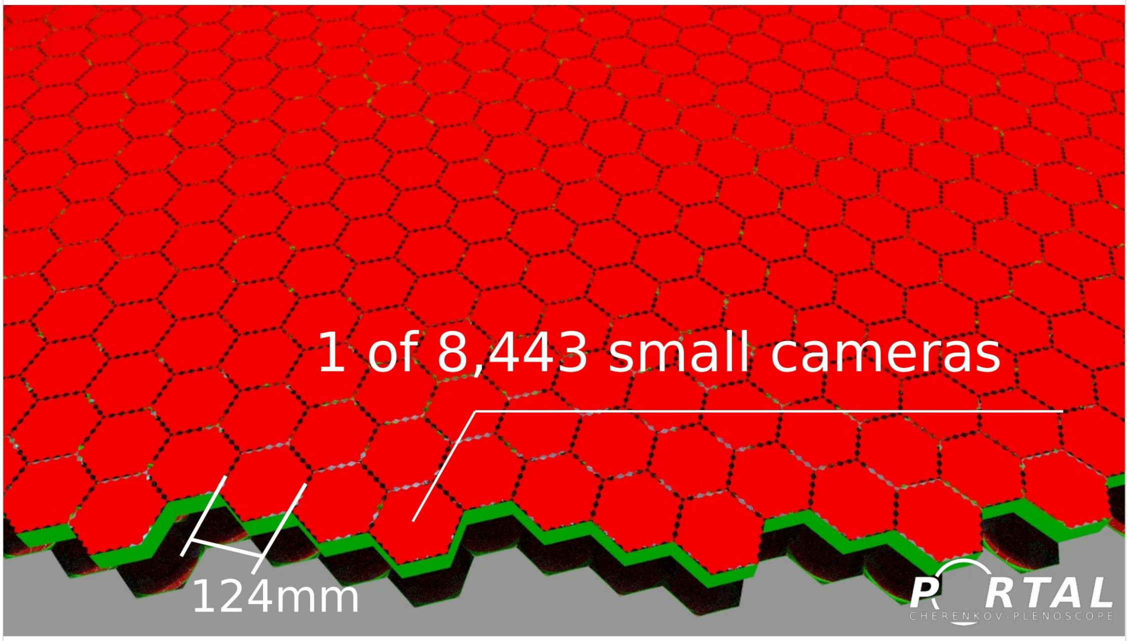

the small-cameras are densely packed.

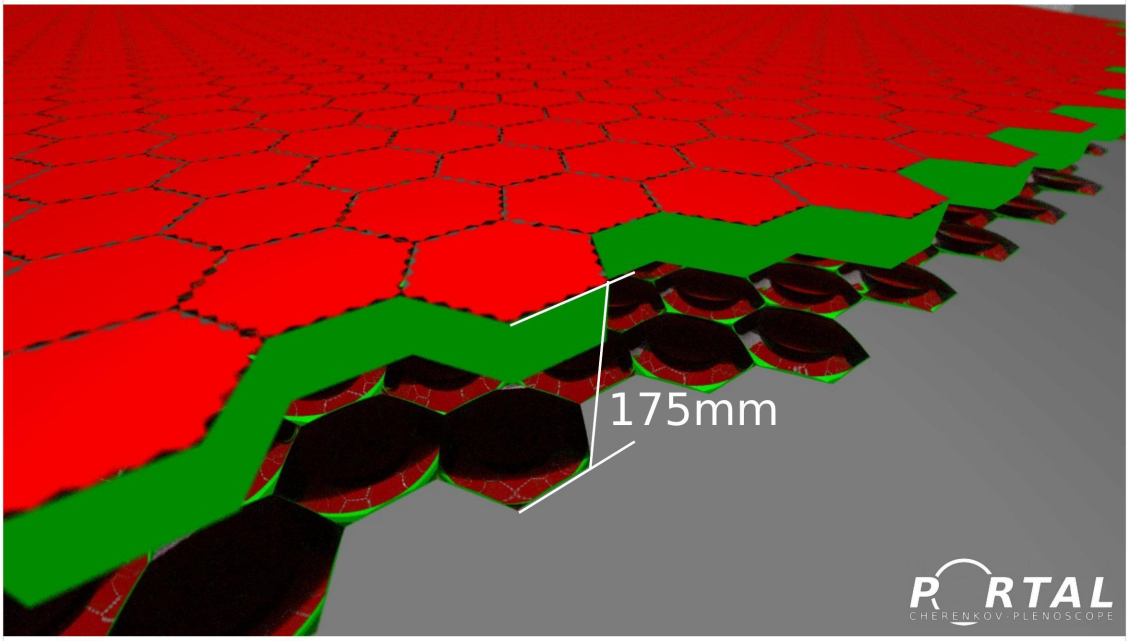

Photo-sensors on top

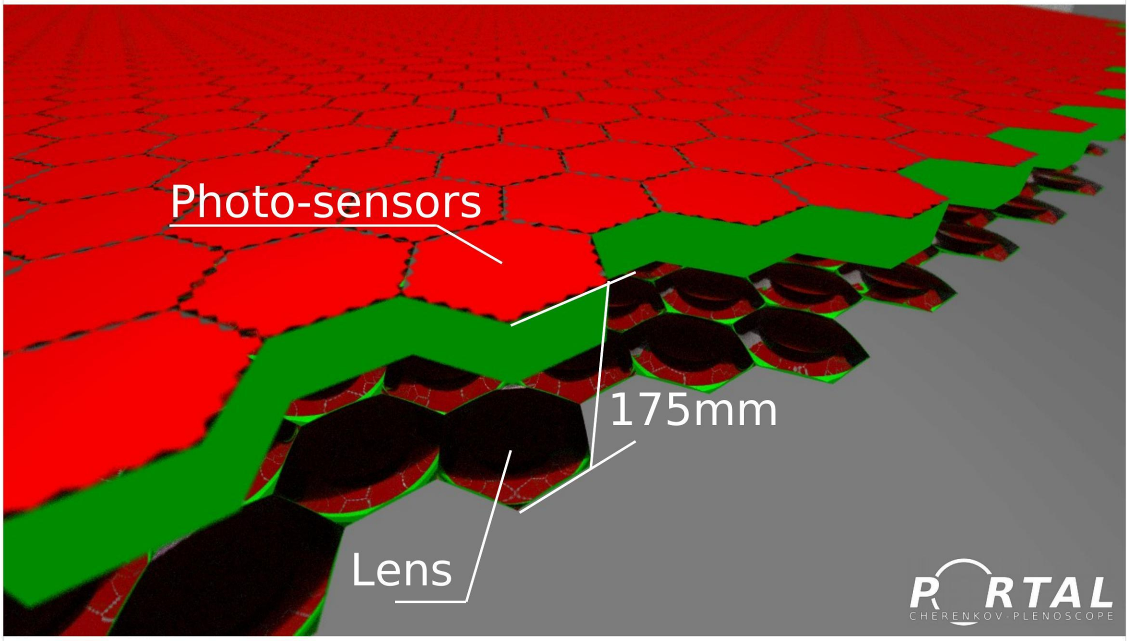

And lenses at the bottom.

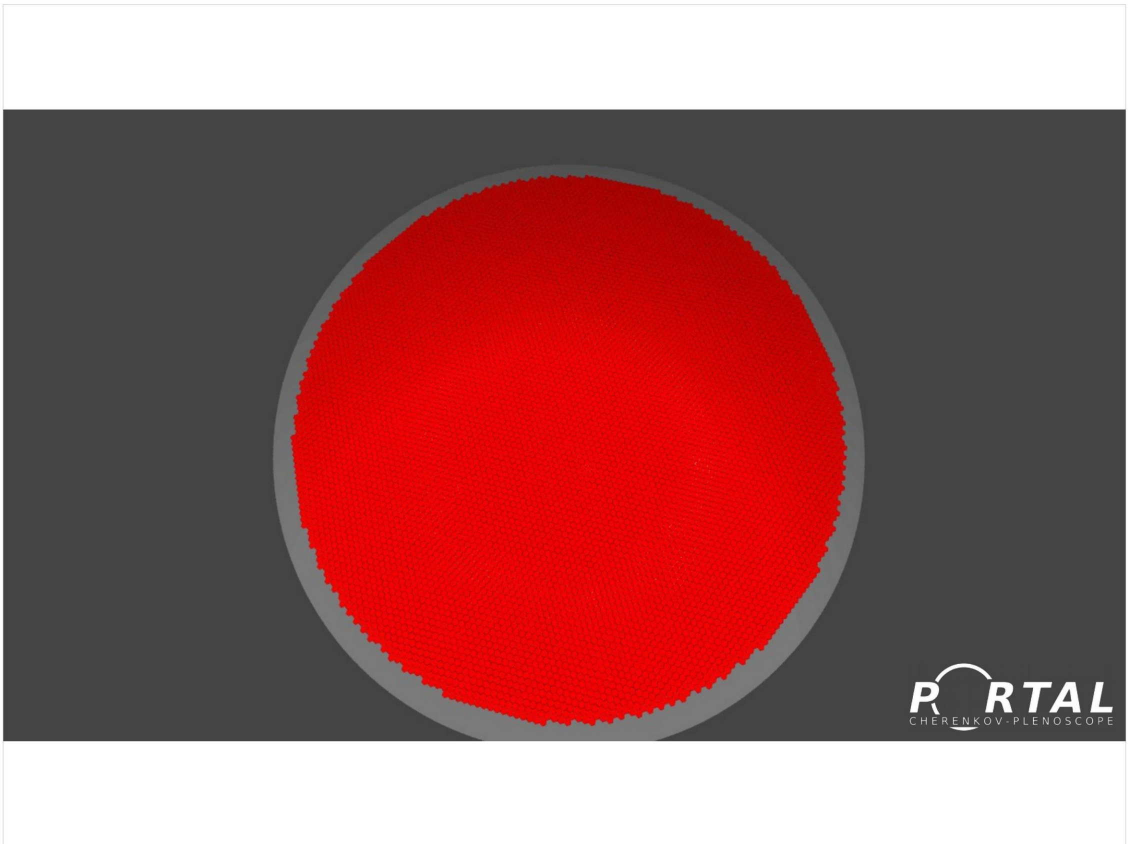

Here we look down onto the entire sensor-plane within Portal’s light-field-sensor.

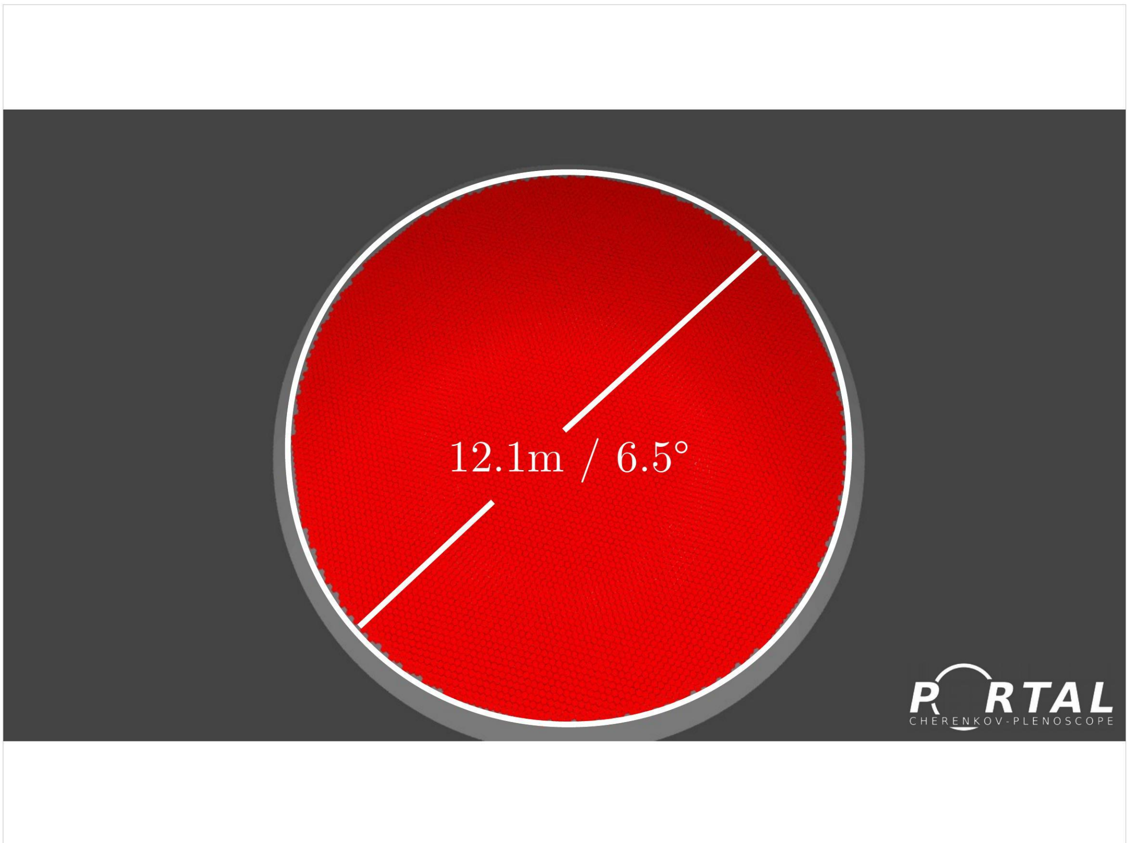

Six point five degrees field of view correspond to twelve point one meter in diameter.

Overcoming Aberrations

with

PORTAL

CHERENKOV-PLENOSCOPE

Overcoming aberrations

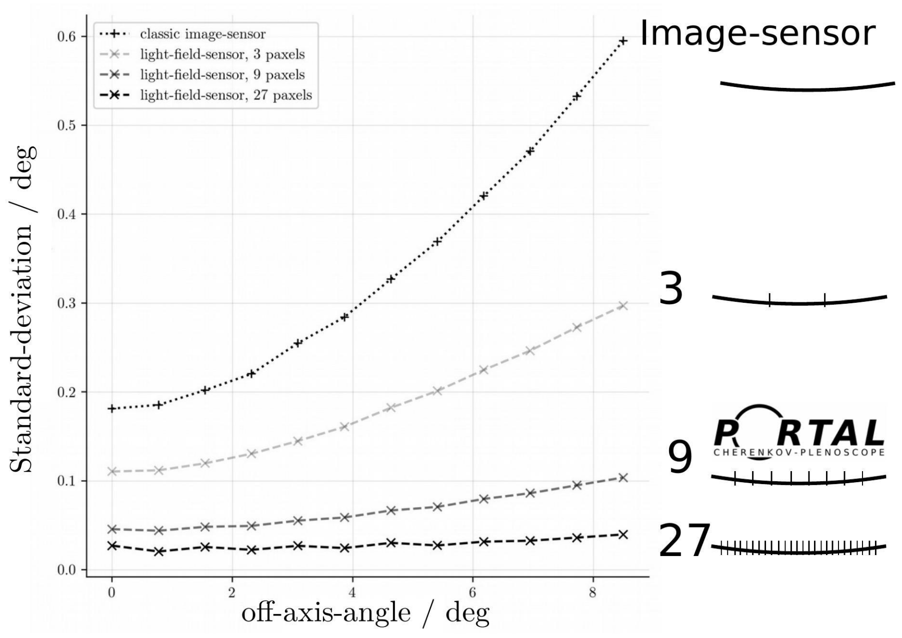

In a simulation, I explore how plenoptic-perception can overcome aberrations.

This is the spread found in images reconstructed from an image-sensor, and from light-field-senors which can distinguish three, nine and twenty seven distinct sections along the aperture's diagonal.

(Point on simplified imaging-reflectors with vertical bars to indicate segmentation.)

Portal has nine distinct sections along its aperture's diagonal.

Portal's field-of-view is exceptionally flat.

It might be possible to build Cherenkov-plenoscopes with twenty degrees field-of-view.

Refocusing Images in Post

with

PORTAL
CHERENKOV-PLENOSCOPE

Refocusing images in post.

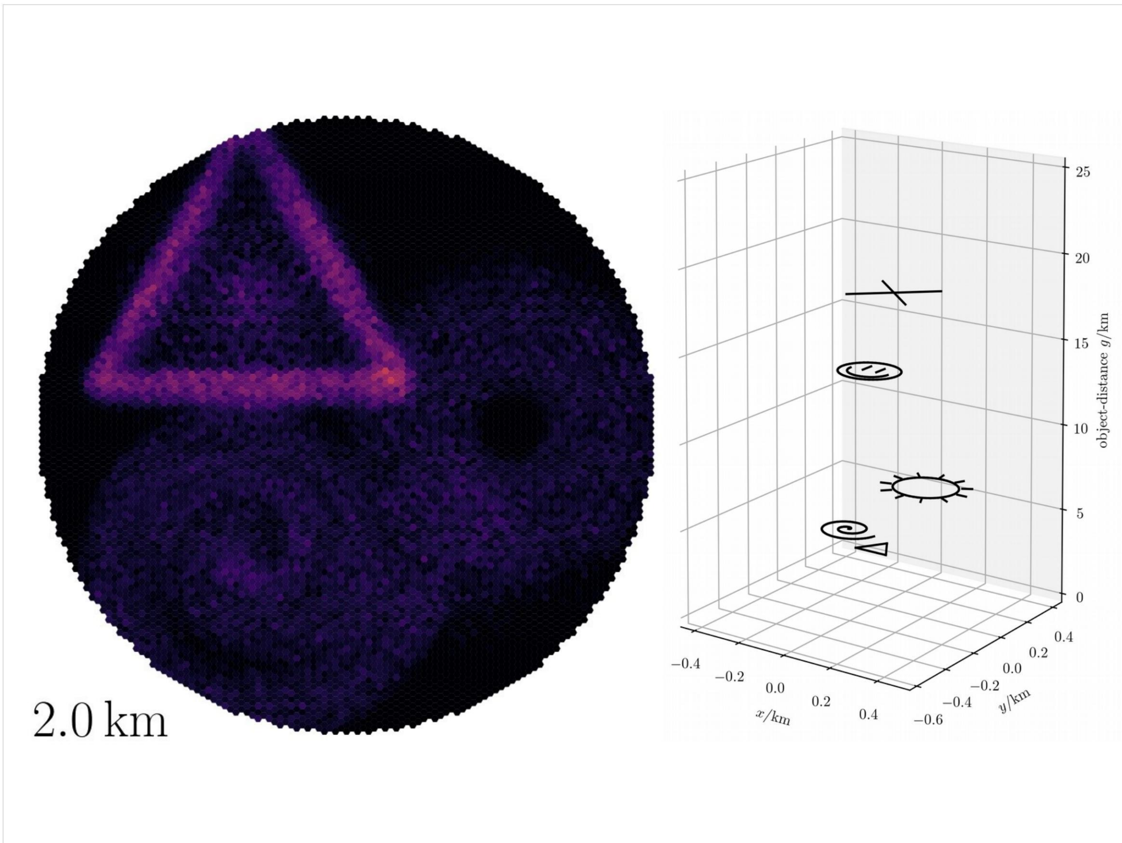

I set up a phantom source.

The phantom source reaches from two kilometers to twenty kilometers in object-distance above Portal's aperture-plane.

In what we are about to see, we do not go through the dimension of time.

Here we project the light-field recorded by Portal onto images refocused to different object-distances, starting at two kilometers.

We only see the triangle.

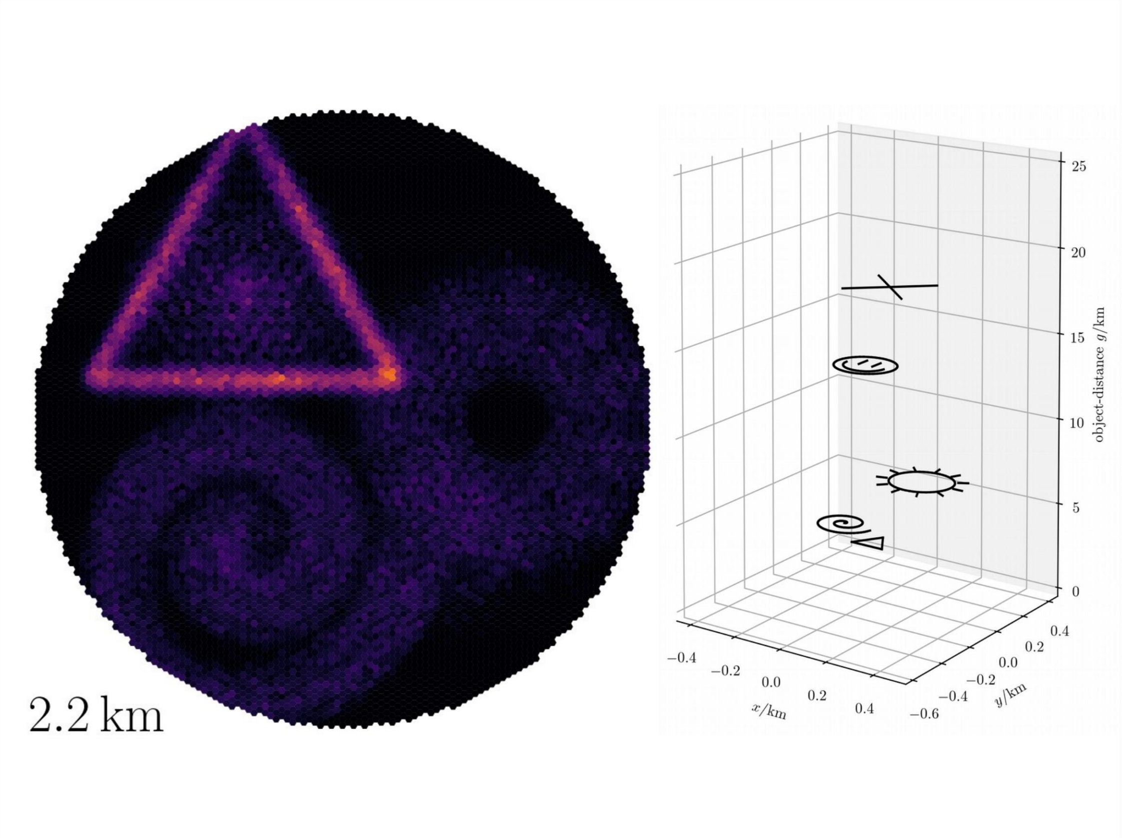

When we refocus the images, we see the different symbols poping up in the image at different object-distances.

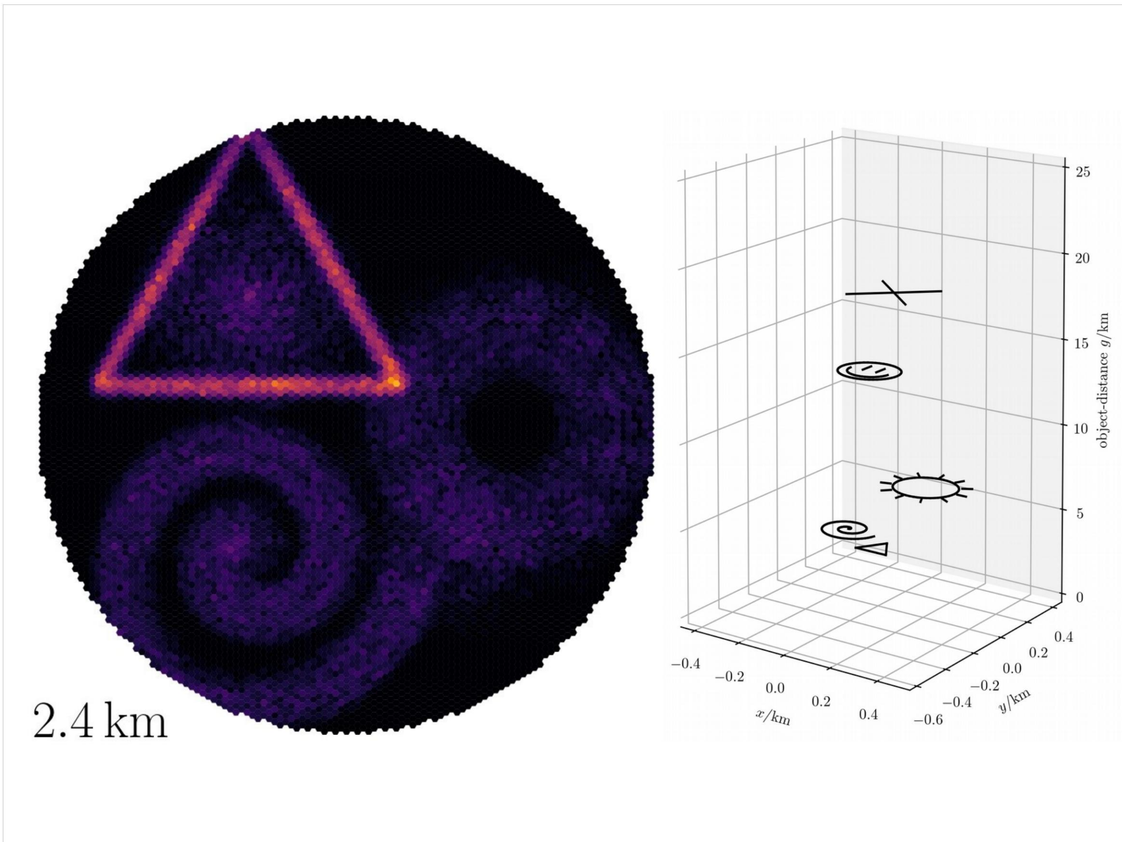

2.4 km
object-distance g/km
x/km
y/km
0
5
10
15
20
25
−0.4
−0.2
0.0
0.2
0.4
−0.6
−0.4
−0.2
0.0
0.2
0.4

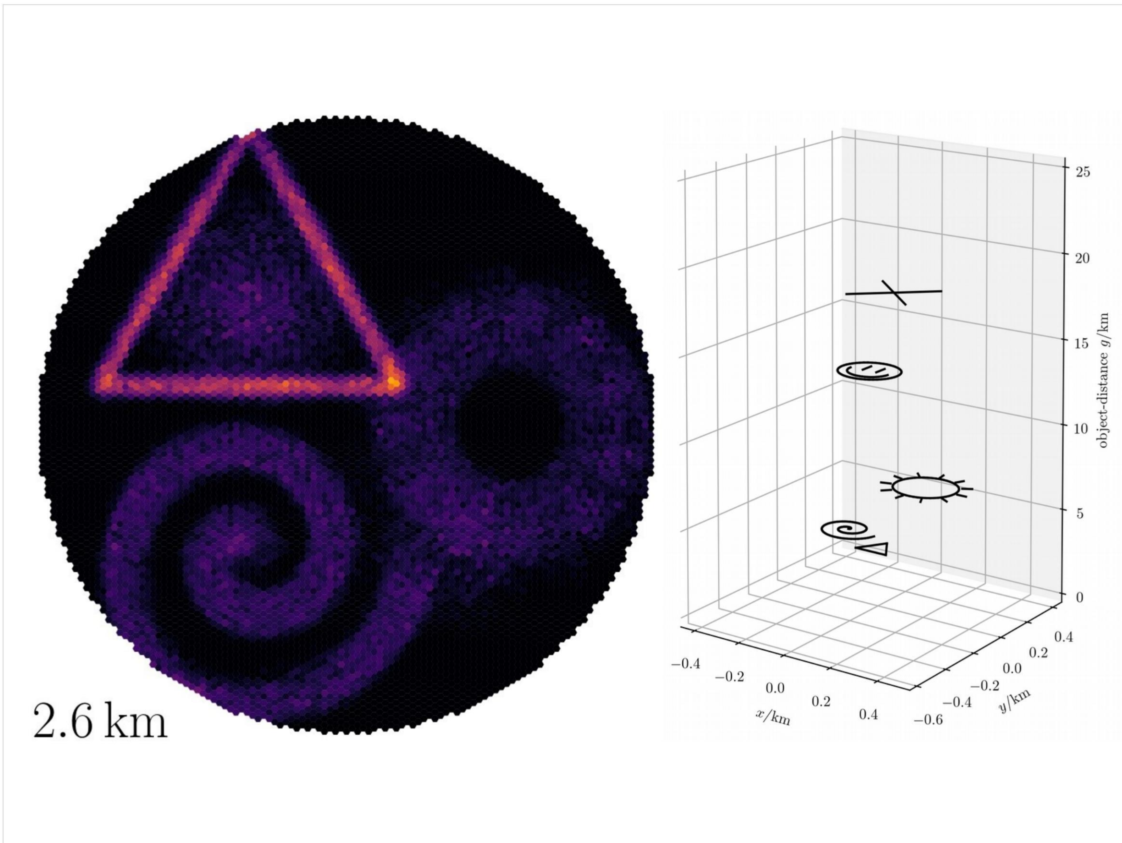
2.6 km
object-distance g/km
x/km
y/km
0
5
10
15
20
25
−0.4
−0.2
0.0
0.2
0.4
−0.6
−0.4
−0.2
0.0
0.2
0.4

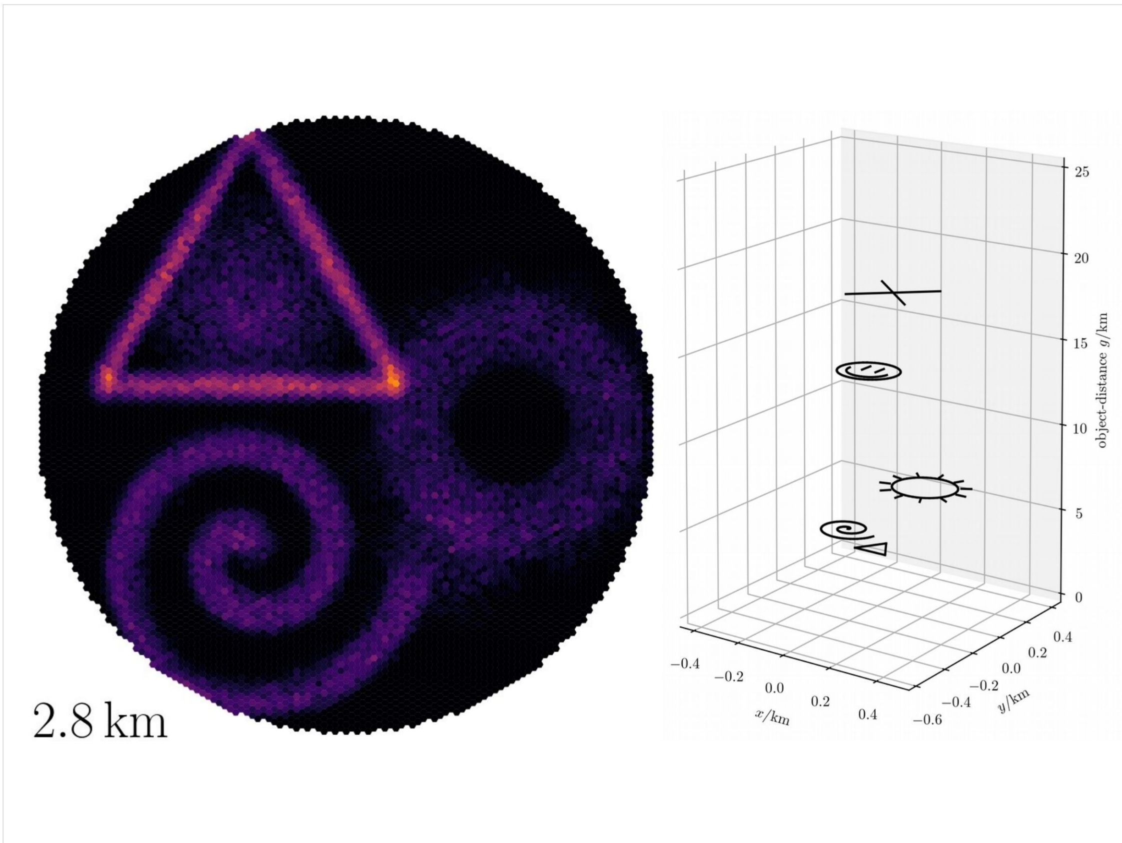

2.8 km
object-distance g/km
x/km
y/km

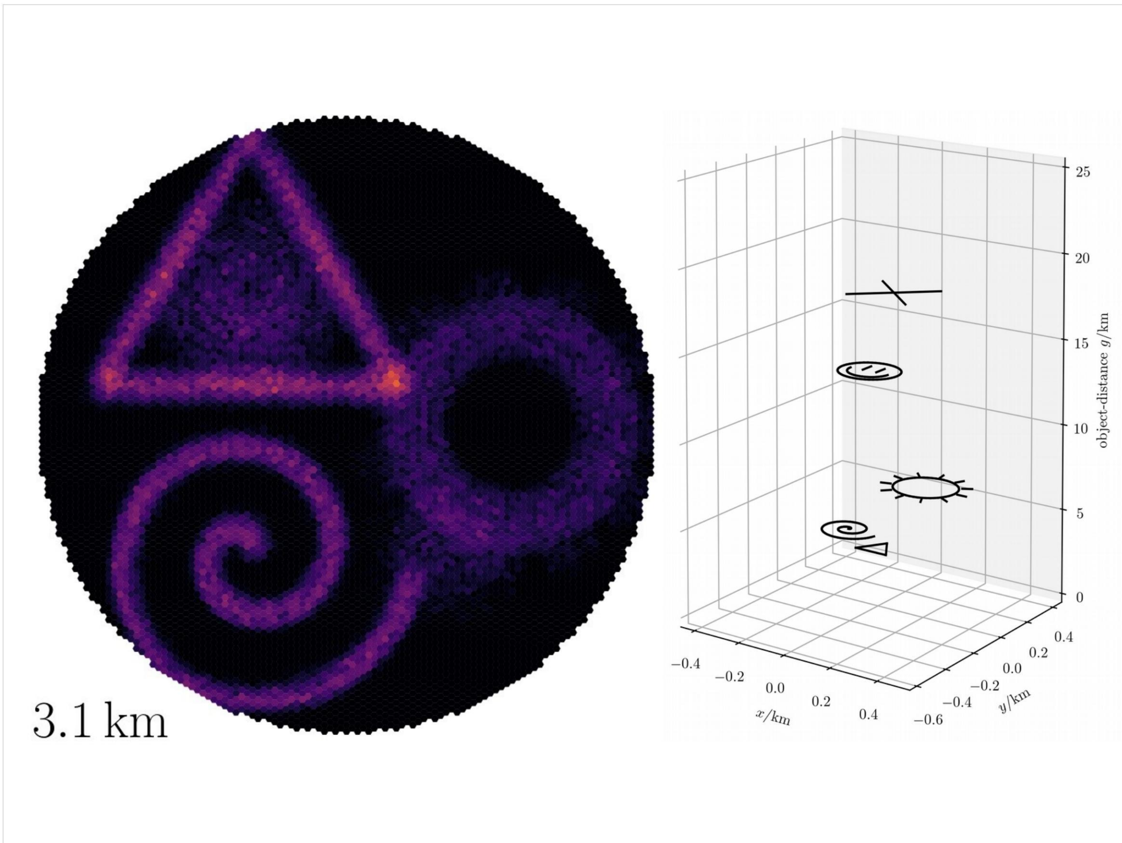

3.1 km
object-distance g/km
x/km
y/km

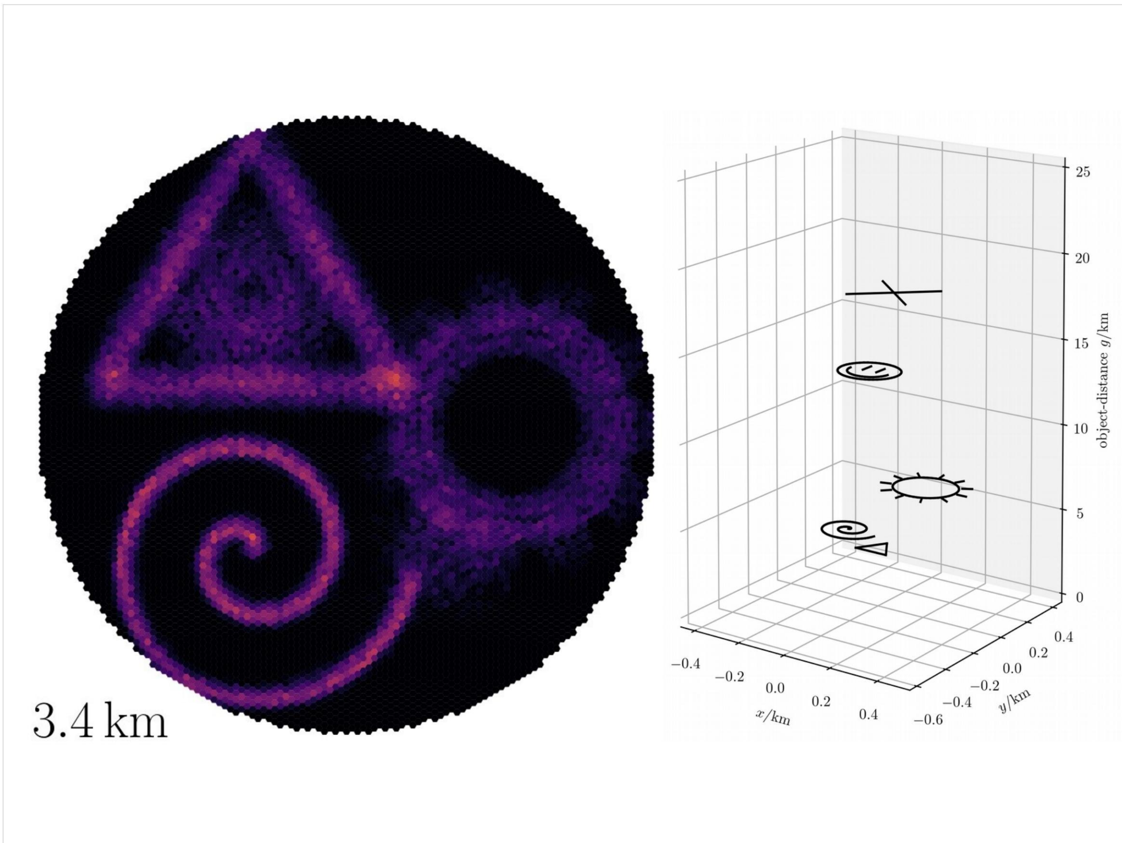
3.4 km
object-distance g/km
x/km
y/km

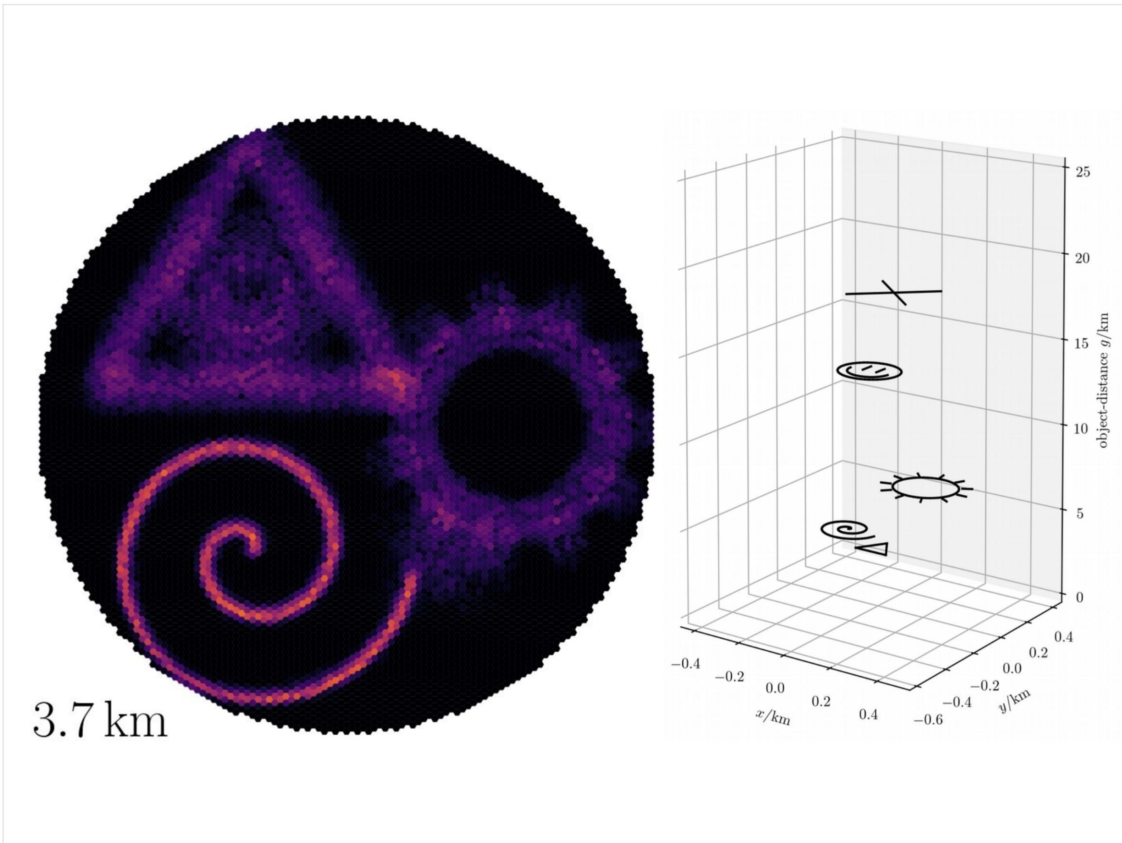

3.7 km
object-distance g/km
x/km
y/km

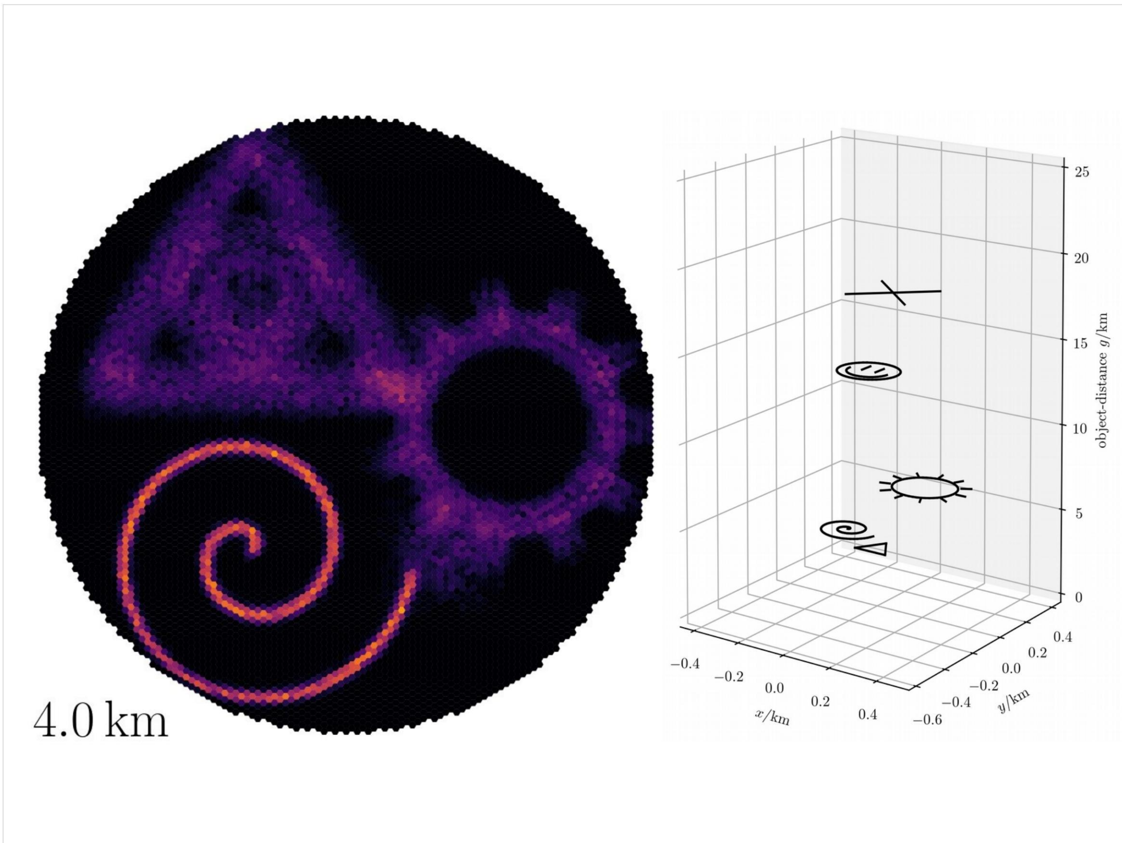
4.0 km
object-distance g/km
x/km
y/km

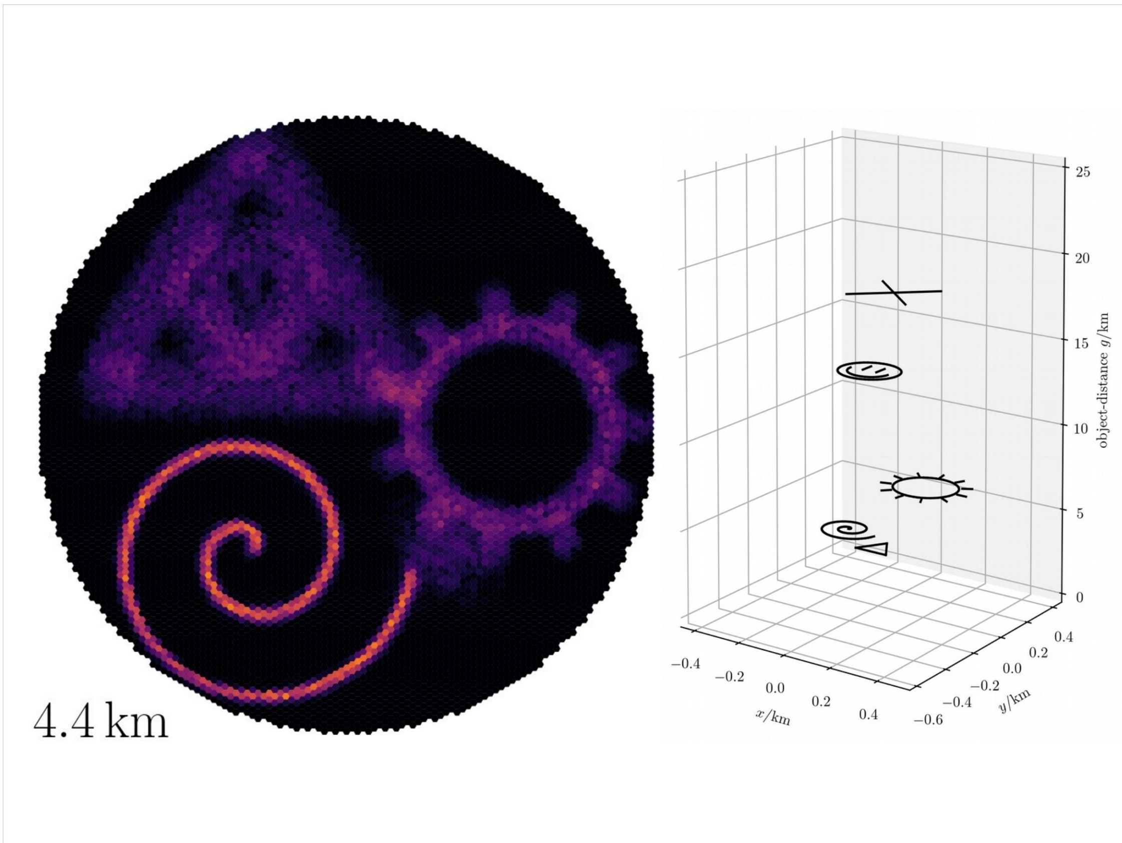
4.4 km
object-distance g/km
0
5
10
15
20
25
−0.4
−0.2
0.0
0.2
0.4
x/km
−0.6
−0.4
−0.2
0.0
0.2
0.4
y/km

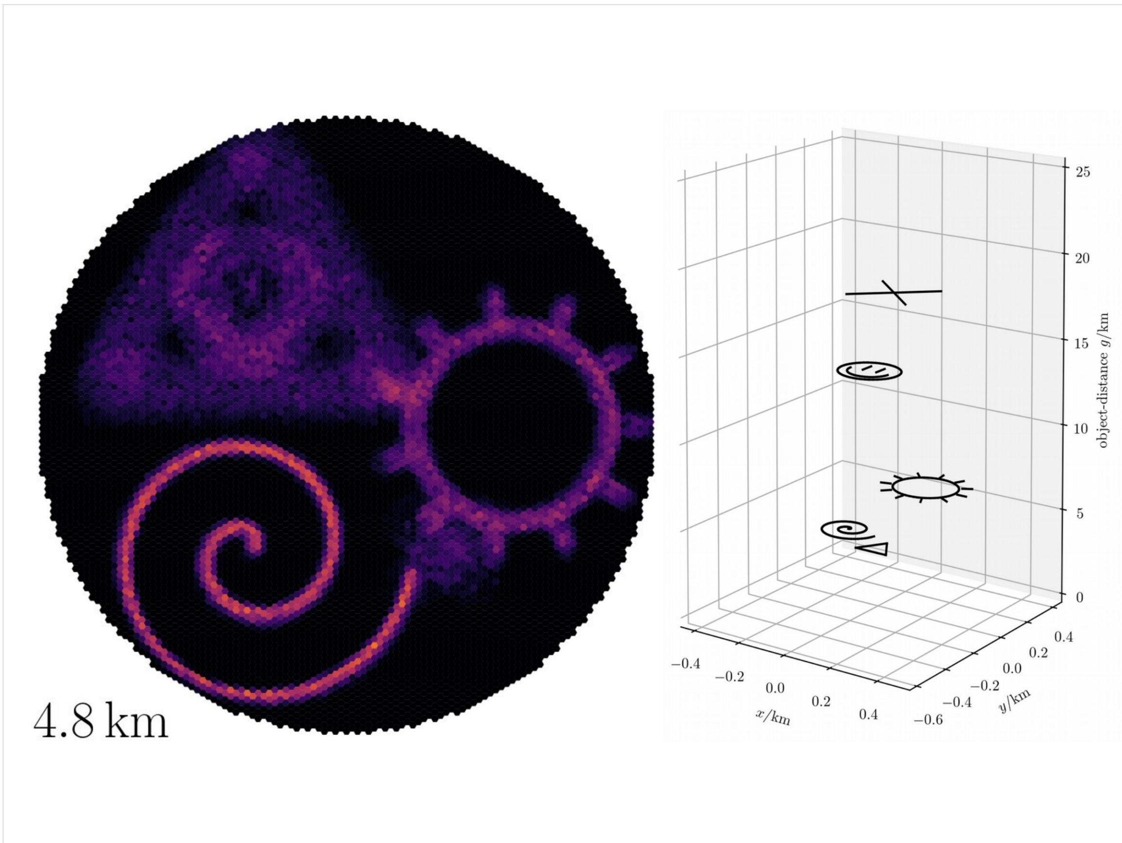

The spiral...

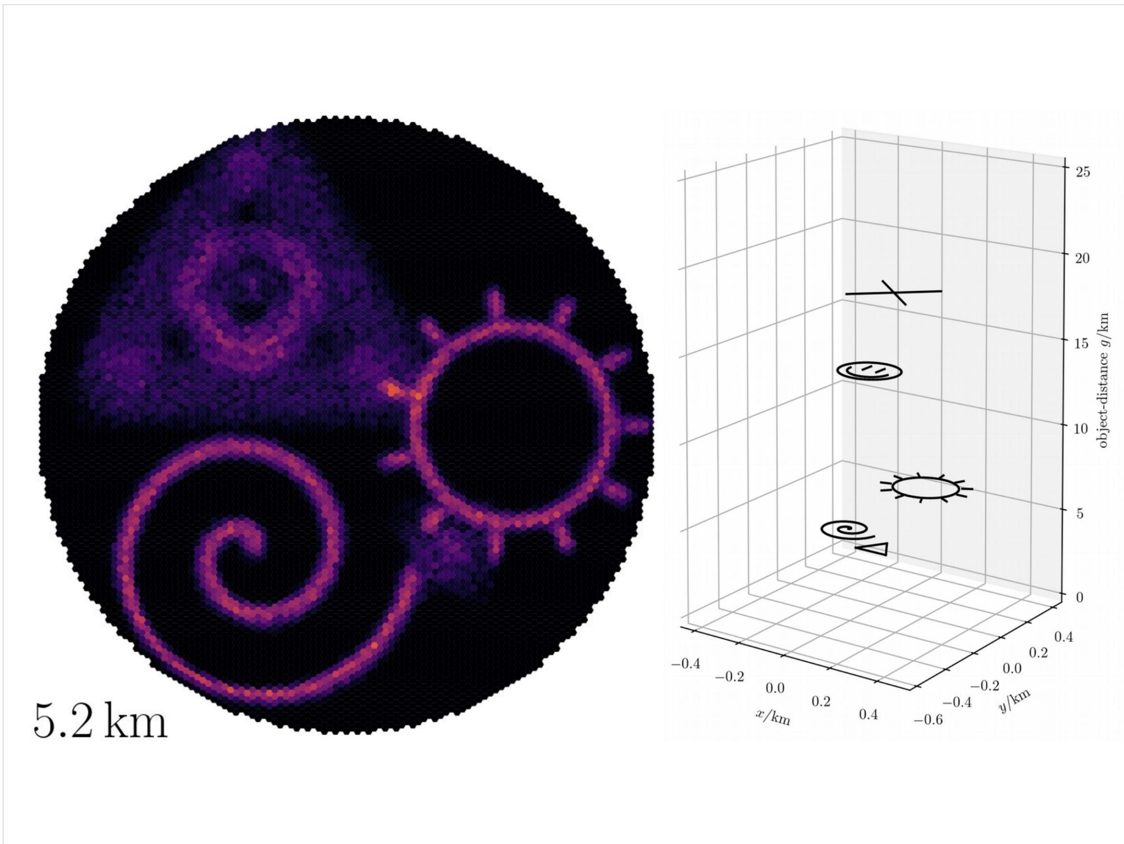
5.2 km
object-distance g/km
x/km
y/km

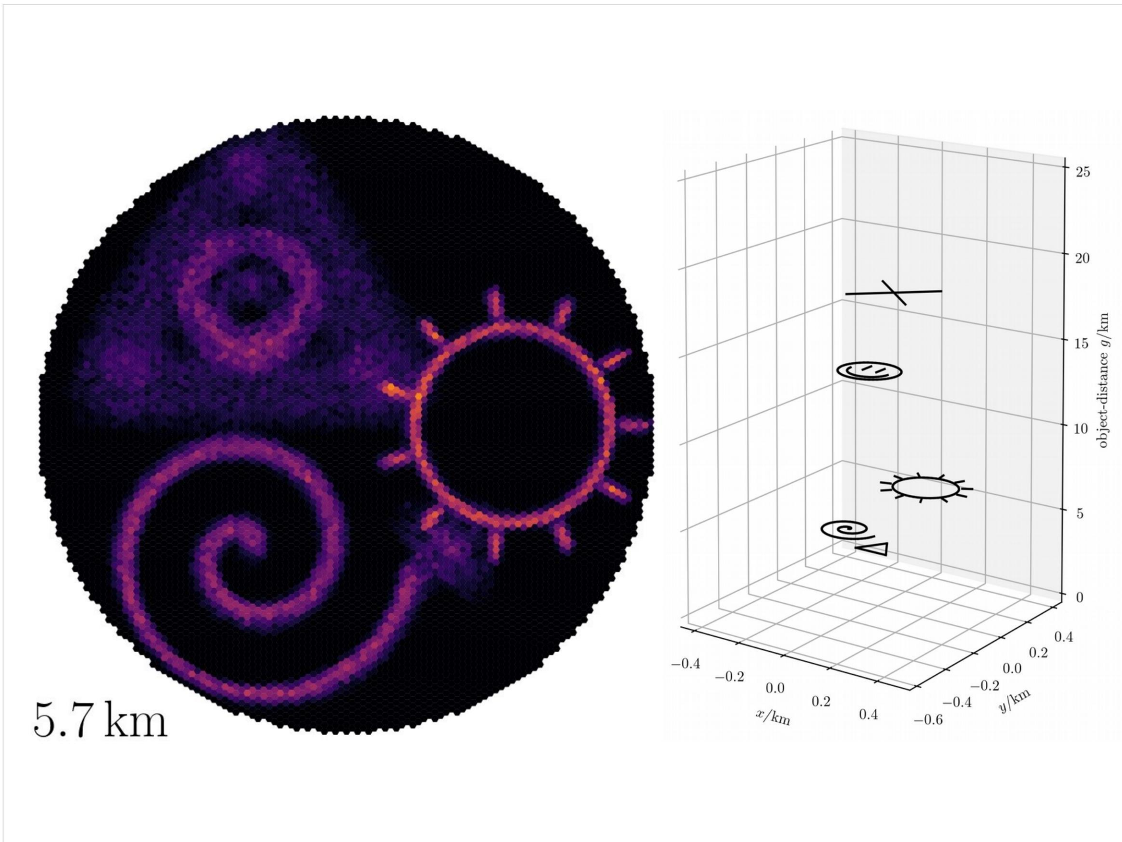
5.7 km
25
20
15
10
5
0
object-distance g/km
−0.4
−0.2
0.0
0.2
0.4
x/km
−0.6
−0.4
−0.2
0.0
0.2
0.4
y/km

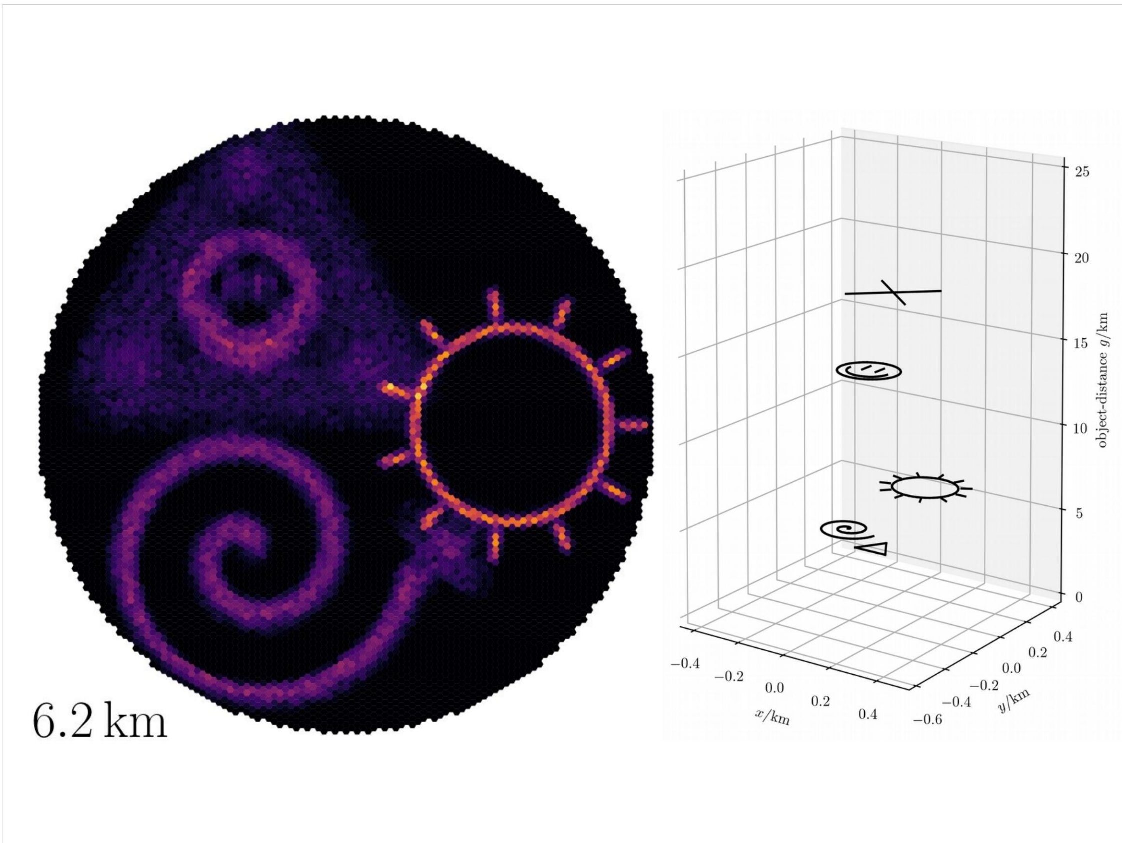

6.2 km
object-distance g/km
x/km
y/km

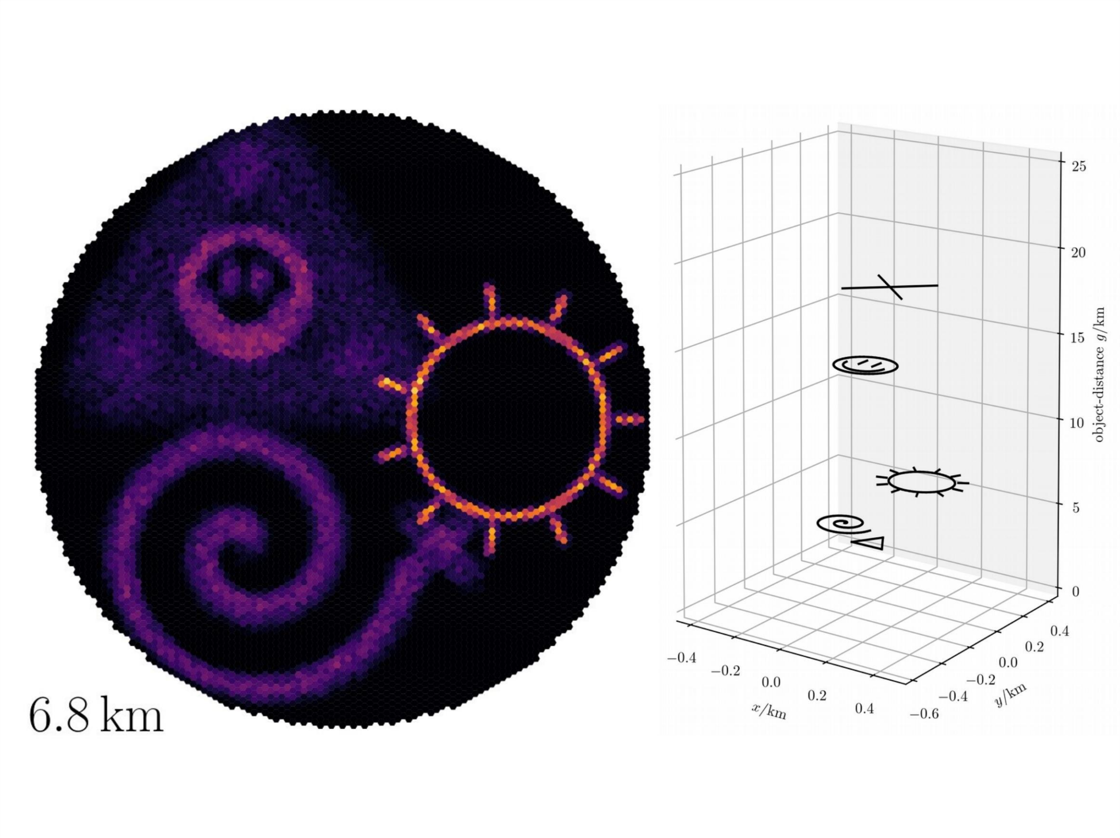
6.8 km
object-distance g/km
x/km
y/km
25
20
15
10
5
0
−0.4
−0.2
0.0
0.2
0.4
−0.6

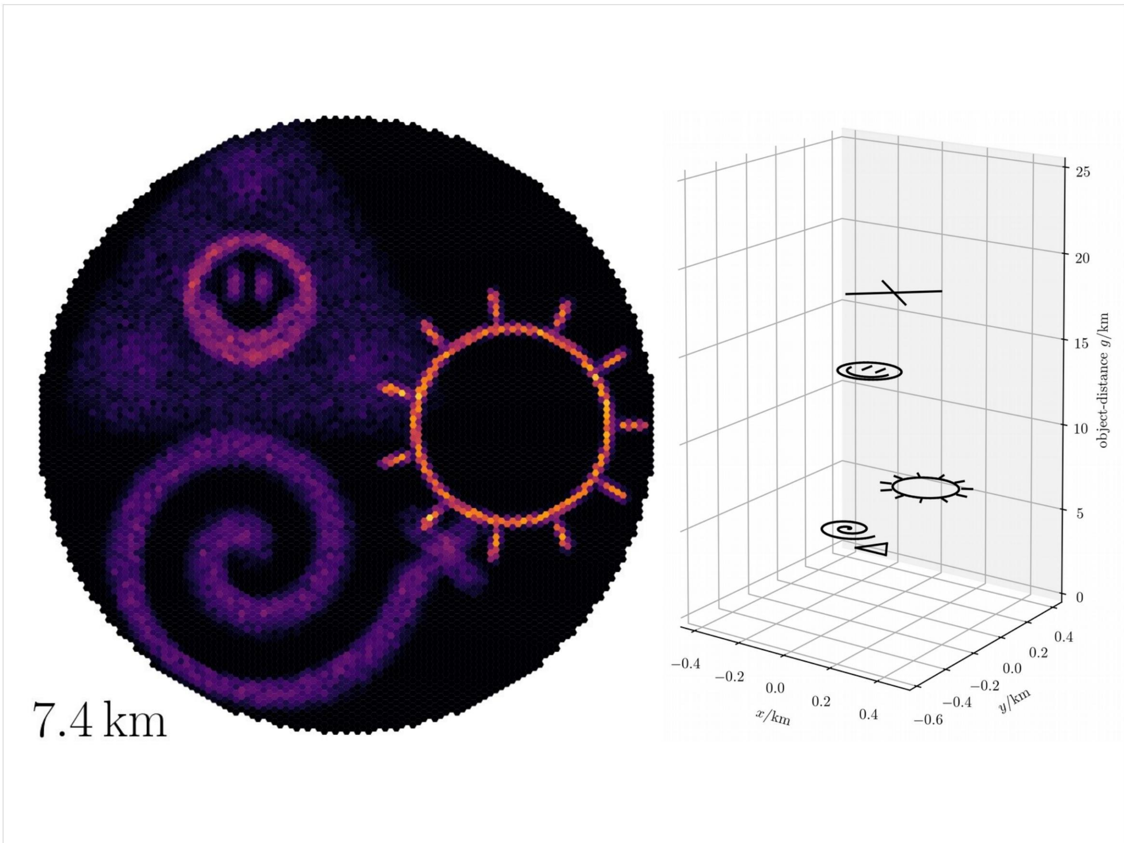

The sun symbol...

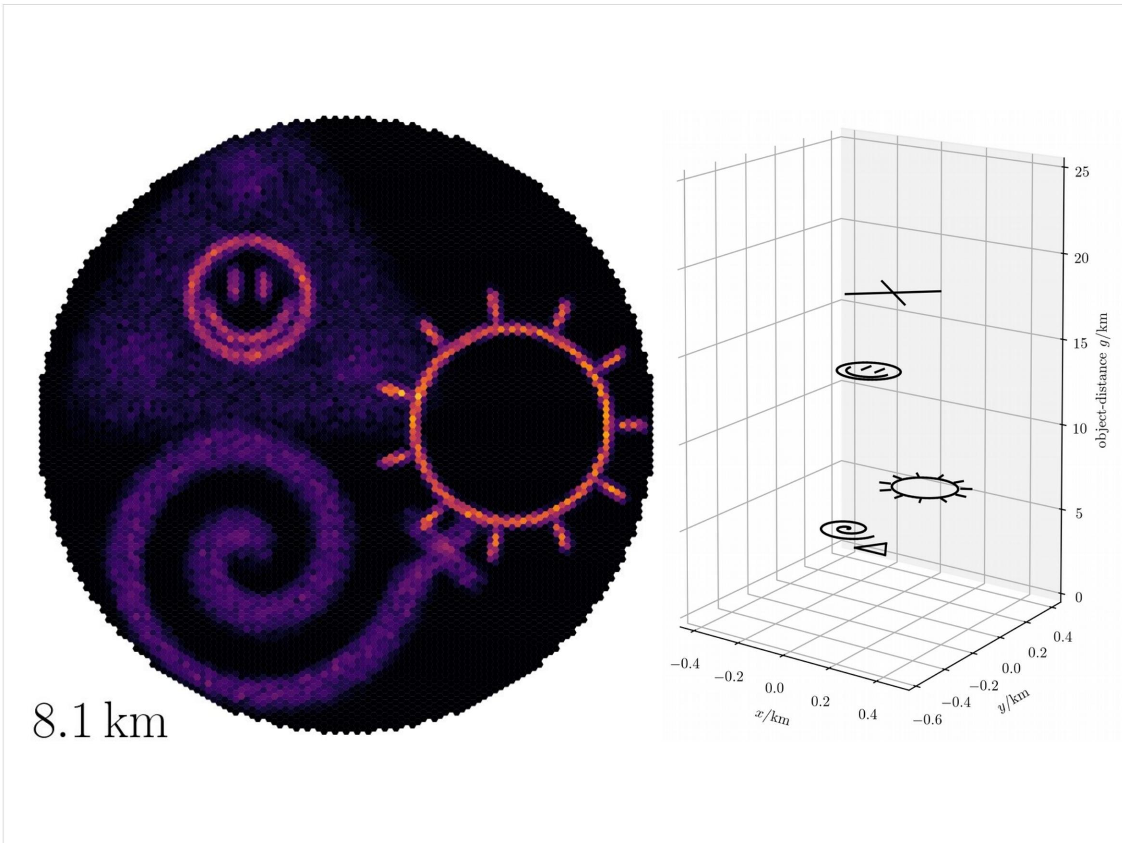

8.1 km
object-distance g/km
x/km
y/km

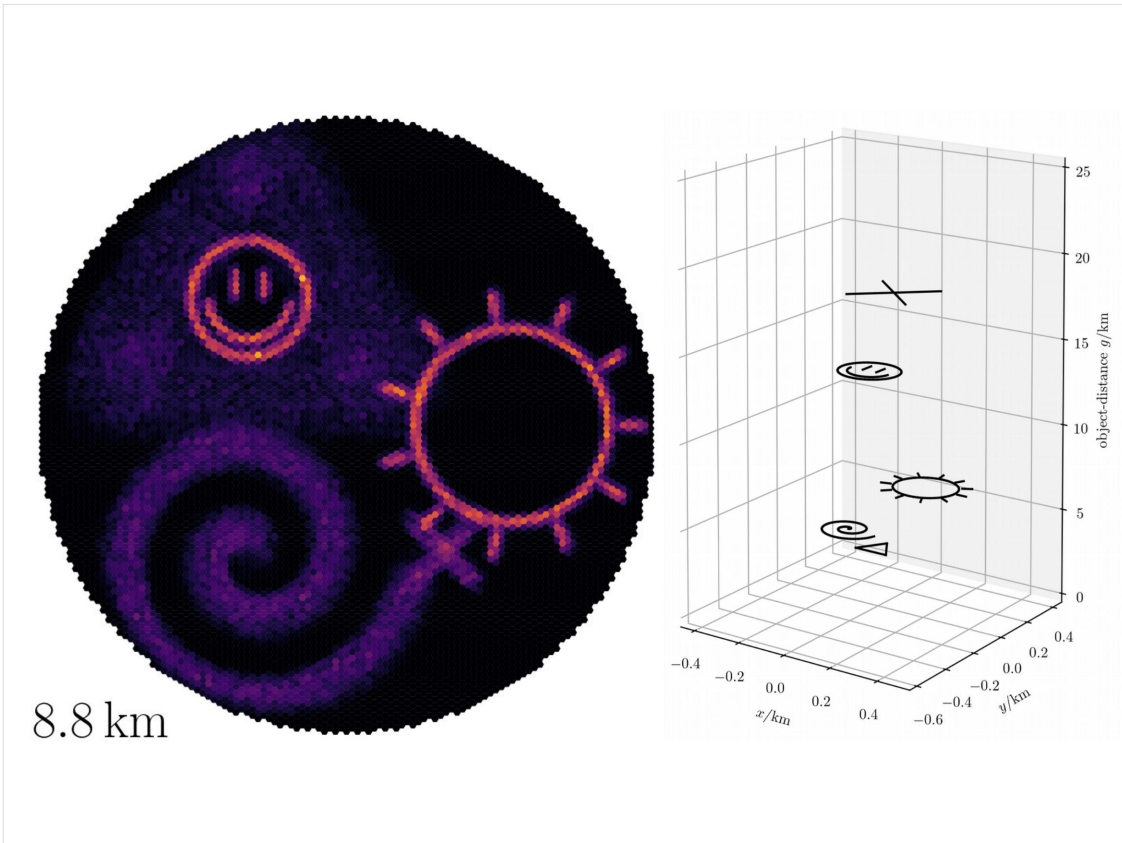
8.8 km
object-distance g/km
x/km
y/km

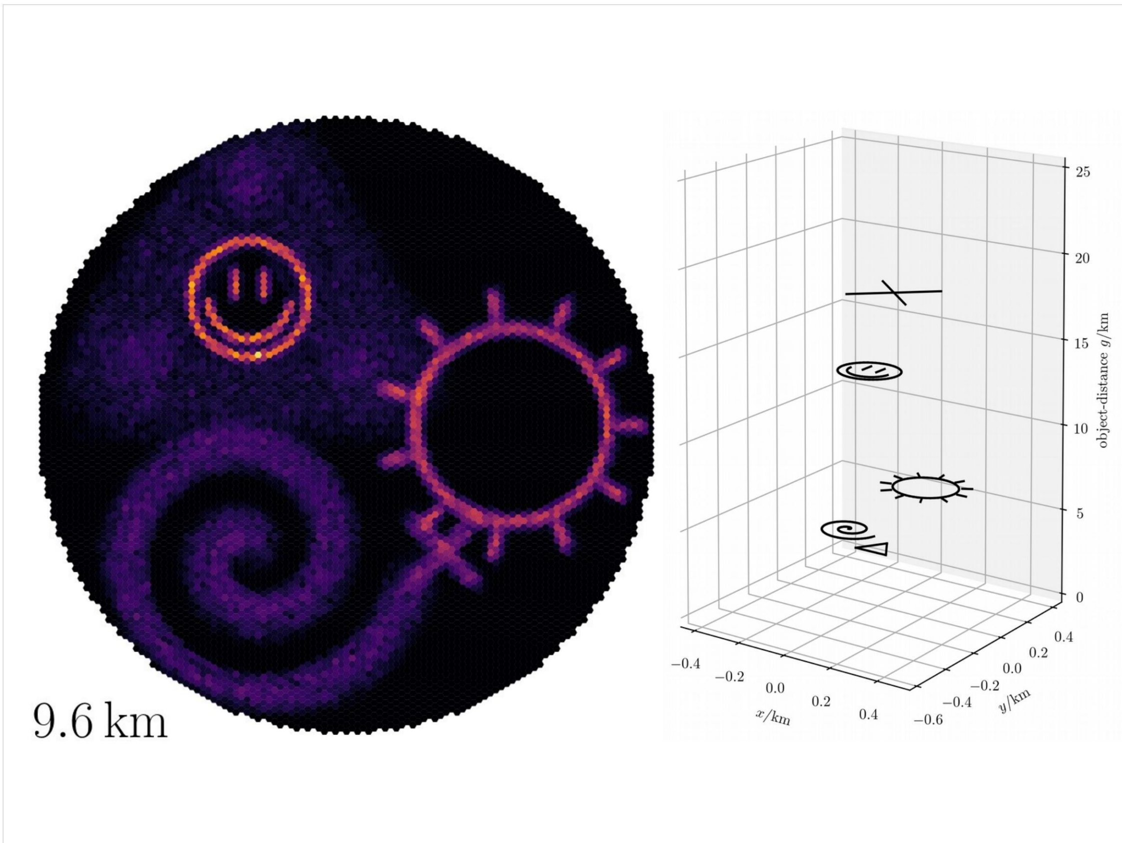
9.6 km
object-distance g/km
x/km
y/km

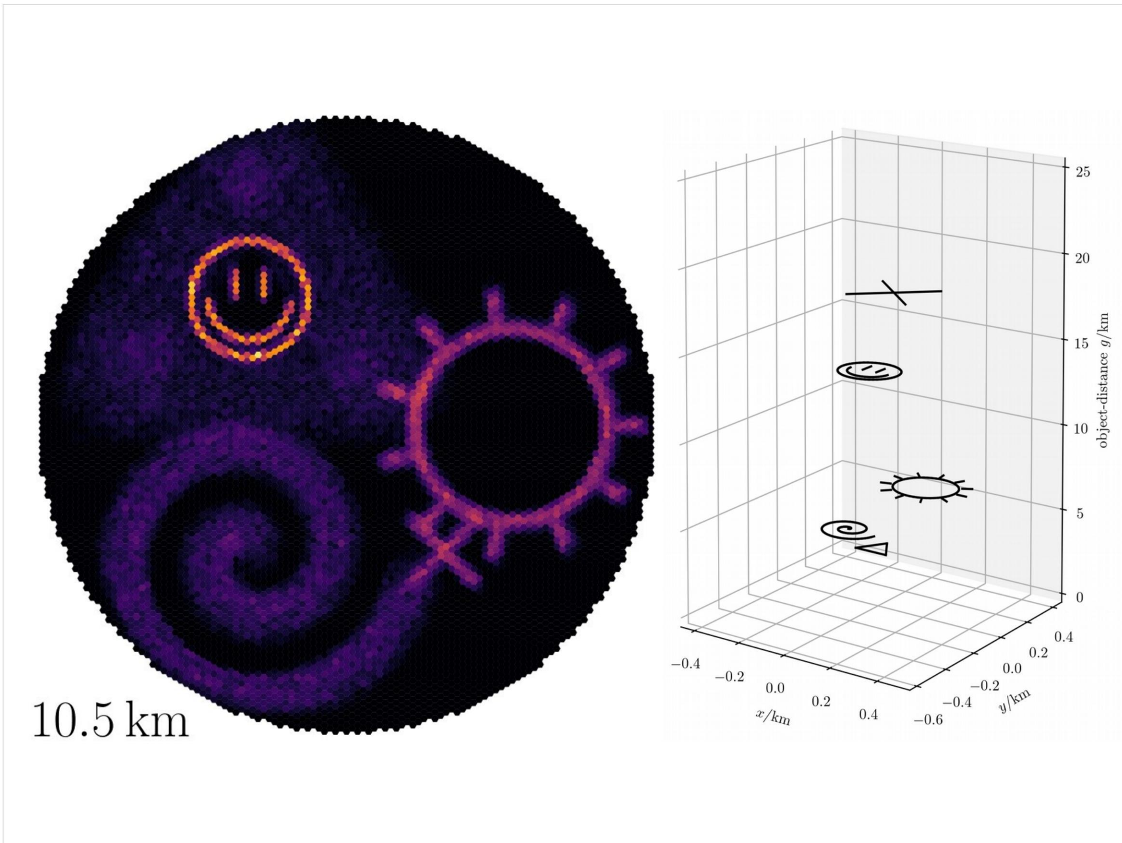

10.5 km
object-distance g/km
x/km
y/km

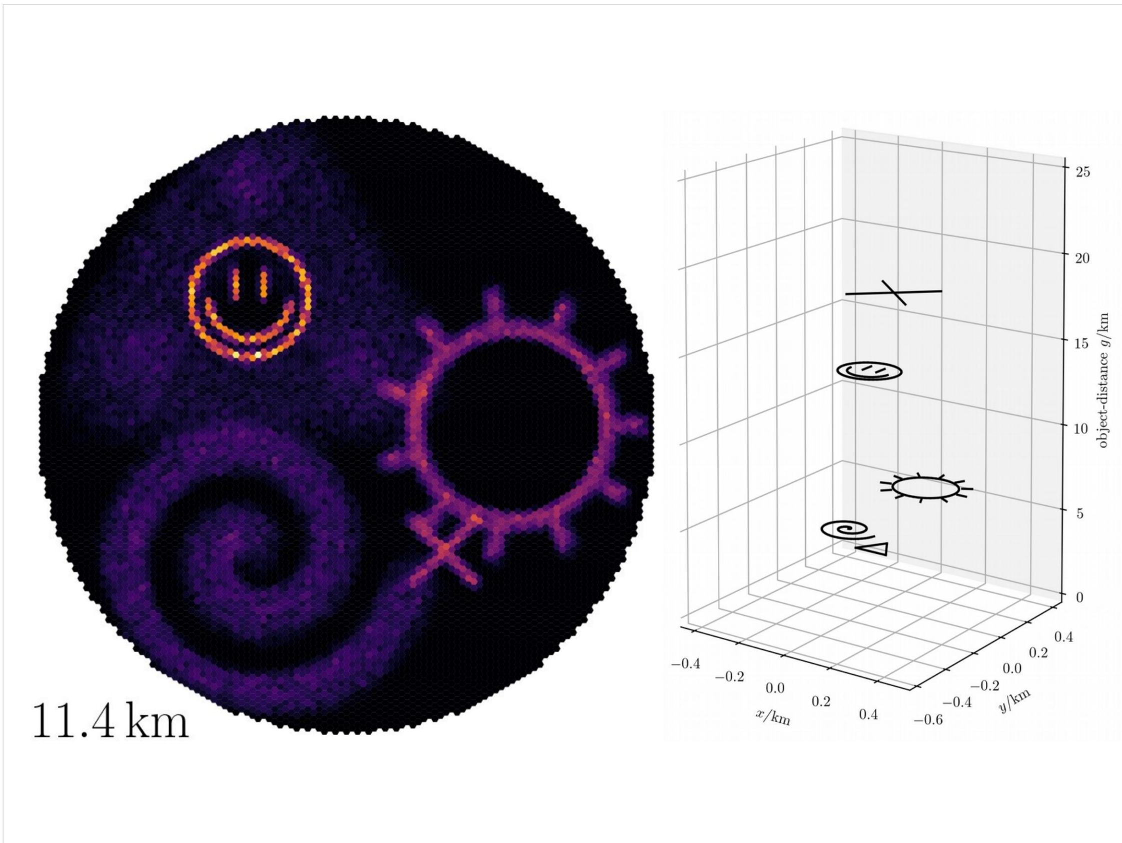

The smiley…

Where is the triangle?

It is gone.

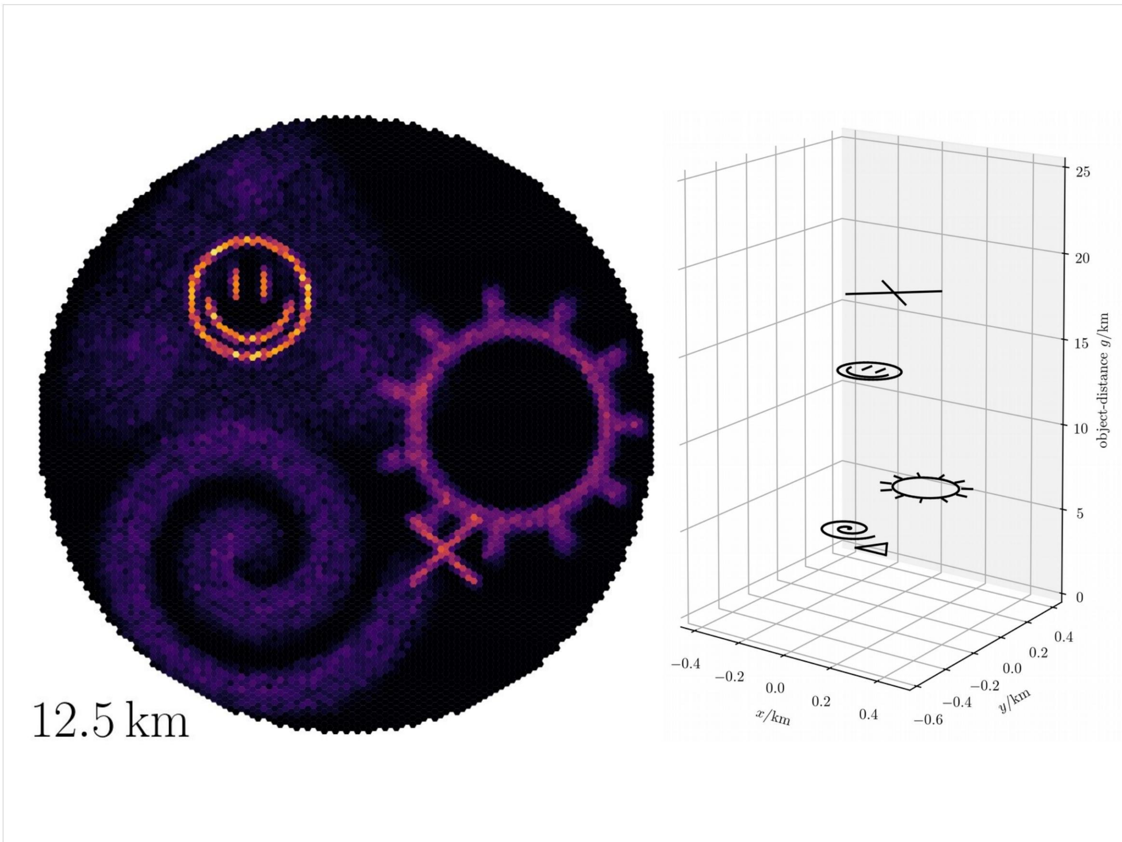
12.5 km
object-distance g/km
x/km
y/km

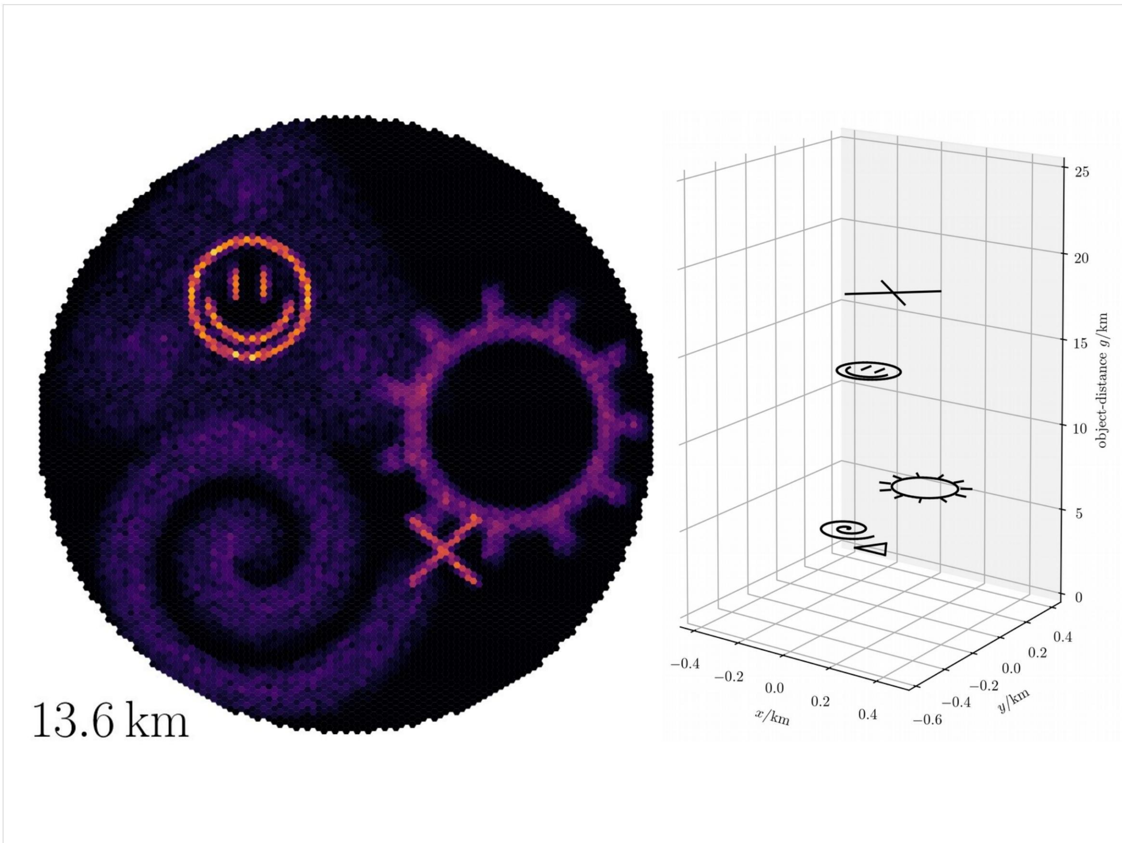
13.6 km
object-distance g/km
x/km
y/km

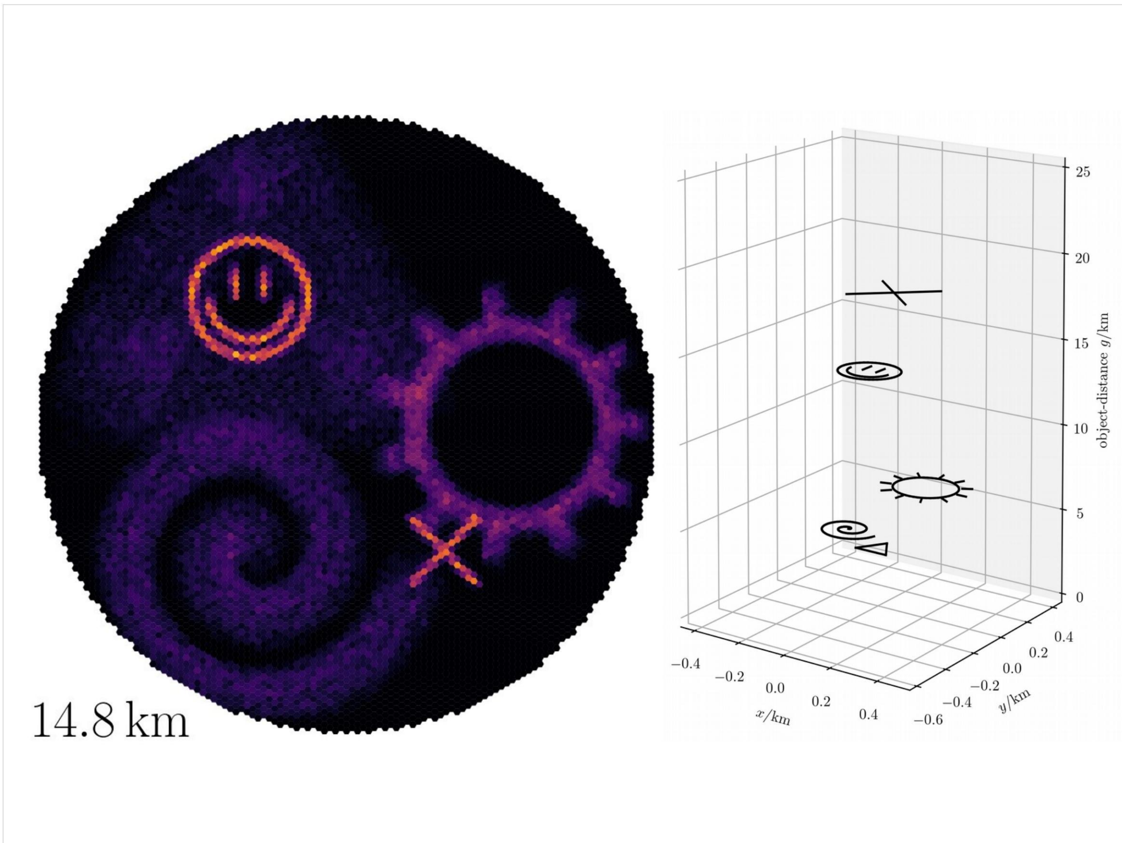
14.8 km
object-distance g/km
x/km
y/km

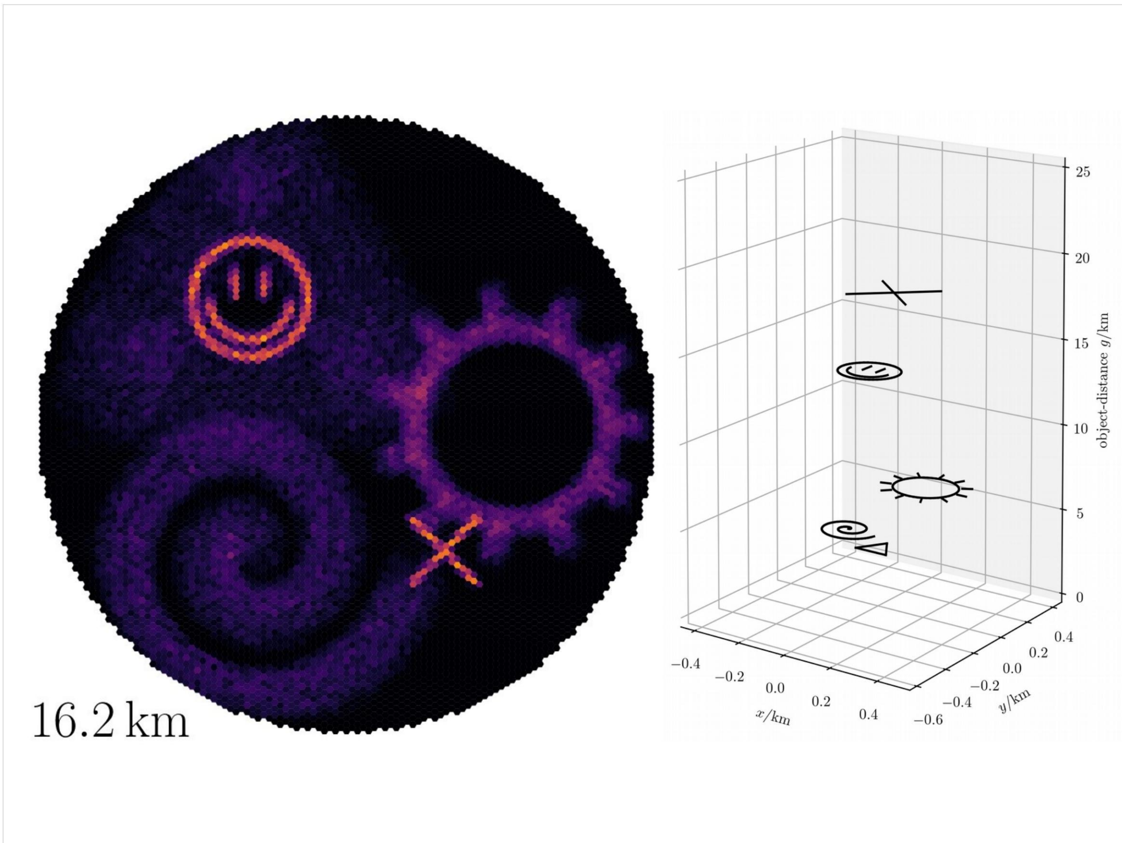
16.2 km
object-distance g/km
x/km
y/km
0
5
10
15
20
25
−0.4
−0.2
0.0
0.2
0.4
−0.6
−0.4
−0.2
0.0
0.2
0.4

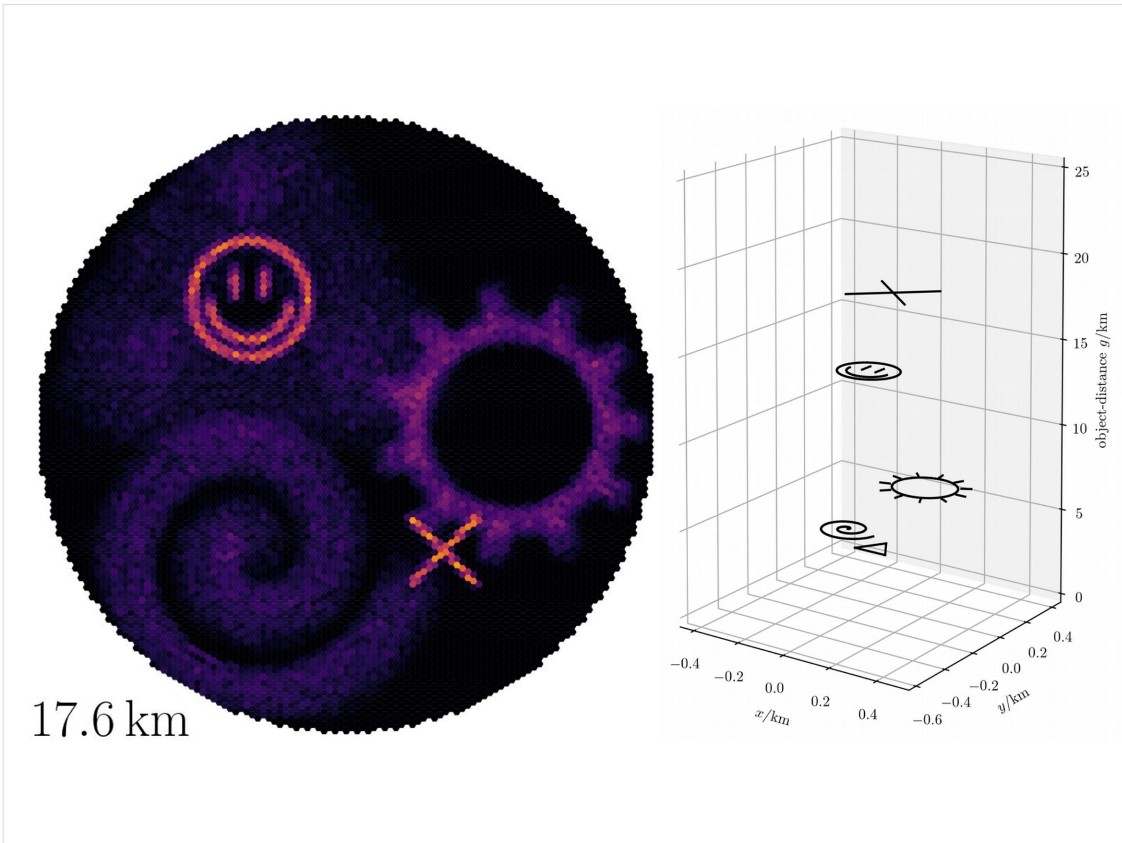

17.6 km
object-distance g/km
x/km
y/km

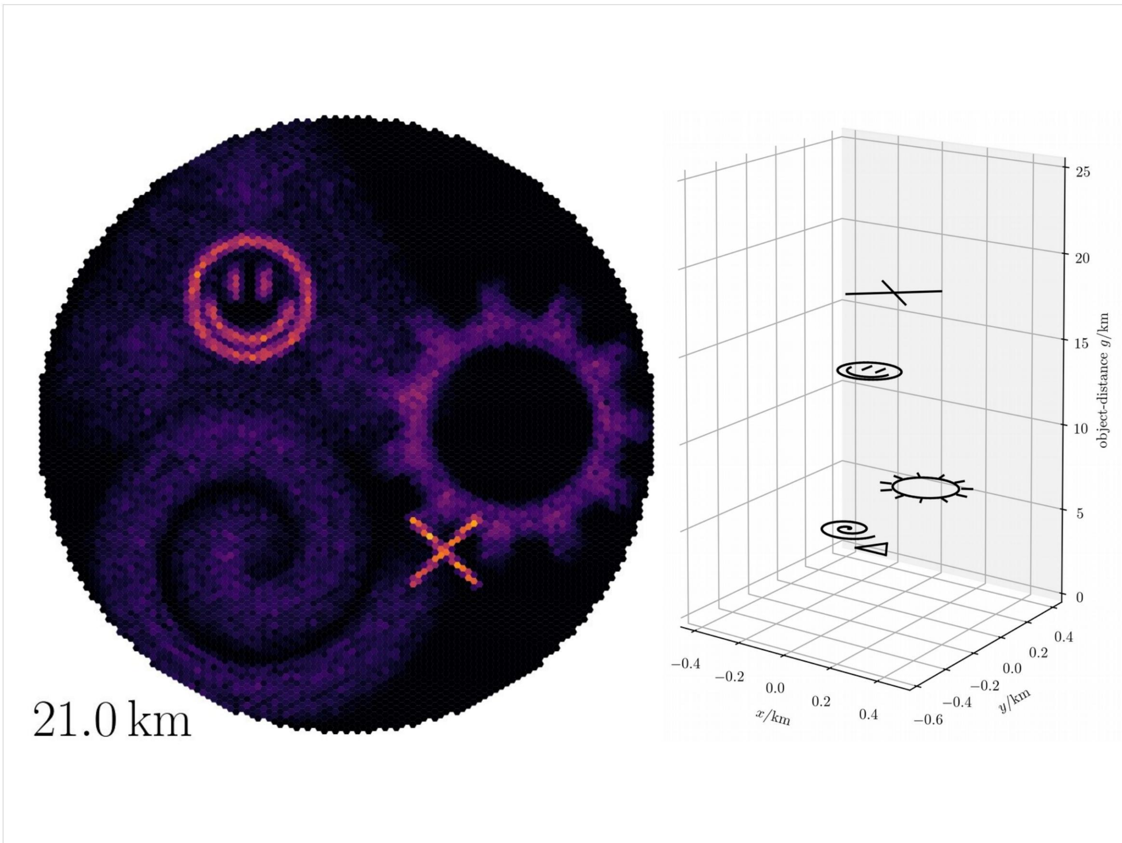
21.0 km
object-distance g/km
x/km
y/km
−0.4
−0.2
0.0
0.2
0.4
−0.6
0
5
10
15
20
25

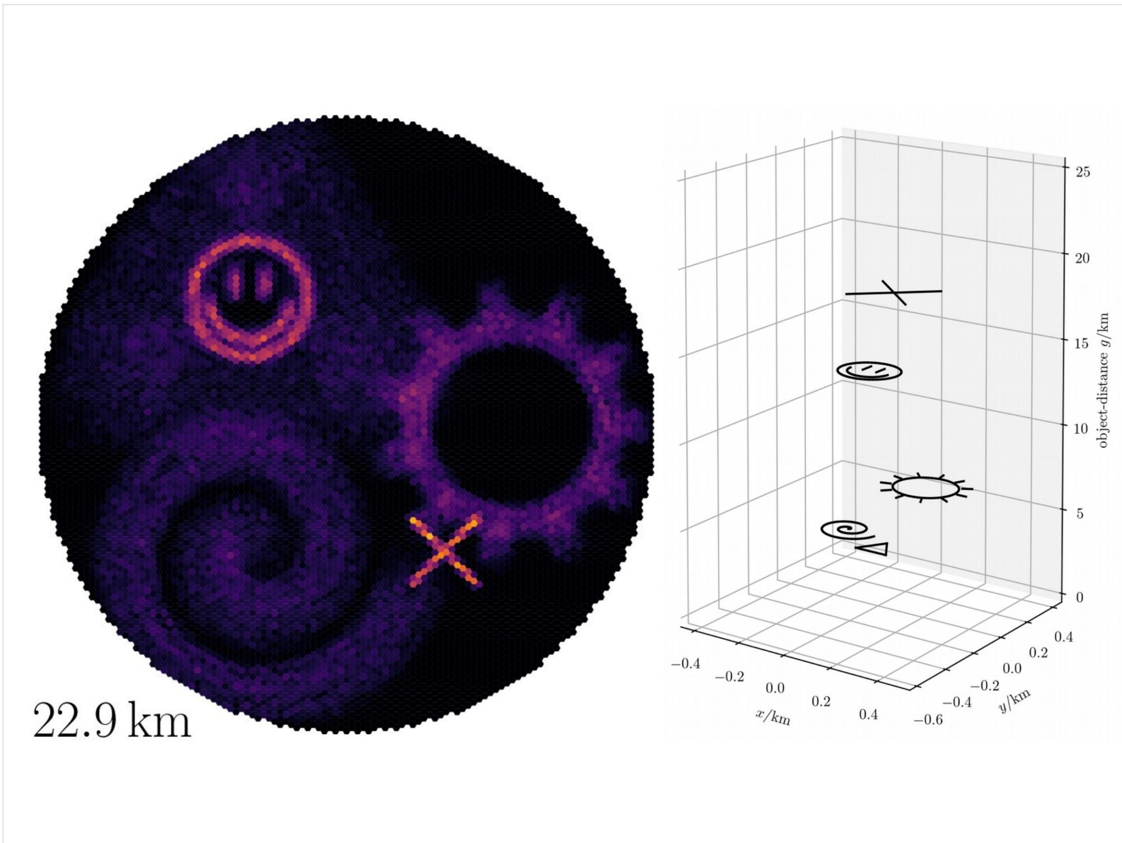
22.9 km
object-distance g/km
x/km
y/km

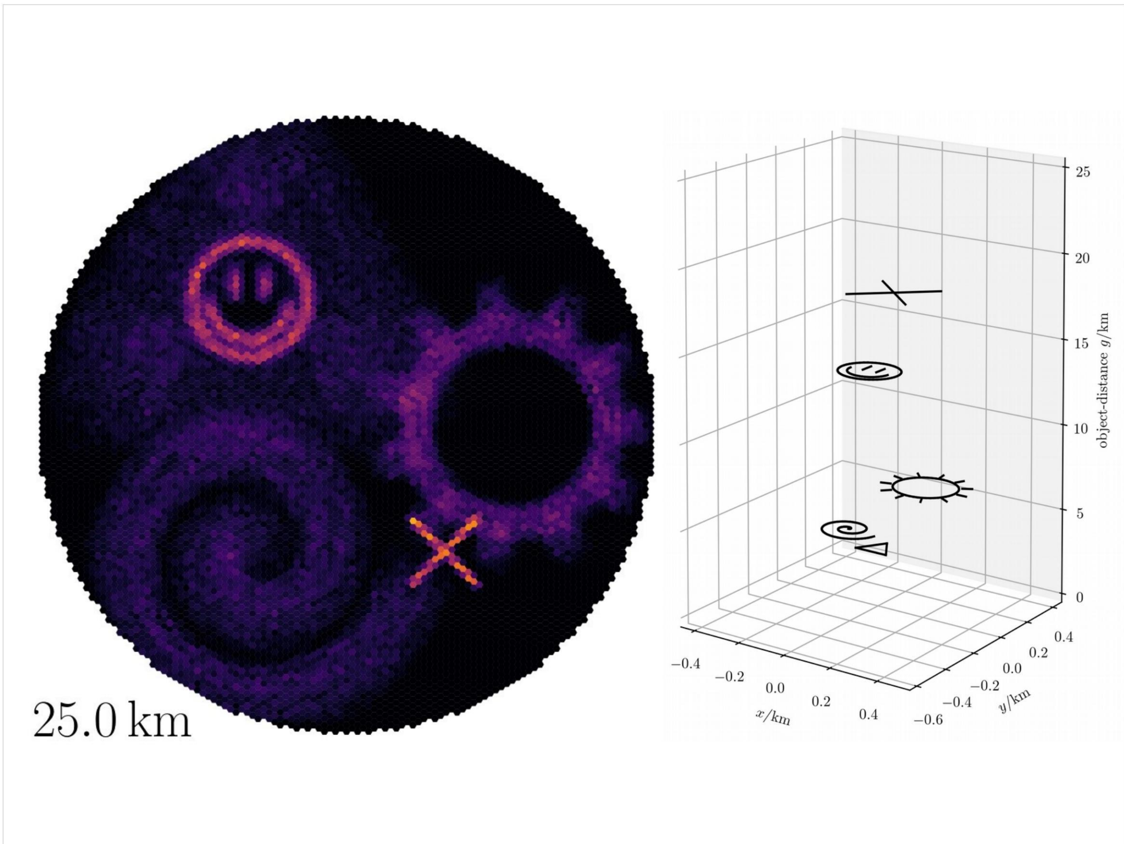

And the cross.

The Cherenkov-plenoscope turns a narrow depth-of-field into three-dimensional reconstruction-power for air-showers.

(Once more back and forth through the refocused images)

Note the flat field-of-view, note how the spiral and the sun-symbol look the same in the inner and outer regions of the field-of-view.

Light-Field-Microscopy

Marc Levoy Ren Ng Andrew Adams Matthew Footer Mark Horowitz

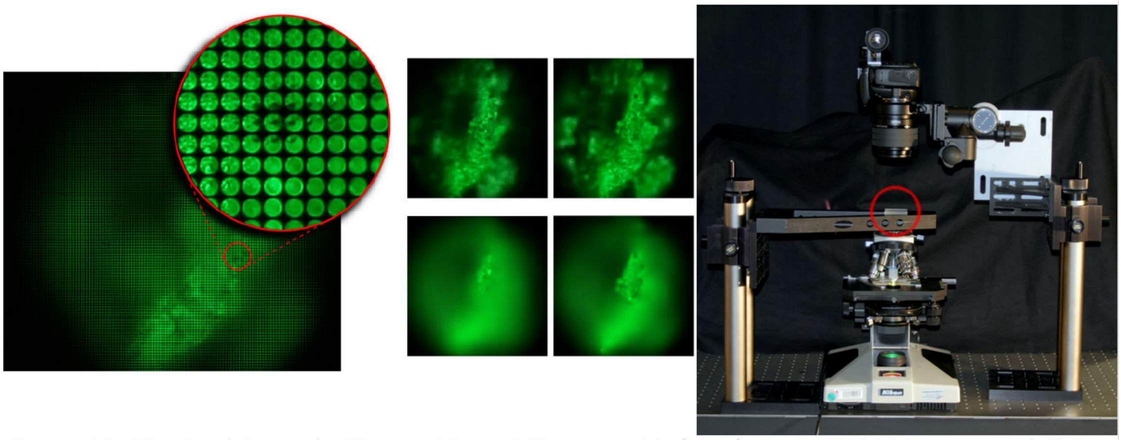

Levoy, M., Ng, R., Adams, A., Footer, M., and Horowitz, M. (2006). Light Field Microscopy. ACM Transactions on Graphics (TOG), SIGGRAPH, 25(3):924–934.

Light-field-microscopy,

Narrow-angle-tomography,

Focus-stack-deconvolution,

are three different names for the same mathematical procedure which can now be directly adopted to reconstruct air-showers with the Portal Cherenkov-plenoscope.

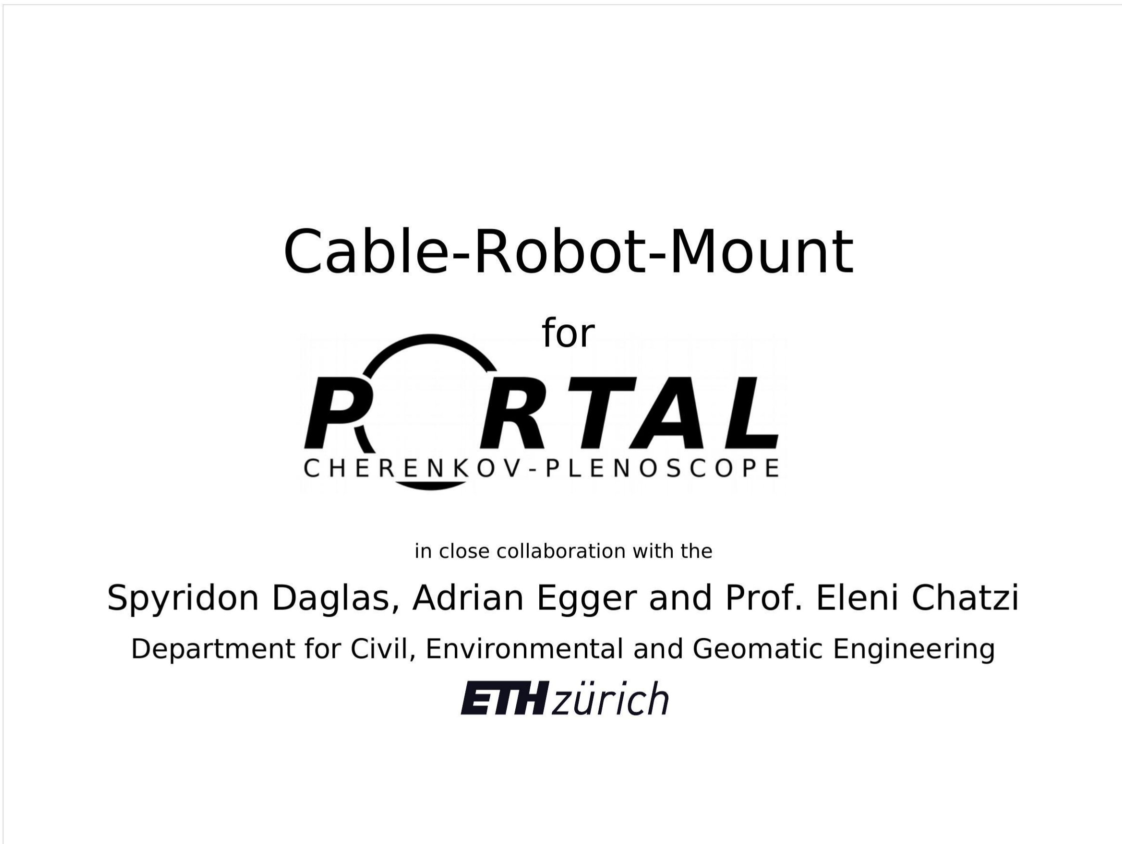

Cable-robot-mount

In close collaboration with Spyridon Daglas, Adrian Egger, and Professor Eleni Chatzi from the department for Civil, Environmental, and Geomatic Engineering at ETH-Zurich.

Since Porta’s light-field-sensor can compensate misalignments, we decouple the light-field-sensor from the imaging-reflector.

This way, the imaging-reflector has only to support itself and does not deform due to additional forces induced by long lever arms where the sensor-plane is mounted.

During the day, the light-field-sensor is parked on ground.

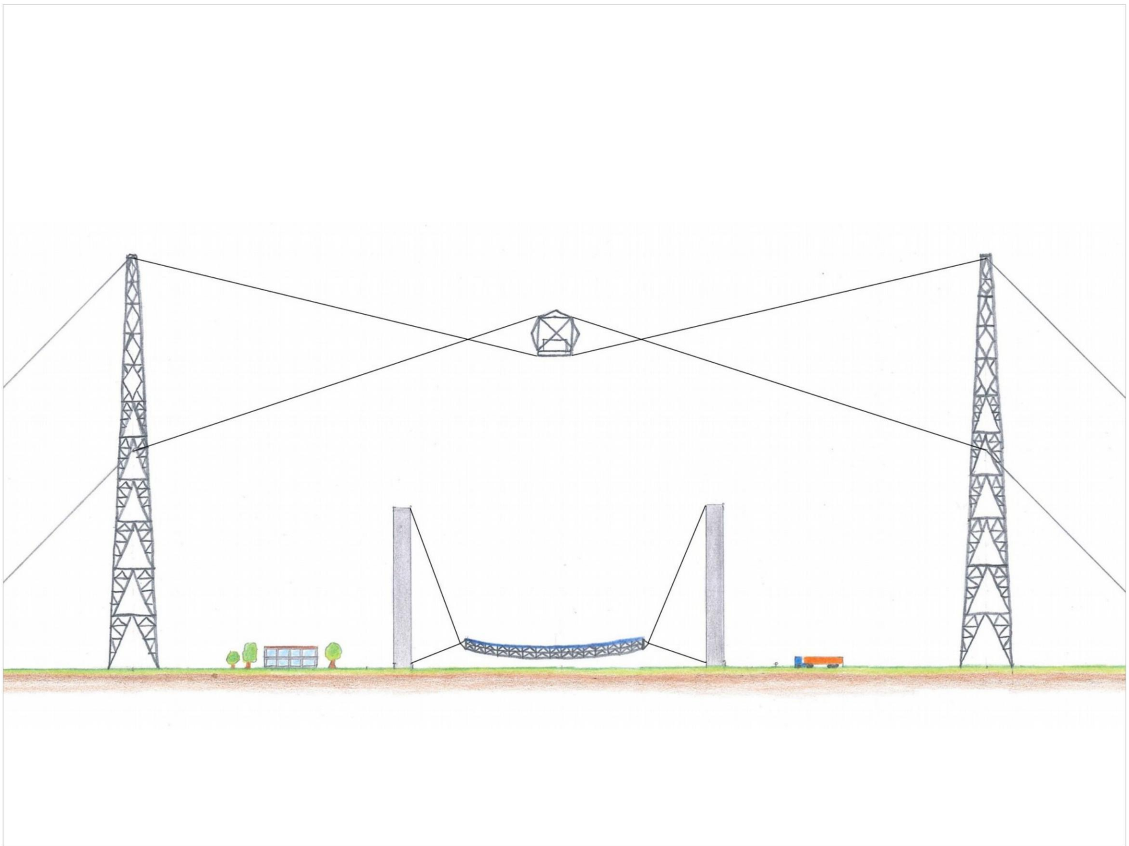

In the night, the cable-robot-mount tries to establish the desired target geometry between the imaging-reflector and the light-field-sensor.

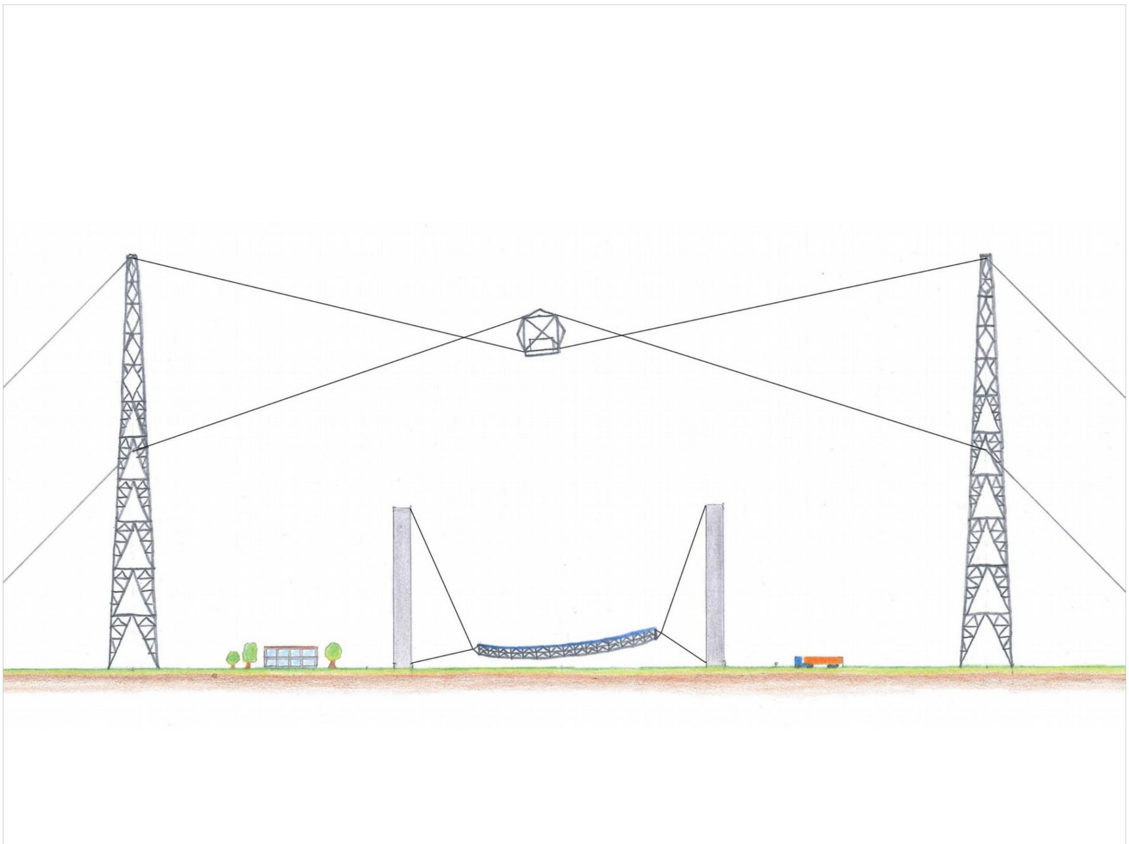

Portal’s cable-robot-mount can point up to zenith distances of forty five degrees.

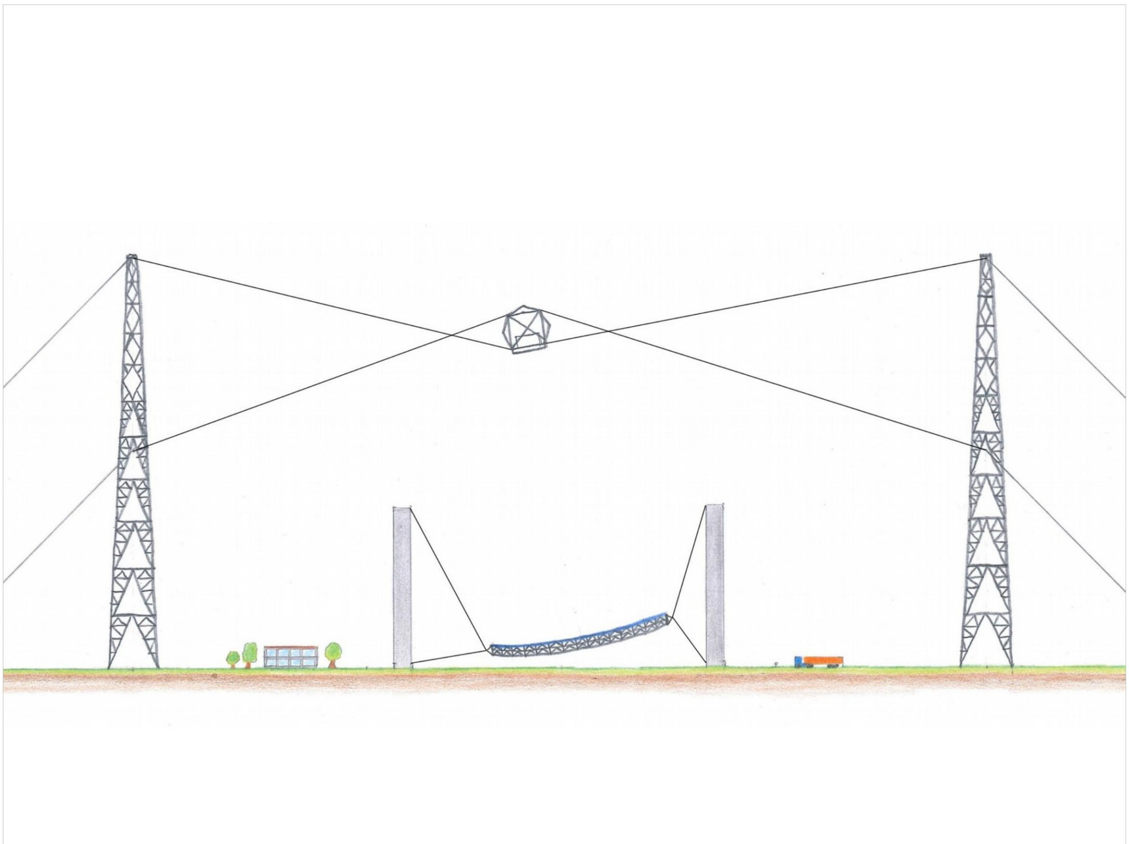

Unlike the alitute-azimuth-mount, the cable-robot-mount has no near zenith-singularity which makes it intrinsically faster for the hunt of transient-sources.

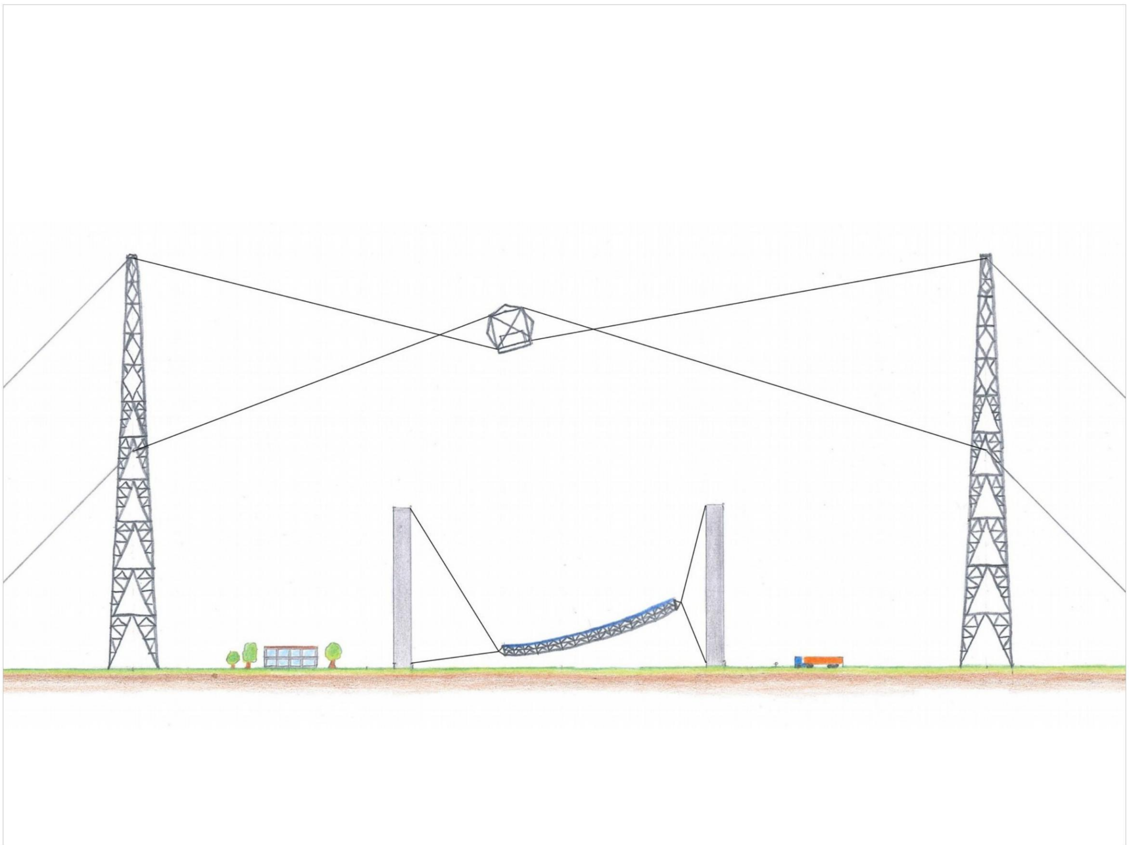

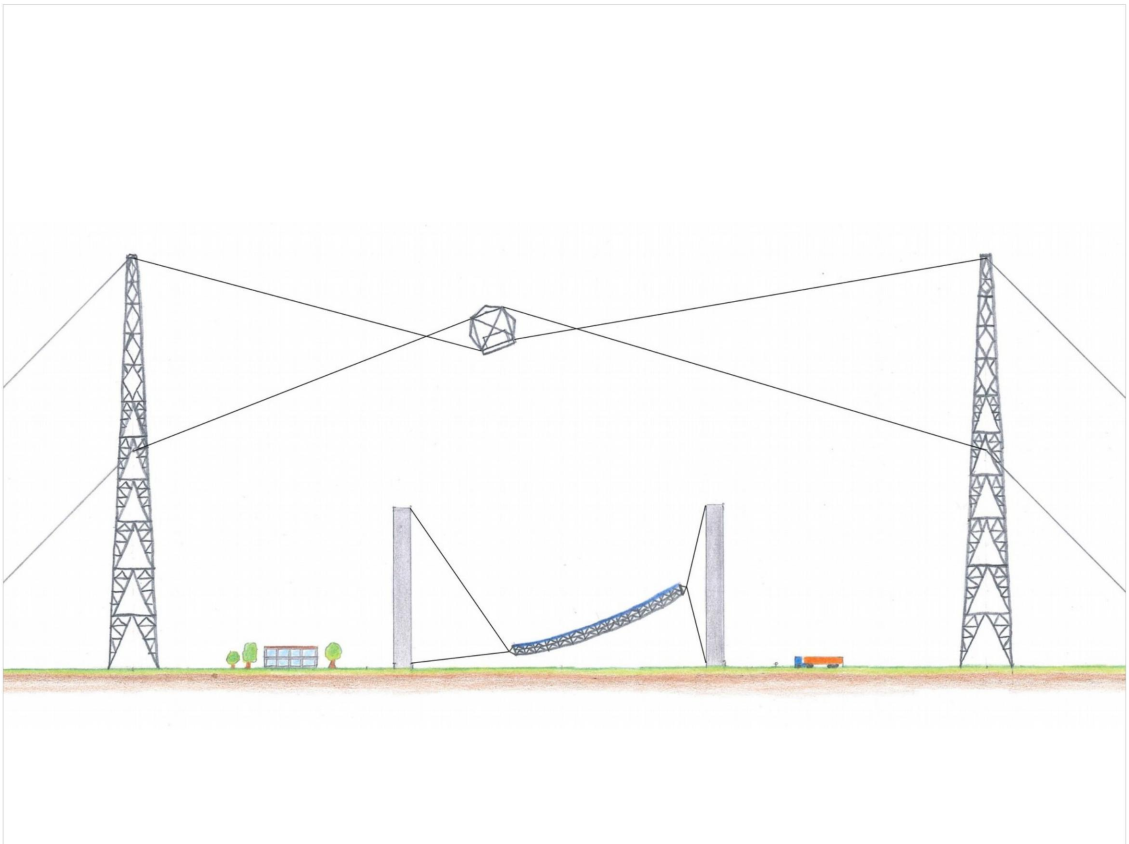

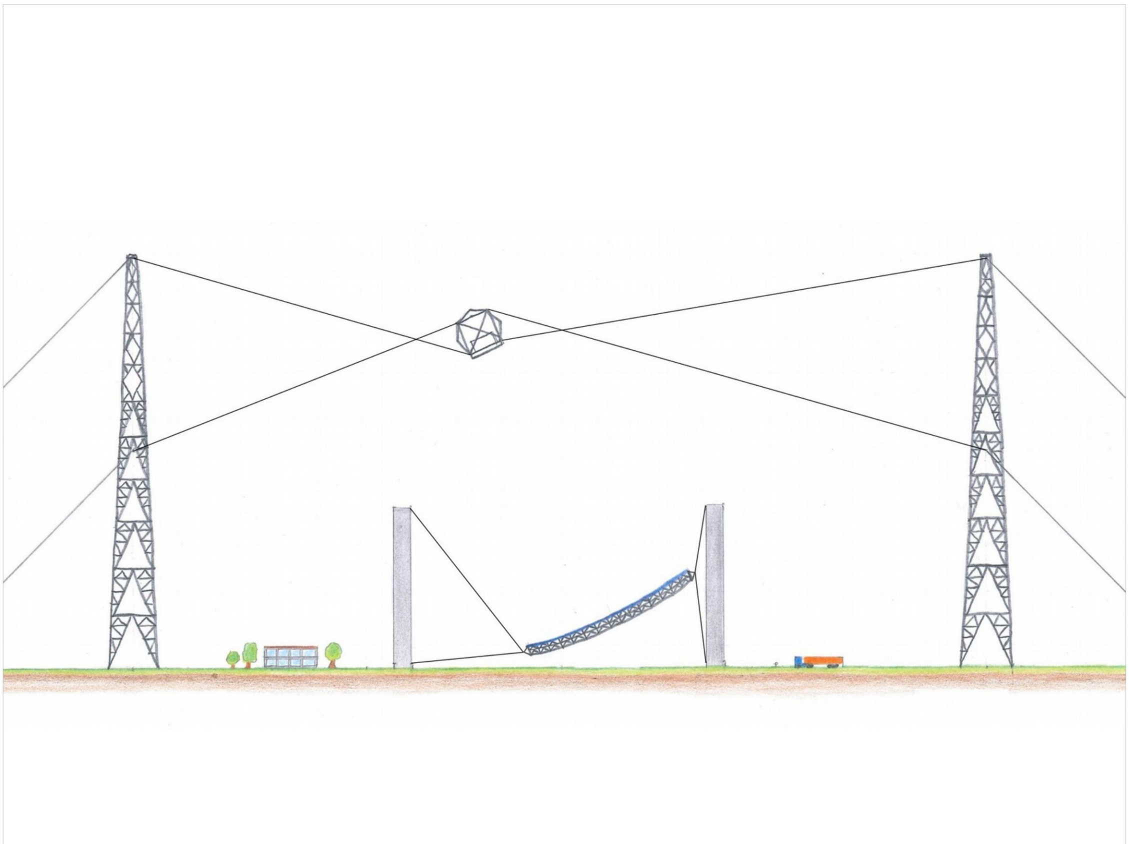

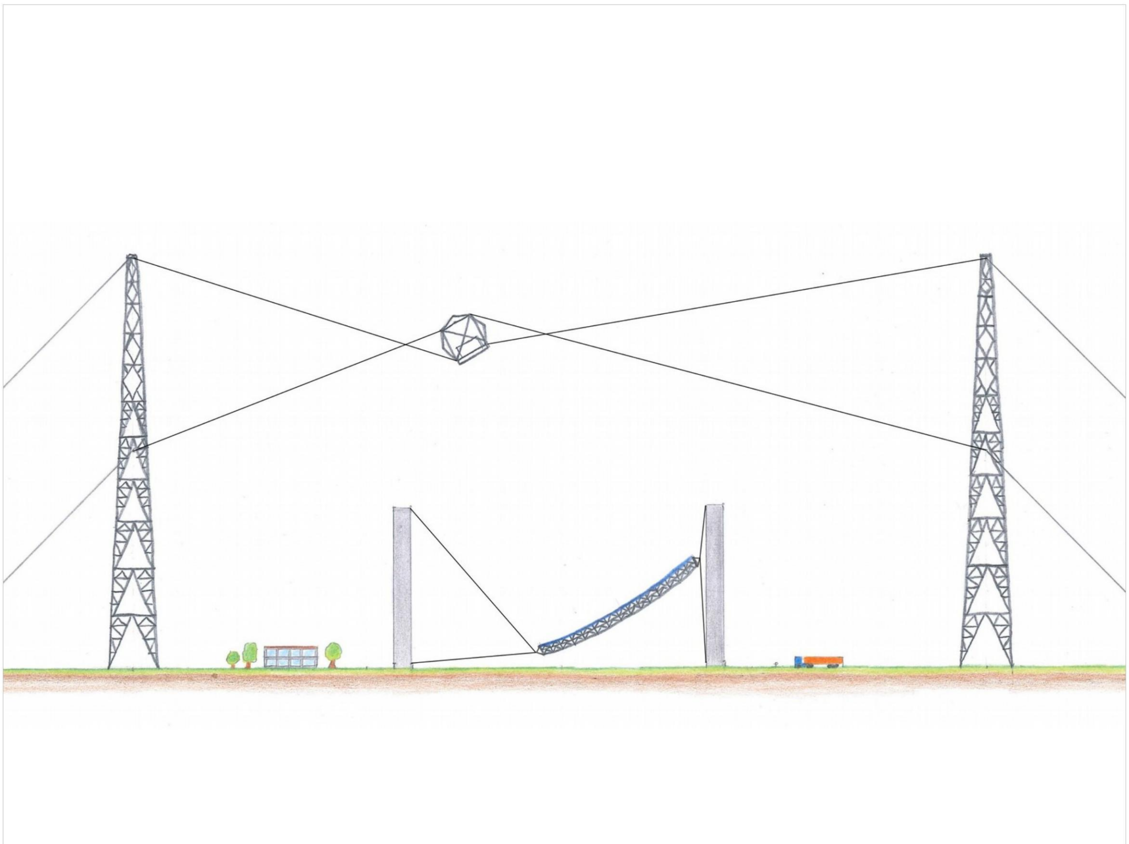

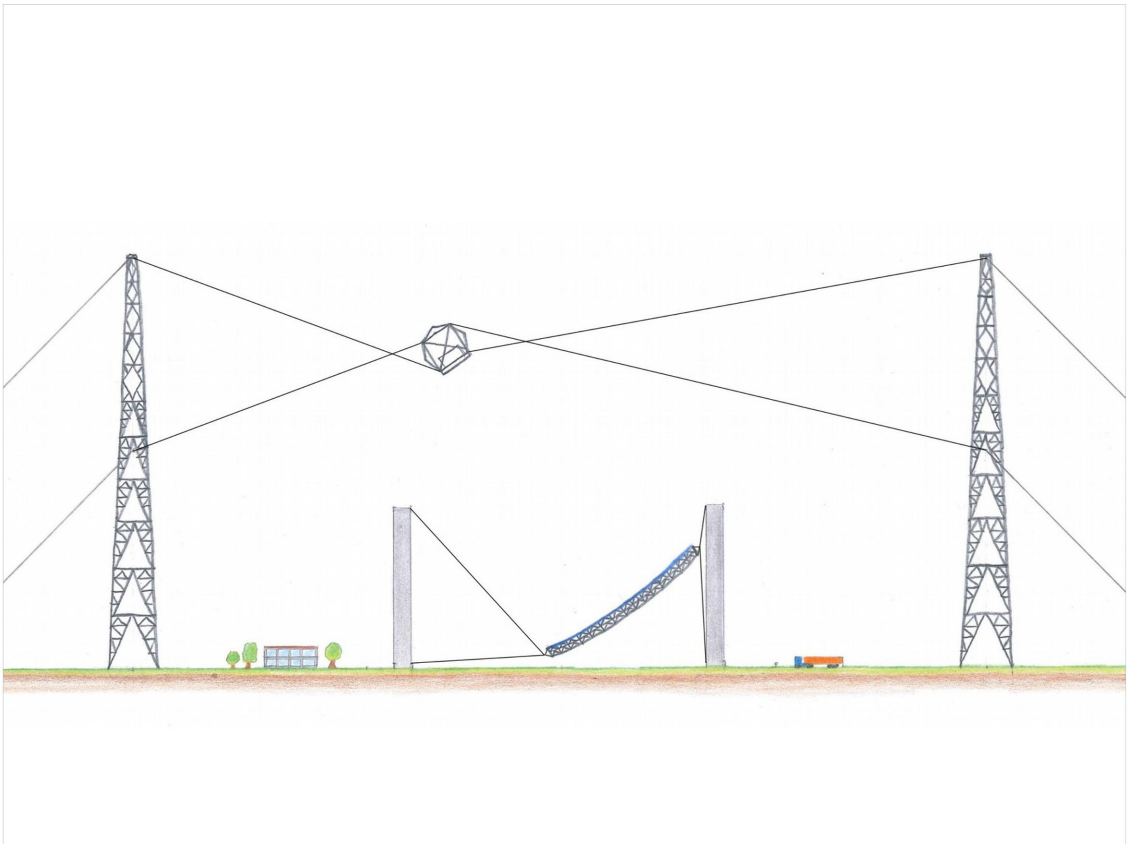

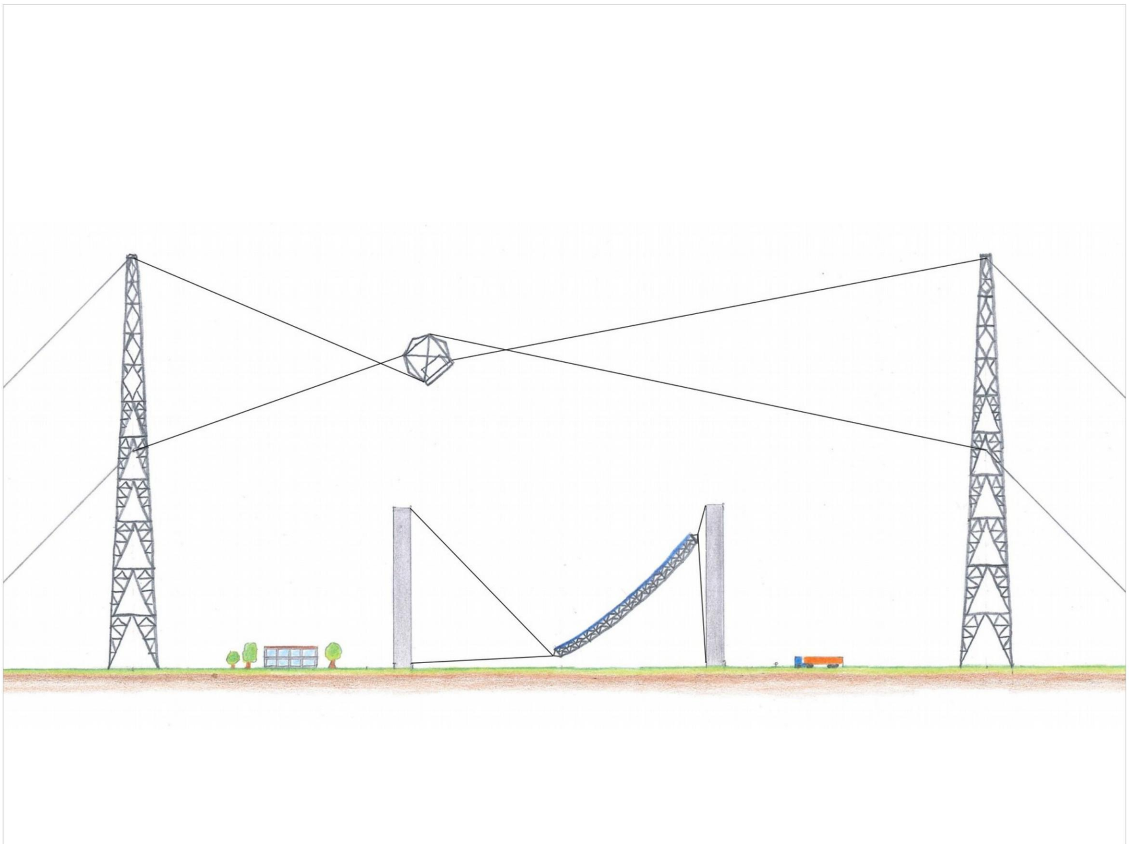

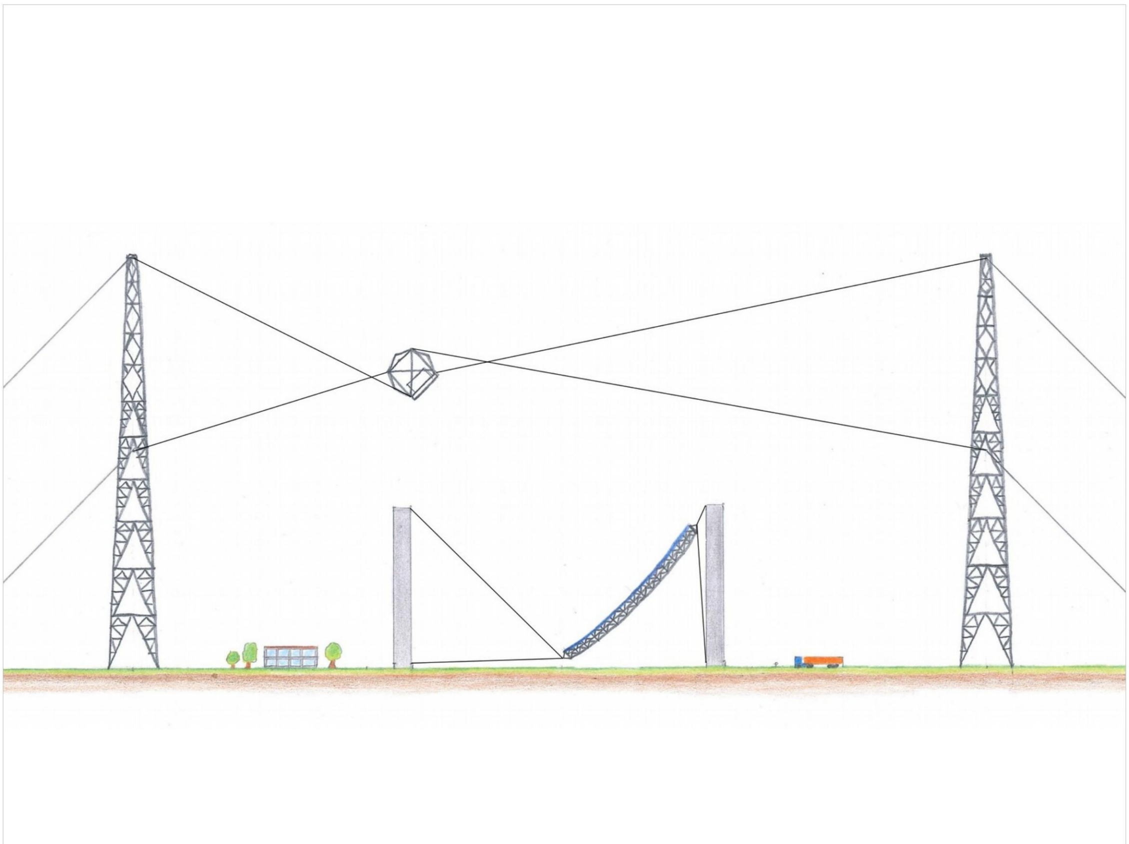

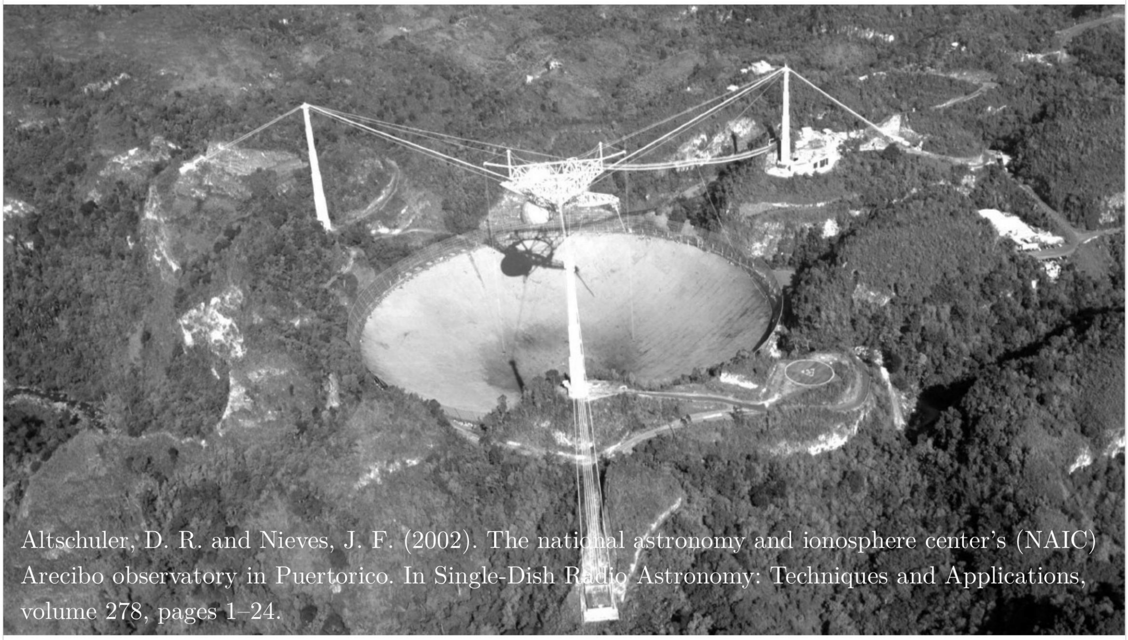

Altschuler, D. R. and Nieves, J. F. (2002). The national astronomy and ionosphere center's (NAIC) Arecibo observatory in Puertorico. In Single-Dish Radio Astronomy: Techniques and Applications, volume 278, pages 1–24.

The Cable-robot-mount is inspired by the Arecibo radio-telescope

Miermeister, P., et al. (2016). The CableRobot Simulator: Large Scale Motion Platform Based on Cable Robot Technology. In IEEE/RSJ International Conference on Intelligent Robots and Systems.

And the cable-robot-simulator, an impressive demonstration of parallel kinematics.

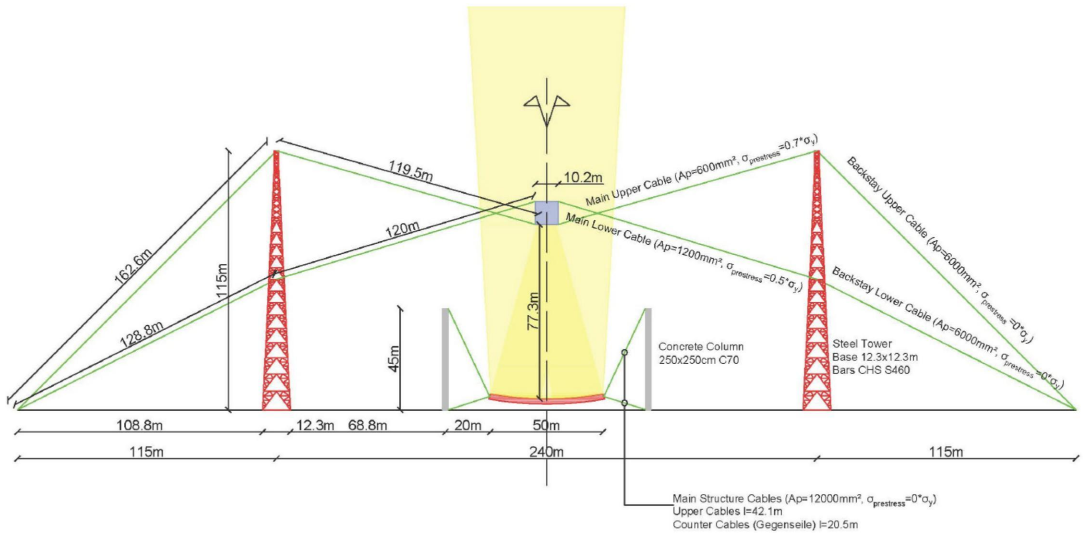

Daglas, S. (2017). Structural Optimization of a Next Generation Gamma-Ray Telescope. ETH Zurich, Research Collection, Department of Civil Engineering

Civil engineer Spyridon Daglas took my childish, and hand made drawings and contributed real engineering to the project.

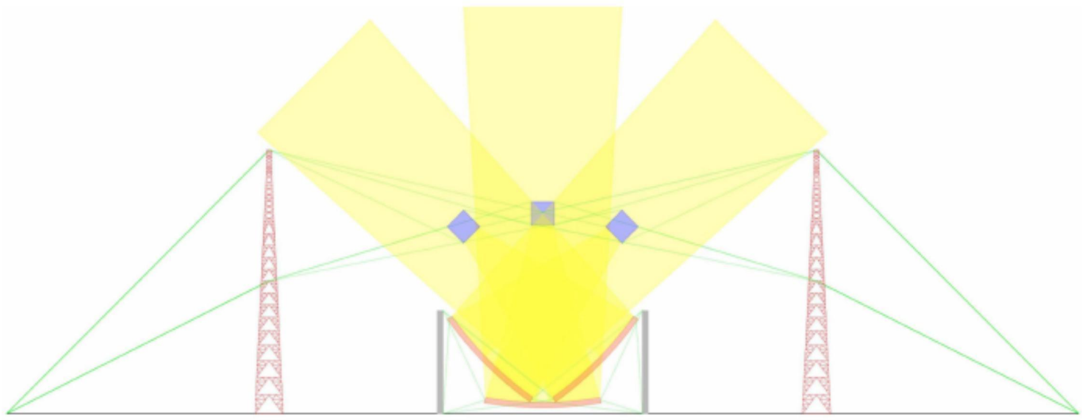

Daglas, S. (2017). Structural Optimization of a Next Generation Gamma-Ray Telescope.
ETH Zurich, Research Collection, Department of Civil Engineering

He thought about shadowing

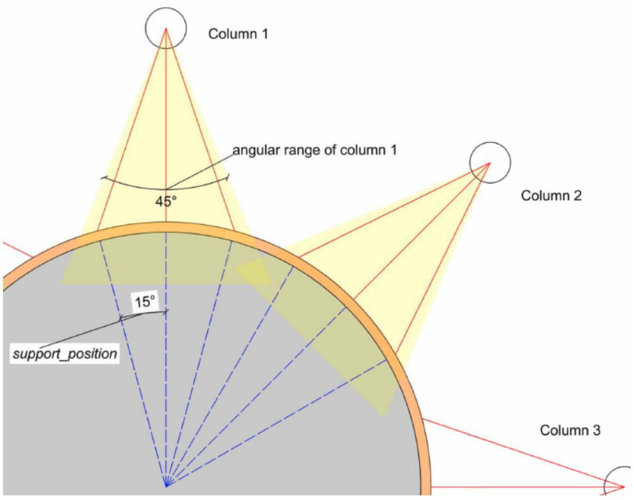

Daglas, S. (2017). Structural Optimization of a Next Generation Gamma-Ray Telescope. ETH Zurich, Research Collection, Department of Civil Engineering

He thought about cables

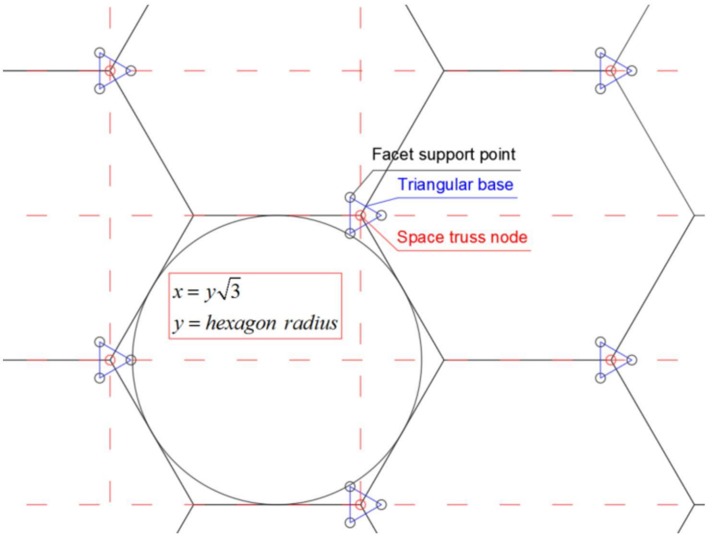

Daglas, S. (2017). Structural Optimization of a Next Generation Gamma-Ray Telescope. ETH Zurich, Research Collection, Department of Civil Engineering

He thought about space-truss-latices in combination with the mirror-facets

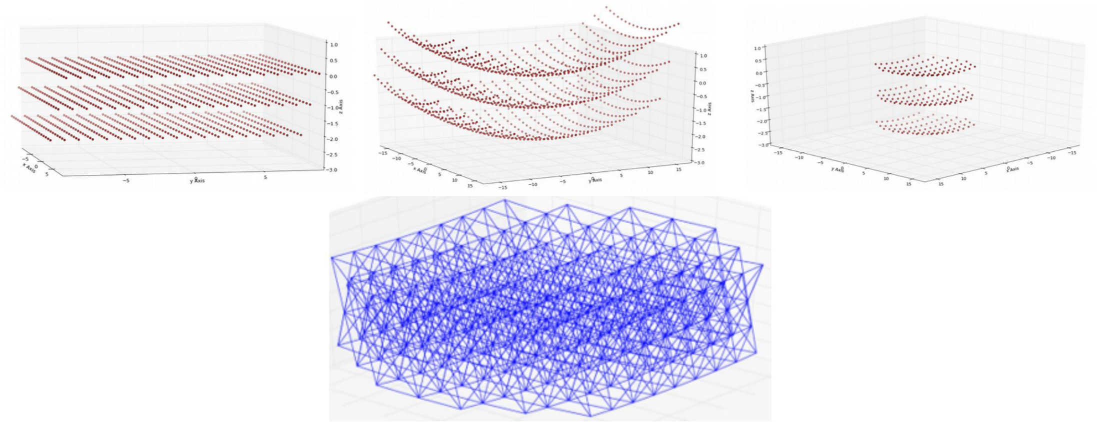

Daglas, S. (2017). Structural Optimization of a Next Generation Gamma-Ray Telescope.
ETH Zurich, Research Collection, Department of Civil Engineering

And together with me in equal parts implemented a parametric computer-simulation of the Cherenkov-plenoscope.

In his master-thesis, Spyridon uses finite-elements and my ray-tracing as a feed-back

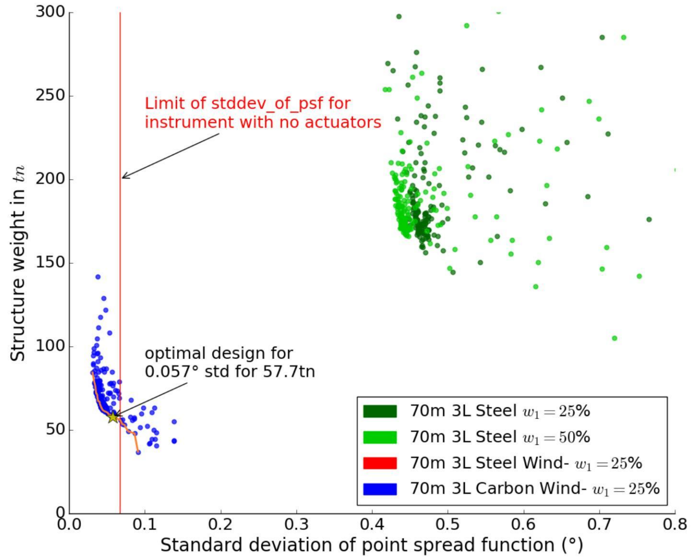

Daglas, S. (2017). Structural Optimization of a Next Generation Gamma-Ray Telescope. ETH Zurich, Research Collection, Department of Civil Engineering

To explore the parameter-space of the Cherenkov-plenoscope.

And Spyridon finds that a 70 meter Cherenkov-plenoscope can be build today.

The entire imaging-reflector of Portal has a mass of fifty seven point seven tons.

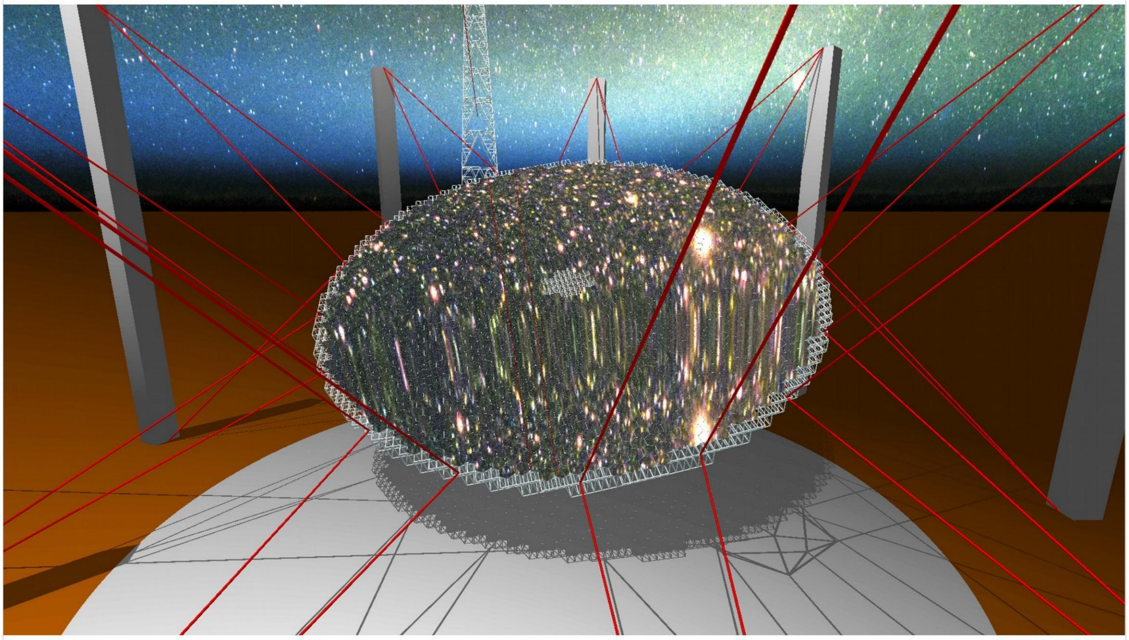

Portal is not just a phd-students dream.

It is a phd-students dream approved by civil engineering.

Of course, Portal has its cost.

Spyridon and I estimate that Portal will be two hundred million give or take when ready for first-light.

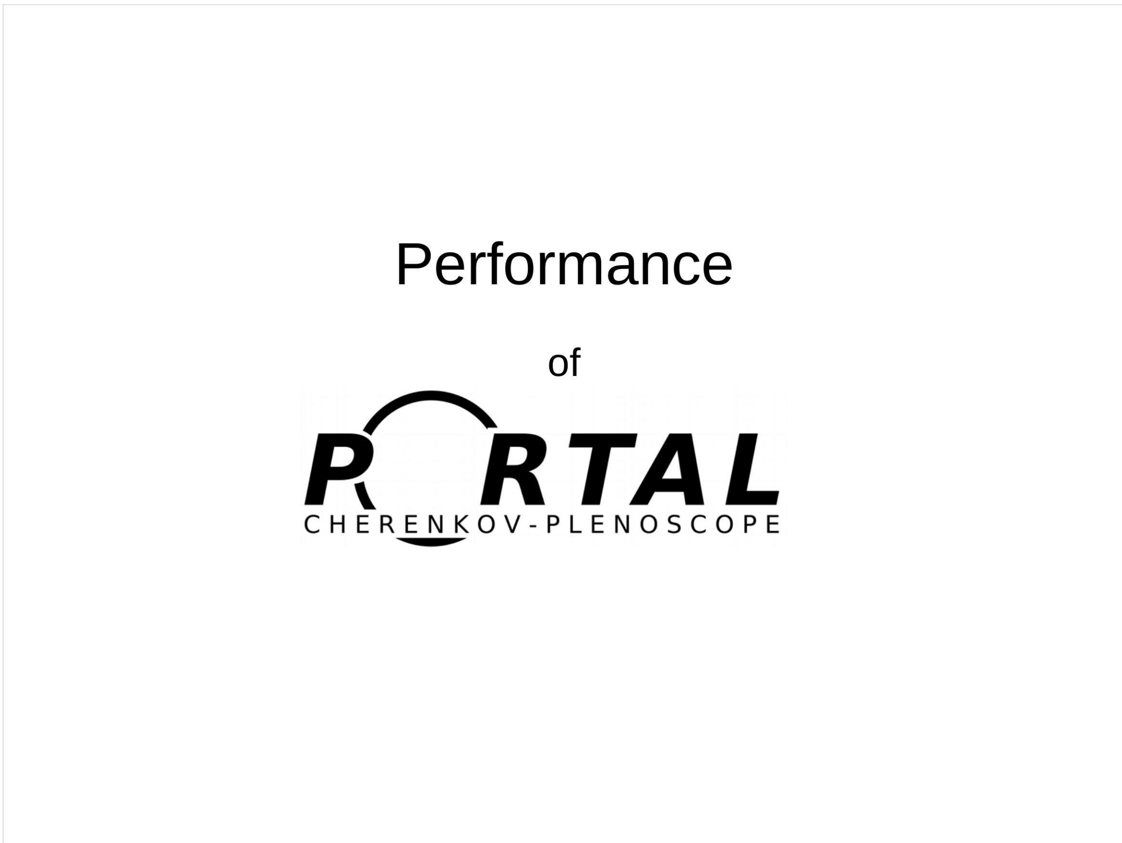

But on the other hand Portal also has quiet some performance to offer.

Night-sky-background

One giga electron Volt is all about the trigger and the night-sky-background.

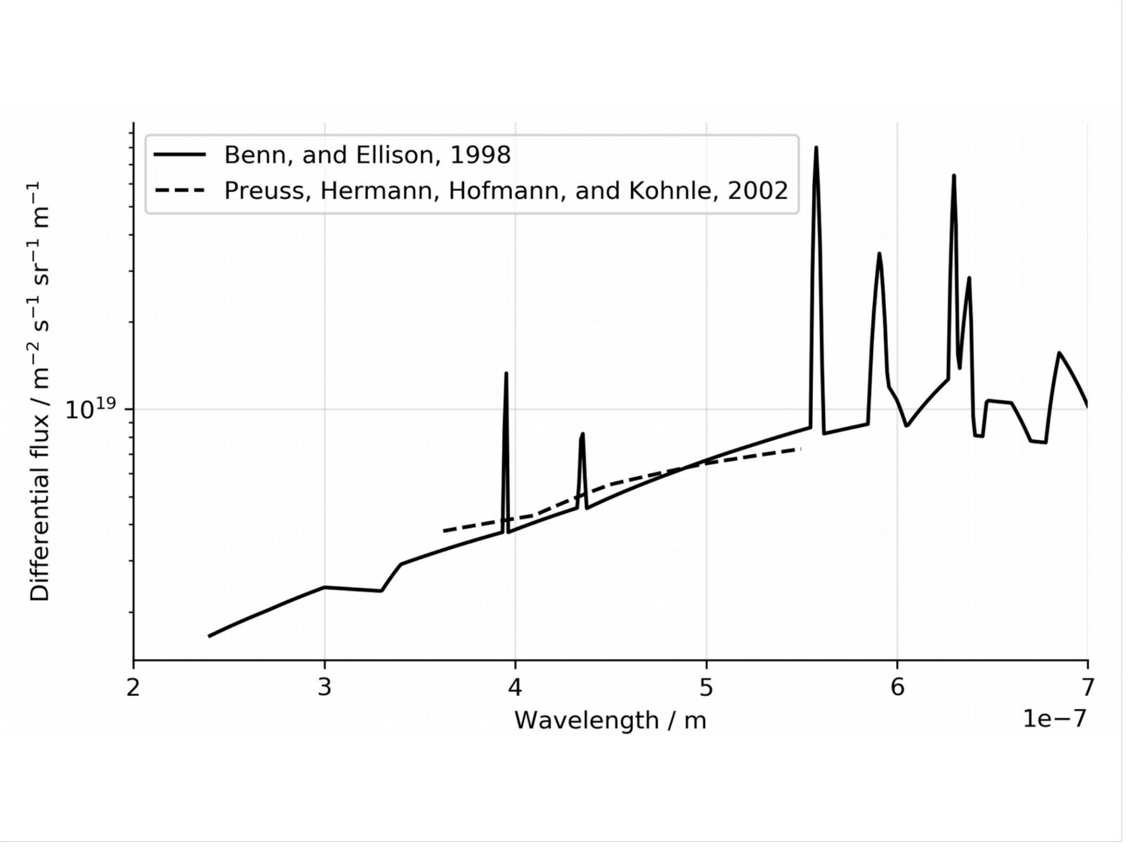

I simulate the night-sky-background of the dark night on Canary island La Palma.

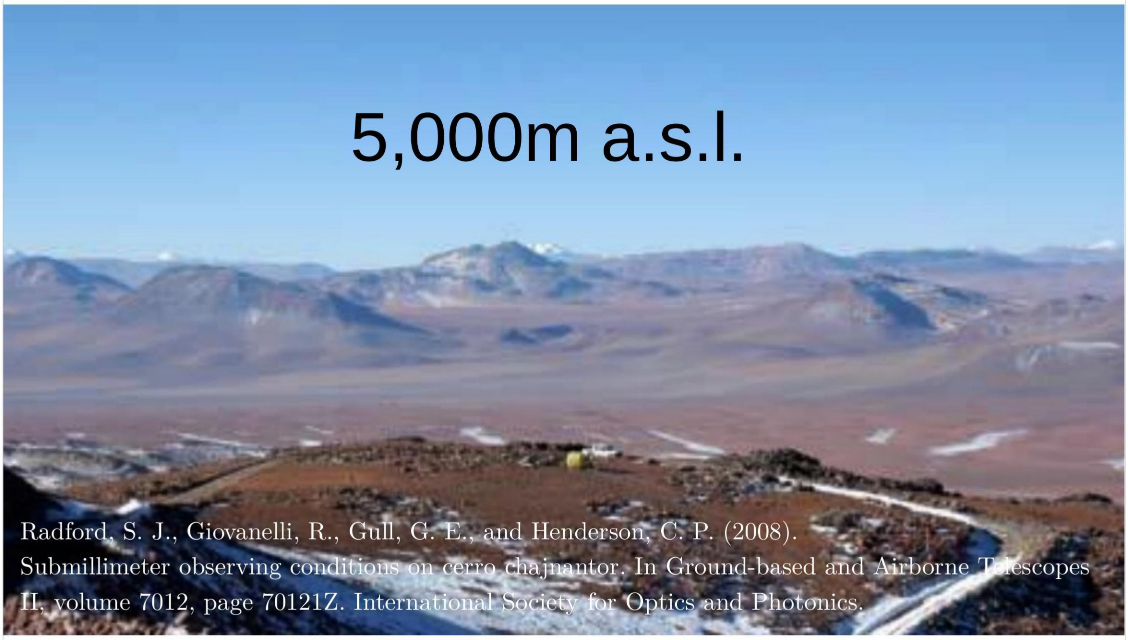

My simulation uses atmospheric models for the Atacama-desert in Chile.

In the simulation, Portal is on 5000m above sea level.

Trigger

Portals trigger

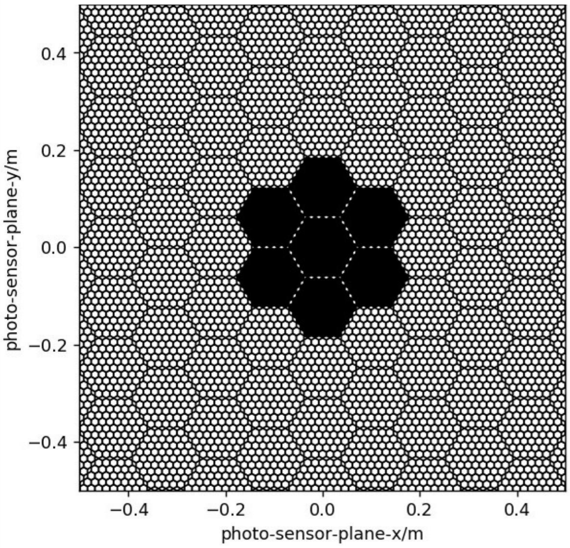

NSB-rate	~25 Ms^{-1} $sensor^{-1}$
Sum	427 sensors
Integration-duration	5 ns
Avg. integral	53.5 p.e.
Threshold	103.0 p.e.
Min. neighbors	2
NSB-accidental	O(22) s^{-1}

Free of distortions
Free of aberrations

Is very similar to the sum trigger of established Cherenkov-telescopes but it has reduced distortions and aberrations.

The average night-sky-background-photon-rate in a single photo-sensor is 25Mega photons per second.

The sum-trigger sums 427 photo-sensors into one trigger-pixel, see the pattern in the figure.

The trigger integrates over a duration of 5 nano seconds.

On average there are 53.5 photon-electrons in a trigger-pixel integrated over 5 nano seconds.

The trigger demands to have at least two neighboring trigger-pixels above the threshold in order to trigger the read-out.

I set the trigger-threshold for a trigger-pixel to 103 photo-electrons such that there are no accidental triggers within all the 45ms in which I exposed Portal to the night-sky-background.

So I estimate that the accidental-rate will not significantly exceed 22 events per second.

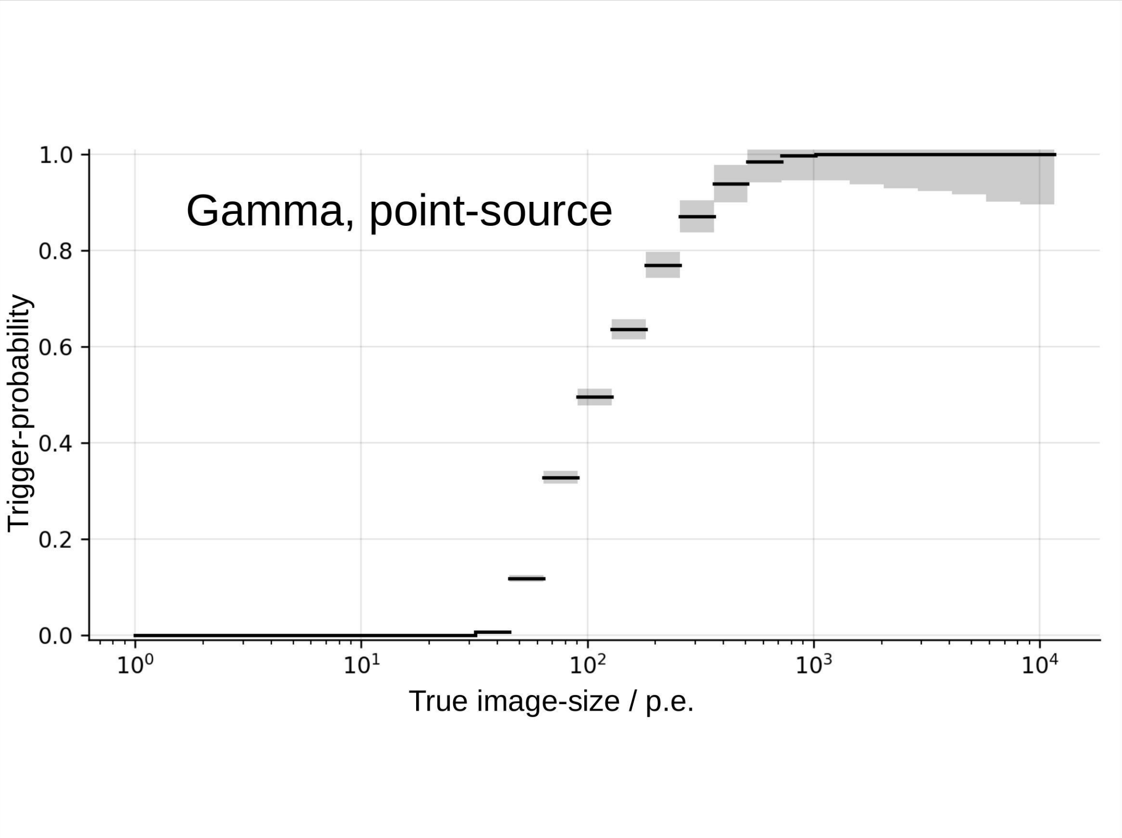

For gamma-rays coming from a point-source we find that events with a true image-size of 100 photo-electrons have a 50% chance to trigger the Portal.

Events with true image-sizes below 30 photo-electrons have almost no chance to trigger.

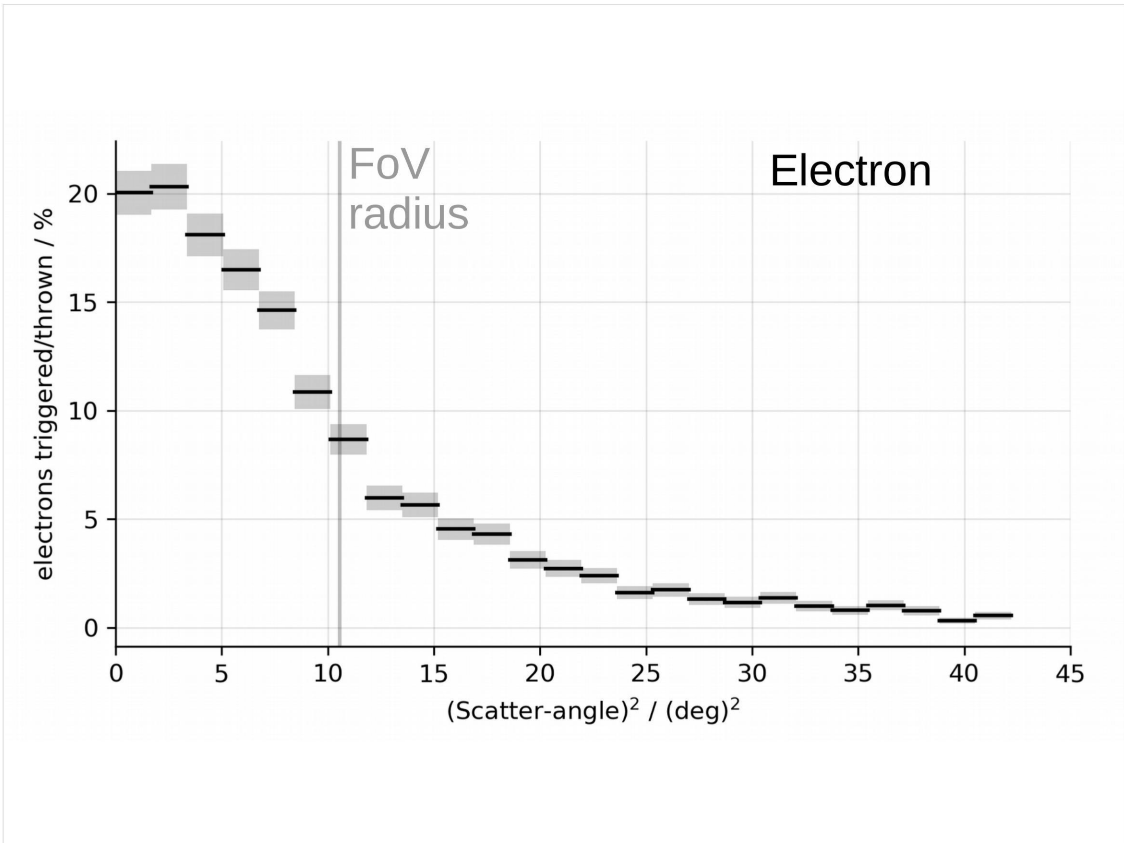

To not spoil the instrument-response-functions too much, we took care that the scatter-radii and scatter-angles are wide enough.

Here we see the scatter-angle for diffuse electrons.

For larger scatter-angles the trigger-probability vanishes to zero.

Instrument-response

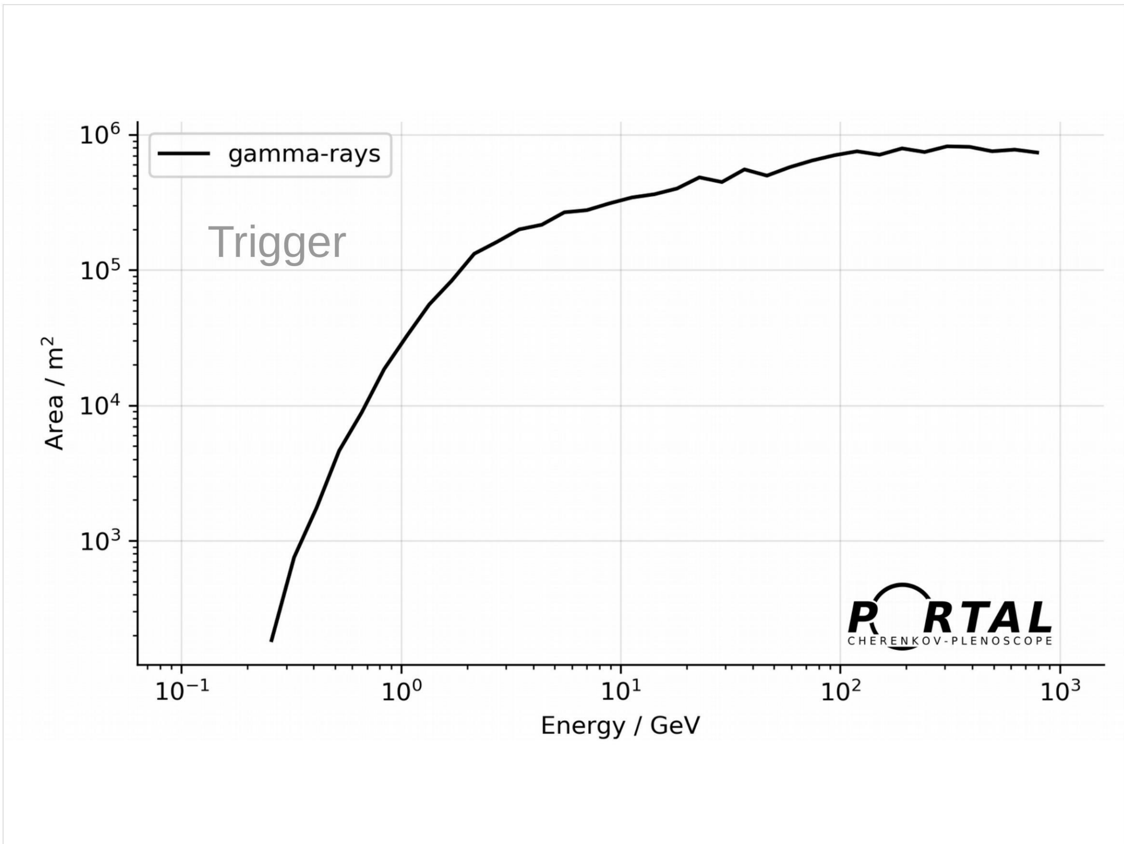

Portal's effective-area for cosmic gamma-rays coming from a point-source is

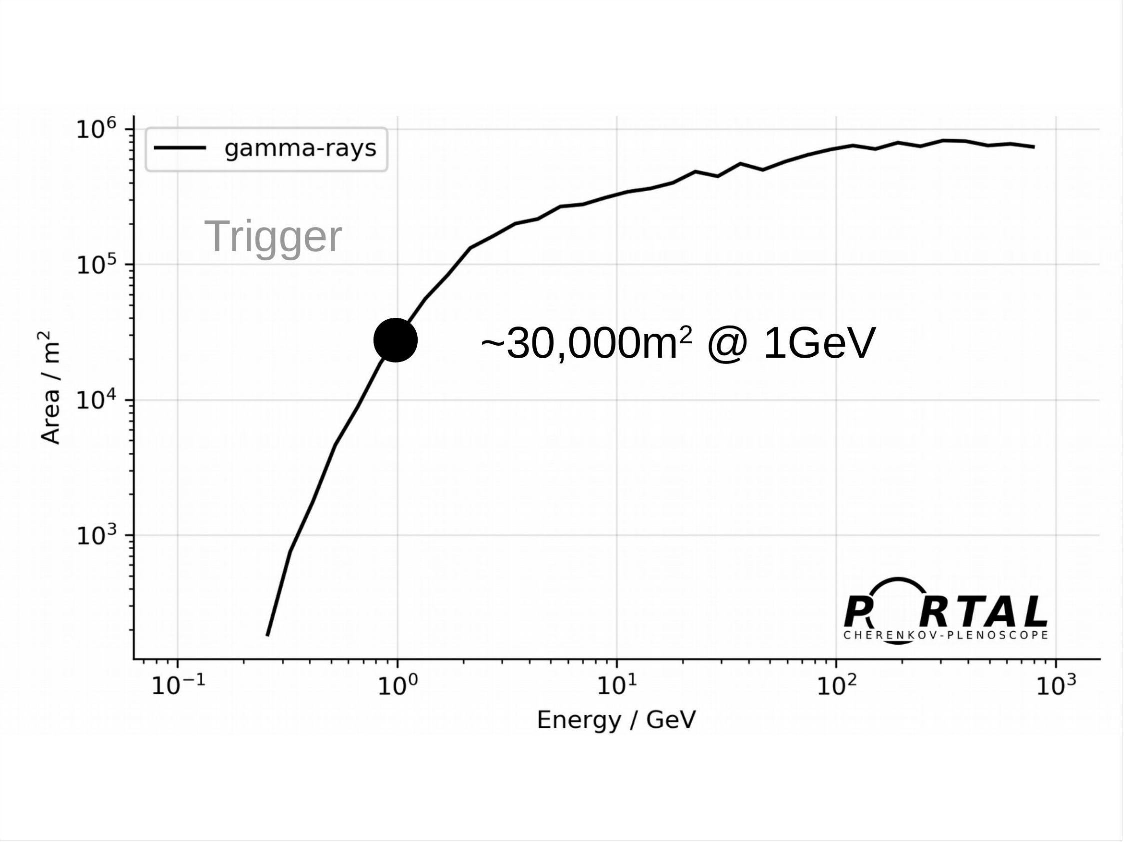

30,000 meter square at one Giga electron Volt.

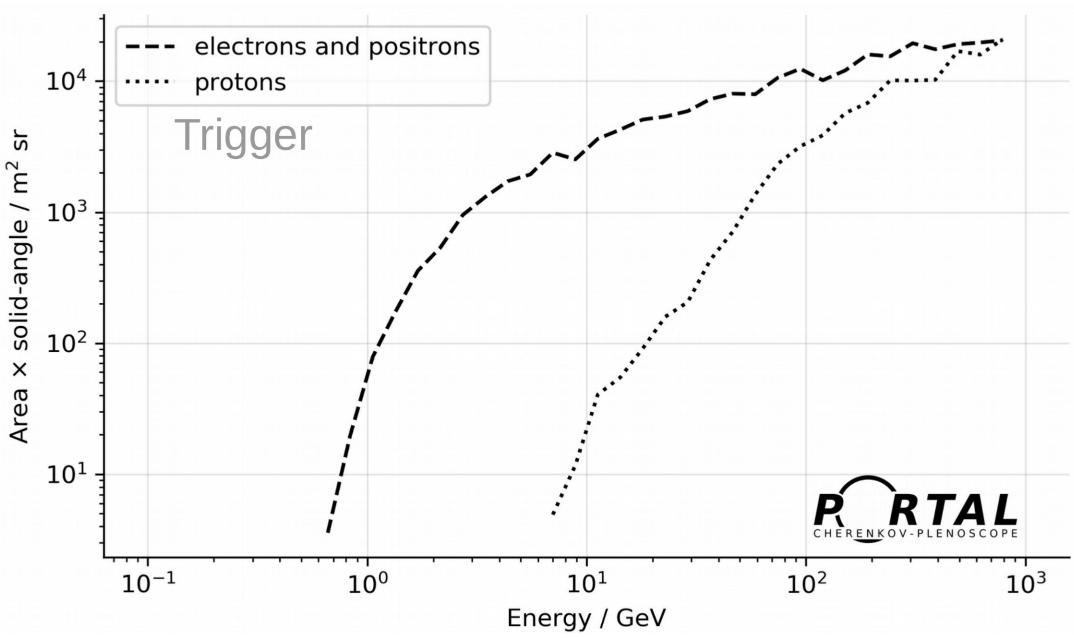

The acceptance for charged cosmic-rays.

Protons do not contribute too much below ten GeV, but electrons and positrons are still running strong.

Angular resolution

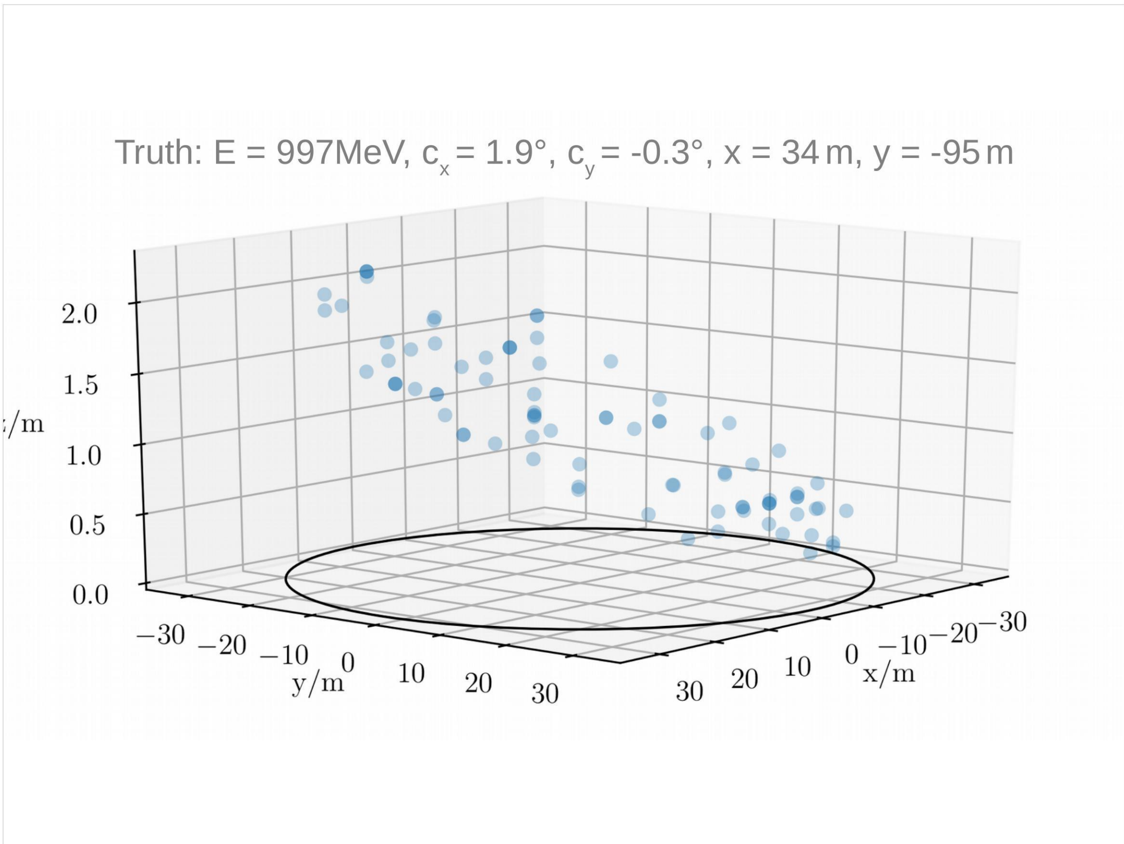

For the direction-reconstruction I use the light-field-sequence to fit a plane to the Cherenkov-photon-light-front just before it rushes into the aperture-plane.

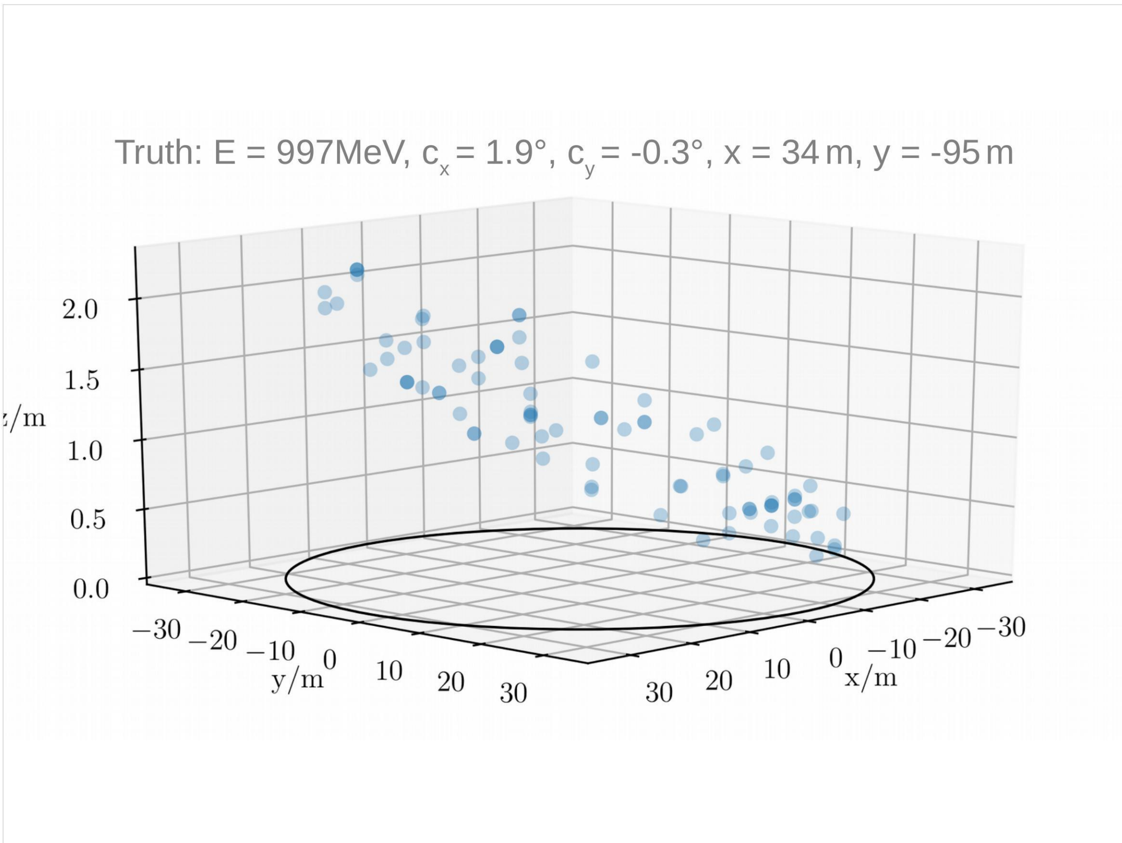

I take the surface-normal of this plane to be the reconstructed source-direction on the sky-dome.

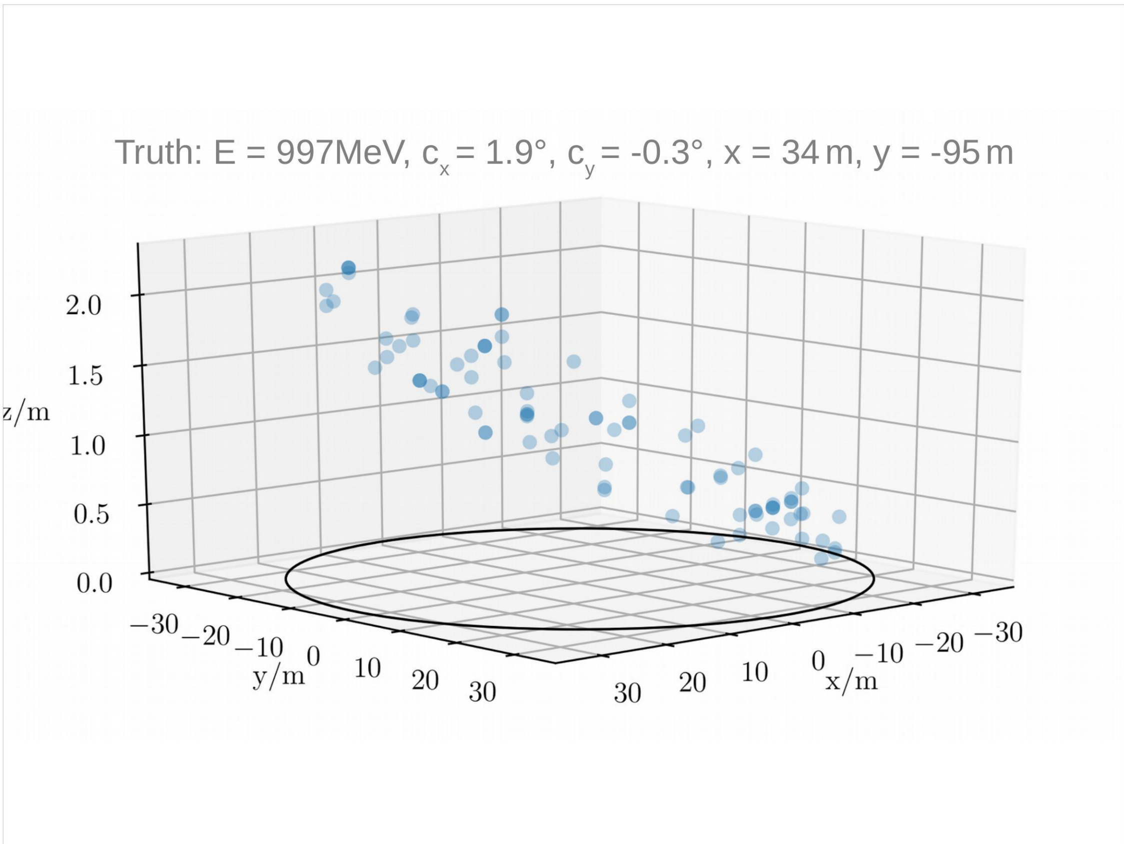
Truth: E = 997MeV, c_x = 1.9°, c_y = -0.3°, x = 34 m, y = -95 m
z/m
2.0
1.5
1.0
0.5
0.0
y/m
−30 −20 −10 0 10 20 30
x/m
30 20 10 0 −10 −20 −30

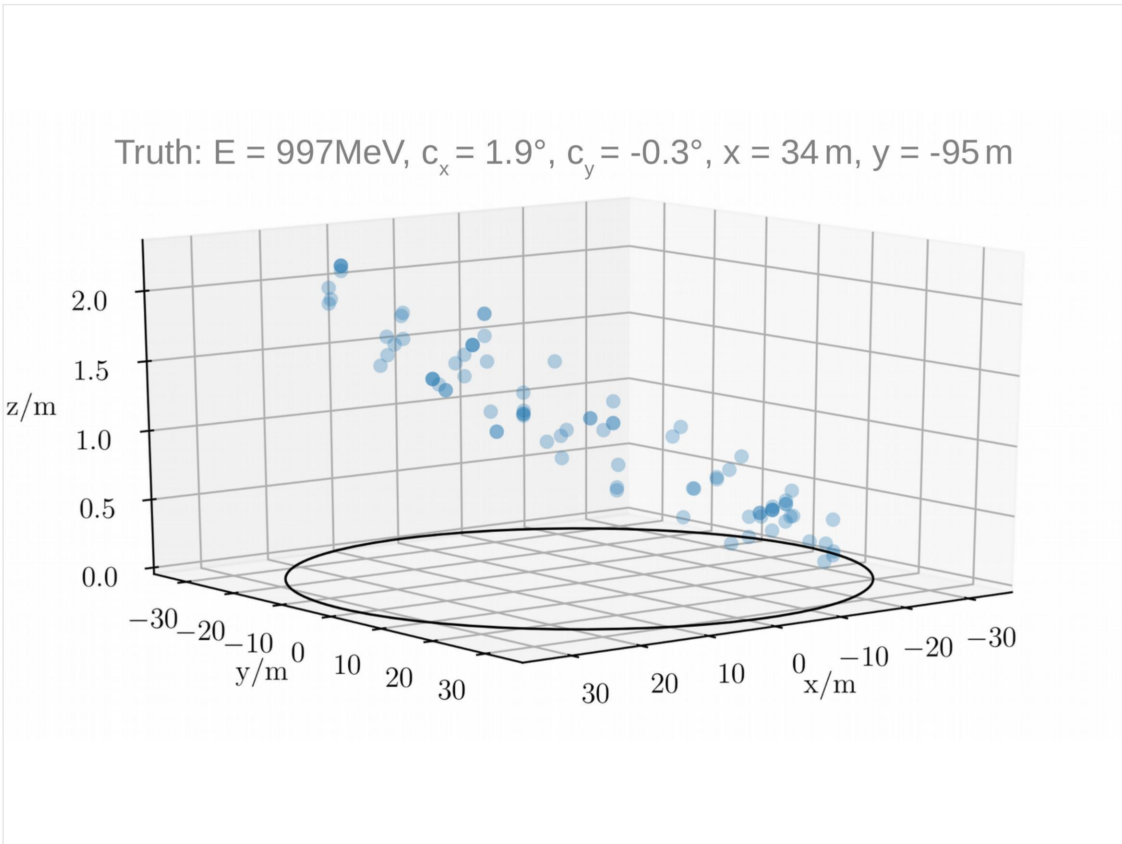
Truth: E = 997MeV, cx = 1.9°, cy = -0.3°, x = 34 m, y = -95 m
z/m
2.0
1.5
1.0
0.5
0.0
−30
−20
−10
0
10
20
30
y/m
30
20
10
0
−10
−20
−30
x/m

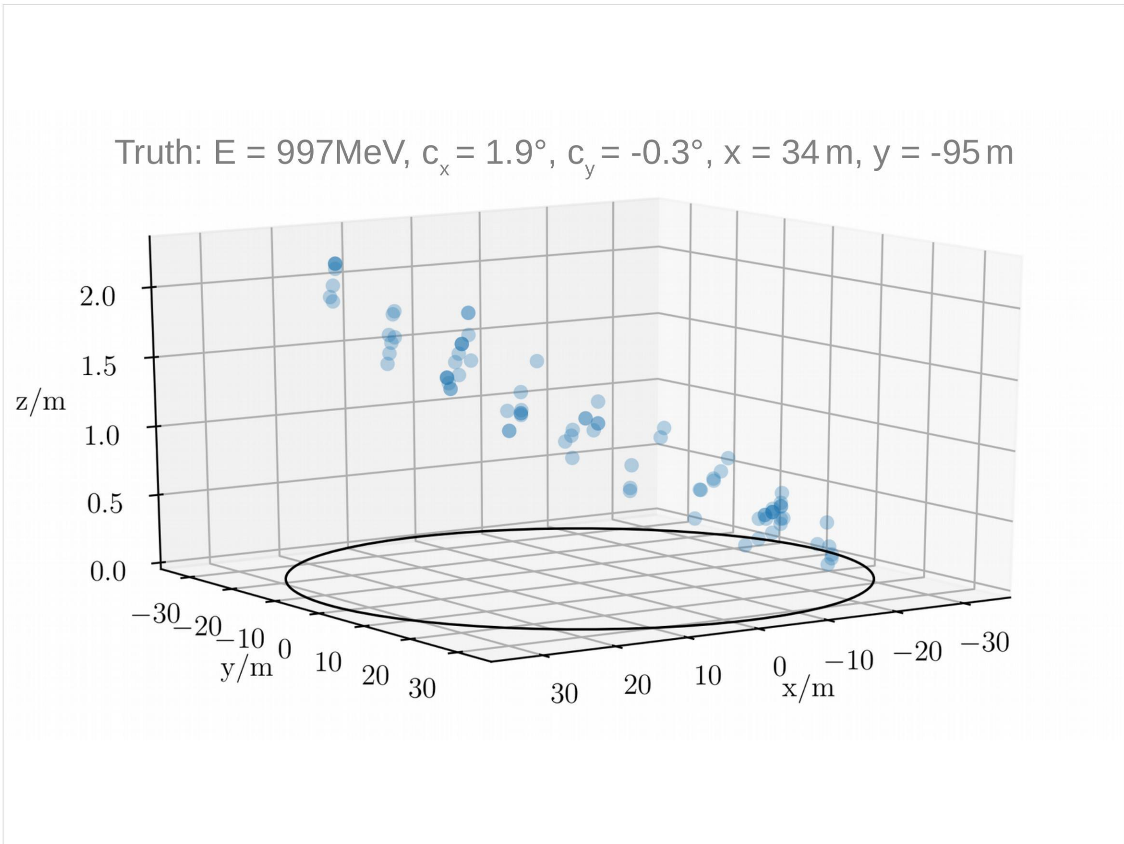

Truth: E = 997MeV, cx = 1.9°, cy = -0.3°, x = 34 m, y = -95 m
z/m
2.0
1.5
1.0
0.5
0.0
−30
−20
−10
0
10
20
30
y/m
30
20
10
0
−10
−20
−30
x/m

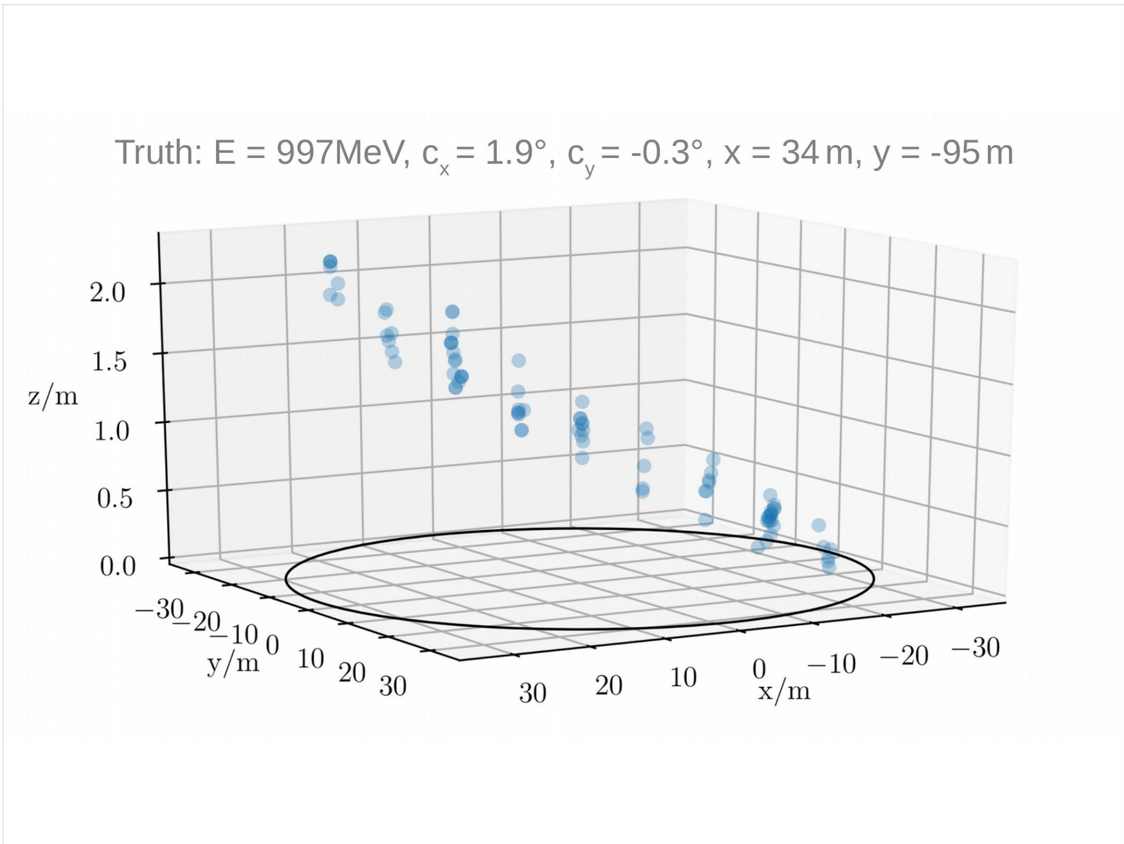
Truth: E = 997MeV, c_x = 1.9°, c_y = -0.3°, x = 34 m, y = -95 m
z/m
y/m
x/m

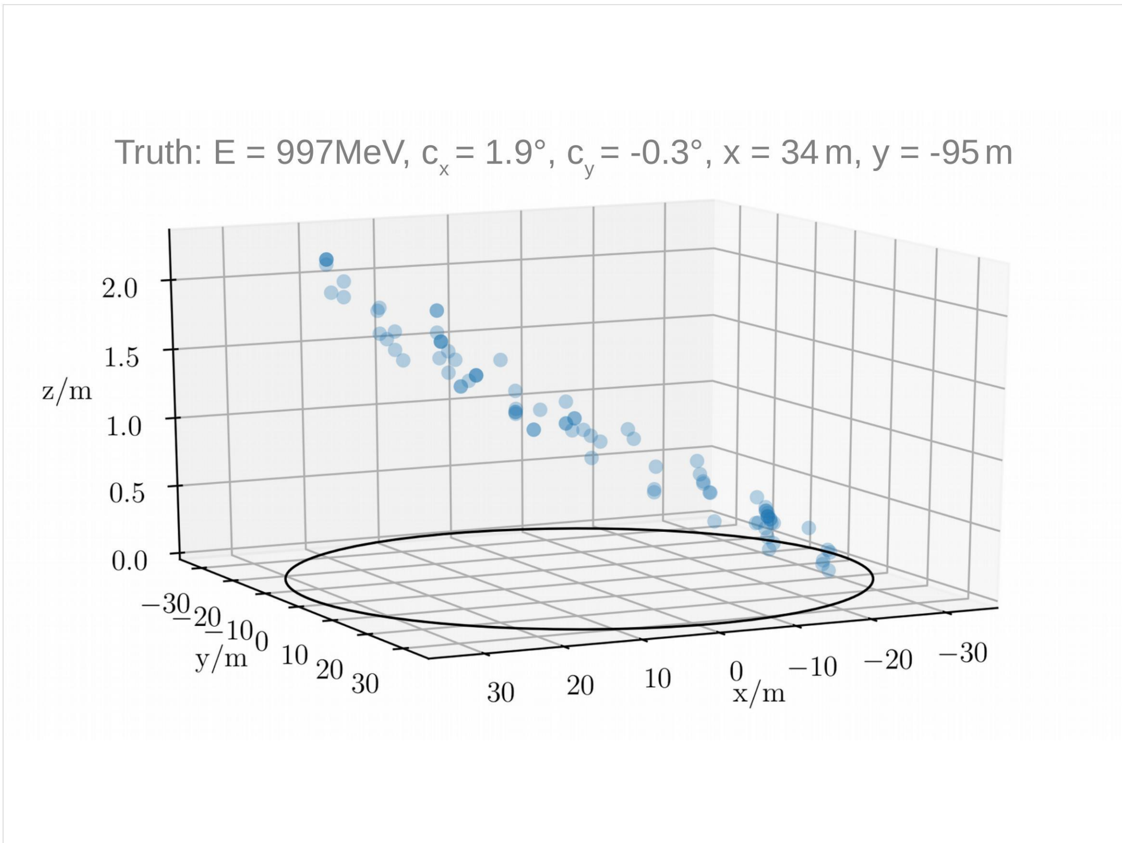
Truth: E = 997MeV, c$_x$ = 1.9°, c$_y$ = -0.3°, x = 34 m, y = -95 m
z/m
2.0
1.5
1.0
0.5
0.0
y/m
−30
−20
−10
0
10
20
30
x/m
30
20
10
0
−10
−20
−30

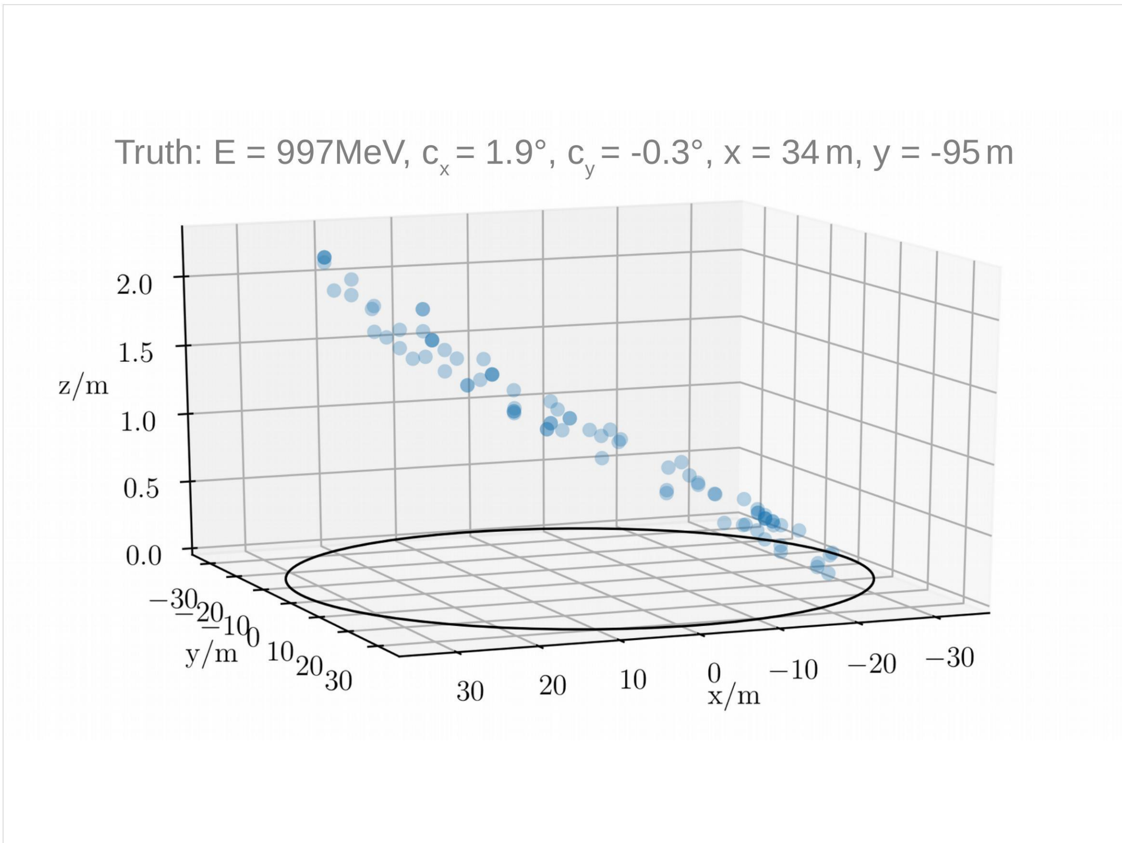
Truth: E = 997MeV, c_x = 1.9°, c_y = -0.3°, x = 34 m, y = -95 m
z/m
2.0
1.5
1.0
0.5
0.0
y/m
−30
−20
−10
0
10
20
30
x/m
30
20
10
0
−10
−20
−30

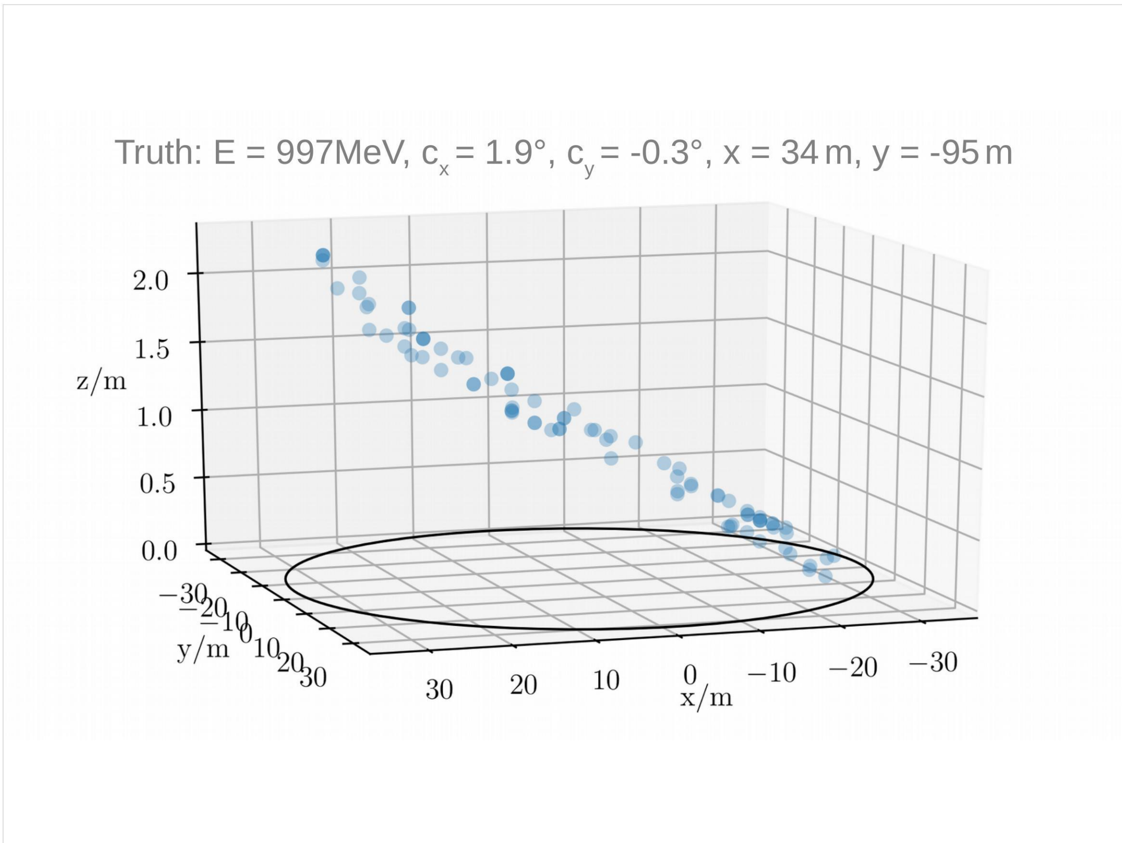

Truth: E = 997MeV, c_x = 1.9°, c_y = -0.3°, x = 34 m, y = -95 m
z/m
2.0
1.5
1.0
0.5
0.0
y/m
−30
−20
−10
0
10
20
30
x/m
30
20
10
0
−10
−20
−30

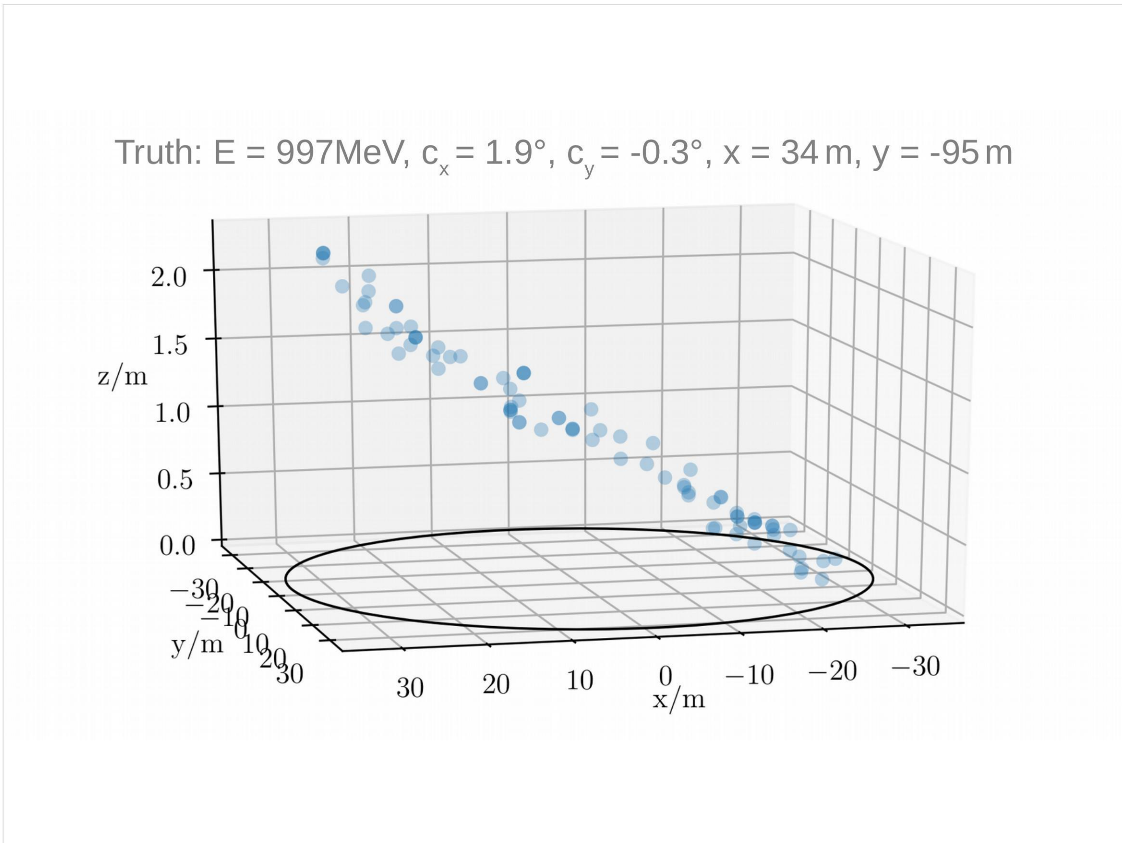

Truth: E = 997MeV, c_x = 1.9°, c_y = -0.3°, x = 34 m, y = -95 m
z/m
2.0
1.5
1.0
0.5
0.0
y/m
−30
−20
−10
0
10
20
30
x/m
30
20
10
0
−10
−20
−30

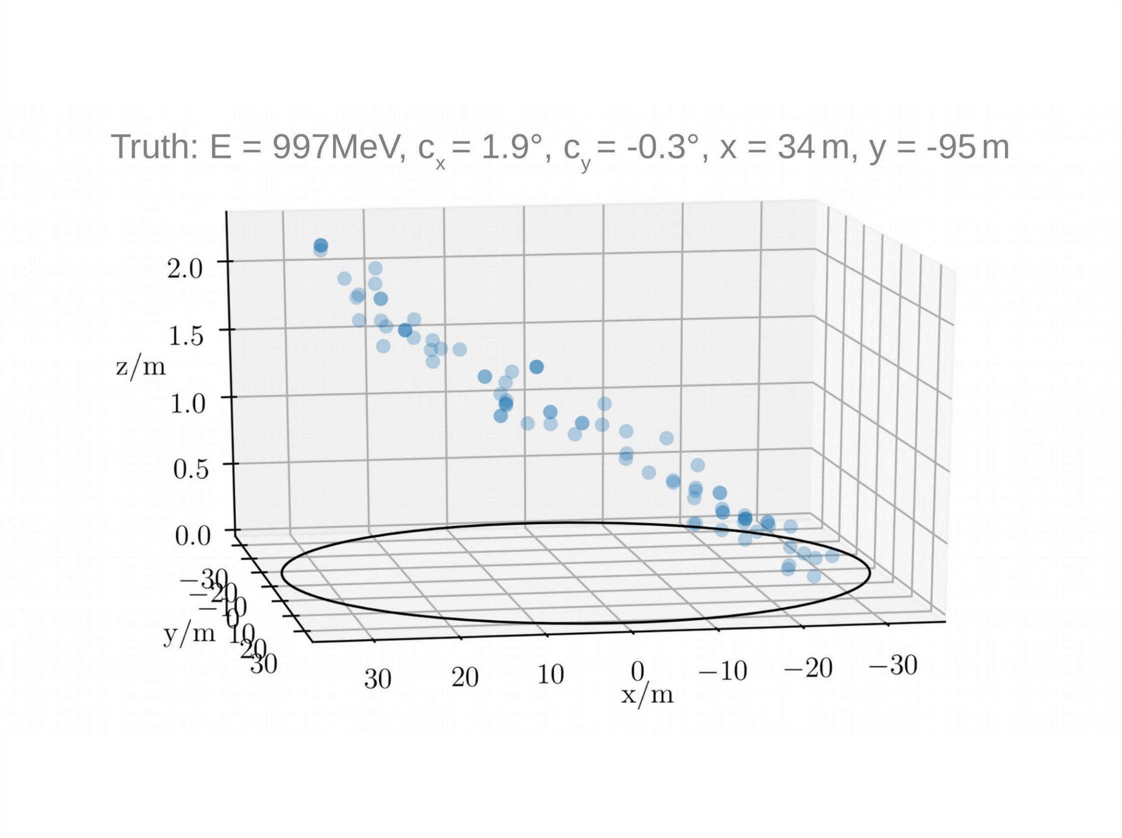
Truth: E = 997MeV, c_x = 1.9°, c_y = -0.3°, x = 34 m, y = -95 m
2.0
1.5
1.0
0.5
0.0
z/m
−30
−20
−10
0
10
20
30
y/m
30
20
10
0
−10
−20
−30
x/m

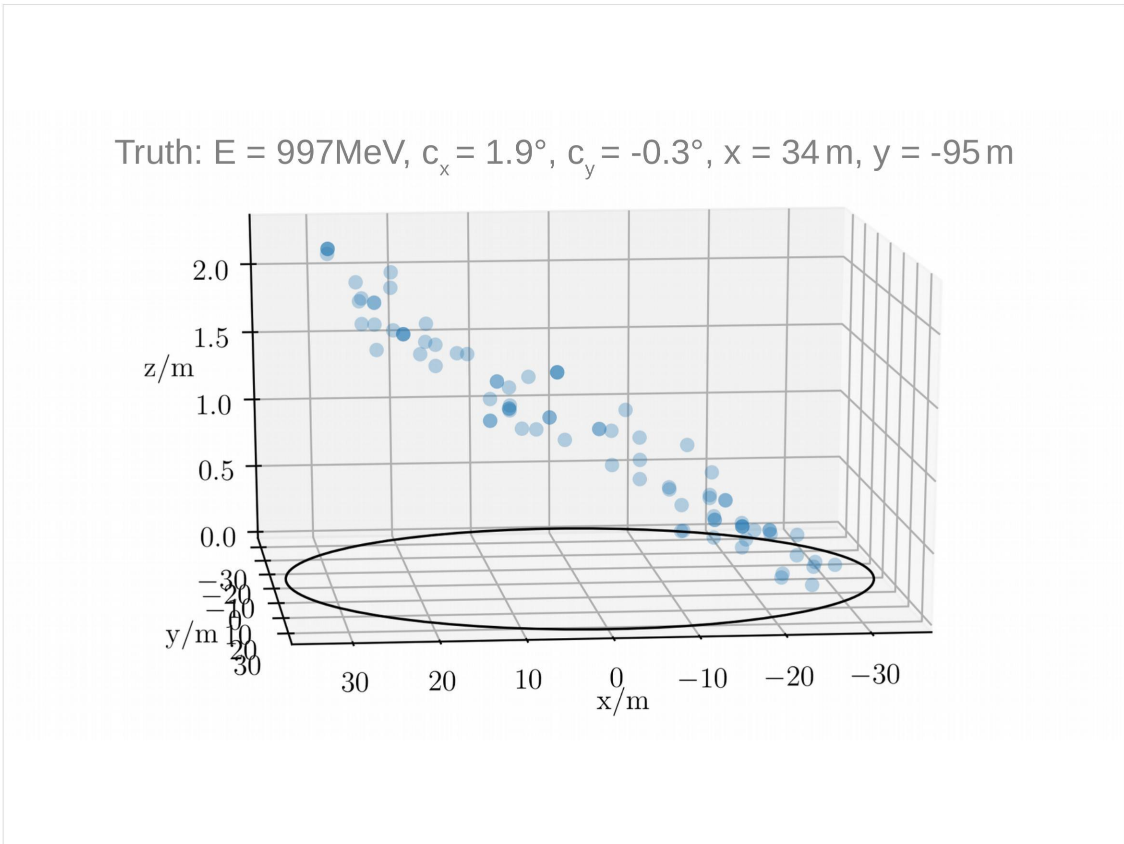
Truth: E = 997MeV, c_x = 1.9°, c_y = -0.3°, x = 34 m, y = -95 m
z/m
2.0
1.5
1.0
0.5
0.0
y/m
−30
−20
−10
0
10
20
30
x/m
30
20
10
0
−10
−20
−30

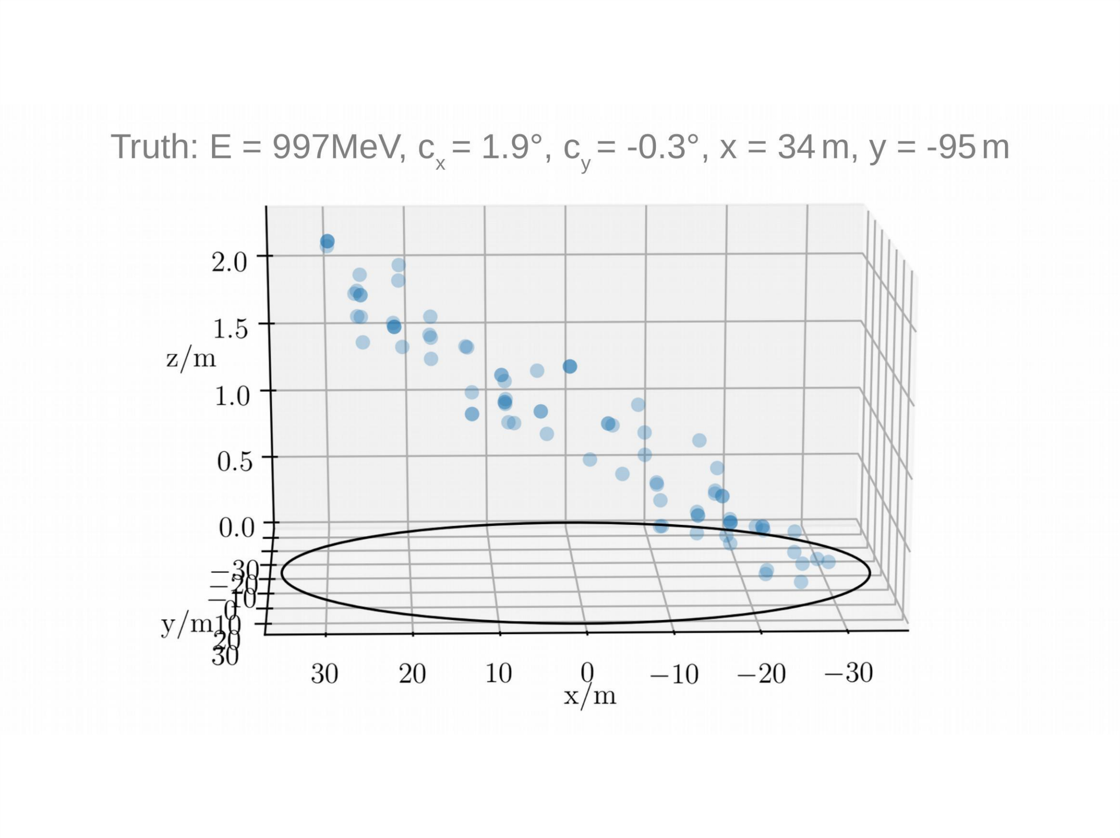
Truth: E = 997MeV, c_x = 1.9°, c_y = -0.3°, x = 34 m, y = -95 m
z/m
2.0
1.5
1.0
0.5
0.0
y/m
−30
−20
−10
0
10
20
30
x/m
30
20
10
0
−10
−20
−30

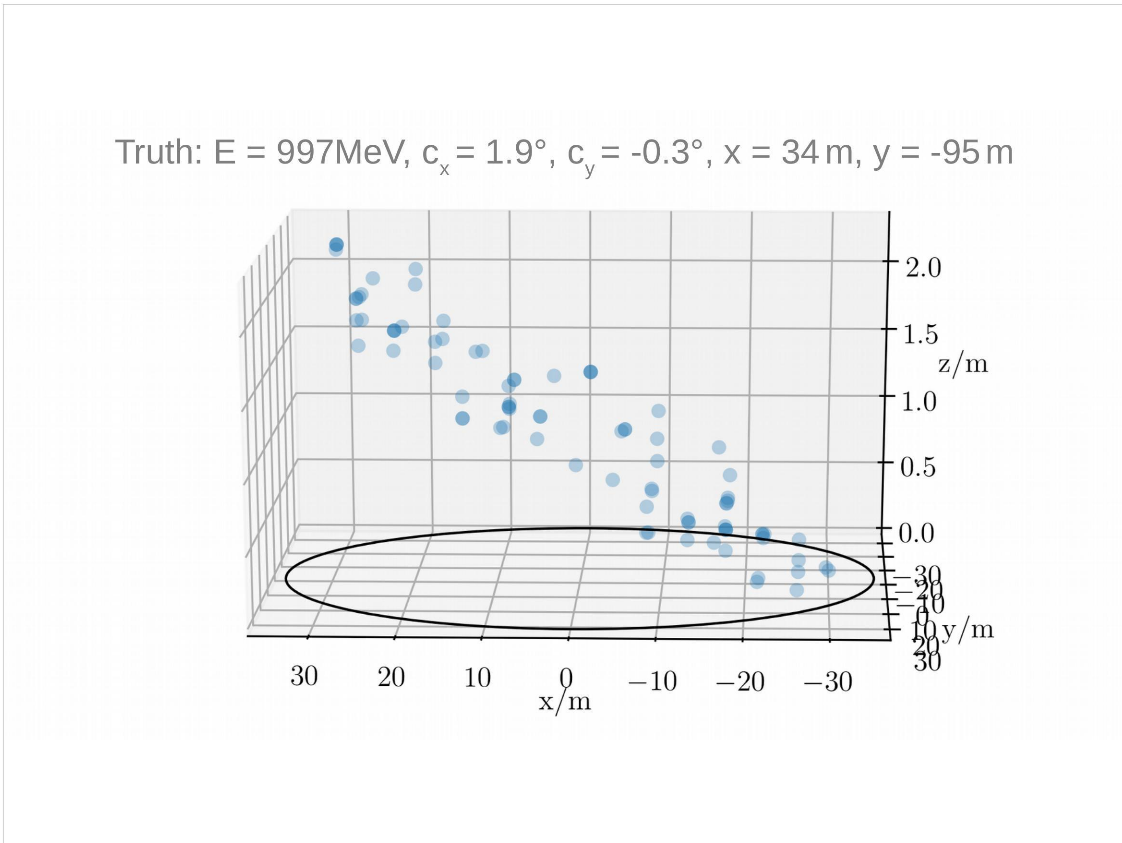

Truth: E = 997MeV, c_x = 1.9°, c_y = -0.3°, x = 34 m, y = -95 m
2.0
1.5
z/m
1.0
0.5
0.0
y/m
30
20
10
0
−10
−20
−30
x/m

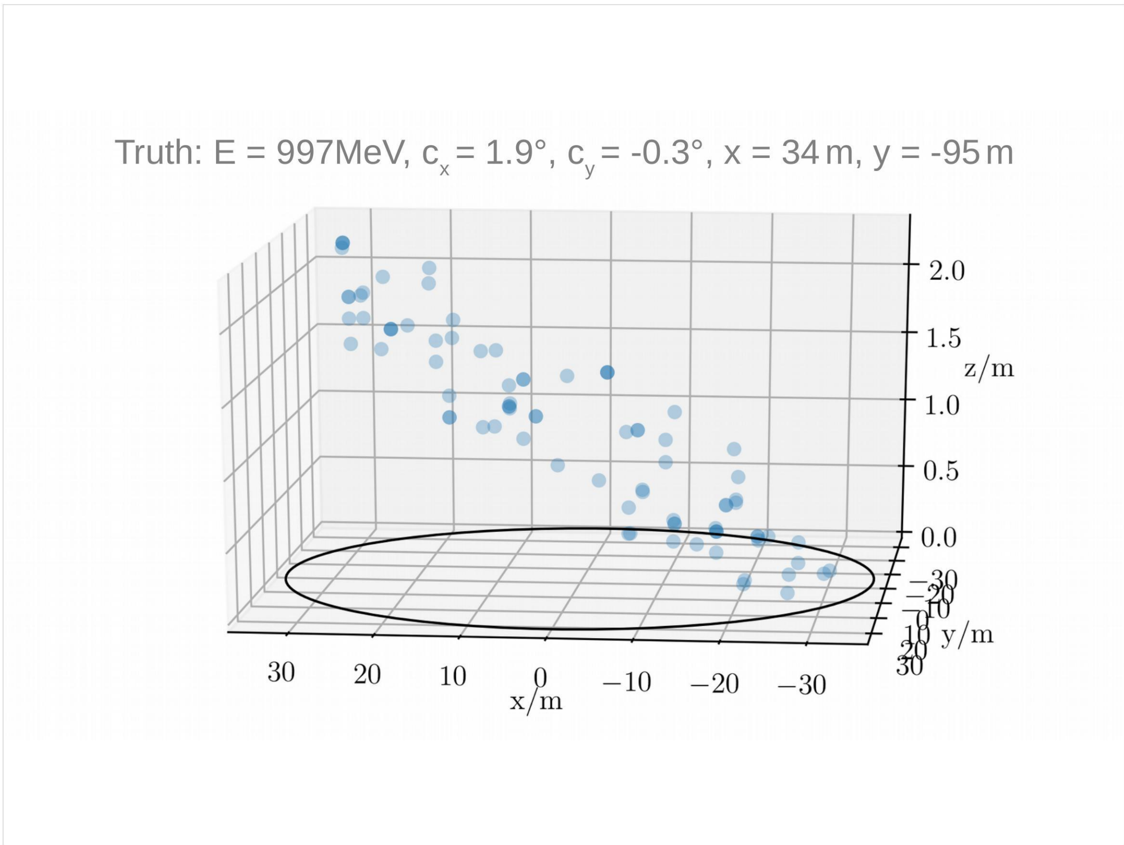
Truth: E = 997MeV, c_x = 1.9°, c_y = -0.3°, x = 34 m, y = -95 m
x/m
y/m
z/m

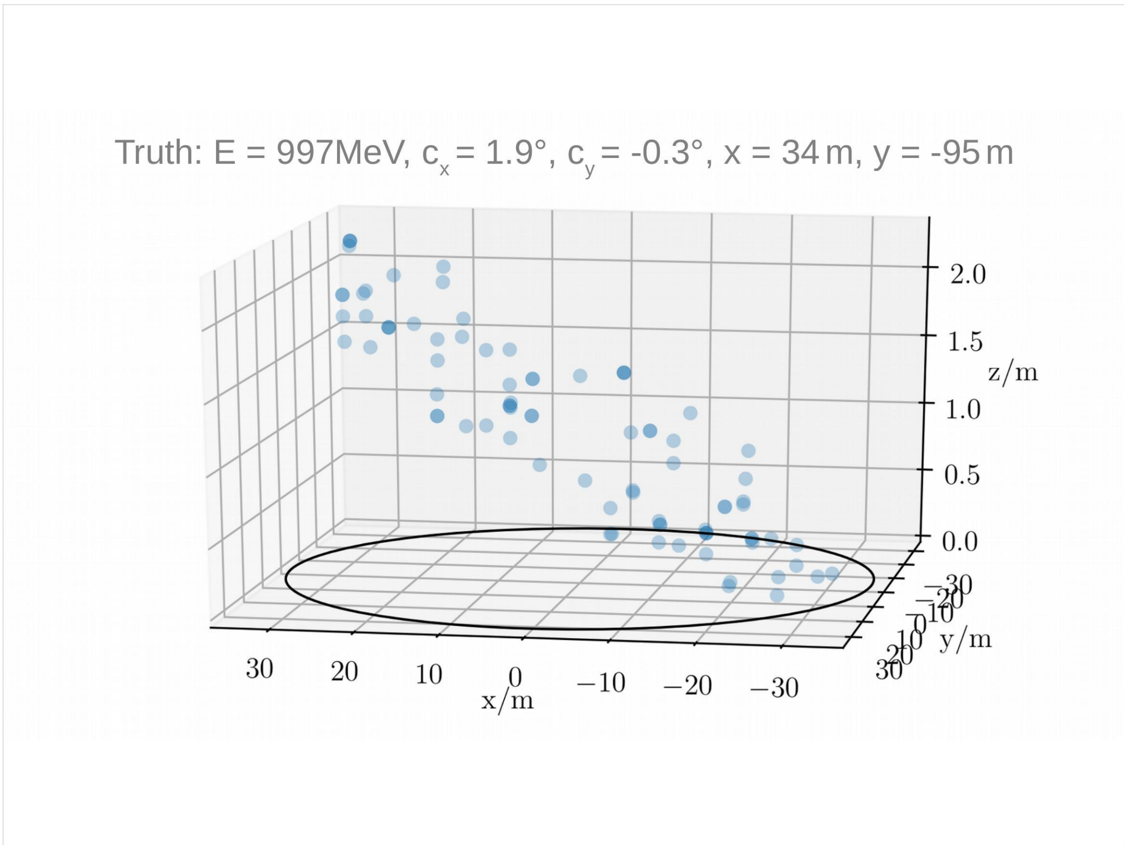
Truth: E = 997MeV, c_x = 1.9°, c_y = -0.3°, x = 34 m, y = -95 m
2.0
1.5
1.0
0.5
0.0
z/m
30
20
10
0
−10
−20
−30
x/m
y/m

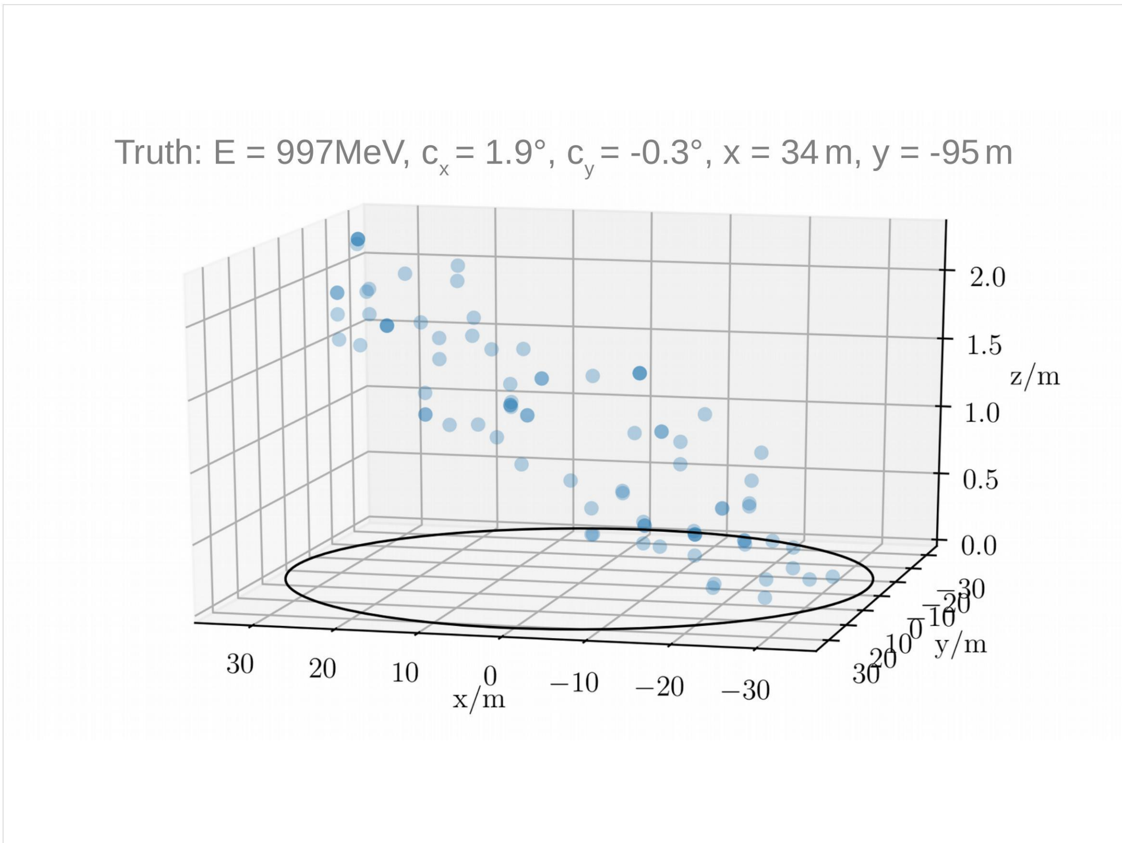
Truth: E = 997MeV, c_x = 1.9°, c_y = -0.3°, x = 34 m, y = -95 m
2.0
1.5
1.0
0.5
0.0
z/m
30
20
10
0
−10
−20
−30
x/m
y/m

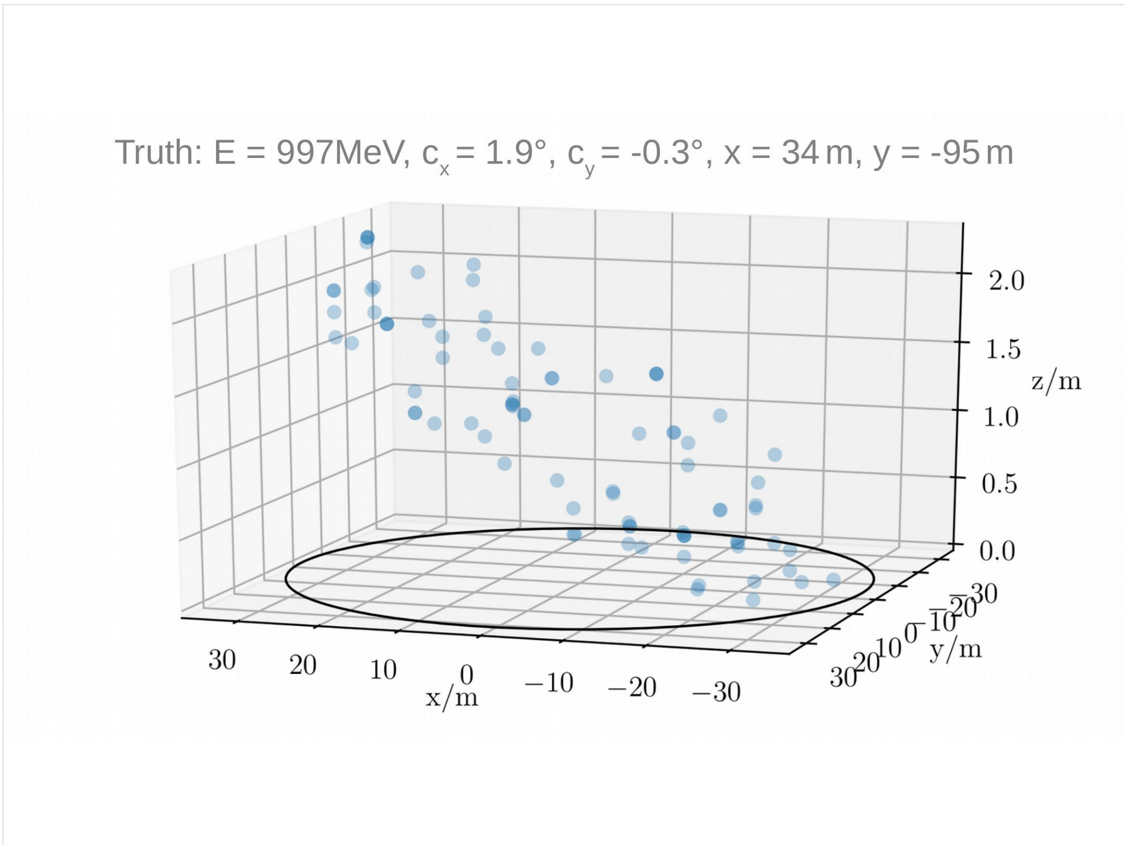

Truth: E = 997MeV, c_x = 1.9°, c_y = -0.3°, x = 34 m, y = -95 m
2.0
1.5
1.0
0.5
0.0
z/m
30
20
10
0
−10
−20
−30
x/m
y/m

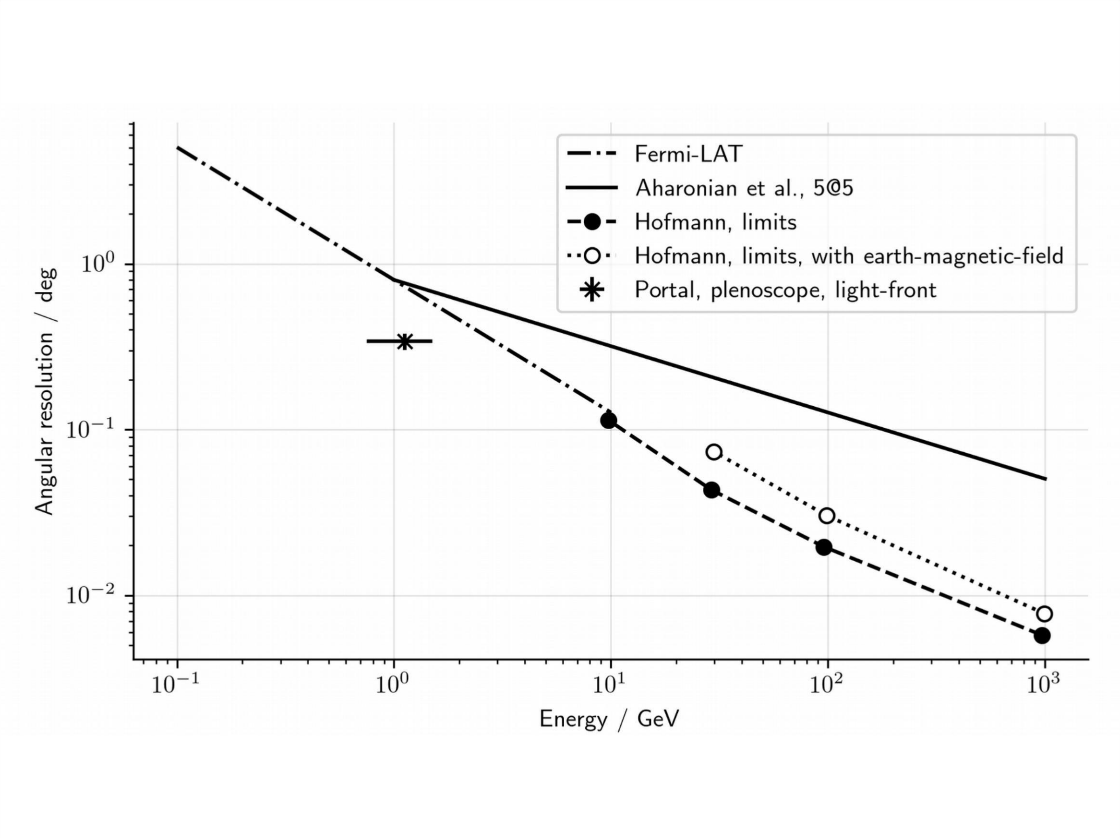

In the energy-range from 750 MeV to 1500MeV, Portal reaches an angular-resolution of 0.35 degrees for the 68% containment-radius, which is in the range of former studies.

Cosmic-ray-background

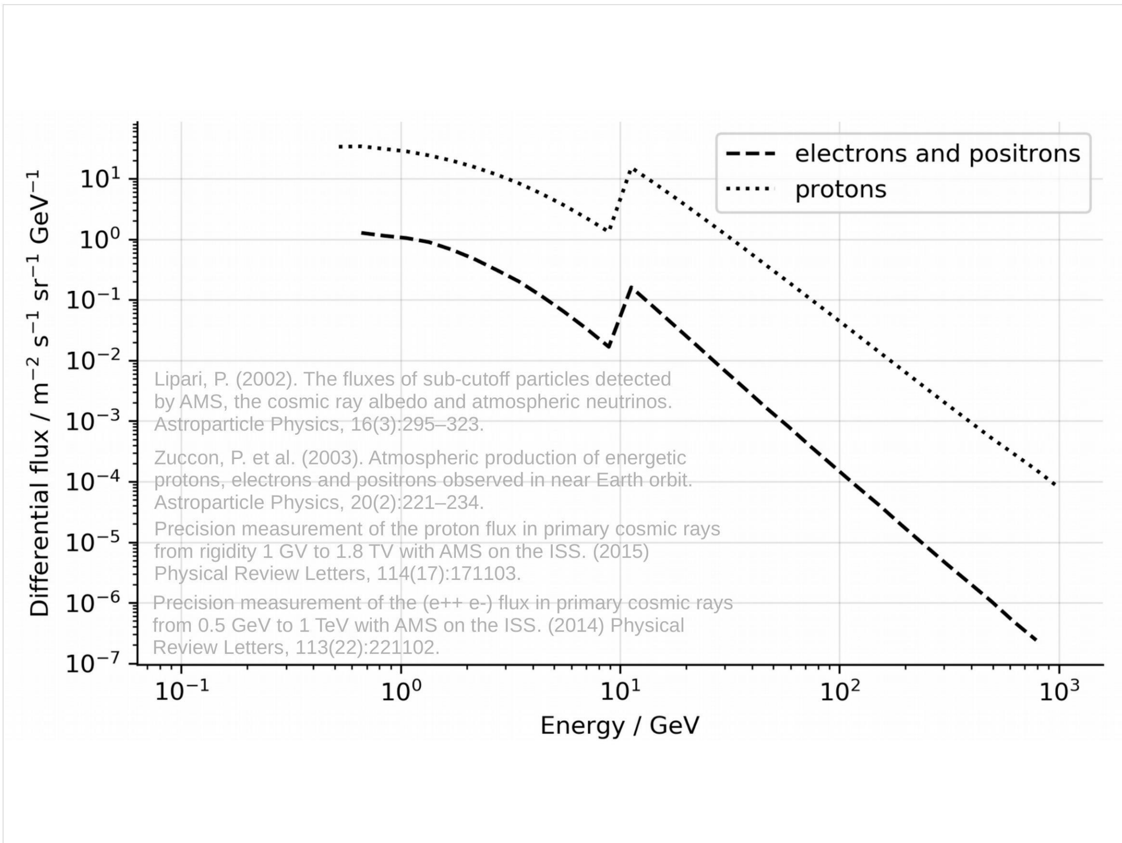

- I take the cosmic-ray background from AMS with a geomagnetic-cutoff applied at a rigidity of ten Giga Volts.

- I follow the arguments of Lipari and Zuccon to conclude that the flux of air-showers does not completely vanish below the cut-off, but is reduced to about five percent.

- This is what AMS calls the second spectrum.

- This is not the flux of charged cosmic-rays, but the flux of air-showers induced by charged cosmic-rays.

Trigger-rate

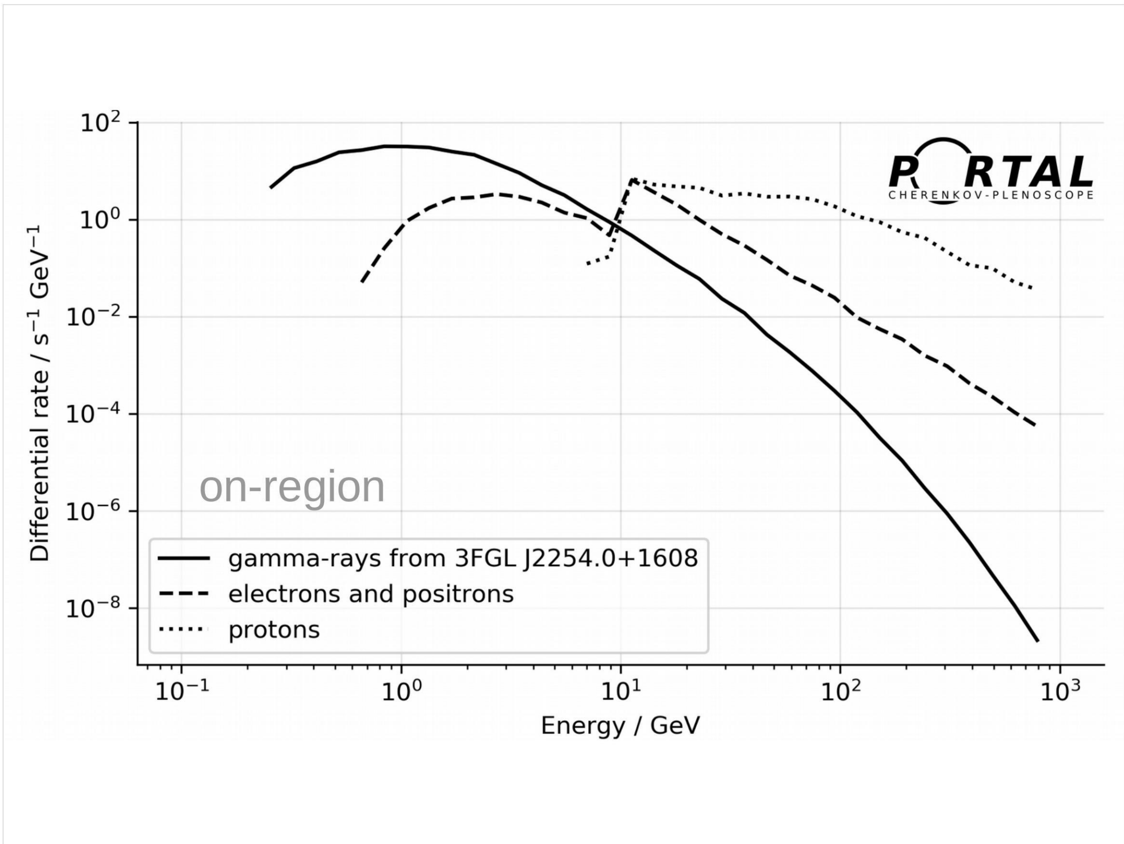

The differential trigger-rate of Portal in the on-region while observing a bright gamma-ray-source.

The radius of the on region is Portal’s angular-resoultion of point three five degrees.

Portal’s energy-thtreshold is one Giga electron Volt.

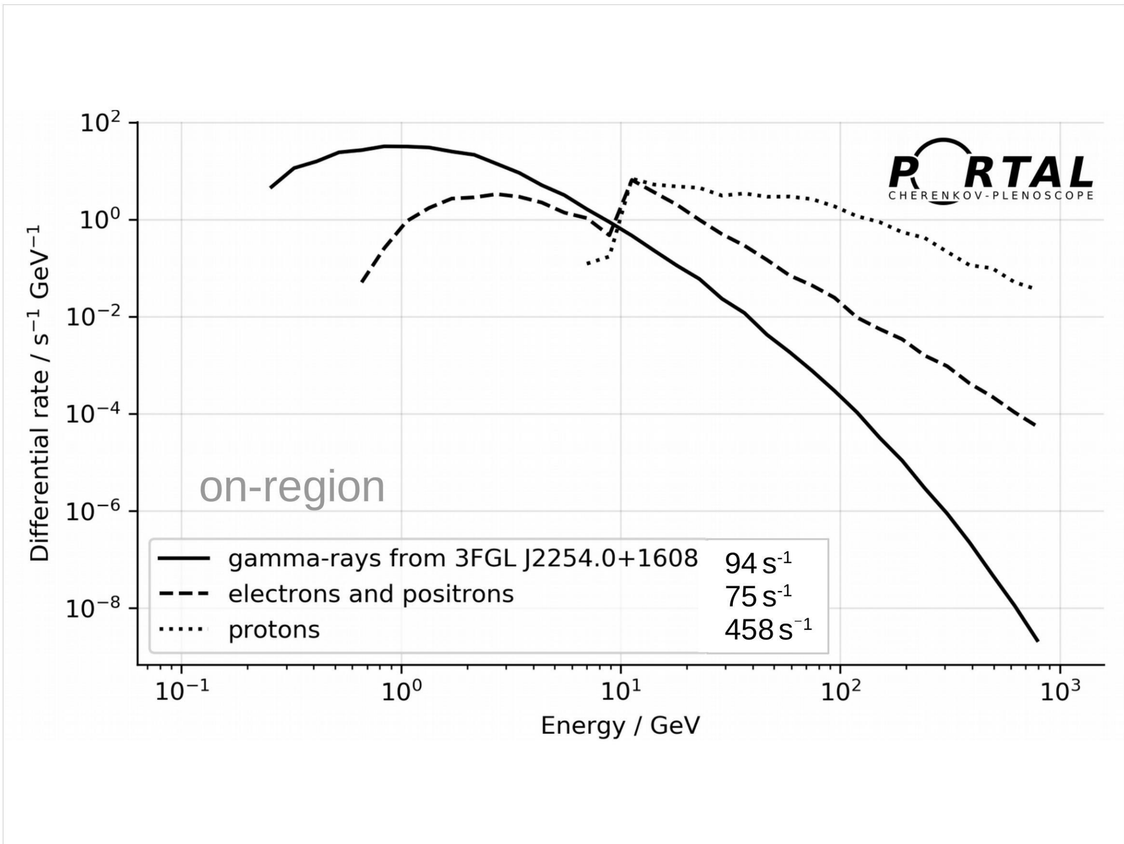

The integrated rates are 94 for gamma-rays, 75 for electrons, and 458 for protons.

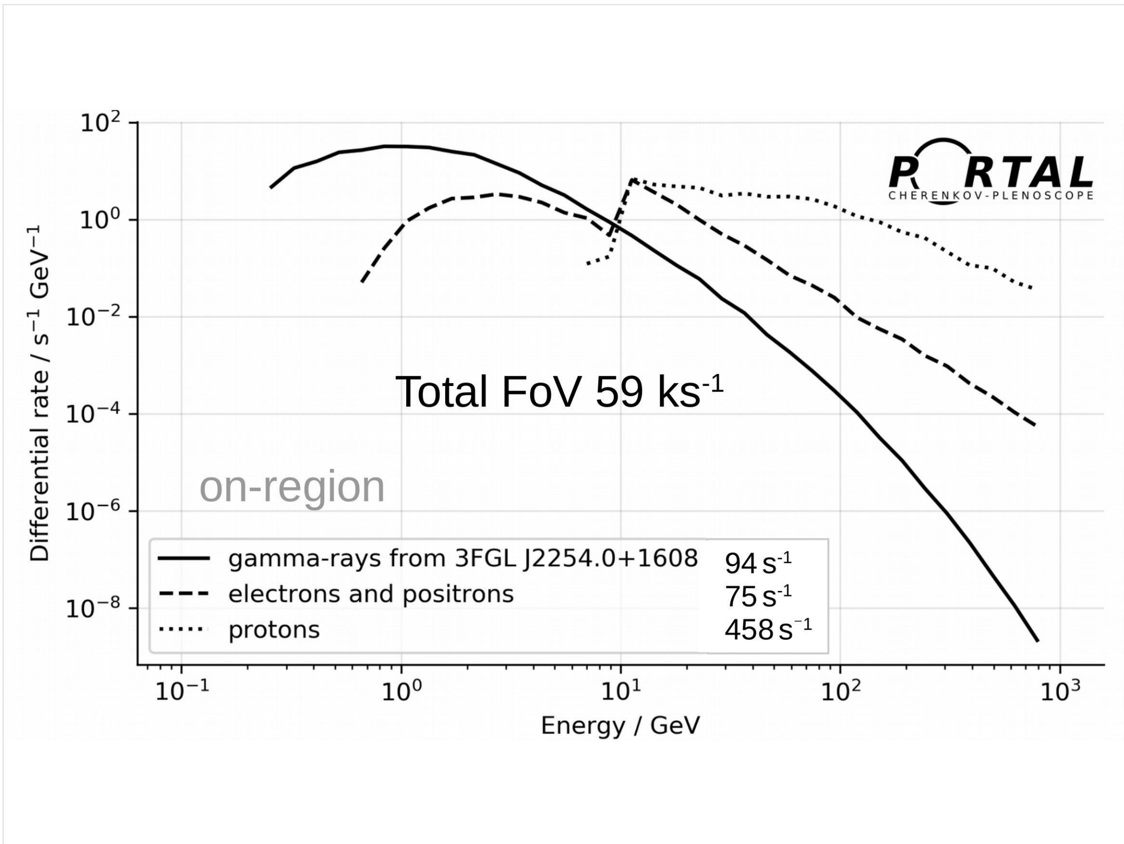

The total trigger rate in the entire field-of-view is 59 kilo events per second.

Remember I estimated the accidental rate to be not significantly larger than 22 events per second.

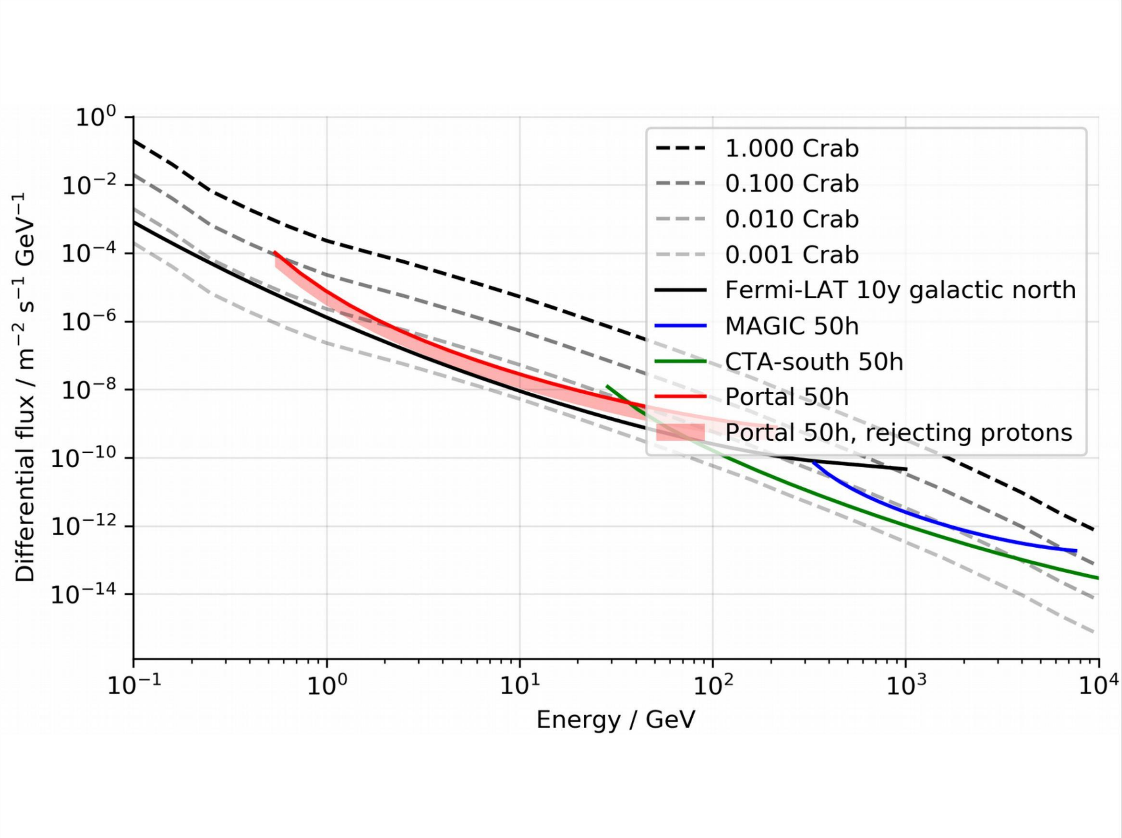

The integrated sensitivities for Portal in red, Fermi-LAT in solid black, and other Cherenkov-telescopes.

If it was possible to implement a gamma-hadron-separation for Portal as we have it on Cherenkov-telescopes, Portal might reach down into the reddish box before the electrons and positrons become the limiting factor.

Watch out, this is integrated sensitivity. There is not yet an energy-reconstruction for Portal.

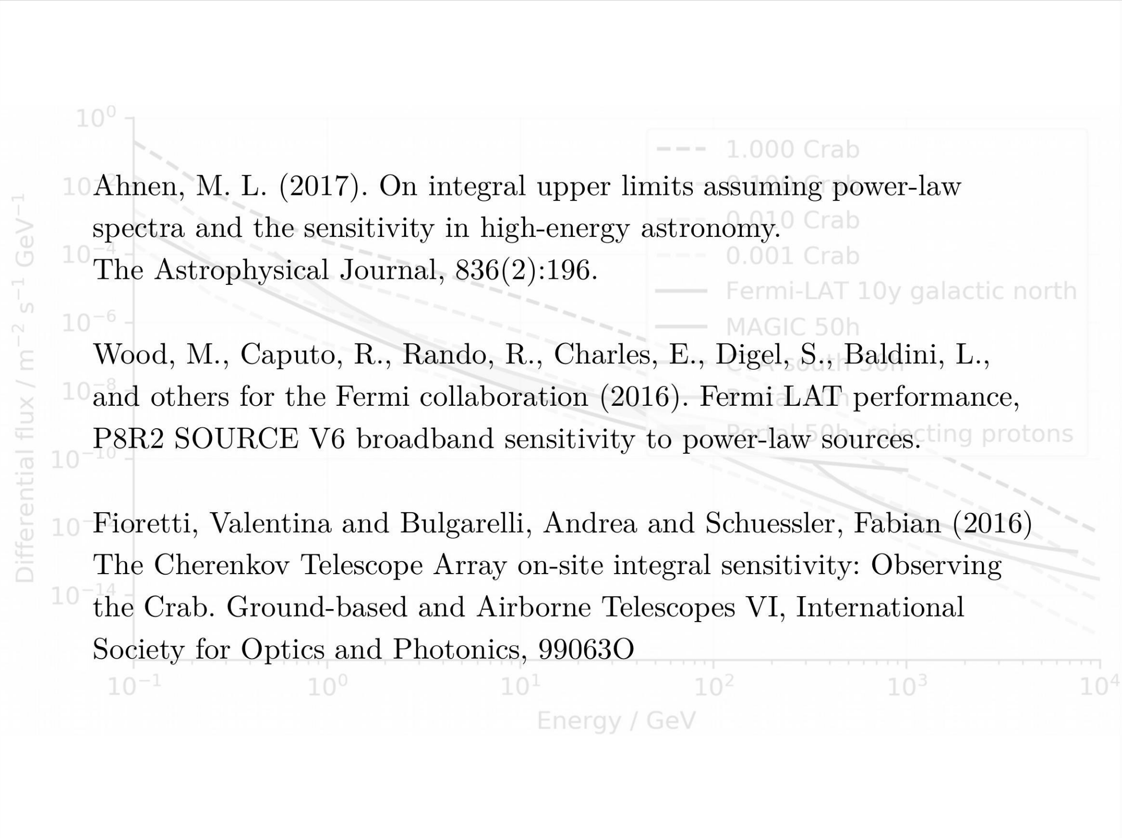

Ahnen, M. L. (2017). On integral upper limits assuming power-law spectra and the sensitivity in high-energy astronomy. The Astrophysical Journal, 836(2):196.

Wood, M., Caputo, R., Rando, R., Charles, E., Digel, S., Baldini, L., and others for the Fermi collaboration (2016). Fermi LAT performance, P8R2 SOURCE V6 broadband sensitivity to power-law sources.

Fioretti, Valentina and Bulgarelli, Andrea and Schuessler, Fabian (2016) The Cherenkov Telescope Array on-site integral sensitivity: Observing the Crab. Ground-based and Airborne Telescopes VI, International Society for Optics and Photonics, 99063O

MAGIC, Fermi-LAT, CTA in combination with effective-areas from CTA-web-pages.

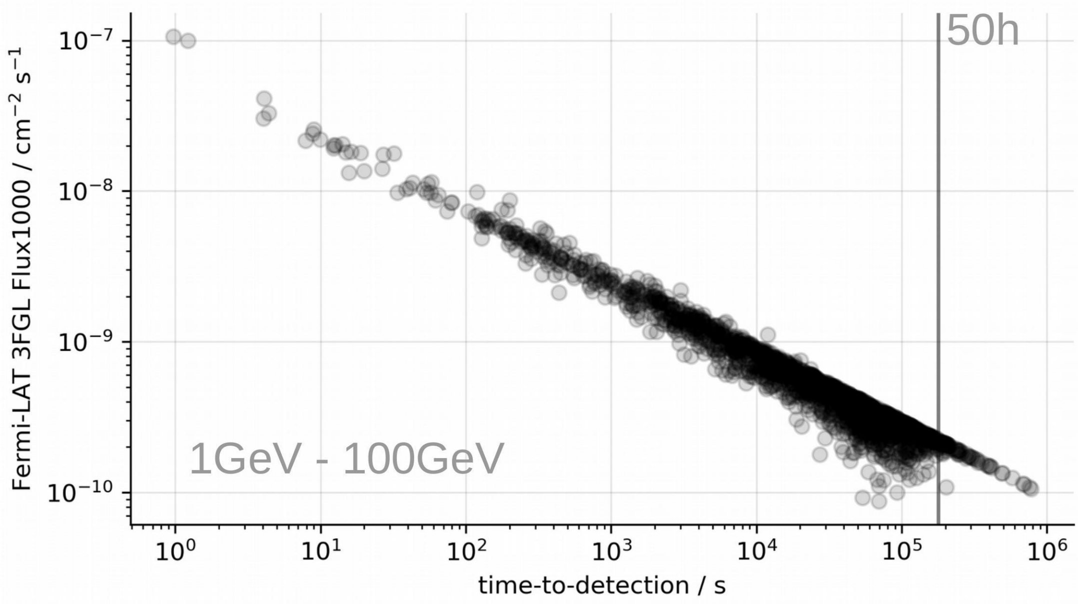

This is the flux of gamma-ray-sources measured by Fermi-LAT in the range from 1 to 100 GeV versus the estimated time-to-detection of these sources with the Portal Cherenkov-plenoscope.

Almost all known sources in the static gamma-ray-sky can be detected within 50 hours.

And with a few sources in the regime of one second time-to-detection, the Portal Cherenkov-Plenoscope becomes the gamma-ray-timing-explorer.

As Felix Aharonian phrased it: “...The scientific reward of a ground based approach in GeV gamma-ray-astronomy will be enormous…”

We can now ask him whether he still thinks so today.

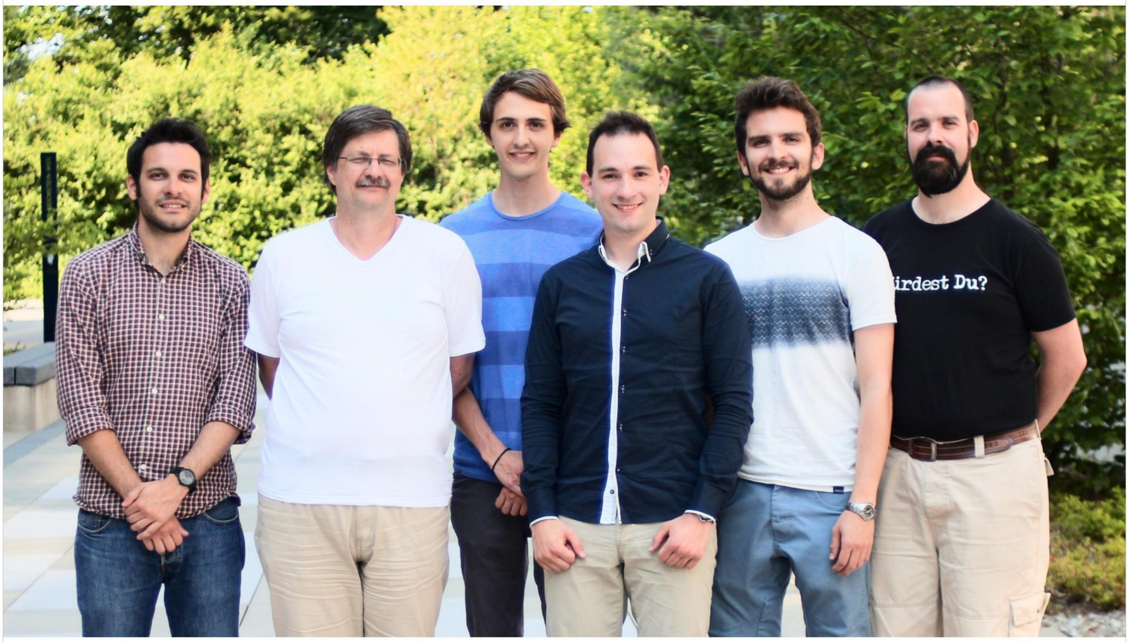

I want to thank Civil engineer Spyridon Daglas, Axel Arbet Engels, Max Ludwig Ahnen, Dominik Neise, and Professor Adrian Biland for supporting my ground based approach into the one Giga electron Volt gamma-ray-sky.

From left to right:
Spyridon Daglas (Civil-engineer),
Prof. Adrian Biland,
Axel Arbet Engels,
Sebastian Achim Muller (Speaker),
Max Ludwig Ahnen,
Dominik Neise.

Hoenngerberg-campus ETH-Zurich, 2017-May-30